Sophorolipid assisted enhanced solubility of hydrophobic biomolecules and development of nano-carriers as advanced drug delivery systems

Thesis Submitted to AcSIR
For the Award of the Degree of
DOCTOR OF PHILOSOPHY
In
BIOLOGICAL SCIENCES

By
Priti Anand Darne
10BB15A26040

Under the guidance and co-guidance of
Dr. Narendra Kadoo and Dr. Asmita Prabhune

Biochemical Sciences Division
CSIR-National Chemical Laboratory
Pune-411008, India

November 2018

सीएसआयआर–राष्ट्रीय रासायनिक प्रयोगशाला
(वैज्ञानिक तथा औद्योगिक अनुसंधान परिषद)
डॉ. होमी भाभा मार्ग, पुणे – 411 008. भारत

CSIR-NATIONAL CHEMICAL LABORATORY
(Council of Scientific & Industrial Research)
Dr. Homi Bhabha Road, Pune - 411008. India

CERTIFICATE

This is to certify that the work incorporated in this Ph.D. thesis entitled "**Sophorolipid assisted enhanced solubility of hydrophobic biomolecules and development of nano-carriers as advanced drug delivery systems**" submitted by Priti Anand Darne for the Degree of Doctor of Philosophy to Academy of Scientific & Innovative Research (AcSIR) is the record of work carried out by her at Biochemical Sciences Division, CSIR- National Chemical Laboratory, Pune - 411008, India, under our supervision. The thesis embodies original work. Research material obtained from other sources has been duly acknowledged in the thesis. Any text, illustration, table etc., used in the thesis from other sources, have been duly cited and acknowledged.

Dr. Narendra Kadoo
(Research supervisor)

Dr. Mrs. Asmita Prabhune
(Research co-supervisor)

Biochemical Sciences Division
CSIR-National Chemical Laboratory
Dr.HomiBhabha Road, Pashan
Pune – 411008
Maharashtra, India

November 2018

☎
Communications Channels
NCL Level DID : 2590
NCL Board No. : +91-20-25902000
Four PRI Lines : +91-20-25902000
FAX
Director's Office : +91-20-25902601
COA's Office : +91-20-25902660
SPO's Office : +91 20 25902664
WEBSITE
www.ncl-india.org

DECLARATION BY RESEARCH SCHOLAR

I hereby declare that the thesis entitled "**Sophorolipid assisted enhanced solubility of hydrophobic biomolecules and development of nano-carriers as advanced drug delivery systems**" submitted by me for the Degree of Doctor of Philosophy to Academy of Scientific & Innovative Research (AcSIR) is the record of work carried out by me at Biochemical Sciences Division, CSIR- National Chemical Laboratory, Pune - 411008, India, under the supervision of Dr. Narendra Kadoo (Research supervisor) and Dr. Asmita Prabhune (Co-supervisor). The work is original and I further declare that the material obtained from other resources has been duly acknowledged in the thesis.

Priti Anand Darne **Dated: 7.11.2018**

Biochemical Sciences Division
CSIR-National Chemical Laboratory
Dr.HomiBhabha Road, Pashan
Pune – 411008
Maharashtra, India

Acknowledgment

Firstly, I would like to express my sincere gratitude to my advisor Dr. Mrs. Asmita Prabhune for her continuous support of my Ph.D. study and related research, for her patience, motivation, and immense knowledge. Her guidance helped me incredibly throughout my research and writing of this thesis. I could not have imagined having a better advisor and mentor for my Ph.D. study. Prabhune ma'am has understood me better than I would ever understand myself. She has absorbed all of my emotional and frustrated tantrums whenever my research was stuck. She never objected my ideas and gave freedom to work as I please. This helped me to become a more organized and independent researcher. She was always there to encourage me and give timely advice whenever required. Her suggestions were at first impossible to do, but when tried always worked wonders. She is an incredible human being, the strength and wisdom that she has shown is an encouragement for a young researcher like me. She is my role model. I would also like to express my gratitude towards Dr. Narendra Kadoo my other advisor. He was always there to support me. His calm presence and concern have always touched me. I really am lucky to get such people as my guides.

Besides my advisors, I would like to thank the rest of my thesis advisory committee: Dr. Sushama Gaikwad, Dr. Bhushan Chaudhari, and my DAC chairman Dr. Ulhas Karul, for their insightful comments and encouragement, but also for the hard question which urged me to widen my research from various perspectives.

My sincere thanks to Dr. Giri, Head of Department, Biological Sciences Division; CSIR-NCL and Prof. Nangia, Director, CSIR-NCL for letting me use the workplace and providing with world-class facilities. I also thank Dr. Pundle for her presence and timely inputs in the lab and introducing a few wonderful people in my life who eventually become my close friends.

My sincere thanks also go to Dr. Kalpana Joshi of Sinhgad College of Engineering, Pune who provided me an opportunity to join their team for a short time and who gave access to the laboratory and research facilities. Without their precious support to understand and help me learn the cell biology work, it would not be possible to conduct part of this research.

I would also like to thank Mrs. Ashwini Rane from Savitribai Phule Pune University (SPPU) and Dr. Deopurkar who let me use their tensiometer which is an important aspect in surfactant characterization. And the whole team of Centre for Material Characterization (CMC), CSIR-NCL, Pune for various instrumentation and characterization of my compounds and nanoparticles. With their timely help, the thesis work was completed within stipulated time. I am very grateful for the same.

I thank all my fellow past and present labmates for the stimulating discussions, for the fun talks when we were working together before deadlines, and for all the excitement we have had in the last six years. My tenure as a Project assistant and later as a Ph.D. student was made wonderful by these amazing bunch of people. Dr. Kasturi, Dr. Vrushali, Dr. Pradeep, Dr. Ruchira, Dr. Pooja, Dr. Madhura, Dr. Animesh, Dr. Parul have made me strive to work hard and diligently to achieve the similar success that they had. Dr. Pushpa and Dr. Avinash were my dearest friends among them. They not only taught me about science but also how to live life. We had a great time together. I am forever grateful towards them.

In recent years Pooja, Amruta, Swarali, Isha, Mihir, Sahana, Shraddha, Palna, Megha, Dr. More made my life in lab enjoyable and work environment pleasant. Amruta and Swarali have become like sisters to me and Isha a very good friend of mine. They have pushed me and spared me from menial work of lab to finish my thesis in time. Their motivation was much needed at times, whenever I thought it as a daunting task. I am very blessed to have met all of my lab mates who have become lifelong friends of mine.

I am truly thankful to all the project students who worked hard with me to complete their Master's project. Prachiti, Arun, Bismoy, Avinash, Shamitha, Swati, Pradnya, Ajit, Mahesh, Snehal, Sonakshi and many more have enriched my life and shown me how to be a patient and understanding mentor.

Last but not the least; I would like to thank my family: my parents and my brother and Vahini (sister-in-law) for supporting me unconditionally throughout working and writing this thesis and my life in general. The precious bundle of joy, Jia my niece made my life fun and happy ever since she is born. I love them all to the bits. I am eternally thankful to God who gave me such amazing parents and brother.

Thanks to all who have entered my life in the past six years, everyone has taught me a thing or two and made me the person that I am today.

Sincerest Thanks

Priti Anand Darne

Table of Contents

	Page
List of Figures	i
Thesis Abstract	1
Chapter 1: Introduction	
1. Drug Solubility	3
1.1. The various techniques employed for drug solubilization of poorly soluble drug	3
2. Surfactant	5
2.1. Biosurfactant	7
3. Sophorolipid (SL)	8
3.1. Properties of Sophorolipid	9
3.2. Production	9
3.3. Producing Organism	10
3.4. The Structure of Sophorolipid	10
4. Application of SL	11
5. Sophorolipid in Nanoparticles synthesis	15
6. Curcumin	20
7. Calcium carbonate	22
8. Sericin	22
9. The scope of work	23
10. Outline of thesis	23
References	27
Chapter 2: Bioavailability studies of curcumin-sophorolipid nano-conjugates: Their role in synthesis of uniform gold nanoparticles	
1. Introduction	38
1.1 Curcumin	38
1.2 Formulation for solubility of curcumin	38
2. Our strategy for curcumin solubility	39
2.1 Sophorolipid	39
2.2 Gold nanoparticles synthesis for drug carrier	39
3. Materials and Methods	41
3.1. Reagents and Chemicals	41
3.2 Organism and maintenance	41
3.3 Synthesis of oleic acid sophorolipid (OASL) and Extraction	41
3.4 Synthesis of aqueous Curcumin- Sophorolipid Nanoconjugates (CurSL)	41
3.5 Gold Nanoparticles synthesis	41
3.6 Characterization	42

3.7 Scanning Electron Microscopy (SEM) 42
3.8 Transmission Electron Microscopy (TEM) 42
3.9 Pharmacokinetic study 42
3.10 High-Resolution Mass Spectroscopy (HR-MS) 43
3.11 Histopathological study 43
4. Results and Discussion 45
4.1 Spectrophotometric analysis 45
4.2 FTIR Characterization 47
4.3 Particle Size Distribution and Stability 50
4.4 Pharmacokinetic Plasma Studies 52
4.5 Histopathological Analysis 55
4.6 Energy Dispersive X-ray (EDX) analysis 55
5. Conclusion 56
References 58

Chapter 3: Derivatization of curcumin via biotransformation and exploring its applied aspects

1. Introduction 63
1.1 Curcumin 63
1.2 Degradation products of Curcumin 66
1.3 Sophorolipid 67
1.4. The Scope of the study 68
2. Materials and Methods 69
2.1 Maintenance of Micro-organisms 69
2.2. Production of Curcumin derived Sophorolipid (CSL) 69
2.3. Resting Cell Method 69
2.4 Extraction of CSL 70
2.5 Rota-Evaporation and Purging 72
2.6 Characterization 73
2.6.1 Oil displacement 73
2.6.2 Thin Layer Chromatography (TLC) 73
2.6.3 Surface tension measurement and critical micelle concentration 73
2.6.4 High-Performance Liquid Chromatography (HPLC) 74
2.6.5 High-Resolution Mass Spectroscopy (HRMS) 74
2.6.6 Fourier Transform Infrared Spectroscopy (FTIR) 75
2.6.7 Nuclear Magnetic Resonance (NMR) 76
2.6.7 Photoluminescence (PL) 76
2.7 Fluorescence Microscopy 76
2.8Bio-imaging 77
2.9 Anti-biofilm assay 77
2.10 Antioxidant Activity [DPPH Assay] 77

2.11 Anti-Tyrosinase Property 78
2.11.1 Role of Melanin 79
2.11.2 Deleterious Effect of Melanin 80
2.11.3 Anti-Tyrosinase assay 81
2.12 Anti-cancer activity 81
3. Results and Discussion 83
3.1 Oil displacement 83
3.2 Surface tension analysis 84
3.3 TLC 85
3.4 HPLC 86
3.5 HRMS 87
3.6 FTIR 89
3.7 NMR 93
3.8 Photoluminescence 94
3.9 Fluorescence Microscopy 95
3.10 Bio-imaging 96
3.11 Anti-biofilm 97
3.12 Anti-Oxidant activity 98
3.13 Anti-Tyrosinase assay 99
3.14 Cell viability and anti-cancer study 100
4. Conclusion 101
Reference 103

Chapter 4: Synthesis of biocompatible Calcium carbonate ($CaCO_3$) microparticles as a drug delivery system using sophorolipid as a capping agent to increase the porosity of synthesized particles

1. Introduction 112
1.1 Calcium carbonate 112
1.2 Synthesis methods for $CaCO_3$ particles 112
1.3 Applications of Calcium carbonate 113
1.4. Sophorolipids 113
1.5. The scope of work 114
2. Materials and Methods 115
2.1. Synthesis of $CaCO_3$ particles 115
2.1.1. Probe sonication for the synthesis of $CaCO_3$ particles 115
2.1.2. Magnetic stirring for the synthesis of $CaCO_3$ particles 116
2.2. Nucleation of Calcium carbonate particles in presence of sophorolipid 116
2.3. Determining the presence of SL on $CaCO_3$ particles 117
2.4. Drug loading and release study 117
3. Results and discussion
3.1.1 Set I of sonication 118

3.1.2 Set II of sonication 119
3.2. Magnetic stirring for the synthesis of $CaCO_3$ particles 121
3.3. Nucleation of Calcium carbonate particles in presence of sophorolipid 122
3.4. Determining the presence of SL on $CaCO_3$ particles 123
3.5. Drug loading and release study 124
4. Conclusion 125
References 127

Chapter 5: Sericin based synthesis of Tunable, Monodispersed and Stable Gold nanoparticles: Role of Temperature and pH
1. Introduction 131
1.1 Gold Nanoparticles (GNPs) 131
1.2 Synthesis Methods 131
1.3 Sericin 131
2. Materials and Methods 133
2.1. Extraction of Sericin 133
2.2. Synthesis of Sericin Gold Nanoparticles (Seri-GNPs) and Characterization 133
3. Results and Discussion 135
3.1. UV-Vis spectroscopic and MALDI 135
3.2. Particle size distribution and Analysis via DLS and TEM 140
3.3. X-Ray Diffraction Analysis XRD 142
3.4. Fourier Transform Infrared Spectroscopy (FTIR) 143
4. Conclusion 144
References 145

Chapter 6: Conclusion and Future work 148
List of publications and Seminar and Workshop attended 154

List of Figure

Figure no.	Chapter 1	Page no.
Fig. 1	Structure of Sophorolipid (a) Acidic SL (b) Lactonic SL (Dubey et al., 2013)	11
Fig. 2	Curcumin I, II, III (curcumin, demethoxycurcumin, and bisdemethyoxy curcumin) and keto-enol tautomers of curcumin. (Naksuriya et al 2016)	21
	Chapter 2	
Fig.1a.	The UV-Vis spectrum of Curcumin in water, sophorolipid (OASL) solution and synthesized CurSL nano-conjugate solution. λmax observed at 424 nm and 440 nm for CurSL and Curcumin in water respectively.	46
Fig.1b.	The UV-Vis spectra of CurSL-GNPs, where λmax is observed at 540 nm.	46
Fig. 2	The PL spectra when excited at 400 nm for CurSL nano-conjugate, curcumin (cur) in water and sophorolipid (OASL) solution. Emission λmax was observed at 504nm and 548 nm with the inset images of solutions for CurSL nano-conjugate and curcumin (cur) in water respectively.	47
Fig. 3	FTIR analysis of (a) Curcumin (powder) and CurSL solution, (b) OASL and (c) CurSL-GNP, inset CurSL solution.	49
Fig. 4	a) DLS and (b) Zeta Potential of synthesized CurSL nanoparticles indicating the hydrodynamic size of 275 nm and the mean zeta potential of -65.79 mV.(c) DLS of CurSL-GNPs with hydrodynamic size as 5 nm and -42.39 mV zeta potential (d).	50
Fig. 5	SEM images of Curcumin control (a) showing large irregular pieces about 8-10 μ in size. (b) CurSL solution evenly dispersed nearly spherical nanoparticles of size between 40-60 nm. (c) TEM image of CurSL-GNPs, scale represented is 50 nm and the size of particles is nearly 8-10 nm.	51
Fig. 6	An HR-MS spectrum of standard curcumin in ACN (a) and spectrum of extracted plasma samples from Wistar rats administered with CurSL (100 μg/ml) solution after 2 h time interval (b).	53
Fig. 7	Microscopic images of the Histopathology of organs viz., Lung, Liver, Heart, Kidney, and Spleen	55
	Chapter 3	
Fig. 1	Curcumin I, II, III (curcumin, demethoxycurcumin, and bisdemethyoxy curcumin) and keto-enol tautomers of curcumin. (Naksuriya et al 2016)	64
Fig. 2	The metabolic and degradation pathways of curcumin. (a) Reduction; (b) conjugation; (c) oxidation; and (d) cleavage (Claus Schneider**,** 2015)	67
Fig. 3	Schematic illustration of production method for CSL (a). Flask containing *C. bombicola* cells in MGYP broth incubated for 48 h. (b). Re-suspended cells in 10% glucose medium with addition of 10 mg Curcumin.	70
Fig. 4	The product (CSL) settled at the bottom of the flask	71
Fig. 5	(a) Separation of cell mass from the solvent phase (b) Partially extracted CSL with sodium sulphate crystals	71
Fig. 6	(a) Filtering the partially extracted CSL of any sodium sulphate crystals. (b) The solution before subjecting it to Rota-evaporation (c) Concentrating the extracted product by Rota-evaporation	72
Fig. 7	(a) The concentrated CSL after rota-evaporation. (b) The final product CSL.(c) Crystallization of CSL	72

Fig. 8	Block diagram of an FTIR spectrometer	76
Fig. 9	The scavenging reaction between DPPH and an antioxidant (R-H) (MacDonald et al, 2006)	78
Fig. 10	Biosynthetic pathway of melanin synthesis. (Chang, T.S, 2009)	79
Fig. 11	Oil displacement activity of CSL, showing detergent property	83
Fig. 12	Graph displaying the surface tension lowering property of CSL. The CMC was calculated by extrapolating graph to obtain the lowest surface tension started being stable	84
Fig. 13	(a) TLC of Curcumin-Sophorolipid (b) Comparative TLC of OASL and CSL (b) 1: Sophorolipid synthesised from oleic acid (OASL) 2: CSL 3: Oleic acid oil 4: Curcumin	85
Fig. 14	(a) Chromatogram of Standard Curcumin. (b) Chromatogram of Crude-CSL. The HPLC chromatogram of Standard curcumin shows a retention time at 12^{th} minute, on the other hand, a shift in the retention time is seen in the CSL chromatogram observed at 5^{th} minute. The CSL compound resolved to give 4 peaks that were collected at their specific retention time.	86
Fig. 15	HR-MS spectra showing molecular weight of the seven predicted compounds viz., Deacetylated acidic SL, Acidic diacetylated SL , Vanillic acid acidic deacetylated SL, Vanillic acid acidic diacetylated SL, 4-vinyl guaicol acidic acetylated SL, Diguaiacol acidic deacetylated SL, and Bicyclopentadione acidic diacetylated SL	87-90
Fig. 16	(a) FTIR of Standard Curcumin. (b) FTIR of CSL compound	91
Fig. 17	H1 NMR spectra of curcumin and CSL in deuterated methanol	93
Fig. 18	Vials containing sample observed under Ultra-violet light. 1: Only distilled water sample (1 mL) 2: Curcumin (5 mg) in distilled water (1 ml) 3: CSL (5 mg) in distilled water (1 ml)	94
Fig. 19	Photoluminescence study of Curcumin and CSL in water and ethanol	94
Fig. 20	(a) View of under light microscope (40x) (b) View under blue filter for fluorescent imaging (40x)	95
Fig. 21	Confocal microscopy	96
Fig. 22	Anti-biofilm activity of CSL and Curcumin	97
Fig. 23	DPPH activity of CSL compound	98
Fig. 24	Graph representing percent scavenging activity of CSL	98
Fig. 25	(a) The plate observed after 30 mins. (b) The plate observed after 24 h. C1: No inhibitor C2: No enzyme C3: Curcumin in water C4: Curcumin in ethanol C5: Ethanol C6: CSL in ethanol	99
Fig. 26	Percent inhibitory activity graph of Tyrosinase activity of CSL	99

Fig. 27	Toxicity study on L6 cell line. Curcumin shows detrimental effect with increasing concentration, while CSL helps in cell proliferation	100
Fig. 28	MTT assay of curcumin and CSL against cancer cell line MCF-7 and HeLa	101
	Chapter 4	
Fig. 1	Schematic representation of $CaCO_3$ particle formation by sonication method	116
Fig. 2	An illustration of the probable mechanism for spindle shape formation	119
Fig. 3	SEM of Control $CaCO_3$ and SL influenced $CaCO_3$ micro particles	119
Fig. 4	An illustration of the probable mechanism for spherical shape formation	120
Fig. 5	SEM image of control $CaCO_3$ micro-particle and change in the morphological form of $CaCO_3$ with increasing SL concentration in set II experiment.	120
Fig. 6	Illustration for $CaCO_3$ particle formation by magnetic stirring	121
Fig. 7	SEM images of the particles formed by magnetic stirring	121
Fig. 8	SEM study for the nucleation and formation of particles	122
Fig. 9	Elemental mapping of the formed micro-particles	122
Fig. 10	TEM study validating the presence of SL on $CaCO_3$ particles	123
Fig. 11	EDAX graph showing elemental presence on the TEM grid, inset showing a SAED pattern indicating crystalline nature of whole assembly.	123
Fig. 12	a. Bare $CaCO_3$ and b. $CaCO_3$ loaded with drug furosemide	124
Fig. 13	Furosemide drug release profile from $CaCO_3$ microparticles	125
	Chapter 5	
Fig. 1	Process used for obtaining sericin in this thesis	133
Fig. 2	MALDI of sericin in different pH (5.0 to 9.0) at 80^oC	135-137
Fig. 3	Seri-GNP synthesis in different conditions. Control represents $HAuCL_4$ in pH buffers 0.1M (pH 5.0 to pH 9.0) without sericin at 80^oC. Rest represents Sericin-$AuCL_4$ sample in different buffers of 0.1M (pH 5.0 to pH 9.0) at respective temperatures (30^oC to 80^oC).	138
Fig. 4	Seri-GNP synthesized at 80^oC with varying pH 5.0 to pH 9.0. SPR band was observed at 540 nm typical of gold nanoparticles	139
Fig. 5	DLS size distribution temperature 80^oC, pH 5.0 and pH 9.0	140
Fig. 6	TEM of Seri-GNPs synthesized at different conditions	141
Fig. 7	XRD pattern of Seri-GNPs synthesized at 80^oC and pH 5.0 (red) and pH 9.0 (black).	142

Fig. 8	FTIR of Sericin, legends SGNP5 and SGNP9 indicate Seri-GNP pH 5.0 and Seri-GNP pH 9.0 respectively synthesized at 80^{o}C	143
	Chapter 6	
Fig. 1	SEM images (a) Control solution of ZnO nano-material in aggregates (scale 10µm) (b) CSL reduced/capped ZnO particles as separate (scale 1µm) (c) CSL reduced/capped ZnO particles as separate (scale 500 nm)	151-152
Fig. 2	Anti bacterial activity of ZnO against *S.aureus* and *E. coli*	153

Chapter 1

Sophorolipid assisted enhanced solubility of hydrophobic biomolecules and development of nano-carriers as advanced drug delivery systems

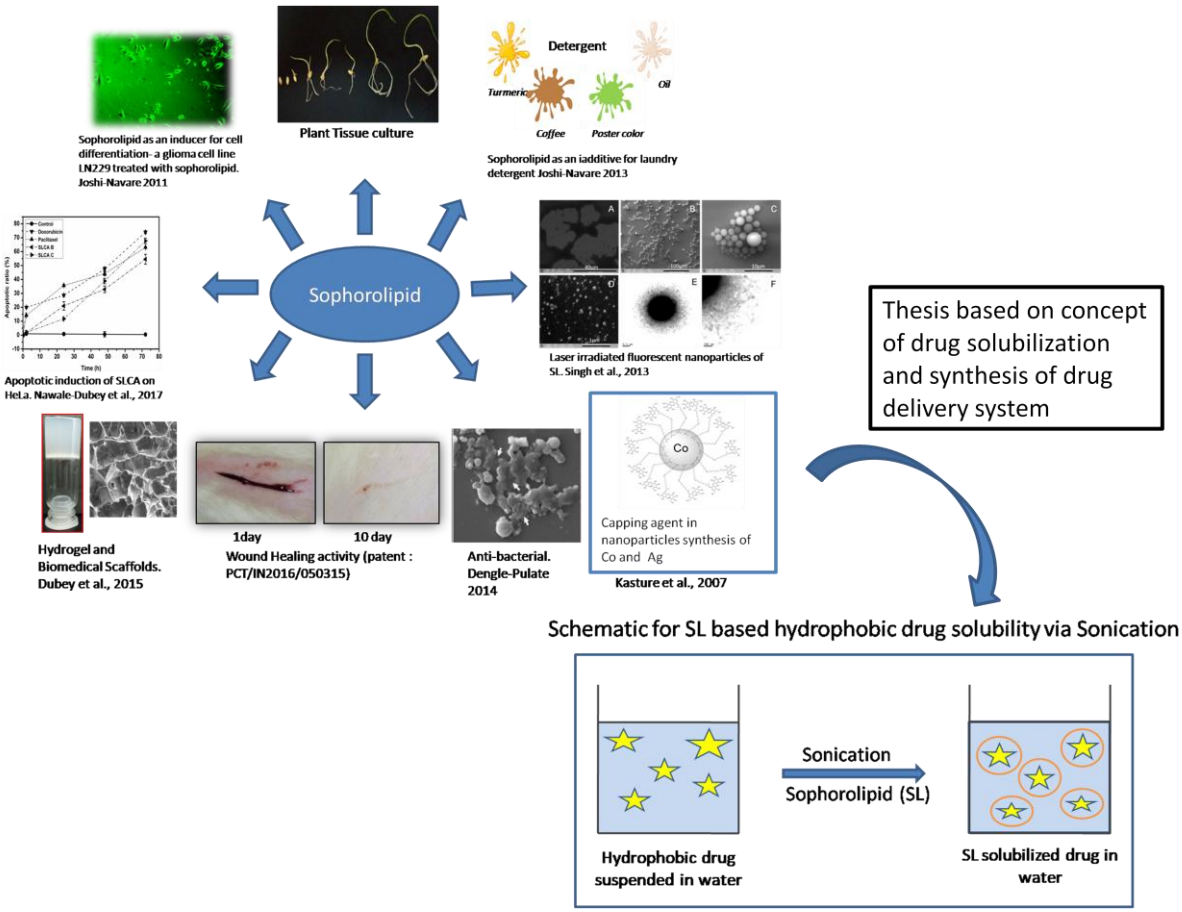

Thesis Abstract:

Nearly 40% New Chemical Entities (NCE) that is developed in the pharmaceutical industry and 90% of molecules in the discovery pipeline are hydrophobic in nature. Many such marketed drugs not only have poor solubility but low permeability, rapid metabolism and easy elimination from the body along with safety and tolerability issues. Physical Modifications, Chemical Modifications, Miscellaneous Methods (Adjuvants like Surfactant, PEG, PVP, SDS, Tween 80, etc.) are some of the applied solutions. Liposomes are currently being investigated as a delivery vehicle, but this system is expensive and alternative needs to be identified. Among all these strategies, the use of surfactant seems attractive and

economical. Currently, synthetic surfactants like Tween 80 and SDS are used in drug formulation which has very low bio-degradability when used in drug formulation; besides, it causes side effects like nausea. Additionally, these chemical surfactants have higher critical micelle concentrations (CMC) leading to higher amounts being used in the formulation leading to cause tolerance issues. Strategies which use biological surfactants can address this challenge. Amongst many biosurfactants, Sophorolipid (SL) is the most promising based on its production yield and unique properties. Sophorolipids are glycolipid in nature and synthesized by non-pathogenic yeast *Candida bombicola*. Sophorolipids are reported to have many activities, like anti-microbial, anti-cancer, biomedical scaffolds, wound healing etc. Many reports of nanoparticles reduced/capped via sophorolipid are published in last decade. Nanoparticles currently are intensively studied topic due to its immense applicability. For targeted drug delivery, nanoparticles are preferred carriers, but given the chemical nature of synthesis, their use is limited. In this thesis, we are using SL for solubilizing hydrophobic drug molecules (model drug as curcumin) and for the synthesis of drug delivery vehicles. Microparticles like calcium carbonate are attempted in conjunction with SL. This whole assembly is biocompatible and free from the chemical method. Also, another bio-based material the sericin is used for the synthesis of gold nanoparticles as a model drug delivery vehicle. The thesis covers the synthesis and characterization of these drug delivery systems.

Introduction:

1. Drug solubility

Drug solubility is considered a challenge in the current pharmaceutical scenario. Many are trying to conquer this challenge by employing various means. Amongst them, the interest lies when done by abiding the principles of green chemistry. Drugs are usually administered via many different routes like injections, rectal, vaginal, ocular, etc., but generally, the preferred route is oral administration. Moreover, the role of drug solubility and permeability plays a significant part in drug formulation and designed for oral administration. According to the Biopharmaceutics Classification System (BCS), drugs are classified based on their solubility and permeability. There are four classes viz., Class I drugs with high solubility and high permeability, Class II drugs with low solubility and high permeability, Class III contains drugs having high solubility, but low permeability and Class IV category consist of drugs with both lower solubility and permeability. To overcome the issue of solubility methodologies have been adopted by pharmaceutical manufacturers to ensure that poorly soluble drugs achieve improved bioavailability. Bioavailability is the term referred to the drugs or substances that enter the circulation for the desired effect. When a drug is orally given, its complete absorption through gastric juices is considered to be an excellent bioavailable drug. Not only absorption but bioavailability depends on many factors including drug solubility in aqueous medium and drug permeability via lipidic membranes. Different techniques employed for solubilization of drugs mainly includes a chemical modification, micronization, pH adjustment, co-solvency, solid dispersion, complexation, hydrotrope, micellar solubilization, etc. Nearly 40% of the new chemical entities developed as drugs are practically insoluble in water. [1] Another report stated that 40% of approved drugs and nearly 90% of drugs under development are poorly soluble. This leads to slower drug absorption and in the process to lower bioavailability of the drug. To overcome this issue drug dosage is increased to achieve the desired effective concentration for the drug to act. However, this, in turn, leads to side effects hence the development of newer drugs remains a challenge.

1.1. The various techniques employed for drug solubilization of poorly soluble drugs are given in brief below:

Solid dispersions: This is a physical method where the drug is dispersed in a solid form in a carrier that is inert in nature and water soluble.

Amorphous form: Drug with its stable crystal form causes poor solubility, therefore changing the form of crystal into more amorphous nature imparts more solubility in water to the drug. Hence this method is widely explored in pharmaceutics production.

Co-crystals: In the last decade co-crystals has seen tremendous interest due to its achievement in the delivery of insoluble drugs. Drug and conformer in a crystal at ambient temperatures are known as co-crystals. Interactions like acid -amide, amide-amide, acid -acid through hydrogen bonds between a drug and conformer are seen in a co-crystal. The GRAS (generally regarded as safe) excipients like organic acids (glutaric acid, oxalic acid), neutraceuticals (quercetin, saccharine), etc are considered as conformers.

pH modification and salt forms: Almost 70% of drugs are said to be ionizable, and the majority of them are weakly basic. A pH-dependent solubility is observed by ionizable drugs, i.e. weakly acidic drugs are much soluble at pH is more than its pKa (ionization constant) while in weakly basic drugs pH in lower than its pKa. This pH-dependent solubility is widely explored in drug designing and development.

Complexation: This is the method where the hydrophobic drug is filled in a hydrophobic cavity of cyclodextrin, enabling the hydrophobic interactions to keep the drug in place and due to a hydrophilic outer layer of cyclodextrin the complex becomes water soluble. Cyclodextrin also helps in drug stabilization and protects the drug from exposures of light, heat and oxidative stress along with its action to reduce dermal, gastrointestinal and ocular irritation. Many marketed drugs with insoluble nature are formulated with cyclodextrin.

Size reduction and nanonization: The advent of nanoparticles technology has opened up a new and exciting area for drug design, development, and formulation. By reducing the particle size to nano range leads to improved cellular uptake of insoluble drugs. Drugs can be nanonized by top down or bottom up methods.

Liposomes: Vesicles of phospholipid bilayer entrapping an aqueous phase are referred to as liposomes. Liposomes are considered the model drug delivery system transporting drugs to target site efficiently.

Solid lipid nanoparticles: GRAS cleared lipids are used as an excipient for carriers of insoluble drugs for site-specific actions. These lipids are usually biocompatible and biodegradable.

Microemulsions and self-emulsifying drug delivery systems: Microemulsions are a mixture of oil, water, surfactant, and a co-surfactant. These are thermodynamically stable and produced as a clear emulsion when mildly agitated.

Polymeric micelles: Encapsulation of hydrophobic drugs into the hydrophobic core of micelles enables the solubility of drugs. Hydrophilic surfactants were used for drug formulation initially, but due to higher critical micelle concentration (CMC), limited solubilization and slightly adverse effects of these micelles have limited their utilization. Polymeric micelles formed by using diblock polymers like PEG-PLA or triblock polymers PLA-PEG-PLA have shown greater solubilization, lower CMC, and reduced the tolerability issues hence have become a well-studied drug delivery system.

Co-solvency and surfactant solubilization: For the solubilization of hydrophobic or poorly soluble drugs use of surfactants and co-solvents have been studied extensively for oral and intravenous drugs. To prevent precipitation by dilution and to increase solubility, co-solvents in the conjugation of surfactants with lower CMC values are used along with pH modifiers. However chemical surfactants can cause hypersensitivity reactions leading to tolerability issues, and uncontrolled precipitation of drug may happen when diluted with physiological fluids. [1–6]

2. Surfactants:

The world that we live in today depends tremendously on the ever-evolving science. The growth of humankind closely relates to the growth of science. Our daily routine is based on the scientific accomplishments, be it the use of toothpaste, soap, detergents, instant food, preserved food, drugs, and many more such things where science and scientific discoveries have made our life's more comfortable. Among most of the toiletries and drug formulation, a prominent compound is ever present without which washing and drug solubility become unimaginable. This incredible compound is a surfactant. Surfactants are used in detergents, emulsions; inks, herbicides, biocides and even your shampoo [7,8]. Surfactants also act as effective emulsifiers while allowing for miscibility of liquids having poor solubility.

The high number of potential utilization of surfactants due to their ability to influence and enhance the properties and dynamics of various surfaces and interfaces has led to the production of synthetic surfactants using chemicals. Chemical surfactants are produced from non-renewable sources such as petrochemical or oleochemicals. Different surfactants possess

different properties such as dissimilarities in the solubility, the ability to reduce surface and interfacial tension and ability to form micelles at different critical micellar concentrations when used with detergents while allowing for foaming and wetting thereby displaying application-specific utilities [9–11]. These many applications lead to widespread usage of surfactants causing an increase in surfactant discharge through various mediums into the environment.

Chemical based surfactants are not readily biodegradable, resulting in the pollution and degradation of aquatic ecosystems as well as posing severe health risks to human beings. The total utilization volume of the major surfactants and detergent alcohols from 1990 to 2004 in North America (US and Canada) ranges from 719,000 metric tons in 1990 to 895,500 metric tons in 2004 with an average of approximately 787,000 metric tons. This clearly displays the quantity of usage of such products and thereby the accumulated harm to the environment [12]. Chemical surfactants have multiple effects on the environment with a direct proportionality observed between the concentrations of the surfactant. Some of these harmful effects are listed as follows [13]:

- Promote and assist the growth of algae in the water, thus decreasing the productiveness of water bodies and undermining aquatic food chain systems.
- Increases the toxicity of aquatic animals through feeding and skin penetration, causing bioaccumulation. Through the food chain, eventually building up a high concentration of toxins in the human body leading to inhibited enzyme activity and loss of immunity.
- Chemical surfactants promote improper filtering and purification of wastewater due to emulsification and dispersion of pollutants, reducing the efficiency of sewage treatment plants.
- They are reported to cause damage to the skin, skin irritations, and liver damage and in some cases are also known to promote carcinogenic formations.
- Chemical surfactants have the ability to disturb fetal development and hence come under the category of teratogens.

The multitude of harmful effects due to the concentration of chemical surfactants in the environment and the dependence on the use of surfactants has led to a focus on the development of environmentally friendly yet effective surfactants using the principles of Green Chemistry. The availability of surfactants produced from animal or plant sources are

readily available sources of biosurfactants but the cost of obtaining such surfactants by using the methods of extraction, precipitation or distillation is much higher as compared to the production of chemical surfactants, thus making them economically unviable.

2.1. Biosurfactants:

A better alternative was the utilization of fermentation techniques to tap the potential of microbial organisms for the production of high yield natural surfactants. Due to reduced costs and sustainable production methods with bacteria, fungi, and yeast, highly efficient production of biosurfactants was possible.[10] The use of glycolipids for the production of biosurfactants using bacteria and yeasts led to the growth of three types of surfactants: sophorolipids, rhamnolipids and mannosylerythritol lipids; with sophorolipids being easy to produce and displaying high yields while the remaining require further studies and development to understand and enhance their potential applications [10,14].

A recent report published by Zion Research on the growth of the Market for Microbial Biosurfactants has estimated that the demand for sophorolipids will grow to about USD 17.5 million globally by the end of 2020, with major requirements being in the fields of detergents, industrial cleaners, oilfield clearing chemicals, personal care, agricultural pesticides and herbicides and food processing [15].

Biosurfactants are currently in demand based on their increased applications in various industries such as paint, detergents, cosmetics, agriculture, pharmaceutical, textile, food, etc. They have many properties that are better than their chemical counterparts, currently the major player in the business. These properties include biodegradability, low toxicity, stability in the wide range of pH, temperatures, high tolerance towards salinity, low foaming, detergency, and interfacial properties [7,16,17]. The presence of biosurfactants is estimated to be 11.2 million metric tons in the global surfactants market. Although it is very limited; a recent market analysis projected a significant market penetration in the range of 8–25%, depending on the sector of applications in the year [17]. Biosurfactants basically consist of hydrophilic and hydrophobic components, making them amphiphilic in nature. Unlike the chemical surfactants that are characterized based on their charge, biosurfactants are characterized by their composition. There are five categories of biosurfactants: Glycolipids, Lipopeptides, Fatty acids, Polymer type, and Particulate biosurfactants.

Glycolipids are the largest of biosurfactant groups. They are a combination of carbohydrate

head group and lipidic tail. The most well-known glycolipids are rhamnolipids, sophorolipids, and trehalolipids.

Lipopeptides and **lipoproteins** include a number of cyclic lipopeptides like decapeptide antibiotics (gramicidin) and polymyxins and are known to possess surface active properties. Many micro-organisms can synthesize **fatty acids** and phospholipids when supplemented with n-hexane.

The **polymeric biosurfactants** are the known compounds like emulsan, mannoprotein, liposan, etc.

Extracellular membrane vesicles containing hydrocarbons behave as **particulate biosurfactants**. [18,19]

3. Sophorolipid (SL):

In this thesis, we will be focusing on sophorolipids (SL). These are interesting molecules to study having shown applications in many fields. Based on their therapeutic potential, SL has been commercialized in form of anti-dermatitis soap, body washes and in creams by Soliance and MG Intobio Co. [20]. We will cover briefly these applications but mostly our emphasis is to understand their role in nanoparticles synthesis. Sophorolipids were first synthesized by Gorin *et al*. in the early 1960s using *Candida apicola*. Later many SL producing strains were identified viz. *Rhodotorula bogoriensis, Starmerella bombicola* (previously known as *Torulopsis bombicola* and *Candida bombicola*) and *Wickerhamiella domericqiae*. Among these, *Starmerella bombicola* which is known non-pathogenic yeast has emerged as the best candidate due to its high yielding capacities (up to 400 g/L) and the greater substrate to product conversion rate[20–22]. As the name suggests, sophorolipids are made of sophorose head and fatty acid chain. The two glucose units in sophorose are linked via a unique β 1-2 linkage that may or may not is acetylated with one or two acetyl groups. The fatty acid chain is typically C16-18 long with varying degrees of saturation. During synthesis, if a hydrophobic carbon source is not provided, the organisms form fatty acids *de novo* via acetyl-CoA pathway. The fatty acids are then oxidized at the terminal (ω) or subterminal (ω − 1) position by a cytochrome P450 mono-oxygenase enzyme. These results into formation of hydroxylated fatty acids that are β-glycosidically linked to a first glucose molecule at the 1'-position by a glycosyltransferase I. A second glucose molecule is linked to the 2'-position of the first one by a glycosyltransferase II, yielding sophorolipid acid. [7,10,21] There are two basic

structures of sophorolipid viz., the open chain acidic SL and the closed chain lactonic SL. The proportion of acidic and lactonic in crude SL depends on many factors like organisms used for production, carbon, nitrogen and salt sources in medium, environmental conditions, temperature, agitation, pH, aerations, dissolved oxygen etc. [7]

3.1. Properties of Sophorolipids (SL):

Sophorolipids, being a class of biosurfactants, possess all the basic properties like stability in the wide range of pH, temperatures, and salinity. They have low-foaming and detergent properties; they can sustain water hardness (high concentration of divalent cations) without affecting their interfacial properties. The increased proportion of acidic form of SL increases its surfactant activity. They are highly biodegradable and have low critical micelle concentration (CMC) values with good surface tension and emulsification behavior. Also, SL can be synthesized in large quantities using renewable resources, agro-industrial by-products, and residues with simplified product recovery. [7,22,23] Sophorolipids do not cause irritation to skin and eyes, have an oral safety level which is greater than or equal to 5 mL per kg body weight and causes no allergic reactions hence are preferred for food, cosmetic and pharmaceutical applications. [21]

Sophorolipids display properties and advantages which are comparable to or even better than other surfactants (chemical or biosynthesized). Some of these advantages are listed as follows [7,11]:

- Environmental compatibility.
- High biodegradability.
- Low toxicity.
- Higher tolerance to a broad range of temperature, pH and salinity conditions.
- Eco-friendly.
- Follow the approach of Green chemistry.

3.2. Production:

Sophorolipid is produced extracellularly when grown on a certain hydrophilic and lipophilic carbon source. The lipophilic substrate is usually in the form of a free fatty acid, methyl ester (biodiesel), triglyceride or alkane and the hydrophilic source is glucose [24,25]. Sophorolipid synthesis starts when the yeast cells enter the stationary phase after the exhaustion of nitrogen, in the presence of suitable carbon and energy sources [26]. Declined levels of

phosphate or nitrogen lead to a reduction in the specific activities of NAD+ and NADP+ dependent isocitrate dehydrogenase, thereby causing accumulation of isocitrate as well as citrate in the mitochondria. A transport of isocitrate and citrate occurs into the cytosol, where it is cleaved by adenosine triphosphate (ATP): citrate synthase to give rise to acetyl-CoA, the precursor for fatty acid synthesis [27]. As sophorolipid producing organisms are usually found in areas of high osmotic levels (high sugar content), production of sophorolipid is a means of dealing with high levels of sugar. [23, 28]

3.3. Producer Organisms:

Gorin, Spencer, and Tulloch were the first to describe an extracellular glycolipid produced by the yeast, *Torulopsis magnoliae* in the year 1961, later confirming it to be *Torulopsis apicola* in 1968 *(Candida apicola).* In the same year, a new sophorolipid was identified from *Rhodotorula bogoriensis* [29,30] A third SL yielding strain was identified as *Candida bombicola* [31]. However, the production of sophorolipids is not restricted to one single yeast species. SLs are also produced by several microorganisms such as *Wickerhamiella domericqiae*, *Candida batistae* (CBS 8550), *Candida floricola* (TM1502), *Candida riodocensis*, *Candida stellata*, *Candida rugosa*, *Candida kuoi*, *Candida tropicalis* and *Rhodotorula mucilaginosa* [32–37]. Among these species, *Candida bombicola* (ATCC 22214) is the most studied yeast that exhibits the highest productivity. Furthermore, *Candida bombicola* comes under the title of being GRAS (Generally Recognized as Safe) [38].

3.4. The Structure of a Sophorolipid

Sophorolipids, being surfactant molecules are amphiphilic in nature that interact with the phase boundary in heterogeneous systems and reduce the repulsive forces between phases having different polarity (air-water /oil-water), thereby helping the phases to mix easily. They comprise of the hydrophobic fatty acid tail of 16-18 carbon atoms and sophorose, a hydrophilic carbohydrate head [23,28,39]. Sophorose (a dimeric sugar) and a hydroxyl fatty acid are linked together by a glycosidic bond [40]. Two different types of SLs are synthesized by the yeast, the non-lactonic (or acidic) SLs, and the lactonic SLs. The hydroxyl fatty acid moiety of the acidic SLs has a free carboxylic acid functional group. On the other hand, the lactonic SL forms a macrocyclic lactone ring with the 4”- hydroxyl group of the sophorose by intramolecular esterification. In some rare cases, 17- hydroxy oleic acid is found at 6’- or 6”- position. This is the most common lipophilic moiety used for the production of sophorolipids by *Candida bombicola* [28]. Stearic, linoleic and palmitic acid are some of the commonly found

fatty acids, all of which are hydroxylated on the ultimate or penultimate carbon that is used as a lipophilic carbon source [40].

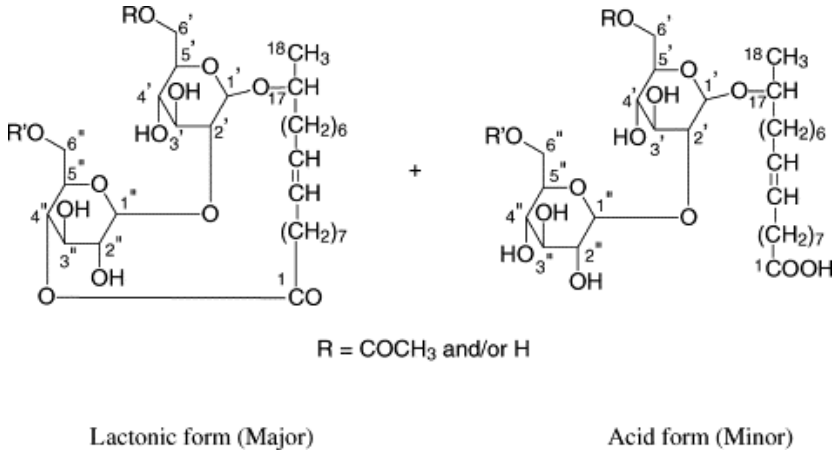

Structure of Sophorolipid (a) Acidic SL (b) Lactonic SL

Image Ref. Zhang et al., 2003 [101]

4. Application of SL

Agriculture:

Sophorolipids have proven to be highly effective in the field of agriculture because of their antimicrobial and anti-fungal properties. They can also act as an adjuvant in the formulation of herbicides with their impressive surfactant property. SL is also effective against plant pathogenic fungi, *Phytophthora* sp. and *Pythium* sp. These fungi cause 'damping-off', a soil-borne root disease, and are capable of spreading rapidly through the soil in the form of zoospores with the aid of water for migration, infecting seeds, leaves, and stems of water culturing plants. Addition of SL has proven to inhibit the mycelial growth and motility of the zoospore while causing lysis of the zoospore. As SL possess low toxicity and are biodegradable in nature, they have a great potential as an environment compatible bio-control agent [16,42]. They are also useful in inhibiting algal bloom that affects the aquatic system [43].

Food:

Addition of surfactants helps to improve the creaminess, appearance, palatability, texture, stability, rheology and overall quality of foods [44] When SL is added to wheat flour or a product constituting wheat flour; it improves the quality of the final product. SL containing wheat flour when used for making bread gives the bread a better volume, improving the appearance and extending its shelf-life [7]. Microbial and chemical contaminations in food can

have a severe impact on public health and the economy. Agricultural workers that are involved in handling the fruits and vegetables during transport or delivery provide opportunities for contamination with microbial hazards such as *Salmonella* spp., verotoxin producing *Escherichia coli* (VTEC) and Norovirus (NoV) [Van Boxstael et al, 2013]. Germicide formulation containing 1% SL is capable of killing 100% of *Escherichia coli*, *Salmonella typhi and Shigella dysenteriae* in 30 seconds [45]. Food contamination may also be caused due to the presence of biofilm. These biofilms are key sources of contamination, leading to food spoilage and disease transmission [7]. Biofilm is a protective matrix made up of extracellular polysaccharide or proteinaceous material that is secreted by bacteria helping them to adhere to the surface [46,47]. Preventing the adherence of pathogenic microorganisms to food surfaces is an important step in providing contamination–free and good quality products to consumers [44]. The biofilm formed by Gram-positive (*Ralstonia eutropha* ATCC 17699) and Gram-negative microorganism (*Bacillus subtilis* BBK006) is effectively disrupted by SL owing to its antimicrobial properties against these organisms [48].

Cosmetics:

SL biosurfactants have gained importance as an active ingredient in the field of cosmetics. SLs are known to be biocompatible as they show low cytotoxicity towards human keratinocytes and fibroblasts [49,50]. Incorporation of SL in creams and lotions promotes the metabolism of fibroblasts and collagen neo-synthesis in the dermis layer of the skin, thereby aiding in skin repair and skin toning [51]. Skin aging is caused due to an increase in the elastase activity from dermal fibroblasts, leading to formations of freckles and wrinkles. SL inhibits the elastase formation by reducing the generation of free radicals that are responsible for skin aging. [52]. SL helps to activate macrophages, fibrinolytic agents, desquamating agents and also acts as a de-pigmenting agent through partial inhibition of melanogenesis that helps to reduce brown spots [53]. The French company Soliance, uses sophorolipid in their cosmetic formulations [28], as the bactericidal and bacteriostatic property of SL is useful in the control of dandruff, acne treatment and in reducing body odor in the form of deodorants [7]. There is a product from Soliance (France, http://www.groupesoliance.com) called Sopholiance S, that uses rapeseed oil SL against body odors and acne

Anti-Microbial Activity:

SLs are anti-microbial in nature. They are capable of destabilizing and altering the permeability of the cellular membrane causing cell rupture which leads to extrusion of the

cell contents [43]. Besides this, SL can also act as anti-algal, antifungal and antiviral agent [42,43,54,55]. Effect of SL on Gram-positive and Gram-negative organisms differs due to the differences in their cell wall structure and in osmotic level [7]. SL produced by *Candida bombicola* using lauryl–myristyl alcohol as its hydrophobic moiety, shows potent activity against Gram-positive and Gram-negative organisms. It shows complete inhibition of Gram-negative bacteria *Escherichia coli* and *Pseudomonas aeruginosa*, which is mainly responsible for causing cross infections in hospitals and clinics. It also exhibits substantial activity against Gram-positive bacteria such as *Staphylococcus aureus* and *Bacillus subtilis*, which are majorly involved in food poisoning. Gram-positive bacteria are killed by cell rupturing (lysis) while shrinking of the cells occurs in the case of Gram-negative bacteria [56,57]. Lactonic sophorolipid inhibited cell growth more effectively than acidic for both *B. subtilis* and *P. acne*.[58]

SL as a cleaning agent:

Sophorolipids are the preferred biosurfactants for cleaning purpose due to its ability as an antimicrobial agent and properties like emulsifier and low-high foaming surfactant. A Japan-based company Saraya has commercialized “Sophoron”, a sophorolipid based low-foam dishwasher detergent. “Sophogreen” is a bio-solubilizer recently designed by Soliance using sophorolipids that serves as a better alternative to petroleum-based solubilizers. Belgian-based Ecover (http://www.ecover.com) and South Korea-based MG Intobio also commercialize products made using Sophorolipids. The skin irritability test (Episkin test) conducted by Ecover on SL based product confirmed that SL does not cause skin irritation. Toxicity and biodegradability test conducted on Ecover product SL18 revealed that SL based product was in orders of magnitude less toxic than non-ionic surfactants, alkyl polyglucosides (APG) and 100% biodegradable after 28 days. Sophorolipids mild nature, low aquatic toxicity and considerable surface activity have resulted in the launching of SL based products by Ecover such as all-purpose cleaner, window cleaner, floor soap, and wax cleaner. [25,59] Germany based Henkel has also been employing sophorolipid for its glass cleaning products such as Sidolin, Tenn, Instanet and Sonasol. A study conducted by Navare et al. (2013) also demonstrated that SL synthesized using jatropha oil, to curtail the production cost by using cheap sources, had potential to be used as a fabric cleaner. [14]

Anti- Cancer:

Sophorolipids induced differentiation of human acute promyelocytic leukemia cell line HL60

at a concentration of 10µg/ml. The protein kinase C activity was observed to be inhibited after 2 days and differentiation into monocytes took place. For two other leukemic cell lines, the human myelogenous leukemia cell line K562 and the human basophilic leukemia cell line KU812, differentiation into megakaryocytes was also induced at a sophorolipid concentration of 15 µg/ml. [21] Joshi-Navare et al have shown anti-cancer activity of SL by inducing cell differentiation in human glioma cell LN-229. [22]. A recent study conducted by Nawale et al., 2017 showed the anti-proliferative activity of purified forms of the novel SL derived from cetyl alcohol (SLCA) and their anti-cancer mechanism in human cervical cancer cells. [60]

Self Assembly:

A recent study conducted by Singh et al. 2013, showed the spherical mesoscale molecular assembly of sophorolipid when irradiated by a pulse laser. These assemblies had fluorescent property and a probable use in bio-imaging and drug delivery. The very first attempt to understand acidic SL's assembly behavior at pH 2.0 to 4.1 resulted in the giant twisted helical ribbons with 5-11µm width and several hundred micrometers [61,62]. The self-assembly of molecules depends on the concentration, wherein a study conducted by [63], showed the correlation of concentration and shape of the micelle. Spherical micelles were formed at <1wt% concentration and the shape elongates to a cylindrical shape with increasing concentration from > 0.5 wt% to 5 wt%. Apart from factors like pH and concentration, the changes in structure at the molecular level can also influence the self-assembling behavior of sophorolipids [64]. This was clearly illustrated by using three different sophorolipids of oleic acid (OASL), stearic acid (SASL) and eladic acid (EASL) by [65]. The OASL formed a ribbon-like structure similar to those reported by Zhou et al., 2004 [62], in the case of SASL the self-assembled structures appeared like several open sheets lying on top of each other and EASL (with a trans double bond) formed twisted ribbon structures, which was attributed to a favorable π overlap, leading to squeeze in the middle of the molecule. The effect of unsaturation was clearly evident from the study conducted by Dhasaiyan et al. (2014) [66]. With the help of experimental and simulation studies, the author reported the presence of a double bond in the hydrophobic core of the SL molecule greatly impacts the morphology of the self-assembled structures. They showed that oleic acid SL with one unsaturated bond forms ribbon-like structures (also reported previously), whereas linolenic acid SL with three double bonds assembles into vesicles. [66]. Supporting this recently Pandey et al. (2016) [67] also performed simulation studies and reported that linolenic acid sophorolipid with three double bonds, assembled into vesicle and aggregates depending upon SL to water ratio.

Theranostic application

Quantum dots (QDs) are well known for their optical and electronic properties applicable in the bio-medical field as labeling and imaging tools but due to their toxicity and biocompatibility issues, they are not widely used. To introduce biocompatibility, without the loss of photoluminescence property Singh et al. 2013 [68] synthesized non-toxic cadmium telluride (CdTe) QDs by using acidic SL as a surface-functionalizing agent. SL-CdTe QDs potential as a diagnostic tool was demonstrated by cellular internalization studies in ThP-1 (human acute monocytic leukemia) cells. The cytotoxicity studies confirmed their biocompatibility and hence applicability. [68]

Wound healing and Biomedical Scaffolds

A recent world patent filed by Prabhune et al in 2017 (PCT/IN2016/050315) disclosed a study where SL in combination with silk sericin works at par with commercialized wound healing creams. Rather they observed a distinct property of no scars on the wound site when applied with SL-sericin based cream. This has again opened a new avenue where SL can be explored further and commercial product can be launched. Another study was conducted by the Dubey et al 2016 where they used SL with silk fibroin for rapid gelation and synthesis of scaffolds that can be used for biomedical application. [69]

5. Sophorolipid (SL) in Nanoparticles Synthesis:

Of late synthesis of nanoparticles mediated via surfactants is an emerging field in material science due to their potential for the stabilization of nanoparticles. Although the chemical and physical processes are currently used, stable and size-controlled synthesis still remains a challenge. Certain other disadvantages are that the synthesis process is highly expensive and lead to harmful waste materials for humans as well as the environment. The size and shape of nanoparticles decide the biological applicability of nanoparticles. Here biosurfactants play a role in stabilizing and in determining the shape of the nanoparticles during synthesis, emerging as a viable alternative. [70] Nanoparticles synthesis processes based on biologically produced surfactants are rapidly gaining interest where nanoparticles are formed in a range of 10-1000nm. [19] Following are few of the examples where sophorolipids are used either as a capping agent or both reducing and capping of nanoparticles.

a. The earliest work on nanoparticles based on sophorolipid system started a decade back, where synthesis of cobalt nanoparticles was attempted. The early strategies for

the synthesis of cobalt nanoparticles usually used oleic acid as a capping agent but with few concerns regarding the stability. Apart from this, oleic acid is also insoluble in water hence methanol/ethanol-water mixture was used during the preparation of cobalt nanoparticles. Reports regarding oleic acid capped silver and nickel nanoparticles explain that polar solvents expose oleic acids –COOH group in the solvent and help in its binding with nanoparticles surface via a double bond. But this also leads to exposed $–CH_3$ group into the solvent causing a weak capping and instability during dispersion of nanoparticles. To overcome this obstacle, Kasture et al., 2007 employed sophorolipid biosurfactant that is actually a microbial modification of oleic acid and is soluble in water due to attachment of polar sophorose head group. The superparamagnetic cobalt nanoparticles obtained by SL capping were stable in powder form and readily dispersible in an aqueous medium without substantial morphological modifications [71]

b. After the study with cobalt nanoparticles, the authors began to explore certain molecules having a dual nature of reducing and capping the nanoparticles in one go. These are preferred as they enable greater control over the reaction and use of external reducing agents can be avoided. This can help in scaling the process. In another study, they showed the reduction of Ag^+ ions to Ag nanoparticles and capping with the SL. In this work, the particle size variation was studied as a function of time and temperature. Two different SLs were used for the synthesis of Ag NPs viz., oleic acid SL (OASL) and linoleic acid SL (LSL). OASL reduced-capped AgNPs had a mean size of 20 nm at 40^{o}C with and at 90^{o}C the particles size reduced to 5.5 nm with the almost spherical shape. In the case of LSL, at 40^{o}C the mean size obtained was 22 nm and at 90^{o}C the similar reduction in size to 11 nm was observed. This can be attributed to lower temperatures as the particle formation becomes slow but as the temperature is increased the synthesis becomes rapid. From this study, it was concluded that the OASL derived AgNPs were better than that of LSL derived with respect to size and morphology. [72]

c. Kumar et al 2010 later took this study forward for the continuous synthesis using a microreactor. A batch process is a good approach for understanding the mechanism of nanoparticles synthesis but up-scaling becomes a limiting factor. Limitations viz., inefficient mixing, non-uniformity of temperature throughout the reactor, non-

idealities in flow rates, usually result in a wider range of particle size distribution. Also, the thorough cleaning of the vessel after every batch is required to avoid contamination. To tackle this, micro-fluidic methods have been applied that have many advantages over batch process like reduced consumption of reagents, safety and stoichiometric yield that satisfy all the large-scale synthesis. But mostly, a high surface to volume ratio in micro-channels leads to better heat and mass transfer which gives better control over the reaction rates. Silver nanoparticles have well established anti-microbial activity and are considered a model system for microreactors. Therefore in this study, a continuous flow synthesis of silver nanoparticles in water medium via the use of sophorolipid as a reducing and capping agent was demonstrated. Any use of an external reducing agent was avoided hence reducing the number of reactants in the reaction. [73]

Based on results obtained from previous batch process studies, stearic acid SL was chosen for the continuous flow experiments. The particle size distributions of AgNPs as shown by DLS were between 5-9nm that were synthesized using stainless tube model.

d. The formation of sophorolipid-capped iron oxide nanoparticles was executed by Baccile et al. The magnetic iron nanoparticles were synthesized from iron (II) chloride and iron (III) chloride in presence of ammonia at room temperature and at 80 °C. Both two-step and one-step procedures were applied which resulted in nanoparticles with maghemite (γ-Fe_2O_3) or two-line ferrihydrite ($Fe_5HO_8 \cdot 4H_2O$) structure respectively. A very broad particle size distribution was obtained for the one-way synthesis pathway at room temperature, while monodispersed nanoparticles were obtained in all other synthesis processes mentioned above. A much higher increase in the average particle size for the nanoparticles synthesized at room temperature indicated that sophorolipids were more loosely bonded to the nanoparticle surface. FTIR analysis revealed that the sophorolipids mainly attach to the nanoparticle surface via the carboxylic acid function. Adsorption studies were performed for the sophorolipid-capped iron oxide nanoparticles with two lectins, namely Concanavalin A and lectin from *Bandeiraea simplicifolia*. No specific interaction occurred with the lectin from *Bandeiraea simplicifolia*, but an affinity for Concanavalin A for these capped NPs was observed. Sophorolipid-capped iron oxide

nanoparticles also proved to be interesting to be used as selective targets for sugar/ protein interactions. [74]

e. After identifying that sophorolipids can be used for nanoparticles synthesis, another set of experiment to study the cytotoxic and genotoxic effect of glycolipid synthesized Au NPs and Ag NPs, hepatic cell line HepG2 was selected attempted and exposed to different concentrations of the metal nanoparticles. Oleic acid SL was used as reducing and capping agent for nanoparticles synthesis. Silver NPs were synthesized by the previously mentioned method from the same group. These prepared OASL molecules, AuNPs and AgNPs were tested at different concentrations with human hepatic cells and were found neither cytotoxic nor genotoxic, up to concentrations of 100 mM. [75]

f. Nanostructures that are functionalized with biomolecules can gain antimicrobial properties. Although there are some reports related to the basic guidelines for functionalization and application of specialized nanomaterials, active research on functionalizing nanomaterials with biomolecules and their specific antimicrobial activity is poor. Scanty reports are available on the application of functionalized nanoparticles against pathogenic microbes. Therefore, in this study, an attempt was made to employ the sophorolipid (produced by yeast *Cryptococcus sp*. VITGBN2) as a bio-stabilizer for the synthesis of ZnO nanoparticles (ZnO). In addition, ZnO NPs biofunctionalized by sophorolipids, have also been tested as antimicrobial agents. The activity of acidic diacetate sophorolipid by *Cryptococcus sp*. VITGBN2 against pathogens like *S. enterica* and *C. albicans* was established. Sophorolipid biofunctionalized ZnO showed higher antimicrobial activity compared to naked ZnO NP and other antimicrobial agents. Enhanced bioactivity of these NPs was attributed to the increased permeability through the microbial cells that lead to the loss of cellular transport through the plasma membrane, resulting in cell death. [76]

g. Surface functionalization of gellan gum reduced gold nanoparticles with SL was proposed by Dhar et al. Taking advantage of SLs anti-cancer activity, these nanoparticles were then conjugated and loaded with doxorubicin drug and tested against human glioma cells LN-229 as well as human glioma stem cells HNGC-2. Cytotoxicity was carried out without any labeling. MTT assay was performed on the

24 h old plate. The incubation time was 4 h after which, formazan crystals were dissolved in DMSO and read at 570 nm. TEM analysis and particle size distribution confirmed SL-GG-AuNPs of, average particle size (~17 nm), slightly increased from that of pristine GG-AuNPs (~13 nm). In the cellular uptake study, Gold nanoparticles were clearly observed inside the cells as red dots and were localized mostly in the cytoplasm and perinuclear space of cells. From this study, it can be concluded that SL enhances the cell cytotoxicity of gellan gum nanoparticles against glioma cell lines. [77]

h. Singh et al. demonstrated the use of SL as a stabilizer for CdTe quantum dots that were synthesized using 3-mercaptopropionic acid (MPA) and amine terminated by a coupling reaction between MPA and ethylenediamine (EDA). For the synthesis, the authors used NaHTe that was prepared by reacting $NaBH_4$ and Te powder. The reaction was considered completed once the black Te powder turned to a clear pink solution. NaHTe is then refluxed under nitrogen for 2 h at 100^{o}C with 36 mM MPA and $CdCl_2$ 15 mM at pH 9. Once cooled the CdTe solution was precipitated by acetone, centrifuged and washed to remove un-reacted salts. The dried powder was then again re-dispersed for conjugation with EDC to achieve amine termination via sulfo-NHS (N-hydroxysulfo-succinimide) and EDC coupling. The amine-terminated CdTe QDs were then mixed with acidic SL (100 mg each) under stirring for 30 min.
The QDs obtained via MPA were of 8 nm observed in TEM and DLS, whereas SL capped CdTe QDs were of 118 nm indicating encapsulation via SL. They were tested for their biocompatibility in both normal and cancer cell lines. It was shown that the SL capped CdTe QDs were biocompatible in normal cell line and effective against cancer cell line with enhanced cellular association and uptake, which was detected by the fluorescence of the QDs. Almost 100% viability in case of normal NIH_3T_3 cell lines and 65% viability in case of cancer MCF-7 cell line was observed, clearly indicating that composites provided a mode to diagnose cancer cells using their fluorescence property as well as cytotoxicity towards them. Thus authors have made a composite particle which has a high potential as a theranostic weapon. [68]

i. Singh et al. have used a pulsed UV laser approach for self-assembly of SL molecules in water and achieved mesoporous structures. The structures thus formed were found to be fluorescent in nature. They have also demonstrated easy loading of magnetic nanoparticles on these mesoporous structures during their synthesis for application in

hyperthermia. The time evolution study of self-assembly was observed via SEM imaging at an interval of 10 mins. Both SEM/TEM analyses showed that the defined particles were formed after 40 min of laser irradiation. These particles fluoresced when excited with 330 nm. This property was attributed to the addition of an extra double bond due to laser irradiation and π–π stacking. Cytotoxicity test was carried out on HeLa cell line by MTT assay which revealed that 50 µg/ml was not detrimental for the cells. The hyperthermia experiment was carried out using a radio frequency source. Magnetite loaded SL mesostructure (5 mg/ml Fe_3O_4 nanoparticle) were used for this experiment. The data was collected at 0 min, 4 min, 10 min and 15 min for both the simple SL solution and the magnetite-loaded SL mesostructures. It was observed that the magnetite loaded SL mesoparticles were effective against hyperthermia. [61]

j. A recent example, where SL has been used for the synthesis of Solid Lipid nanoparticles (SLN) that was used to encapsulate rifampicin and dapsone drugs. In this report, lactonic SL with pluronic co-polymer was used to obtain stable SLNs. These SLNs had high entrapment efficiency and loading capacity. The release study conducted revealed a high release rate. Therefore, new areas in solid lipid nanoparticles have been ventured through this study and there is scope for development. [78]

Based on these examples we have attempted to synthesize few drug delivery systems using sophorolipid as reducing, capping or both for the nanoparticles of gold nanoparticles and calcium carbonate which will be explained in chapter 1 and chapter 4 of this thesis.

6. Curcumin

Ayurveda, an ancient Indian medical system makes use of turmeric paste to treat eye infections, to dress wounds and as an anti-inflammatory agent against insect bites, acne, and various skin diseases. Powdered turmeric taken with boiled milk has been commonly used to cure a cough and related respiratory ailments. It can also act as an anti-dysenteric for children suffering from dysentery [79].

Turmeric Band-Aids are being prepared by the American pharmaceutical company Johnson & Johnson for the Indian market [80,81]. Turmeric acts as a healing agent and cures any lacerations in the birth canal when applied to the perineum [82]. This dietary spice is also used

to treat digestive disorders such as dyspepsia, ulcers, stomach pain due to indigestion, and flatulence

Curcumin is an active ingredient in traditional herbal remedies and also in a vibrant yellow dietary spice called turmeric obtained from the rhizome of *Curcuma longa*. It has been used in the traditional medicines of China and India since a long time with the powder being used in Asian cooking, medicine, cosmetics, and fabric dyeing for more than 2000 years [79,83]. Curcumin is currently being used to add a dash of color in perfumes [84].

Vogel first isolated Curcumin in the year 1842 and it was structurally characterized by Lampe and Milobedeska [79]. Curcumin (curcumin I), demethoxycurcumin (curcumin II) and bisdemethoxycurcumin (curcumin III) are the three major curcuminoids present in the commercial Curcumin. The percentage of each curcuminoid present differs. Approximately 77% is comprised of curcumin I with only 17% of curcumin II; curcumin III being the least at about 3% [85]. Curcumin exists in its keto-enol tautomer form as shown in the figure and exhibits limited solubility in water while showing good solubility in organic solvents such as DMSO and chloroform [86]. This property may be responsible for its low bioavailability. Evidence from numerous literature has revealed that curcumin has low bioavailability, poor absorption, low metabolism, and limited biodistribution. Up to 1 g/kg of the body weight is almost completely eliminated by the human metabolic system [87].

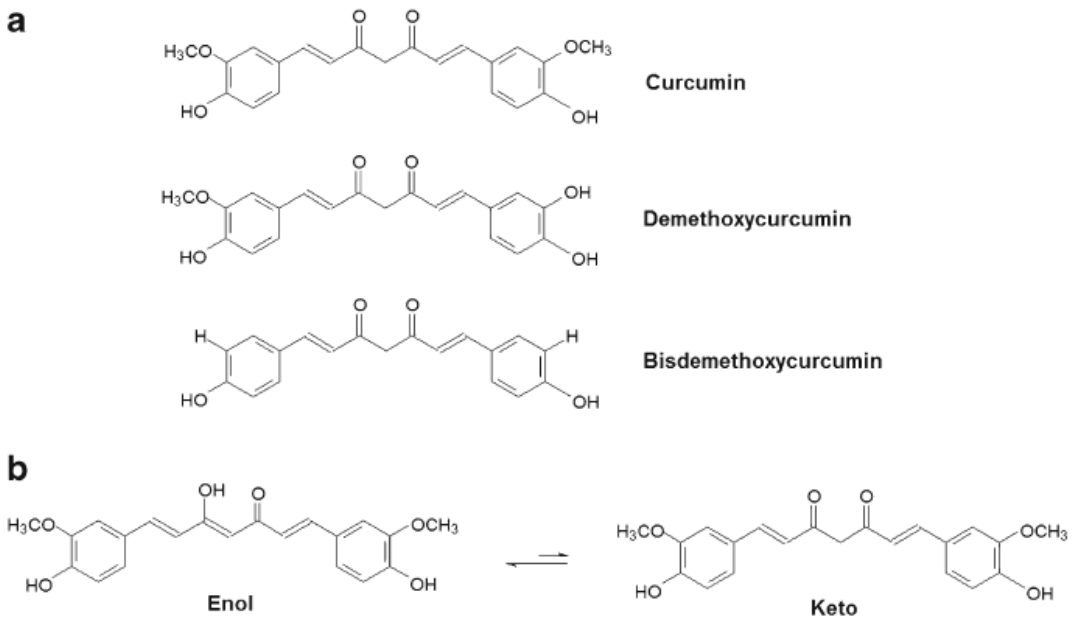

Curcumin I, II, III (curcumin, demethoxycurcumin, and bisdemethyoxy curcumin) and keto-enol tautomers of curcumin. [Image source: Naksuriya et al 2016 [88]]

7. Calcium carbonate

Calcium Carbonate ($CaCO_3$) is a naturally occurring inorganic biomaterial. It is a white, insoluble solid that occurs in nature in form of chalk, limestone, marble, and calcite, and is the main component of shells of marine organisms, snails, pearls, and eggshells [89]. In the chemical industry, it acts as raw material owing to its varied applications such as to produce cement, mortars, plasters, refractories, and glass as building materials. It also is used to produce quicklime, hydrated lime and a number of calcium compounds. The latter consists of finer particles of greater purity and more uniform in size. Diverse calcium carbonate forms are currently being used in several commercial products, like textiles, papers, paints, plastics, adhesives, sealants, and cosmetics [90].

Nano calcium carbonate synthesis has received significant importance due to their industrial applications in the quantum dots, catalysis, flame retardant, clean-up of toxic contamination from chemical warfare, and bone replacement [91]. The applications of nanoparticles of $CaCO_3$ strictly depend on parameters such as morphology, size, specific surface area, oil adsorption capacity, and chemical purity. Therefore, the control of particle morphology via its shape and size is crucial from the perspective of the technical applications [92].

$CaCO_3$ nanoparticles show unique advantages due to their ideal biocompatibility and are ideal as the potential drug delivery systems offering a range of drug loading options [93]

8. Sericin

Silk is a continuous protein fiber produced by the silkworm and consists of two main groups of proteins, sericin, and fibroin. Fibroin constitutes the fibrous component and has great tensile strength and property to withstand wear and tear [94]. Fibroin is being used in textile manufacturing and for several biomaterial applications. Whereas sericin is a natural macromolecular protein, that serves as an adhesive binding the fibroin threads.

Sericin is a glue-like protein that binds the silk fibers in a cocoon of *Bombyx mori*. It is highly hydrophilic in nature due to the higher content of hydrophilic amino acids like serine (35%) and threonine (10%). This also means they are rich in hydroxyl groups due to serine and this is expected to have a major role in its structure conformation. Sericin is secreted by the middle silk gland of *B. mori* larvae as a watery solution during spinning. Afterward, it solidifies to give toughness to cocoon. [95]

Sericin is considered as waste material in the textile industry, with nearly 250 to 300 tons of sericin per year being discarded [96]. Recently sericin has been found to activate the proliferation of several cell-lines and has also shown various biological activities [97] like Anti-oxidant [98], Anti-tyrosinase [96], Anti-bacterial [99] and Anti-aging [100]. Nanoparticles capped with sericin can have these advantageous properties as well and this needs to be further studied.

9. The scope of work:

As we have understood the difficulty faced by the pharmaceutical industry in developing new drug entities and some of the solution suggested by researchers around the globe are of interest. We identified an area where a biosurfactant that can be produced on a commercial scale can be used for the solubility of class II to class IV drugs using curcumin as our model. Since ancient times turmeric is boasted of its medical applicability but its full potential is yet to be utilized. Hence we have used curcumin and sophorolipid as our model for drug solubility and in turn tried to bio-transform curcumin into a more water-soluble form.

Apart from solubility, drug delivery is also a major challenge. Therefore biocompatible and biodegradable drug delivery systems, in the form of calcium carbonate have been aimed to study in this thesis.

We also aim to utilize a waste protein viz. sericin for the synthesis of gold nanoparticles as part of my thesis as a development of newer and greener drug delivery system.

10. Outline of the Thesis:

Chapter I:

The first chapter gives a general description of the problem associated with drug solubility and the current method used to solve these shortcomings. It also introduces readers to components used in the following chapters like sophorolipids, curcumin, calcium carbonate, and sericin. The scope of the work and certain objectives are also highlighted in the introduction section.

Chapter II:

Bioavailability studies of curcumin-sophorolipid nano-conjugates in the aqueous phase: role in the synthesis of uniform gold nanoparticles

The major limiting factors for curcumin to be accepted as a modern drug, despite its

widespread applications, are its low aqueous solubility, low retention time and poor bioavailability. When subjected to a mild physical stress, curcumin is observed to internalize within the micellar hydrophobic core of oleic acid sophorolipid resulting in the formation of curcumin–sophorolipid nanoconjugates (CurSL). These bio-composites show enhanced retention time and increased bioavailability of curcumin in rat models. In the presence of gold salts, CurSL act as potent reducing and capping agents, resulting in the synthesis of monodispersed, spherical gold nanoparticles (CurSL–GNPs) of 8–10 nm in size. Physicochemical, morphological and optical characteristics of both the nanoparticles are discussed based on spectroscopic absorption, photoluminescence (PL), dynamic light scattering (DLS), zeta potential, SEM and TEM measurements. FTIR spectroscopy signatures of these nanoparticles confirm the retention of functional groups in the end products. A retention time of 2 hours in blood plasma and an increase in curcumin recovery by about 150 times that previously reported were observed in the pharmacokinetic (pKa) studies performed on Wistar rats. The bio-distribution of gold nanoparticles in rats was studied using EDX, which revealed their presence in different vital organs. The absence of unusual legions or necrosis in histopathological analysis of vital organs in all the rat models suggests the use of curcumin–sophorolipid nano-conjugates enhances curcumin bioavailability and the Cur–SL based nano-gold formulation is a good drug delivery carrier.

Chapter III:

Derivatization of curcumin via biotransformation and exploring its applied aspects

Low solubility in aqueous solution and poor bioavailability of Curcumin has lead to the synthesis of various formulations by scientists worldwide to enhance the physiochemical characteristics of this bright yellow molecule. In this study, a novel compound is being proposed Curcumin-sophorolipid (CSL) synthesized by *Candida bombicola* cells that have helped to improve the water solubility, stability, and bioavailability of curcumin. The objective of this study was to synthesize CSL compound and carry out its extraction. Further partial purification and characterization of CSL were done using UV-Vis spectrophotometry, Thin Layer Chromatography and High-Performance Liquid Chromatography. The further understanding about the compound structure and its interaction were made by carrying out HRMS, FTIR, NMR and Photoluminescence studies. The application of synthesized compound, CSL in various areas, such as its property of being anti-tyrosinase, anti-oxidant, anti-biofilm and fluorescence were studied. CSL shows good anti-biofilm activity against *P.*

aeruginosa. It shows scavenging activity and anti-tyrosinase activity. Under UV light it emits green fluorescence and shows strong emission in 700nm range when excited at 350nm. To study its toxicity, MTT assay was carried out on L6 cell line and anti-cancer activity against MCF-7 and HeLa were also studied.

Chapter IV:

Synthesis of biocompatible Calcium carbonate microparticles as a drug delivery system using sophorolipid as a capping agent and increasing the porosity of synthesized particles

A simple yet effective method is developed for the synthesis of calcium carbonate micron-sized particles. The 0.1M aqueous solution of calcium chloride is drop-wise added in a 0.1M solution of sodium bicarbonate under probe sonication for 30 minutes to obtain spindle-shaped 2-3 micron particles. To reduce the particles size, we added a biologically synthesized glycolipid (sophorolipid) during the synthesis by two different approaches. In one method sophorolipid is solubilized in aqueous calcium chloride solution and probe sonicated for 10 minutes. To this mixture, drop-wise sodium bicarbonate solution was added and further sonicated for 20 minutes. This approach leads us to produce spherical and porous calcium carbonate nanoparticles in the size range of 100-400 nm. While in the second method, sophorolipid was solubilized in sodium bicarbonate solution and sonicated for 10 minutes. Here, calcium chloride solution is added gradually and sonicated for 20 minutes. The particles observed here were spindle shaped with size 1-3 μm. Scanning electron microscopy and EDS have confirmed the shape, size, and composition of these particles. Also when using these two approaches if we change the method to magnetic stirring, porous and spherical microparticles of CaCO3 obtained. The sizes of these were also in the range of 1-2μm. The nucleation of the particles was studied via time-dependent SEM analysis. These particles can be an effective host for the fabrication of biocompatible composite materials as they are natural biomineral available in nature and can be used for oral drug delivery.

Chapter V:

Sericin based synthesis of Tunable, Monodispersed and Stable Gold nanoparticles: Role of Temperature and pH

Sericin a protein from silk cocoon of *Bombyx mori* has got many properties like anti-bacterial, moisture retaining, anti-oxidant etc, but it is not reported for the synthesis of gold

nanoparticles. Therefore, in this chapter, we study the synthesis of gold nanoparticles in different pH and temperature mediated by sericin. Sericin is extracted from the silk cocoons and lyophilized to obtain the powder. Different buffers from pH 5.0 to pH 9.0 were tested at varying temperatures from modest 30^{o}C to higher 80^{o}C. UV-vis spectroscopy confirmed the characteristic surface plasmon bands of gold nanoparticles, while dynamic light scattering and Transmission electron microscopy confirmed the size of particles between 10-50nm. The near-spherical nanoparticles obtained can be applied as a drug delivery vehicle. These particles are highly stable confirmed by zeta potential studies. The study confirmed the role of temperature and pH for the size modulation of sericin nanoparticles.

Chapter VI:

Conclusion

In this thesis, we have covered different topics from hydrophobic drug solubility to drug-biosurfactant bio-transformed product to various nano-micro carriers for drug delivery. The model drug curcumin was solubilized in a crude sophorolipid solution and its bioavailability in rats was tested and it was retained in the rat body up to 2 h confirmed via HR-MS study of blood plasma. Based on the Cur-SL solution, gold nanoparticles were synthesized and their bio-distribution in the rat was analyzed. Curcumin was later used as a hydrophobic source for derivatization via biotransformation using yeast *C. bombicola* to obtain solubilized glycol form of curcumin. This compound was found to have many applications at minimum concentration than its parent molecule. Oleic acid sophorolipid was used to cap calcium carbonate microparticles that can be used as a biocompatible drug delivery vehicle. Another biomaterial, sericin was explored for the synthesis of gold nanoparticles for drug delivery purpose

References

1. Chaudhary A, Nagaich U, Gulati N, Sharma VK, Khosa RL. Enhancement of solubilization and bioavailability of poorly soluble drugs by physical and chemical modifications: A recent review. *J Adv Pharm Educ Res*. 2012;2(1):32-67. doi:10.1016/S0040-6031(02)00451-3.
2. Kalepu S, Manthina M, Padavala V. Oral lipid-based drug delivery systems – an overview. *Acta Pharm Sin B*. 2013;3(6):361-372. doi:10.1016/j.apsb.2013.10.001.
3. Kalepu S, Nekkanti V. Insoluble drug delivery strategies: Review of recent advances and business prospects. *Acta Pharm Sin B*. 2015;5(5):442-453. doi:10.1016/j.apsb.2015.07.003.
4. Junyaprasert VB, Morakul B. Nanocrystals for enhancement of oral bioavailability of poorly water-soluble drugs. *Asian J Pharm Sci*. 2015;10(1):13-23. doi:10.1016/j.ajps.2014.08.005.
5. Vandana KR, Prasanna Raju Y, Harini Chowdary V, Sushma M, Vijay Kumar N. An overview on in situ micronization technique - An emerging novel concept in advanced drug delivery. *Saudi Pharm J*. 2014;22(4):283-289. doi:10.1016/j.jsps.2013.05.004.
6. Barkat Ali Khan,. Basics of pharmaceutical emulsions: A review. *African J Pharm Pharmacol*. 2011;5(25):2715-2725. doi:10.5897/AJPP11.698.
7. Oliveira MR De, Magri A, Baldo C, Camilios-neto D. Review : Sophorolipids A Promising Biosurfactant and it ' s Applications. 2015;6:161-174.
8. Vijayakuma S, Saravanan V. Biosurfactants-Types, Sources and Applications. *Res J Microbiol*. 2015;10(5):181-192. doi:10.3923/jm.2015.181.192.
9. Desai JD, Banat IM. Microbial production of surfactants and their commercial potential. *Microbiol Mol Biol Rev*. 1997;61(1):47-64. doi:10.1016/S0140-6701(97)84559-6.
10. Marchant R, Banat IM. Biosurfactants: A sustainable replacement for chemical surfactants? *Biotechnol Lett*. 2012;34(9):1597-1605. doi:10.1007/s10529-012-0956-x.
11. Banat IM, Franzetti A, Gandolfi I, et al. Microbial biosurfactants production, applications and future potential. *Appl Microbiol Biotechnol*. 2010;87(2):427-444. doi:10.1007/s00253-010-2589-0.
12. Cowan-Ellsberry C, Belanger S, Dorn P, et al. Environmental safety of the use of major surfactant classes in North America. *Crit Rev Environ Sci Technol*. 2014;44(17):1893-1993. doi:10.1080/10739149.2013.803777.
13. Yuan CL, Xu ZZ, Fan MX, Liu HY, Xie YH, Zhu T. Study on characteristics and harm

of surfactants. *J Chem Pharm Res*. 2014;6(7):2233-2237. doi:10.1023/A:1011908323811.

14. Joshi-Navare K, Khanvilkar P, Prabhune A. Jatropha oil derived sophorolipids: production and characterization as laundry detergent additive. *Biochem Res Int*. 2013;2013:169797. doi:10.1155/2013/169797.
15. Zion. Microbial Biosurfactants Market (Rhamnolipids, Sophorolipids, Mannosylerythritol Lipids (MEL) and Other) for Household Detergents, Industrial & Institutional Cleaners, Personal Care, Oilfield Chemicals, Agricultural Chemicals, Food Processing, Textile and. 2014;2020:2018-2021. http://www.reportlinker.com/.
16. Kim K, Yoo D, Kim Y, Lee B, Shin D, Kim EK. Characteristics of sophorolipid as an antimicrobial agent. *J Microbiol Biotechnol*. 2002;12(2):235-241.
17. Solaiman DKY, Ashby RD, Foglia TA, Nuñez A, Marmer WN. Sophorolipids - Emerging microbial biosurfactants. *Inf - Int News Fats, Oils Relat Mater*. 2004;15(4).
18. Gharaei-Fathabad E. Biosurfactants in pharmaceutical industry: A mini-review. *Am J Drug Discov Dev*. 2011;1(1):58-69. doi:10.3923/ajdd.2011.58.69.
19. Rodrigues LR. Microbial surfactants: Fundamentals and applicability in the formulation of nano-sized drug delivery vectors. *J Colloid Interface Sci*. 2015;449:304-316. doi:10.1016/j.jcis.2015.01.022.
20. Dolman BM, Kaisermann C, Martin PJ, Winterburn JB. Integrated sophorolipid production and gravity separation. *Process Biochem*. 2017;54:162-171. doi:10.1016/j.procbio.2016.12.021.
21. Delbeke EIP, Movsisyan M, Van Geem KM, Stevens C V. Chemical and enzymatic modification of sophorolipids. *Green Chem*. 2016;18(1):76-104. doi:10.1039/C5GC02187A.
22. Darne P, Mehta M, Dubey P, Prabhune A. Bauhinia Seed Oil, a Novel Substrate for Sophorolipid Production. *World J Pharm Pharm Sci*. 2014;3(11).
23. Bogaert INA Van, Zhang J, Soetaert W. Microbial synthesis of sophorolipids. *Process Biochem*. 2011;46(4):821-833. doi:10.1016/j.procbio.2011.01.010.
24. Fleurackers SJJ. On the use of waste frying oil in the synthesis of sophorolipids. *Eur J Lipid Sci Technol*. 2006;108(1):5-12. doi:10.1002/ejlt.200500237.
25. Fleurackers SJJ, Van Bogaert INA, Develter D. On the production and identification of medium-chained sophorolipids. *Eur J Lipid Sci Technol*. 2010;112(6):655-662. doi:10.1002/ejlt.200900158.
26. Davila A-M, Marchal R, Vandecasteele J-P. Sophorose lipid fermentation with

differentiated substrate supply for growth and production phases. *Appl Microbiol Biotechnol*. 1997;47(5):496-501. doi:10.1007/s002530050962.

27. Albrecht A, Rau U, Wagner F. Initial steps of sophoroselipid biosynthesis by Candida bombicola ATCC 22214 grown on glucose. *Appl Microbiol Biotechnol*. 1996;46(1):67-73. doi:10.1007/s002530050784.
28. Van Bogaert IN a, Saerens K, De Muynck C, Develter D, Soetaert W, Vandamme EJ. Microbial production and application of sophorolipids. *Appl Microbiol Biotechnol*. 2007;76(1):23-34. doi:10.1007/s00253-007-0988-7.
29. P. A. J. Gorin, J. F. T. Spencer APT. Hydroxy fatty acid glycosides of sophorose from Torulopsis magnoliae. *Can J Chem*. 1961;39(6199):846-855. doi:10.1139/v61-104.
30. A. P. Tulloch and J. F. T. Spencer. A new hydroxy fatty acid sophoroside from Candida bogoriensis'. *Can J Chem*. 1968;46(21):3291-3300. doi:10.1139/v68-545.
31. P. A. J. Gorin, J. F. T. Spencer APT. Torulopsis bombicola sp. n. *Antonie Van Leeuwenhoek*. 1970;36(11234):129-133. doi:https://doi.org/10.1007/BF02069014.
32. Chandran P, Das N. Characterization Of Sophorolipid Biosurfactant. 2011;2(1):63-71.
33. Chandran P, Das N. Biosurfactant production and diesel oil degradation by yeast species Trichosporon asahii isolated from petroleum hydrocarbon contaminated soil. *Int J Eng Sci Technol*. 2010;2(12):6942-6953. http://www.ijest.info/docs/IJEST10-02-12-045.pdf. Accessed September 28, 2014.
34. Kitamoto D, Morita T, Fukuoka T, Konishi M, Imura T. Self-assembling properties of glycolipid biosurfactants and their potential applications. *Curr Opin Colloid Interface Sci*. 2009;14(5):315-328. doi:10.1016/j.cocis.2009.05.009.
35. Price NPJ, Ray KJ, Vermillion KE, Dunlap C a, Kurtzman CP. Structural characterization of novel sophorolipid biosurfactants from a newly identified species of Candida yeast. *Carbohydr Res*. 2012;348:33-41. doi:10.1016/j.carres.2011.07.016.
36. Kurtzman CP, Price NPJ, Ray KJ, Kuo T-M. Production of sophorolipid biosurfactants by multiple species of the Starmerella (Candida) bombicola yeast clade. *FEMS Microbiol Lett*. 2010;311(2):140-146. doi:10.1111/j.1574-6968.2010.02082.x.
37. Chen J, Song X, Zhang H, Qu Y. Production, structure elucidation and anticancer properties of sophorolipid from Wickerhamiella domercqiae. *Enzyme Microb Technol*. 2006;39(3):501-506. doi:10.1016/j.enzmictec.2005.12.022.
38. Bourdichon F, Casaregola S, Farrokh C, et al. Food fermentations: Microorganisms with technological beneficial use. *Int J Food Microbiol*. 2012;154(3):87-97. doi:10.1016/j.ijfoodmicro.2011.12.030.

39. Claus S, Van Bogaert INA. Sophorolipid production by yeasts: a critical review of the literature and suggestions for future research. *Appl Microbiol Biotechnol*. 2017;101(21):7811-7821. doi:10.1007/s00253-017-8519-7.
40. Hans-Joachim Asmer , Siegmund Langa FW and VW. Microbial Production, Structure Elucidation and Bioconversion of Sophorose Lipids. *jaocs*. 1988;65(9):1460-1466. doi:https://doi.org/10.1007/BF02898308.
41. Dubey P, Sevaraj K, Prabhune A. Sophorolipids: in self assembly and nanomaterial synthesis. *WJPPS.*, 2013:1107-1133. http://www.wjpps.com/admin/assets/article_issue/137517738329 WJPPS 540.pdf. Accessed September 28, 2014.
42. Yoo DS, Lee BS, Kim EK. Characteristics of microbial biosurfactant as an antifungal agent against plant pathogenic fungus. *J Microbiol Biotechnol*. 2005;15(6):1164-1169.
43. Baek, Seung-Hak, Xiao-Xia Sun, Young-Ju Lee, Song-Young Wang, Kyung-Nam Han, Joong-Ki Choi J-HN and E-KK. Mitigation of Harmful Algal Bloom by Sophorolipid. *J Microbial Biotechnol*. 2003;13(5):651-659.
44. Kralova I, Sjöblom J. Surfactants used in food industry: A review. *J Dispers Sci Technol*. 2009;30(9):1363-1383. doi:10.1080/01932690902735561.
45. Pierce et al. United States Patent US 6,262,038 B1. 2001;2(12). doi:10.1038/incomms1464.
46. Mukherji R, Prabhune A. Novel glycolipids synthesized using plant essential oils and their application in quorum sensing inhibition and as antibiofilm agents. *ScientificWorldJournal*. 2014;2014:890709. doi:10.1155/2014/890709.
47. Patil A, Joshi-Navre K, Mukherji R, Prabhune A. Biosynthesis of Glycomonoterpenes to Attenuate Quorum Sensing Associated Virulence in Bacteria. *Appl Biochem Biotechnol*. 2017;181(4):1533-1548. doi:10.1007/s12010-016-2300-8.
48. Banat IM, De Rienzo MAD, Quinn GA. Microbial biofilms: biosurfactants as antibiofilm agents. *Appl Microbiol Biotechnol*. 2014;98(24):9915-9929. doi:10.1007/s00253-014-6169-6.
49. Otto RT, Daniel HJ, Pekin G, et al. Production of sophorolipids from whey: II. Product composition, surface active properties, cytotoxicity and stability against hydrolases by enzymatic treatment. *Appl Microbiol Biotechnol*. 1999;52(4):495-501. doi:10.1007/s002530051551.
50. Hirata Y, Ryu M, Oda Y, et al. Novel characteristics of sophorolipids, yeast glycolipid biosurfactants, as biodegradable low-foaming surfactants. *J Biosci Bioeng*.

2009;108(2):142-146. doi:10.1016/j.jbiosc.2009.03.012.

51. Borzeix Frédérique. United States Patent (US006057302A). 2000.
52. Hillion et al. United States Patent (US005756471A). 1998.
53. Martine Maingault. WO1997001343A2.
54. Shah V, Jurjevic M, Badia D. Utilization of restaurant waste oil as a precursor for sophorolipid production. *Biotechnol Prog*. 2007;23(2):512-515. doi:10.1021/bp0602909.
55. Shah V, Doncel GF, Seyoum T, et al. Sophorolipids , Microbial Glycolipids with Anti-Human Immunodeficiency Virus and Sperm-Immobilizing Activities Sophorolipids , Microbial Glycolipids with Anti-Human Immunodeficiency Virus and Sperm-Immobilizing Activities. 2005;49(10):4093-4100. doi:10.1128/AAC.49.10.4093.
56. Dengle-Pulate V, Chandorkar P, Bhagwat S, Prabhune AA. Antimicrobial and SEM Studies of Sophorolipids Synthesized Using Lauryl Alcohol. *J Surfactants Deterg*. 2013;17(3):543-552. doi:10.1007/s11743-013-1495-8.
57. Dengle-Pulate V, Joshi J, Bhagwat S, Prabhune A. Application Of Sophorolipids Synthesized Using Lauryl Alcohol As A Germicide And Fruit-Vegetable Wash. 2014;3(7):1630-1643. http://www.wjpps.com/download/article/1404219095.pdf. Accessed September 28, 2014.
58. Lang S, Katsiwela E, Wagner F. Antimicrobial effects of biosurfactants. *Fat Sci Technol*. 1989;91(9):363-366. doi:10.1002/lipi.19890910908.
59. Develter DWG, Lauryssen LML. Properties and industrial applications of sophorolipids. *Eur J Lipid Sci Technol*. 2010;112(6):628-638. doi:10.1002/ejlt.200900153.
60. Nawale L, Dubey P, Chaudhari B, Sarkar D. Anti-proliferative effect of novel primary cetyl alcohol derived sophorolipids against human cervical cancer cells HeLa. 2017:1-14.
61. Singh PK, Mukherji R, Joshi-Navare K, et al. Fluorescent sophorolipid molecular assembly and its magnetic nanoparticle loading: a pulsed laser process. *Green Chem*. 2013;15(4):943. doi:10.1039/c3gc40108a.
62. Zhou S, Xu C, Wang J, et al. Supramolecular Assemblies of a Naturally Derived Sophorolipid. 2004;(11):7926-7932.
63. Baccile N, Babonneau F, Jestin J, Pehau-arnaudet G, Bogaert I Van. Unusual, pH-Induced, Self-Assembly Of Sophorolipid Biosurfactants. 2012;(6):4763-4776.
64. Baccile N, Selmane M, Le Griel P, et al. PH-Driven Self-Assembly of Acidic

Microbial Glycolipids. *Langmuir*. 2016;32(25):6343-6359. doi:10.1021/acs.langmuir.6b00488.

65. Dhasaiyan P, Banerjee A, Visaveliya N, Prasad BL V. Influence of the Sophorolipid Molecular Geometry on their Self-Assembled Structures. 2013:369-372. doi:10.1002/asia.201200935.
66. Dhasaiyan P, Pandey PR, Visaveliya N, Roy S, Prasad BLV. Vesicle structures from bolaamphiphilic biosurfactants: Experimental and molecular dynamics simulation studies on the effect of unsaturation on sophorolipid self-assemblies. *Chem - A Eur J*. 2014;20(21):6246-6250. doi:10.1002/chem.201304719.
67. Pandey PR, Dhasaiyan P, Prasad BLV, Roy S. Structural insight into self assembly of sophorolipids: A molecular dynamics simulation study. *Zeitschrift fur Phys Chemie*. 2016;230(5-7):819-836. doi:10.1515/zpch-2015-0719.
68. Singh P, Joshi K, Guin D, Prabhune AA. Chemically conjugated sophorolipids on CdTe QDs: A biocompatible photoluminescence nanocomposite for theranostic applications. *RSC Adv*. 2013;3(44):22319-22325. doi:10.1039/c3ra44535f.
69. Advances RSC, Csir PD, Csir LN, Sarkar D. Sophorolipid assisted tunable and rapid gelation of silk fibroin to form porous biomedical scaffolds RSC Advances. 2015;(May 2016). doi:10.1039/C5RA04317D.
70. Kiran GS, Selvin J, Manilal A, Sujith S. Biosurfactants as green stabilizers for the biological synthesis of nanoparticles. *Crit Rev Biotechnol*. 2011;31(December 2009):354-364. doi:10.3109/07388551.2010.539971.
71. Kasture M, Singh S, Patel P, et al. Multiutility Sophorolipids as Nanoparticle Capping Agents: Synthesis of Stable and Water Dispersible Co Nanoparticles. *Langmuir*. 2007;23(23):11409-11412. doi:10.1021/la702931j.
72. Kasture MB, Patel P, Prabhune AA, Ramana C V, Kulkarni AA, Prasad BL V. Synthesis of silver nanoparticles by sophorolipids : Effect of temperature and sophorolipid structure on the size of particles †. 2008;120(6):515-520.
73. Kumar DVR, Kasture M, Prabhune AA, Ramana C V., Prasad BL V., Kulkarni AA. Continuous flow synthesis of functionalized silver nanoparticles using bifunctional biosurfactants. *Green Chem*. 2010;12(4):609. doi:10.1039/b919550e.
74. Baccile N, Noiville R, Stievanod L, Bogaert I Van. Sophorolipids-functionalized iron oxide nanoparticles †. *PhysChemChemPhys*. 2013;15:1606-1620. doi:10.1039/c2cp41977g.
75. Singh S, D'Britto V, Prabhune AA, Ramana C V., Dhawan A, Prasad BL V. Cytotoxic

and genotoxic assessment of glycolipid-reduced and -capped gold and silver nanoparticles. *New J Chem*. 2010;34(2):294. doi:10.1039/b9nj00277d.

76. Basak G, Das D, Das N. Dual role of acidic diacetate sophorolipid as biostabilizer for ZnO nanoparticle synthesis and biofunctionalizing agent against Salmonella enterica and Candida albicans. *J Microbiol Biotechnol*. 2014;24(1):87-96. doi:10.4014/jmb.1307.07081.
77. Dhar S, Reddy EM, Prabhune A, Pokharkar V, Shiras A, Prasad BL V. Cytotoxicity of sophorolipid-gellan gum-gold nanoparticle conjugates and their doxorubicin loaded derivatives towards human glioma and human glioma stem cell lines. *Nanoscale*. 2011;3(2):575-580. doi:10.1039/C0NR00598C.
78. Kanwar R, Gradzielski M, Mehta SK. *Biomimetic Solid Lipid Nanoparticles of Sophorolipids Designed for Antileprosy Drugs*. Vol 122.; 2018. doi:10.1021/acs.jpcb.8b03081.
79. Hatcher H, Planalp R, Cho J, Torti FM, Torti S V. Curcumin: From ancient medicine to current clinical trials. *Cell Mol Life Sci*. 2008;65(11):1631-1652. doi:10.1007/s00018-008-7452-4.
80. MacGregor HE. Out of the spice box , into the lab.2006:1-3.
81. Nair KPP. Neutraceutical Properties of Turmeric. *Agron Econ Turmeric Ginger*. 2013:179-204. doi:10.1016/B978-0-12-394801-4.00012-0.
82. Pandeya NK. Old Wives ' Tales : Modern Miracles — Turmeric as Traditional Medicine in India. *Trees Life J*. 2005;1:3.
83. Aggarwal BB, Bhatt ID, Ichikawa H. Curcumin-Biological and Medicinal Properties. *Tumeric: The Genus Curcuma*. 2006:297-368.
84. Tilak JC, Banerjee M, Mohan H, Devasagayam TPA. Antioxidant availability of turmeric in relation to its medicinal and culinary uses. *Phyther Res*. 2004;18(10):798-804. doi:10.1002/ptr.1553.
85. Verma SP, Goldin BR, Lin PS. The inhibition of the estrogenic effects of pesticides and environmental chemicals by curcumin and isoflavonoids. *Environ Health Perspect*. 1998;106(12):807-812.
86. Payton F, Sandusky P, Alworth WL. NMR study of the solution structure of curcumin. *J Nat Prod*. 2007;70(2):143-146. doi:10.1021/np060263s.
87. Singh PK, Wani K, Kaul-Ghanekar R, Prabhune A, Ogale S. From micron to nano-curcumin by sophorolipid co-processing: highly enhanced bioavailability, fluorescence, and anti-cancer efficacy. *RSC Adv*. 2014;4(104):60334-60341.

doi:10.1039/C4RA07300B.

88. Naksuriya O, van Steenbergen MJ, Torano JS, Okonogi S, Hennink WE. A Kinetic Degradation Study of Curcumin in Its Free Form and Loaded in Polymeric Micelles. *AAPS J*. 2016;18(3):777-787. doi:10.1208/s12248-015-9863-0.
89. Hariharan M, Varghese N, Cherian AB, et al. Synthesis and Characterisation of $CaCO_3$ (Calcite) Nano Particles from Cockle Shells Using Chitosan as Precursor. *Int J Sci Res Publ*. 2014;4(10):1-5. www.ijsrp.org.
90. Devamani RHP, Kavitha M, Bala BL. Synthesis and characterization of Calcium Carbonate nanoparticles. *J Environ Sci Comput Sci Eng Technol*. 2015;4(1):112-120.
91. Islam A, Teo SH, Rahman MA, Taufiq-Yap YH. Seeded growth route to noble calcium carbonate nanocrystal. *PLoS One*. 2015;10(12):1-13. doi:10.1371/journal.pone.0144805.
92. Atchudan R, Na H Bin, Cheong IW, Joo J. Facile Synthesis of Monodispersed Cubic and Spherical Calcite Nanoparticles in the Presence of Cetyltrimethylammonium Bromide. *J Nanosci Nanotechnol*. 2015;15(4):2702-2714. doi:10.1166/jnn.2015.9154.
93. Dizaj SM, Barzegar-Jalali M, Hossein Zarrintan M, Adibkia K, Lotfipour F. Calcium carbonate nanoparticles; Potential in bone and tooth disorders. *Pharm Sci*. 2015;20(4):175-182. doi:10.5681/PS.2015.008.
94. Kunz RI, Brancalhï¿½o RMC, Ribeiro LDFC, Natali MRM. Silkworm Sericin: Properties and Biomedical Applications. *Biomed Res Int*. 2016;2016. doi:10.1155/2016/8175701.
95. Teramoto H, Kakazu A, Yamauchi K, Asakura T. Role of Hydroxyl Side Chains in Bombyx mori Silk Sericin in Stabilizing Its Solid Structure. *Macromolecules*. 2007;40(5):1562-1569. doi:10.1021/ma062604e.
96. Aramwit P, Damrongsakkul S, Kanokpanont S, Srichana T. Properties and antityrosinase activity of sericin from various extraction methods. *Biotechnol Appl Biochem*. 2010;55(2):91-98. doi:10.1042/BA20090186.
97. Mondal, M KT and SNK. The silk proteins, sericin and fibroin in silkworm, Bombyx mori Linn., - a review. *Casp J Env Sci*. 2007;5(2):63-76. http://www.sid.ir/en/journal/ViewPaper.aspx?FID=120920070208.
98. Takechi T, Wada R, Fukuda T, Harada K, Takamura H. Antioxidant activities of two sericin proteins extracted from cocoon of silkworm (Bombyx mori) measured by DPPH, chemiluminescence, ORAC and ESR methods. *Biomed Reports*. 2014;2(3):364-369. doi:10.3892/br.2014.244.

99. Rajendran R, Balakumar C, Sivakumar R, Amruta T, Devaki N. Extraction and application of natural silk protein sericin from Bombyx mori as antimicrobial finish for cotton fabrics. *J Text Inst*. 2012;103(4):458-462. doi:10.1080/00405000.2011.586151.

100. Kitisin T, Maneekan P, Luplertlop N. In-vitro Characterization of Silk Sericin as an Anti-aging Agent. *J Agric Sci*. 2013;5(3):54-62. doi:10.5539/jas.v5n3p54.

101. Zhang L, Somasundaran P, Singh S, Felse A, Gross R. Synthesis and interfacial properties of sophorolipid derivatives. *Colloids and Surfaces A: Physicochem. Eng. Aspects* 240. 2004;75–82. doi:10.1016/j.colsurfa.2004.02.016.

Chapter 2

Bioavailability studies of curcumin-sophorolipid nano-conjugates: Their role in synthesis of uniform gold nanoparticles

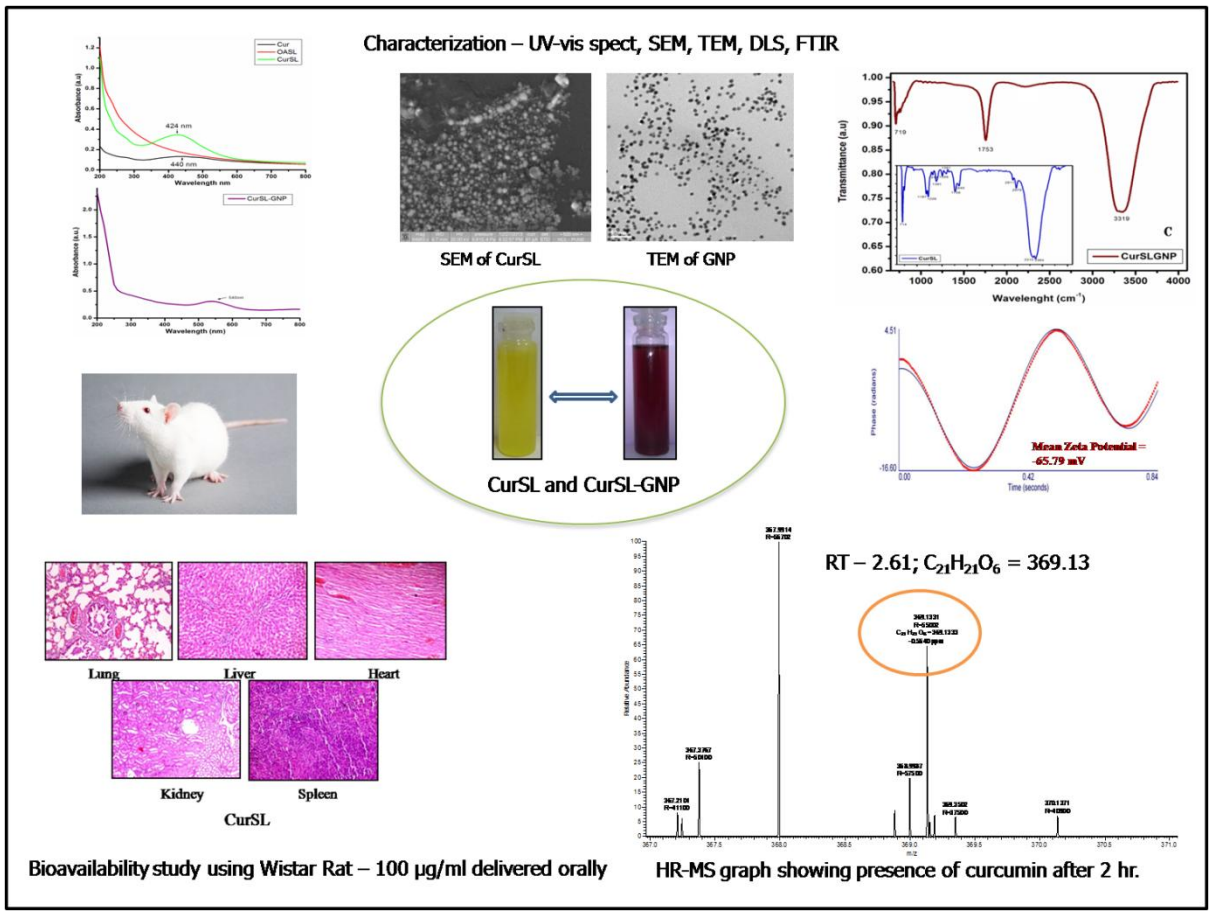

Summary

The major limiting factor for curcumin to be accepted as a modern drug, despite its widespread applications, is the lower aqueous solubility; poor bioavailability and less retention time. When mild physical stress is applied, curcumin is seen to internalize within the micellar hydrophobic core of Oleic Acid Sophorolipid forming Curcumin-Sophorolipid Nanoconjugates (CurSL). These bio-composite displayed enhanced retention time and increased bioavailability of curcumin in Rat models. When gold salts are added to CurSL, it reduces and caps monodispersed, spherical gold nanoparticles (CurSL-GNPs) of 8-10 nm size. Physico-chemical, morphological and optical characteristics of both the nanoparticles are discussed based on spectroscopic absorption, photoluminescence (PL), dynamic light

scattering (DLS), Zeta Potential, SEM, and TEM measurements. FTIR spectroscopy signatures of these nanoparticles confirm the retention of functional groups in the end products. Pharmacokinetic (PKa) studies performed on Wistar rats revealed a manifold increase in curcumin recovery by about 150 times than previously reported; the retention time is up to 2 h in blood plasma. The bio-distribution of gold nanoparticles in rats was studied using EDX which showed their presence in different vital organs. Histopathological analysis confirmed that no unusual legions or necrosis were seen among the vital organs of all the rat models. These results thus suggest the use of curcumin-sophorolipid nano-conjugate for curcumin bioavailability and Cur-SL based nano-gold formulation as a drug delivery carriers.

1. Introduction

1.1 Curcumin

Curcumin is the main active ingredient of Turmeric, a well known ancient Indian spice, belonging to the *Zingiberaceae* (ginger) family responsible for the characteristic yellow color of turmeric[1]. It is a polyphenolic compound consisting of two aromatic rings that give hydrophobicity and tautomerism influencing the polarity of curcumin, while the linker olefin bond between the β-diketone provides flexibility[10-14]. Curcumin found its role in various activities like potent antioxidant, anti-diabetic, anti-inflammatory, antiproliferative, anti-metastatic, anti-angiogenic, hepatoprotective, anti-atherosclerotic, anti-arthritic and anti-thrombotic an agent in cell culture, animal studies, and clinical trials[15,16]. Studies also prove curcumin to be potent against Cancer[17], Alzheimer's disease, Rheumatoid arthritis, hepatic disorders, cystic fibrosis, antineoplastic, anti-viral activity[1,10,11].

1.2 Formulation for solubility of curcumin

Reports of natural analogs of curcumin, curcuminoid derivatives, and curcumin bio-conjugates have been synthesized and challenged to be effective anti-bacterial and anti-viral agents[2,3,4]. Some have also prepared solid dispersions of curcumin-polyvinyl pyrrolidone in a bid to increase its solubility and dissolution[5]. Curcumin nanocrystals are proposed by Onoue et al 2010 and Rachmawati et al. 2012 using methods like milling and high-pressure homogenization[6,7]. Feng et al. 2012 report Polymer-based nanoparticle formulation using poly (ε-Caprolactone)-poly (ethylene glycol)-poly (ε-Caprolactone) copolymer for self-assembly and delivery of curcumin in cancer[8]. Poly(lactic-co-glycolic acid) (PLGA) copolymer based Curcumin uptake are shown by Anand et al 2010, Yallapu et al 2010[9].

Despite these broadly applicable properties, the hydrophobic nature of curcumin prevents the aqueous solubility and invariably restricts its use in the pharma industry. The attributing cause is negligible absorbance, easy elimination, excretion, no distribution, very little retention time and enhanced metabolism in the body. All these factors combined together results in low plasma and tissue level concentration of curcumin which ultimately contributes towards curcumin being non-bioavailable[2,4,17]. Research among various groups in recent years has been positively working on improving the bioavailability of curcumin and to explore its potential application as a modern drug.

2 Our strategy for curcumin solubility

An approach of micelles formation, which is an attractive and known property displayed by amphiphilic surfactants in hydrophilic or hydrophobic solutions (reverse micelles) can be used to address the solubility issue of hydrophobic drugs in water. Surfactants help in wetting of solids and hence improve the rate of disintegration of solids to smaller particles when applied with external physical force. Anisotropic water distribution in micelles aids in better entrapment of hydrophobic drugs within its core rather than adsorption on the surface of micelles. This also stabilizes the whole micelles-drug hybrid[18,19].

2.1 Sophorolipid

Hence to achieve the solubility of curcumin in the water we explore the use of non-ionic glycolipid surfactant viz. Sophorolipid. Sophorolipids are a class of extracellular biosurfactants produced by a non-pathogenic yeast *Candida bombicola* (ATCC 22214). These molecules have a disaccharide unit (sophorose) linked by a glycosidic bond to the hydroxyl group at the penultimate carbon of monounsaturated C18 fatty acid. This arrangement of molecule renders sophorolipid its amphiphilic property[20]. Sophorolipids have negligible toxicity, higher biodegradability and the production media is derived from renewable sources. They are US FDA approved (oral route) for use in food and pharmaceutical industry[21].

To tackle the question of solubility of curcumin in water, we investigated the property of sophorolipids to form micelles while encapsulating curcumin to its core and forming nano-conjugates under the physical force of sonication. The aspects of these nano-conjugates towards an increase in bioavailability of curcumin *in-vivo* are studied in this chapter. With complete characterization and animal study, we compared the possibility of these conjugate as a next level or advances in the heavily researched area of drug solubility. Also in the drug delivery facet, metal nanoparticles are explored as safe carriers for drugs in-vivo.

2.2 Gold nanoparticles synthesis for drug carrier

In this regards gold nanoparticles are vastly studied wherein gold salts are reduced generally by a reducing agent such as citric acid which leads to the formation of gold nanoparticles. In addition, a stabilizing/capping agent is required in most cases and a surfactant plays this role efficiently either by adsorbing or chemically binding to the gold surface with the other end exposed in solution. Thereby, providing stability to the Au nanoparticles in colloidal solution while imparting a charge on the particles which prevent aggregation and settlement[24].

The tunability and multivalent surface chemistry of Au nanoparticles elicit the potential to integrate multiple therapeutic molecules on the surface. And the stabilizing compound actually plays a very important role in the toxicity of these particles *in vivo*[25]. Therefore, in this chapter, we have also ventured to study the gold nanoparticles synthesized using the curcumin-sophorolipid (Cur-SL) nanoconjugate. The characterization and bio-distribution are examined in a rat model which is clarified in the discussion part of this chapter.

3. Materials and Methods

3.1 Reagents and Chemicals

All chemicals and reagents used in this study are of analytical grade unless mentioned otherwise. Curcumin 99% was procured from Sigma Aldrich, media components like peptone, yeast extract, malt extract were obtained from Hi-media, India, and glucose from Qualigens, India. Sodium sulfate was purchased from Merck, India. Solvents namely Ethyl Acetate and Acetonitrile HPLC grade were procured from Rankem (India) and Merck, India respectively.

3.2 Organism and maintenance

Candida bombicola (ATCC 22214), a non-pathogenic yeast was maintained on MGYP slants at 4^{o}C which were subcultured every four weeks prior to use for sophorolipid production. MGYP stands for Malt extract 0.3%, Glucose 2%, Yeast extract 0.3% and Peptone 0.5%[20].

3.3 Synthesis of oleic acid sophorolipid (OASL) and Extraction

Yeast *Candida bombicola* ATCC 22214 was used for the synthesis of sophorolipid via resting cell method. The method in detail is as follows: Initially, *C. bombicola* cells are grown in MGYP medium for 48 h and harvested via centrifugation (5000 rpm, 20 min). These cells are then suspended in 10% glucose medium along with a hydrophobic substrate, in this case, 2ml of oleic acid. The production broth is incubated in a shaking condition at 28^{o}C for nearly 5-6 days, where a brown viscous product is seen visible. Extraction, purification of sophorolipid (viscous product) is explained elsewhere[20].

3.4 Synthesis of aqueous Curcumin- Sophorolipid Nanoconjugates (CurSL)

The synthesis of sophorolipid induced curcumin nanoconjugates (CurSL) was initiated by adding 1mg of Curcumin and 40mg of OASL in 10mL distilled water. This suspension was then probe sonicated using Branson Digital Sonifier 250 at an amplitude of 70 Hz with a constant pulse of 10seconds at an interval of 3 seconds each for 40 minutes. The homogeneous mixture thus obtained was a bright yellow color dispersion of soluble curcumin in sophorolipid solution.

3.5 Gold Nanoparticles synthesis

Gold nanoparticles (CurSL-GNPs) were synthesized using the CurSL solution as a reducing and capping agent. Chloroauric acid ($HAuCl_4$) was added to 10ml of CurSL solution, making

a 1 mM solution of $HAuCl_4$ and kept under 50^oC in water-bath at shaking condition of 50 rpm for 1 h.

3.6 Characterization

The UV-visible spectrum of both dispersion CurSL and CurSL-GNP was recorded on a Jasco V-630 UV-Vis spectrophotometer, with a 10 mm quartz cuvette cell. The spectrum from 200 nm to 800 nm was recorded. Curcumin (100 µg/ml) dispersed in water was kept as a control. Fluorescence spectroscopy was used to record the emission spectra for CurSL solution by providing excitation at 400 nm on a Varian CARY 100 Bio UV-Vis spectrophotometer with a 10 mm quartz cell at 25 ± 0.1°C. Dynamic Light Scattering (DLS) using a Brookhaven 90 plus nanoparticle size analyzer instrument was employed to understand the hydrodynamic size of the particles in the dispersion and their zeta potential. The average surface charges of the particles were determined without diluting the prepared sample for both cases of CurSL solution and CurSL-GNPs. FTIR signatures of CurSL were studied on a Bruker, Alpha FTIR, over the spectral range of 450-4000 cm^{-1}. Controls used were curcumin (powder) and OASL individually. CurSL-GNPs FTIR signatures were also studied over the same range. 25 scans per sample were recorded. All FTIR signatures of the samples and controls were recorded in their nascent state.

3.7 Scanning Electron Microscopy (SEM)

The particles size and morphology of the dispersed particles of CurSL solution were obtained by visualizing them under SEM using an FEI Quanta 200 3D model. The dispersion was drop cast on a clean silicon wafer which was left to dry overnight. These were then sputtered with gold for enhanced contrast. The voltage provided was between 15-20 kV.

3.8 Transmission Electron Microscopy (TEM)

For CurSL-GNPs, 1:1 dilution of the CurSL-GNP solution was drop cast on a carbon-coated copper grid 200 mesh size obtained from Icon analyticals Pvt. Ltd, India and were left to dry overnight. They were observed via TEM of FEI Technai G^2 200kV model.

3.9 Pharmacokinetic study

Nine Albino Wistar rats (approx. 200g) were the subject of this pharmacokinetic study. All the rats were housed under standard ethical conditions provided with *ad libitum* access to standard lab diet and water all throughout the experiment. The experiment on animals was

conducted after obtaining permission from the Institutional Animal Ethical Committee. The rats were divided into three groups; three each for curcumin control, CurSL nanoconjugates, and CurSL-GNPs. All the animals were kept for fasting 12 h prior to the start of the experiment. Three of the rats were orally administered with a dose of 1 mL each of CurSL formulation containing 100 µg of curcumin per 200 g body weight of each rat (maintaining 0.5 mg/kg weight), while the control animals were provided with 100 µg of standard curcumin dispersed in water. The CurSL-Gold Nanoparticles solution (1 ml each) was administered as synthesized to the third group. The oral dosing was performed using a gavage of 3 inches long and 2.25 mm in diameter. Blood was collected alternatively (1 mL) by a retro-orbital method from venous plexus of rats at an interval of 0, 0.15, 0.30, 1, 2, 3, 4, 5, 6, and 24 h into vials pre-treated with EDTA. The plasma from the blood samples was separated by centrifugation at 2000 rpm for 5 minutes at 10^{o}C. These plasma supernatant were collected and stored at -20^{o}C for further analysis.

3.10 High-Resolution Mass Spectroscopy (HR-MS)

The stored plasma specimens were thawed and precipitated in presence of acetonitrile[23]. The supernatant thus obtained was analyzed using HR-MS for the presence of curcumin traces. High-resolution mass spectroscopy was performed on Thermo Scientific, Hybrid Quadrupole Q-Exactive Orbitrap mass spectrometer to identify and analyze the presence of curcumin in the plasma samples. Liquid chromatography pump (Accela 1250) was used with Thermo Scientific Hypersil ODS C18 column 100 mm lengths with 3µm particle size. Isocratic solvent elution was carried out, using acetonitrile/water (60:40, v/v) with a flow rate of 0.5 mL/min for 15 minutes. The mass spectrometer was operated in positive electrospray ionization mode where the spray voltage was at 3.6kV, the capillary temperature at 320°C, S-lens RF level at 50, automatic gain control (AGC) at 1×10^{6}, and maximum injection time at 120ms. Nitrogen was used as the sheath gas, sweep gas and auxiliary gas, set at 45, 10, and 2 (arbitrary units) respectively. A volume of 3 µL of sample was injected and the full HR-MS scan was performed using positive polarity. Data were analyzed with Thermo Scientific Xcalibur software. The mass spectra associated with chromatographic peaks were analyzed for Curcumin control, CurSL solution administered in rat and compared with Curcumin standard in acetonitrile.

3.11 Histopathological study

After 48 h of administration of the CurSL formulation, rats were sacrificed and part of their

lung, spleen, liver, heart, and kidney was fixed in 10% formalin for preparation of histopathological slides. The tissues were processed in a Leica TP 1020 tissue processor and then embedded in paraffin blocks using Leica EG 1160 paraffin embedder. The paraffin blocks were cut into ribbons of 4 mm using a Microm HM 360 microtome. The slides were stained in hematoxylin and eosin using a Microm HMS-70 stainer. The permanent slides were made and evaluated for histopathological changes under an Olympus BX51 microscope, this study was carried out to test the toxicity of formulation on organs of the administered rats.

The same organs were collected from rats administered with CurSL-GNPs and these organs were lyophilized to obtain a powder. EDX analysis was carried out on the SEM instrument of FEI Quanta 200 3D model to analyze the distribution of gold nanoparticles in the rat.

4. Results and Discussion

4.1 Spectrophotometric analysis

After the synthesis of Curcumin-sophorolipid Nanoconjugates (CurSL), a UV-visible spectrum of the solution was recorded to understand their solubility in aqueous solution. Fig 1a. represent the UV-Vis spectra of CurSL in aqueous solution in comparison with curcumin dispersed in water. The spectrum showed a peak at 424 nm whereas; the lambda maximum of curcumin in water was at 440 nm with relatively very less absorbance. Curcumin in any medium is very sensitive regarding its photophysical properties and shows strong absorbance at varying wavelengths[25]. The soluble curcumin usually is observed to absorb at 420 nm in organic solvents[27]. In our case, we observed that CurSL nano-conjugate showed a perfect peak at 424 nm which point to curcumin being soluble in the sophorolipid solution. But the same was not observed for curcumin in water. This might be due to the insoluble nature of curcumin in water where the fine particles in dispersion are seen to absorb at 440nm when taken a UV-Vis spectrometry of solution. OASL in solution did not show any significant absorbance which can be easily spotted in the Fig 1a.

The physical stress (sonication) that the sophorolipids are subjected to, as mentioned in our methods causes them to form spherical micelles making them suitable vessels for drug delivery [22]. The sophorolipids micelles internalize curcumin in the hydrophobic core, whereas the hydrophilic component of the sophorolipids remains on the outer surface exposed to interact freely with the aqueous environment enabling curcumin solubility[27].

Furthermore, the CurSL solution was used as reducing and capping agent for the formation of gold nanoparticles at 50^{o}C temperature. Within 1-hour chloroauric acid (1mM) got converted into gold nanoparticles giving a characteristic purple colored solution. When measured using UV-Vis spectroscopy the solution gave λ_{max} at 540nm, typical of gold nanoparticles [29] which are shown in Fig. 1b. A sharp SPR band was observed which implies that the aggregation of the nanoparticles is very slow and the solution is relatively stable[28]. Generally, the difference in the intensity of SPR bands is attributed to diverse levels of the size distribution of particles as well as their shape in the solution along with their aggregation[26]

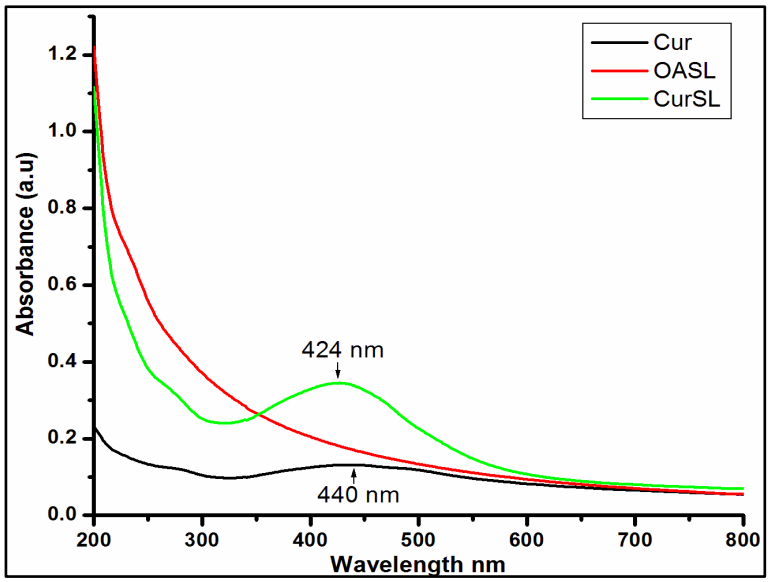

Fig.1a. The UV-Vis spectra of Curcumin in water, sophorolipid (OASL) solution and synthesized CurSL nano-conjugate solution. λmax observed at 424 nm and 440 nm for CurSL and Curcumin in water respectively.

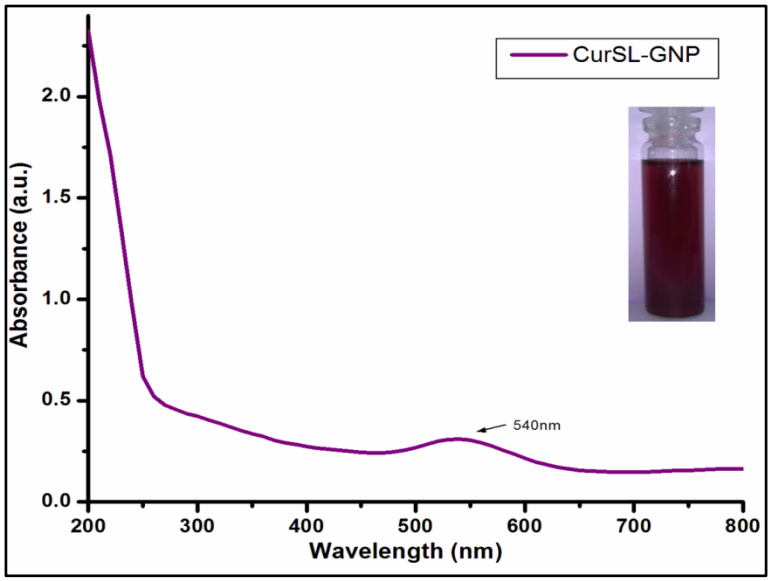

Fig.1b. The UV-Vis spectrum of CurSL-GNPs, where λmax is observed at 540nm.

While interpreting the Photoluminescence (PL) data of Oleic Acid sophorolipid (SL), Curcumin (Cur) in water and the synthesized Curcumin-Sophorolipid nano-conjugate (CurSL) solution a considerable blue shift, of about 50nm in reference to curcumin control, similar to that of the UV-Vis spectra [27]. The PL was recorded at the excitation of 400nm in aqueous solution for all three samples giving us the best comparative results. SL exhibited no photoluminescence, whereas curcumin in aqueous solution displayed a week excitonic emission at 548 nm because of its poor aqueous solubility. However, CurSL nano-conjugate

on excitation at a wavelength of 400 nm exhibited a manifold rise in its intensity yielding a strong emission at 504 nm which concretes the results of strong green fluorescence. In accordance with this observation, a bright yellow colored dispersion of evenly distributed curcumin nano-conjugates is seen in Fig. 2 which emits sharp green fluorescence under UV light.

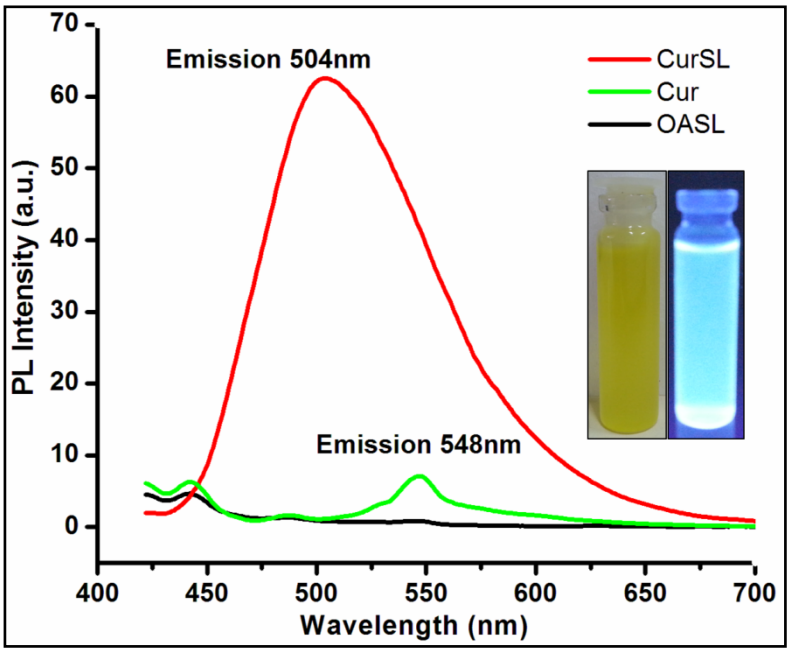

Fig.2. The PL spectra when excited at 400 nm for CurSL nano-conjugate, curcumin (cur) in water and sophorolipid (OASL) solution. Emission λmax was observed at 504 nm and 548 nm with the inset images of solutions for CurSL nano-conjugate and curcumin (cur) in water respectively.

4.2 FTIR Characterization

FTIR spectroscopy was performed to contemplate the chemical changes in curcumin, OASL, CurSL conjugate and CurSL-GNPs that may have occurred during the synthesis process. The curcumin (powder) spectrum showed all the relevant bands including the characteristic 1556cm^{-1} of the C-C aromatic group, 1628cm^{-1} and 1717cm^{-1} of C=O (keto) stretch and 1412cm^{-1} of C-O (enol) stretch. On the other hand, the sophorolipid spectrum displayed a C-H alkane bend at1380cm^{-1} and an aliphatic stretch at 2909cm^{-1} and 2980 cm^{-1}.

While in the spectra of CurSL solution all the bands of the parent molecules were observed, apart from the signature band representing the enol bending of curcumin. In this conjugate, the enol group may be subdued due to the presences of SL micelles. Additionally, the CurSL conjugate showed the presence of a C-O-H duplet at 1226cm^{-1}. This additional group may be formed as a result of the interaction between the enol group of curcumin and SL in the

solution causing a minor shift in the keto group.

The CurSL-GNPs, on the other hand, had very less observable bands viz. 719cm^{-1}, 1753cm^{-1} and 3319cm^{-1} indicating the presence of C-H bend, C=O stretch of Keto and phenolic OH stretch respectively. As the GNPs are stabilized, there was a prominent shift in the keto group from 1628cm^{-1} to 1753cm^{-1}with with respect to that of curcumin. This shift is due to the loss of the hydrogen present in the subdued enolic group, in presence of a strong oxidizing $AuCl_4$ salt[31]. Table 1 mentions the wavelengths and their representing bonds. All these values are consenting with the literature surveyed [27, 32-38].

Table 1: FTIR signatures and their representing bonds

Cur	**CurSL**	**OASL**	**CurSL-GNP**	**Bonds**
717, 886, 976	714	783, 896	719	C-H bend
1014, 1119, 1179	1187	1125, 1179		C-O stretch
	1226			C -OH bend
1301	1314	1313		C-O stretch
	1391	1380		C-H alkane bend
1412				C-O enol bending
1556	1509, 1581	1503, 1574		C-C aromatic
1628, 1717	1759		1753	The C=O stretch of Keto
	1840	1840		Acid anhydride
	2911, 2979	2909, 2980		Alkane stretch
3526	3310, 3364	3410	3319	OH phenolic stretch

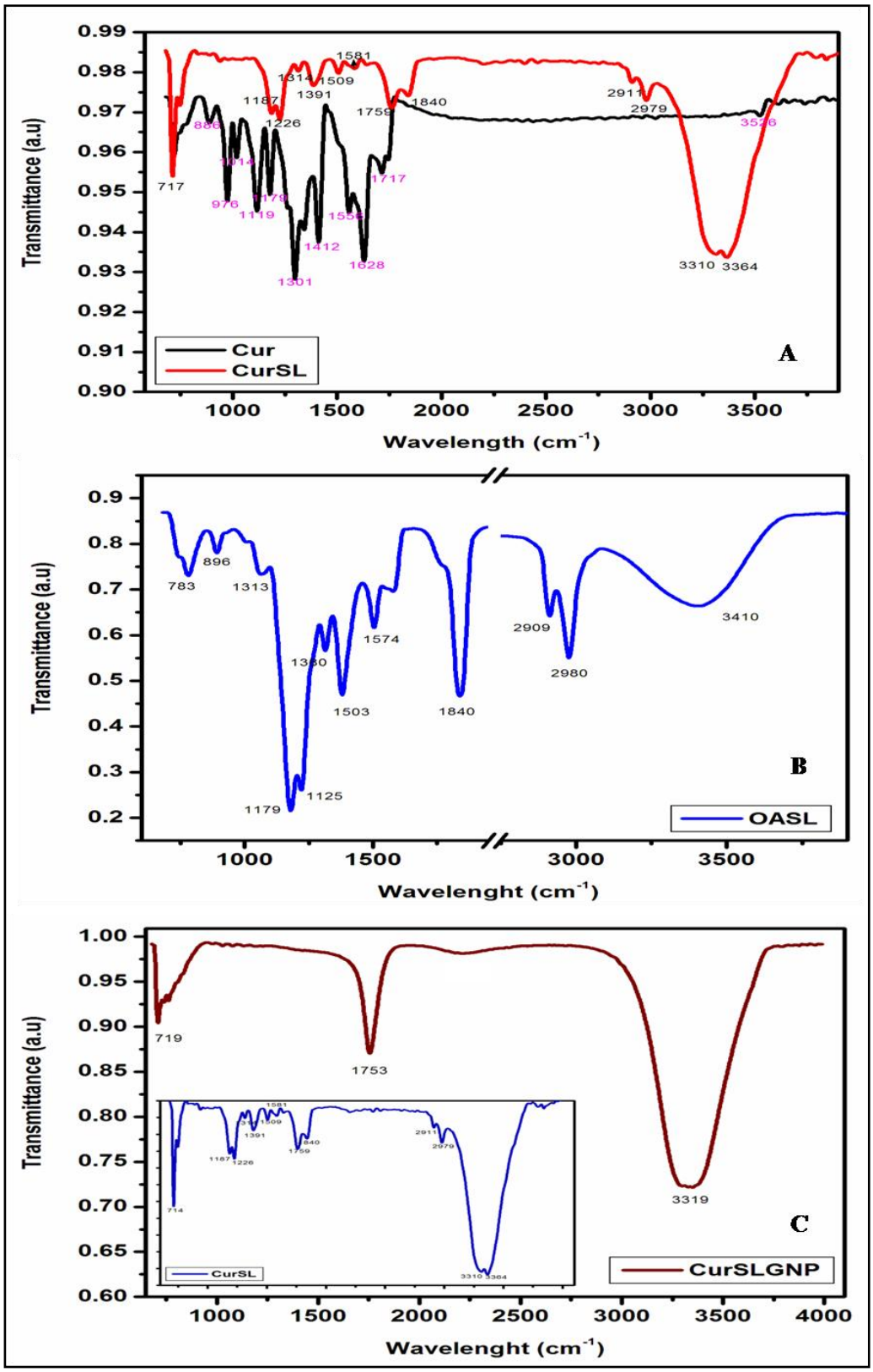

Fig. 3: FTIR analysis of (A) Curcumin (powder) and CurSL solution, (B) OASL and (C) CurSL-GNP, inset CurSL solution.

4.3 Particle Size Distribution and Stability

The particle size of the CurSL nano-conjugates in aqueous solution was measured using the DLS spectra (Fig. 4a.) revealed the formation of monodispersed nanoparticles. The average hydrodynamic size as calculated was around 275 nm with a mean polydispersity index of 0.2. The morphology and particle size distribution using SEM images (Fig. 5b.) of nanoparticles correlates with the DLS analysis. SEM was performed on curcumin dispersed in water as curcumin control (Fig. 5a.). SEM images confirmed that the irregularly shaped curcumin was converted into nearly spherical shaped nanoparticles in presence of sophorolipids with an average size of 40-60 nm. This extreme size reduction and low polydispersity were achieved as a result of physical impulse imparted due to probe sonication in presence of the amphiphilic, biosurfactant SL. Moreover, the surfactant facilitates in reducing the interfacial surface tension enabling synthesis of evenly dispersed nearly spherical nanoparticles[27]. CurSL-GNPs were also subjected for DLS analysis (Fig. 4c.), where it was observed that the polydispersity of these particles is 0.3 and the hydrodynamic size was found to be 5 nm. The TEM analysis (Fig. 5c.) confirms the size of gold nanoparticles to be nearly 5-10 nm which is in agreement with DLS.

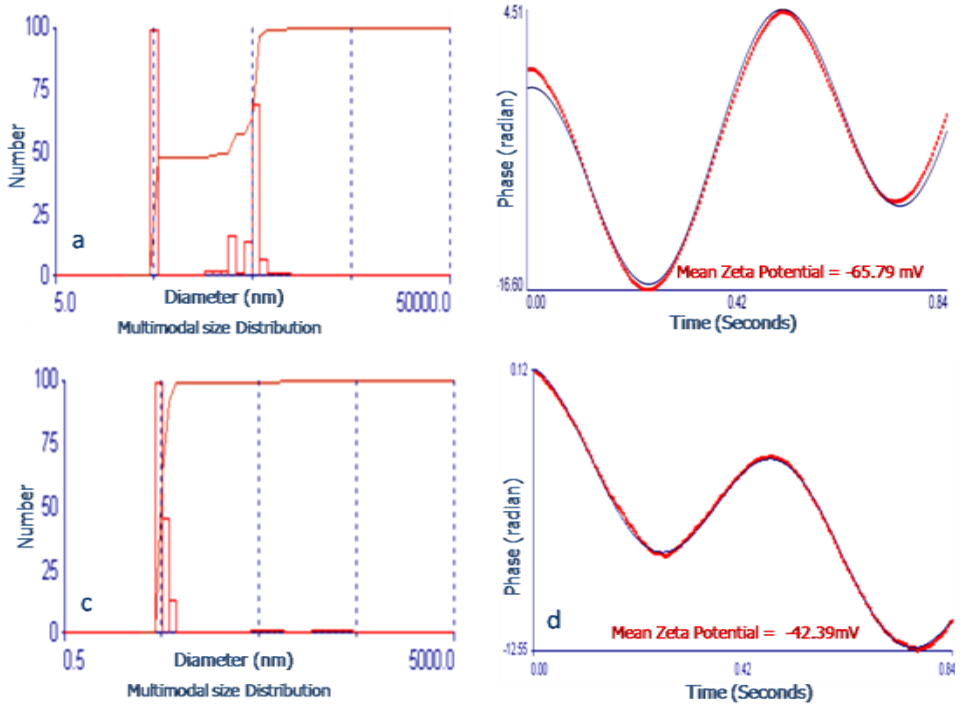

Fig. 4: (a) DLS and **(b)** Zeta Potential of synthesized CurSL nanoparticles indicating the hydrodynamic size of 275nm and the mean zeta potential of -65.79 mV.**(c)** DLS of CurSL-GNPs with hydrodynamic size as 5nm and -42.39 mV zeta potential **(d)**.

Zeta Potential was measured to understand the surface charge and electric potential of CurSL nano-conjugates which is complementary to its stability in aqueous solution. The stability of the solution is in agreement with the calculated zeta potential which shows that the mean surface charge of CurSL nano-conjugates is -65.79mV (Fig. 4b.) which is considered extremely stable[28,38]. K. Sindhu et al, 2013 used green approach to synthesize gold nanoparticles using curcumin alone by manipulating pH to attain spherical shape, and stability up to 6 months with -23mV (Fig. 4d.) zeta potential[49], but the synthesis given in this paper is able to get Gold nanoparticles with higher stability having a zeta potential of -42.39mV. The size of these CurSL-GNPs was observed to be 5-10nm via TEM and DLS. The properties and stability of Cur-SL-GNP solution were retained even after a year.

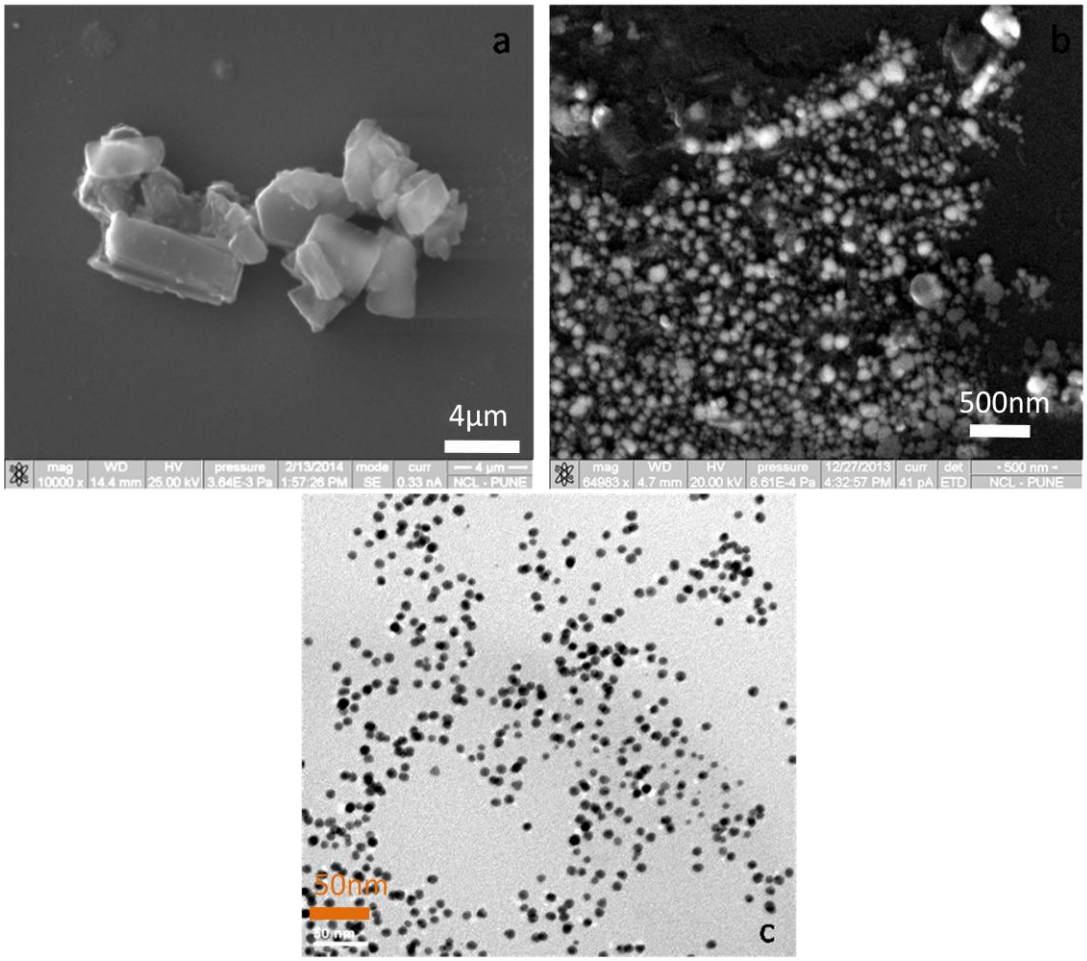

Fig.5: SEM images of Curcumin control **(a)** showing large irregular pieces about 8-10 µm in size. **(b)** CurSL solution evenly dispersed nearly spherical nanoparticles of size between 40-60 nm. **(c)** TEM image of CurSL-GNPs, scale represented is 50 nm and the size of particles is nearly 8-10 nm.

4.4 Pharmacokinetic Plasma Studies:

The pharmacokinetics of curcumin has been ambiguously explained due to its extremely poor water solubility, poor bioavailability and rapid degradation within the body[39]. This leads to an indistinguishable level of curcumin in the plasma, making the calculations of pharmacokinetic very difficult to study. It has also been reported in many studies about the intrinsic properties of curcumin and its ability to act as a therapeutic agent for a host of ailments[2]. Nonetheless, most of these reports lament about poor oral and intestinal bioavailability (≈11 ng/ml) to be one of the biggest barriers for curcumin to exhibit the wide range of its medicinal properties[40]. It has also been studied that even after administration of about 12 g/ml of curcumin through the oral route to human; a negligible amount of 50ng/ml was recovered from the serum[41].

In one of the studies reported by Ravindranath et al 1980, showed that only trace amounts of curcumin, as low as 5μg/ml was found in the blood portal of Rats even when 400 mg of curcumin was administered[42]. In another time-bound experiment, when a single dose of 2 g/kg of curcumin was administered to rats, the maximum quantity of 1.35μg/ml was recovered from the serum sample after 0.83 h whereas in human after 1 hour as low as 0.006μg/ml was recovered[2].

Pan et al 1998 explored the pharmacokinetic properties of curcumin in mice, by oral administration. They found that after oral administration of 1 g/kg of curcumin, the maximum amount found in their plasma was a mere 0.22μg/ml which was obtained after 1 hour; the plasma concentration was further declined with increase in time[43]. According to a recent study conducted by Anand P et al., 2007[2], a distinct peak of curcumin was seen after an hour in the serum sample of curcumin-treated to nude mice. After administering 1 g curcumin per kg rats through the oral route, the maximum serum curcumin level noted was as low as 0.5μg/mL after 45 minutes of dosing[44]. Furthermore, a few other studies displayed a maximum retention of 6.5 ± 4.5 nM of curcumin after 0.5 hours[45]in male rats.

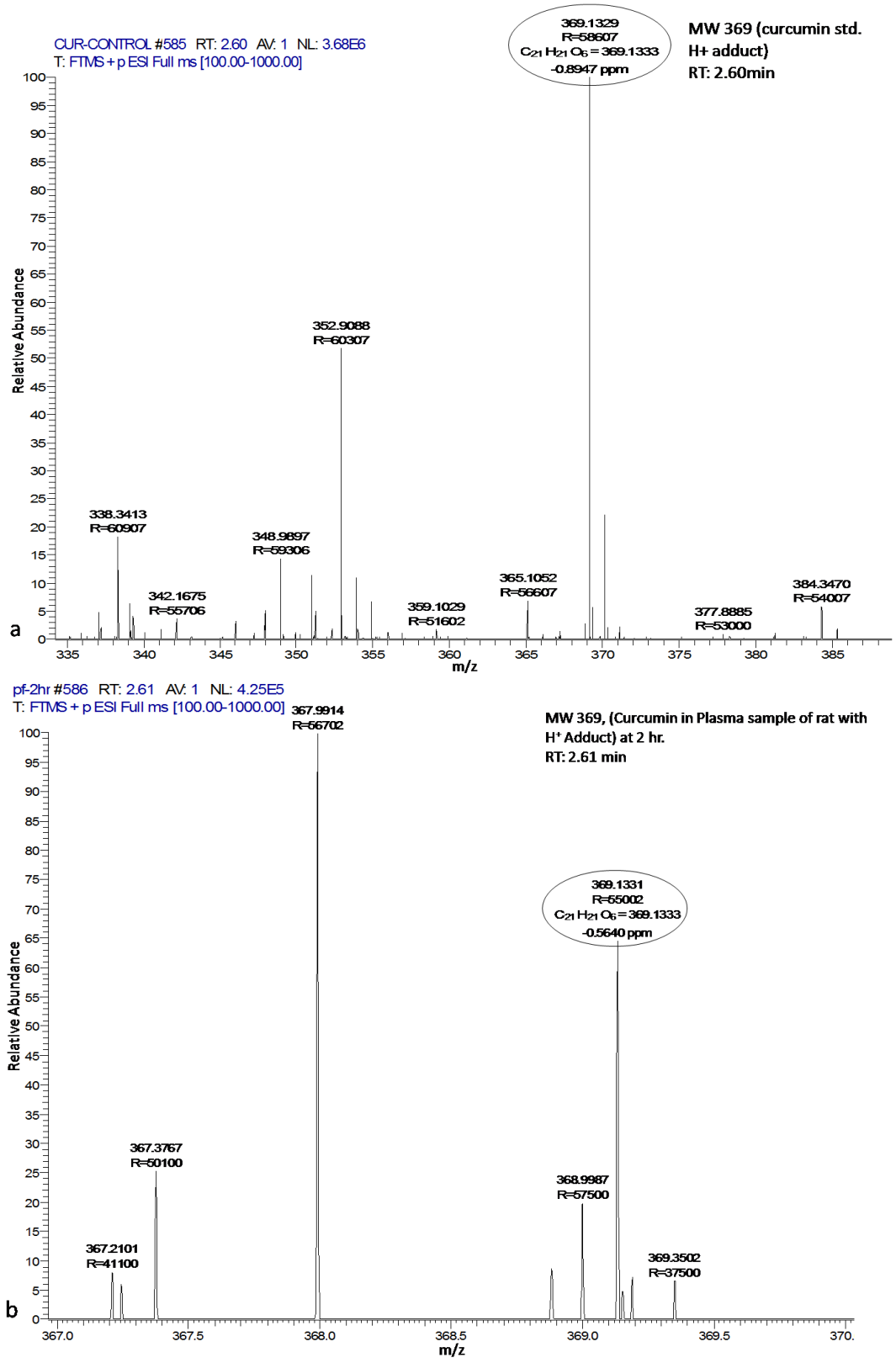

Fig. 6: An HR-MS spectrum of standard curcumin in ACN (a)and spectrum of extracted plasma samples from Wistar rats administered with CurSL (100 µg/ml) solution after 2 h time interval (b).

In our present investigation, as described in the experimental section 100 µg of curcumin in the form of CurSL was administered orally per ~200 g of rats. The retention time and bioavailability of CurSL were compared with that of standard curcumin in water administered in rats. A standard sample was prepared by dissolving curcumin in acetonitrile (ACN) and a method was developed on the HPLC for which an isocratic system of ACN: Water (60:40) at 424 nm was set for 15 minutes. Same parameters were assigned on the HR-MS instrument for which a single sharp peak was observed at a retention time of 2.61 minutes as seen in Fig. 6a. and 6b. Plasma samples from both the groups of rats (Control and CurSL treated) were collected at various time intervals and treated with ACN to denature the proteins and other plasma components[46-48]. Following this, the plasma samples were eluted employing the above-mentioned method by HR-MS technique. The chromatogram of HR-MS for the plasma samples collected at all the time intervals of the control animals showed no elution of curcumin at the retention time of 2.61 minutes. On the other hand, plasma samples of the rats administered with CurSL solution display a prominent peak at the same elution time (2.61 min) as that of the standard at the end of two hours. As there was no further elution of curcumin in the following time intervals, it can be vividly said that CurSL solution was retained in the animals for at least two hours. From this study, we illustrated that intact curcumin was made bioavailable with enhanced retention of up to two hours when 100µg of curcumin (CurSL) was orally delivered to ~200g of rats.

For calculating the exact amount of curcumin found in the plasma of CurSL solution treated rats, a standard Curcumin of 1µg/ml in Acetonitrile was subjected to HR-MS analysis using same column and conditions that were provided for animal study sample. From the results of the plasma studies (Fig. 6b.), the Normalized Level (NL) of curcumin after two hours, was noted to be 4.25×10^5 and that of standard Curcumin (1µg /ml) was marked to be 2.68×10^7. Calculations based on these values showed the concentration of curcumin present in the collected plasma sample after two hours to be nearly 15.87ng/ml of blood. The overall percentage of curcumin in plasma was calculated to be 0.015%. This percentage is many folds higher than that of Pan et al 1998 and Maiti et al 2007 which could achieve 0.00011% and 0.00025% respectively when administered with 1g/kg of curcumin to rats.

4.5 Histopathological Analysis

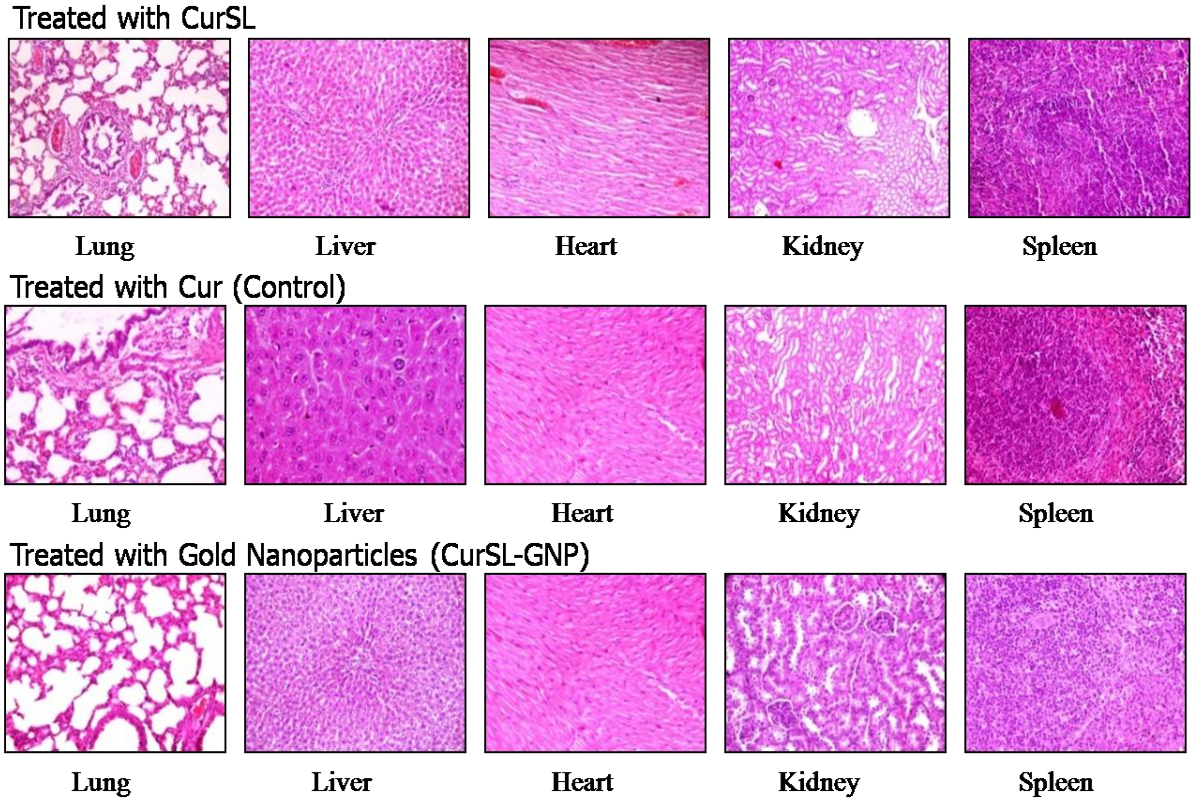

Fig.7: Microscopic images of the Histopathology of organs viz., Lung, Liver, Heart, Kidney, and Spleen.

Once the blood collection for plasma analysis was completed at 48 h, the animals were sacrificed by cervical dislocation. The vital organs of rats from each group viz. CurSL, curcumin control, and CurSL-GNP were instantly fixed in 10% formalin solution. As described in the methodology above, slides of organs were made and analyzed under a light microscope to study any abnormal changes in their cell structure. It was observed that all the animal organs were completely normal with no unusual legions or necrosis. From this, it can be concluded that the CurSL solution and CurSL-GNPs are safe to deliver *in vivo*.

4.6 Energy Dispersive X-ray (EDX) analysis

Part of the vital organs of rats that were administered with CurSL-GNPs was kept in -20^{o}C immediately after their removal from rat body. They were then transferred to -80^{o}C deep freezer for 3-4 h. Later these organs were lyophilized to remove all the moisture from them and then they were ground to fine powder. This powder was subjected to Energy Dispersive X-ray (EDX) analysis provided by SEM using an FEI Quanta 200 3D model.

Table 2 indicates the Carbon and Oxygen Weight % element along with the Au from organs viz. Heart, Kidney, Lung, Liver, and Spleen.

Table 2 Weight% by element from EDX analysis

Organ	CK	OK	AuL
Heart	38.04	22.28	2.78
Kidney	36.17	37.88	3.11
Lung	37.42	31.97	5.59
Liver	39.36	35.02	1.74
Spleen	35.98	39.69	2.38

In our previous studies, we have reported the use of sophorolipid for synergistic delivery and activity of antibiotic. It was theorized that SL spans the cell membrane and delivers the drug within the cell [21]. Also, sophorolipid was used to cap CdTe quantum dots (QDs) to understand the compatibility of QDs on normal and cancer cell line using MTT assay for the theranostic application. It was observed that SL- capped CdTe particles showed biocompatibility with both the cell lines and enhanced the cellular association and uptake of QDs [50]. From these results, we can hypothesize that sophorolipid being amphiphilic in nature may cross the cell membrane and assist the CurSL-GNPs obtained in this report (range of 8-10nm nearly quantum dots size) as drug carrier which can cross the Blood Brain Barrier (BBB).

5. Conclusion:

There is extensive ongoing research among various groups to solubilize curcumin in aqueous solution and improve its bioavailability. One of the aspects for curcumin solubilization is to maintain its properties without altering its structure and chemical bonds. Keeping these concerns in mind, we have successfully solubilized curcumin in a micellar aqueous solution of sophorolipids resulting in the synthesis of curcumin nanoconjugates in this chapter. By employing the physical force of sonication, we were able to form CurSL nanoconjugates of size in the range of 40-60 nm confirmed by SEM and DLS. The physicochemical characterization of CurSL displayed a significant blue shift for maximum absorbance when measured on a UV-Visible spectrophotometer with respect to the non-solubilized curcumin in water. PL studies showed a bright green fluorescence emitted by CurSL sample at 504 nm when excited at 400 nm. During their synthesis, significant chemical bonds were retained indicating no chemical modifications with respect to standard curcumin as indicated by FTIR

signatures. This data is of great significance as any structural and chemical changes in curcumin can result in the loss or modification of activity. The synthesis of CurSL-GNPs was also achieved at ambient temperatures unlike that of the earlier reported studies by Singh et al 2013, where they have used 90^{o}C temperature which may lead to a loss in activity of curcumin. The rate determining step for oral drug formulation is absorption by the gastrointestinal tract with respect to the dissolution and solubility in aqueous solution[18]. The synthesized CurSL nanoparticles when administered to Wistar rats for bioavailability study, showed a remarkable increase in retention time of curcumin in blood plasma up to 2 h. The concentration of curcumin in blood plasma was 0.015% which was calculated using the HR-MS data of standard curcumin of 1µg/ml and which is much higher than 0.00011%[43] and 0.00025%[44] of previous reports. The CurSL bioconjugate acts as a reducing and capping agent for the formation of gold nanoparticles. The distribution of CurSL-GNPs in rat showed presence in all vital organs. The size of particles is very small and in future studies, they can be functionalized and loaded with hydrophobic drugs which can be targeted to specific organs for slow release and delivery of drugs which may even carry them and cross BBB. Our method of solubilization of curcumin can become a solution for the use of curcumin as a therapeutic drug in modern science.

References

1) M. Akram, S. A. Ahmed, K. Usmanghani, A. Hannan, E. Mohiuddin, and M. Asif, *Rom. J. Biol. Plant Biol*, 2010, 55 (2), 65–70.
2) Y. Wang, Z. Lu, F. Lv and X. Bie, *Eur Food Res Technol*, 2009, 229, 391–396
3) O. Naksuriya, S. Okonogi, R. M. Schiffelers and W. E. Hennink, *Biomaterials*, 2014, 35, 3365-3383
4) H. Hatcher, R. Planalp, J. Cho, F. M. Torti, and S. V. Torti, *Cell. Mol. Life Sci*., 2008, 65, 1631 – 1652.
5) S. Balasubramanian, A. R. Girija, Y. Nagaoka, S. Iwai, M. Suzuki, V. Kizhikkilot, Y. Yoshida, T. Maekawa, and S. D. Nair, *International Journal of Nanomedicine*, 2014, 9,437–459.
6) R.A. Sharma, A.J. Gescher, W.P. Steward. *European Journal of Cancer*, 2005, 41, 1955–1968.
7) K. S. Bhullar, A. Jha, D. Youssef and H. P. V. Rupasinghe, *Molecules*, 2013, *18*, 5389-5404.
8) S. C. Gupta, S. Prasad, J. H. Kim, S. Patchva, L. J. Webb, I. K. Priyadarsini and B. B. Aggarwal, *Nat. Prod. Rep.*, 2011, 28, 1937–1955.
9) S. C. Gupta, S. Patchva, and B. B. Aggarwal, *AAPS Journal*, 2013, 15(1), 195-218.
10) S. S. Bansal, M. Goel, F. Aqil, M. V. Vadhanam, and R. C. Gupta, *Cancer Prev Res (Phila)*, 2011, 4(8), 1158–1171.
11) R. Jäger, R. P. Lowery, A. V. Calvanese, J. M Joy, M. Purpura and J. M. Wilson, *Nutrition Journal*, 2014, 13, 11.
12) P. Anand, A.B. Kunnumakkara, R. A. Newman and Bharat B. Aggarwal, *Mol. Pharmaceutics*, 2007, 4 (6), 807-818.
13) M.K. Kim, H. Mok, and Y. Chong, *Bull. Korean Chem. Soc.*, 2012, 33 (9), 2849.
14) R.K. Singh, D. Rai, D. Yadav, A. Bhargava, J. Balzarini, and E. De. Clercq, *European Journal of Medicinal Chemistry*, 2010, 45, 1078–1086.
15) N. Kaewnopparat, S. Kaewnopparat, A. Jangwang, D. Maneenaun, T. Chuchome, and P. Panichayupakaranant, *World Academy of Science, Engineering and Technology*, 2009, 3, 7-29.
16) S. Onoue, H. Takahashi, Y. Kawabata, Y. Seto, J. Hatanaka, B. Timmermann, S. Yamada, *J Pharm Sci.*, 2010, 99 (4), 1871-81.
17) H. Rachmawati, L. Al Shaal, R. H. Müller, C. M. Keck, *Journal of Pharmaceutical Sciences*, 2013, 102(1), 204-214.

18) R. Feng, Z. Song, G. Zhai, *International Journal of Nanomedicine*, 2012, 7, 4089–4098.

19) H. Rachmawati, *Int. J. Res. Pharm. Sci.*, 2013, 4(2), 211-220.

20) K.T.Savjani, A.K. Gajjar, and J.K. Savjani, *International Scholarly Research Network*, 2012, 10.

21) S. Gokturk, E.Caliskan, R. Y. Talman and U. Var, *The Scientific World Journal*, 2012, 12

22) P. Darne, M. Mehta, P. Dubey, and A. Prabhune, *World Journal of Pharmacy and Pharmaceutical Sciences*, 2014, 3 (11), 792-804.

23) K. Joshi-Navare and A. Prabhune, *BioMed Research International*, 2013, 10.1155.

24) R. A. Sperling, P. R. Gil, F. Zhang, M. Zanella, and W. J. Parak, *Chem. Soc. Rev.*, 2008, 37, 1896–1908.

25) D. A. Giljohann, D. S. Seferos, W. L. Daniel, M. D. Massich, P. C. Patel, and C. A. Mirkin, *Angew Chem. Int. Ed.*, 2010, 49, 3280 – 3294.

26) L. Zhongfa, M. Chiu, J. Wang, W. Chen, W. Yen, P. Fan-Havard, L. D. Yee and K. K. Chan, *Cancer Chemother Pharmacol.* 2012, 69 (3), 679–689.

27) A. Barik, K.I. Priyadarsini and H. Mohan, *Photochemistry and Photobiology*, 2003, 77(6), 597-603.

28) P. K. Singh, K. Wani, R. Kaul-Ghanekar, A. Prabhune, and S. Ogale, *RSC Adv.*, 2014, 4, 60334-41.

29) P. Dubey, K. Selvaraj, and A. Prabhune, *World Journal of Pharmacy and Pharmaceutical Sciences*, 2013, 2 (3), 1107-1133.

30) N. Baccile, F. Babonneau, J. Jestin, G. Pehau-Arnaudet, and I. Van Bogaert, ACS Nano, 2012, 6 (6), 4763–4776.

31) A. Rai, A. Prabhune and C. C. Perry, *J. Mater. Chem.*, 2010, 20, 6789–6798.

32) R. Jagannathan, P.M. Abraham and P. Poddar, *J. Phys. Chem. B*, 2012, 116, 14533-14540.

33) D.K. Singh, R. Jagannathan, P. Khandelwal, P. M. Abraham and P. Poddar, *Nanoscale*, 2013, 5, 1882.

34) W. Rechberger, A. Hohenau, A. Leitner, J.K Krenn, B.Lamprecht and F.R. Aussenegg, *Optics communications 220*, 2003, 137-141.

35) C. Sreelakshmi, N. Goel, K.K.R. Datta, A. Addlagatta, R. Ummanni, and B. V. Subba Reddy, *Nanosci. Nanotechnol. Lett.*, 5, 2013, 1–8.

36) Typical Infrared Absorption Frequencies, http://staff.aub.edu.lb/~tg02/IR.pdf, (accessed December 2015).

37) Infrared Spectroscopy, http://www.biomaterial.com.br/FTIR.pdf, (accessed December 2015).

38) S. Bakkialakshmi and G. Jayaranjani, *IJPCBS*, 2015, 5(1), 93-97.

39) S. S. Solanki, P. Paliwal, S. Jain, P. Sharma, and B. Sarkar, *Current Research in Pharmaceutical Sciences*, 2012, 04, 210-214,

40) S. F. Chow, L. Shi, W. Wing Ng, K. H. Yan Leung, K. Nagapudi, C. C. Sun and A. H. L. Chow, *Cryst. Growth Des.*, 2014, 14, 5079−5089.

41) S. N. Abd El-Rahman and S. S. Al-Jameel, *Sch. Acad. J. Biosci.*, 2014, 2(3), 214-223.

42) M. Ibrahim, M. Alaam, H. El-Haes, A.F. Jalbout and A. Leon, *Ecletica Quimica*, 2006, 31, 3.

43) C. Moorthi, K. Krishnan, R. Manavalan and K. Kathiresan, *Asian Pac J Trop Biomed*, 2012, 2(11), 841-848.

44) K. Sindhu, A. Rajaram, K. J. Sreeram and Rama Rajaram, *RSC Adv.*, 2014, 4, 1808-1818.

45) Y. B. Pawar, B. Munjal, S. Arora, M. Karwa, G. Kohli, J.K. Paliwal and A.K. Bansal, *Pharmaceutics*, 2012, 4, 517-530.

46) M.H. Ucisik, S. Kupcu, B. Schuster and U. B. Sleytr, *Journal of Nanobiotechnology*, 2013, 11, 37.

47) C.D. Lao, M.T. Ruffin IV, D. Normolle, D. D. Heath, S. I. Murray, J. M. Bailey, M. E. Boggs, J. Crowell, C. L. Rock, and D. E. Brenner, *BMC Complementary and Alternative Medicine*, 2006, 6, 10.

48) V. Ravindranath and N. Chandrashekhara, *Toxicology*, 1980, 16(3), 259-265.

49) M. Pan, T. Huang, and J. Lin, *Drug Metabolism and Disposition*, 1998, 27(1), 486-494.

50) K. Maiti, K. Mukhurjee, A. Gantait, B. P. Saha and P.K. Mukhurjee, *International Journal of Pharmaceutics*, 2007, 330(1-2), 155-163.

51) T. H. Marczylo, R.D. Verschoyle, D.N. Cooke, P. Morazzoni, W.P. Steward and A. J. Gescher, *Cancer Chemotherapy, and Pharmacology*, 2007, 60 (2), 171-177.

52) S. D. Garbis, A. Melse-Boonstra, C.E. West and R.B. van Breemen, *Anal. Chem.*, 2001, 73, 5358-5364.

53) F. Michopoulos, L. Lai, H. Gika, G. Theodoridis and I. Wilson, *Journal of Proteome Research*, 2009, 8, 2114–2121.

54) R. Kay, C. Barton, L. Ratcliffe, B. Matharoo-Ball, P. Brown, J. Roberts, P. Teale, and C. Creaser, *Rapid Commun. Mass Spectrom.*, 2008, 22, 3255–3260.

55) P. Singh, K. Joshi, D. Guin, and A. A. Prabhune, *RSC Adv.*, 2013, 3, 22319.

Chapter 3

Derivatization of curcumin via biotransformation and exploring its applied aspects

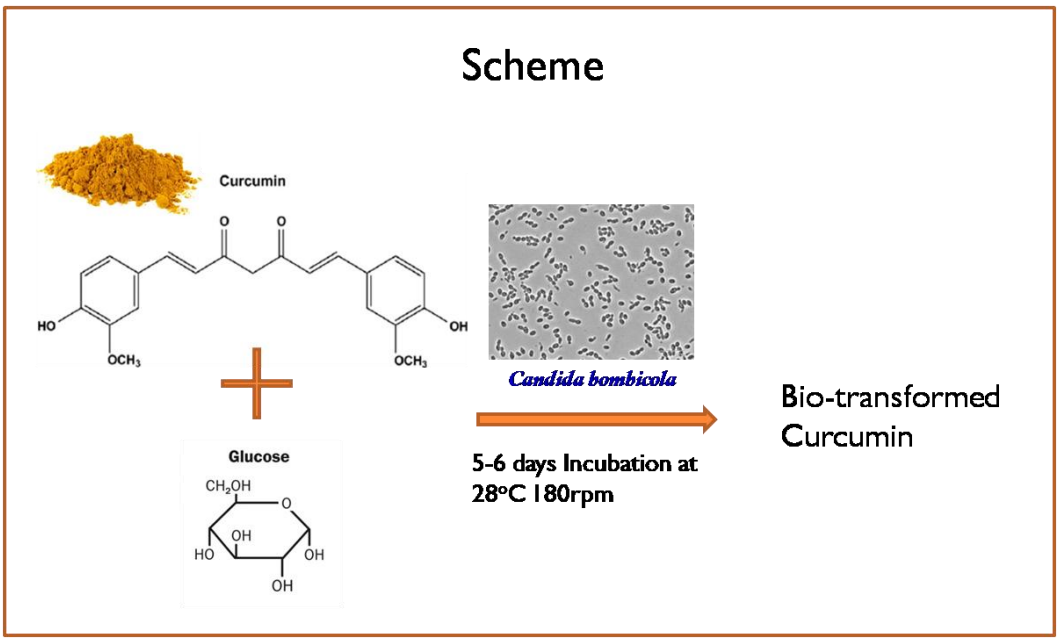

Summary:

Low solubility in aqueous solution and poor bioavailability of Curcumin has lead to the synthesis of various formulations by scientists worldwide to enhance the physiochemical characteristics of this bright yellow molecule. In this study, a novel compound is being proposed Curcumin-sophorolipid (CSL) synthesized by *Candida bombicola* cells that have helped to improve the water solubility, stability, and bioavailability of curcumin. The objective of this study was to synthesize CSL compound and carry out its extraction. Further partial purification and characterization of CSL were done using UV-Vis spectrophotometry, Thin Layer Chromatography and High-Performance Liquid Chromatography. The further understanding of the compound structure and its interaction were made by carrying out HRMS, FTIR, NMR and Photoluminescence studies. The application of synthesized compound, CSL in various areas, such as its property of being anti-tyrosinase, anti-oxidant, anti-biofilm and fluorescence were studied. CSL shows good anti-biofilm activity against *P. aeruginosa*. It shows scavenging activity and anti-tyrosinase activity. Under UV light it emits green fluorescence and shows strong emission in 700nm range when excited at 350nm. To study its toxicity, MTT assay was carried out on L6 cell line and anti-cancer activity against MCF-7and HeLa were also studied.

1. Introduction:

1.1 Curcumin

Ayurveda, an ancient Indian medical system makes use of turmeric paste to treat eye infections, to dress wounds and as an anti-inflammatory agent against insect bites, acne, and various skin diseases. Powdered turmeric taken with boiled milk has been commonly used to cure a cough and related respiratory ailments. It can also act as an anti-dysenteric for children suffering from dysentery[1].

Turmeric Band-Aids are being prepared by the American pharmaceutical company Johnson & Johnson for the Indian market [2,3]. Turmeric acts as a healing agent and cures any lacerations in the birth canal when applied to the perineum [4]. This dietary spice is also used to treat digestive disorders such as dyspepsia, ulcers, stomach pain due to indigestion, and flatulence

Curcumin is an active ingredient in traditional herbal remedies and also in a vibrant yellow dietary spice called turmeric obtained from the rhizome of *Curcuma longa*. It has been used in the traditional medicines of China and India since a long time with the powder being used in Asian cooking, medicine, cosmetics, and fabric dyeing for more than 2000 years [1,5]. Curcumin is currently being used to add a dash of color in perfumes [6].

Vogel first isolated Curcumin in the year 1842 and it was structurally characterized by Lampe and Milobedeska [1]. Curcumin (curcumin I), demethoxycurcumin (curcumin II) and bisdemethoxycurcumin (curcumin III) are the three major curcuminoids present in the commercial Curcumin. The percentage of each curcuminoid present differs. Approximately 77% is comprised of curcumin I with only 17% of curcumin II; curcumin III being the least at about 3% [7]. Curcumin exists in its keto-enol tautomer form as shown in the figure and exhibits limited solubility in water while showing good solubility in organic solvents such as DMSO and chloroform [8]. This property may be responsible for its low bioavailability. Evidence from numerous literature has revealed that curcumin has low bioavailability, poor absorption, low metabolism, and limited biodistribution. Up to 1 g $kg^{-1}$of the body weight is almost completely eliminated by the human metabolic system [9].

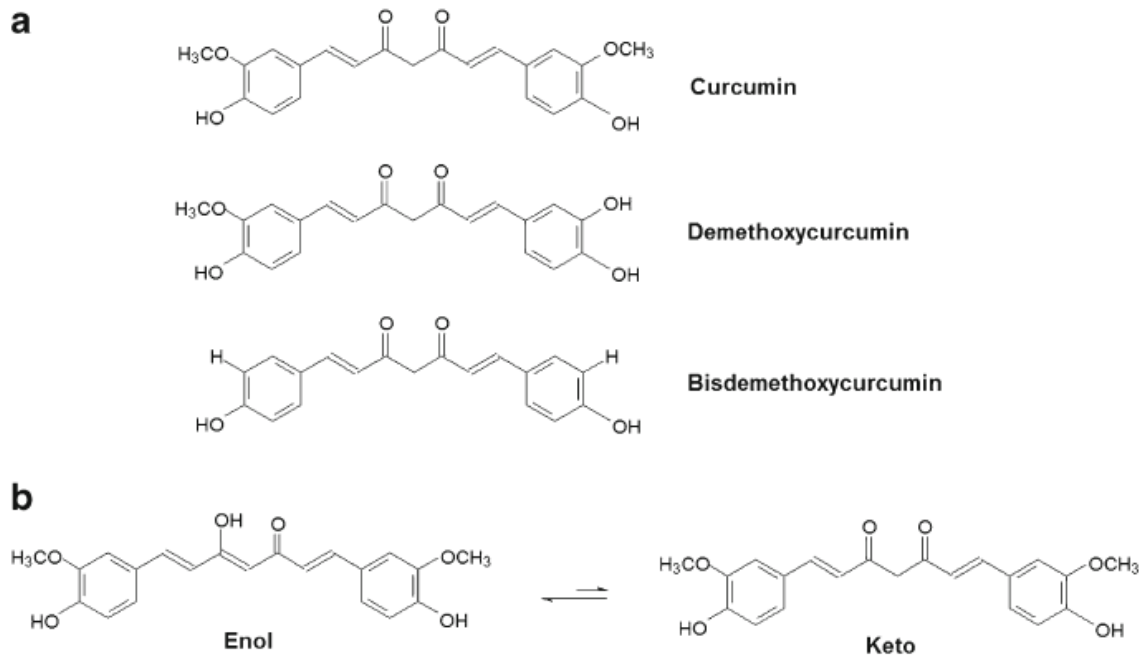

Fig 1: Curcumin I, II, III (curcumin, demethoxycurcumin, and bisdemethyoxy curcumin) and keto-enol tautomers of curcumin. [Image source: Naksuriya et al 2016 [10]]

There is a need of improvising the bioavailability of curcumin a major component turmeric so that maximum utilization of its properties could be done. A wonder drug used by many since ancient times with ample documentation of its therapeutic effects. [1,11]. The properties of turmeric are not limited to only medical ailments but show widespread applications in the field of cosmetics with it being used to maintain skin elasticity and lighten skin tone [12]. Curcumin is a yellow coloured pigment and a major functional constituent (2-5%) of Turmeric [13,14].

The widespread clinical applications of curcumin have led to multiple attempts for the formulation and usage of it as a biomedicine. However, reduced solubility in aqueous medium and the resultant poor absorption coupled with rapid metabolism and systemic elimination have been major setbacks in such attempts; poor bioavailability of curcumin aggravates these issues [15,16].

Continuous research on curcumin has found some possible ways to overcome the above mentioned problems. (Table 1) is a summary of research work done over curcumin to improve its solubility in water and enhance its efficiency

Table 1: Re-formulation of Curcumin for enhanced Bioavailability

Formulation	Reference	Formulation	Reference
Nanosuspension	Gao *et al*, 2011[17]	PEGylated curcumin analogs	Pandey 2011[18]
Aqueous formulation	Gao *et al*, 2010[19]	Curcumin-loaded MPEG-PCL	Wang *et al*, 2013[20]
Nanoemulsion	Zhongfa *et al*, 2012[21]	Aqueous PLGA nanoparticlate	Nair *et al*, 2012[22]
pH-sensitive nanoparticles	Dandekar *et al*, 2010[23]	Curcumin loaded cellulose nanoparticles	Yallapu *et al*, 2012[24]
Curcumin TRC-NPs	Rejinold *et al*, 2011[25]	Curcumin-loaded nanoparticles	Peng *et al*, 2014[26]
Curcumin-loaded carbon nanotubes.	Li *et al*, 2013[27]	Curcumin PLGA-b-PEG-TPP	Marrache *et al*, 2012[28]
Curcumin co-solvent formulation	John *et al*, 2013[29]	Curcumin MPEG-PCL micelles	Gong *et al*, 2013[30]
Curcumin PCL-PEG-PCL	Feng *et al*, 2012[31]	Curcumin-PHEMA-NPs	Kumar *et al*, 2013[32]
Liposomal curcumin	Agarwal *et al*, 2013[33]	Curcumin loaded alginate foams	Hegge *et al*, 2011[34]
Lipid-based oral formulation	Pawar *et al*, 2012[35]	Cyclodextrin-curcumin	Thuillier *et al*, 2014[36]
Curcumin-decorated nanoliposomes	Mourtas *et al*,2011[37]	Curcumin-loaded cationic liposome	Saengkrit *et al*, 2014[38]
Curcumin loaded solid lipid nanoparticles	Sun *et al*, 2013[39]	Pluronic-curcumin formulation	Singh *et al*, 2012[40]
Curcumin Lipid nanoemulsion	Anuchapreeda et al., 2012[41]	Acidic sophorolipid and curcumin (SL(A) + Cur)	Kumar Singh *et al*, 2014[9]

[Modified table: Source: Sahdeo *et al*,2014[42]]

1.2 Degradation products of Curcumin

Including poor solubility, curcumin is also known to be highly unstable in aqueous solution and go through hydrolysis and forms molecular fragments. This adds as another limitation for curcumins therapeutic use. These fragments viz., dihyrdroferulic acid and ferulic acid are speculated to be having biological activity as their presence in the bile of rat administered with curcumin was observed. These compounds were also found to be more soluble than the parent compound [43, 44]. Although, many of such degradation products have been identified, the amount of research indicating their biological activity remains an open question. Few reports suggest the bioactive role of degradation products of curcumin but when compared with curcumin intact they are considerably less active.

It is established that curcumin has poor metabolic stability and solubility thus making it hard to accept the observed various biological activities like anti-cancer, anti-oxidant, and anti-inflammatory are because of curcumin or its degradation products. Yet many studies show that the metabolites of curcumin have less or no biological activity compared to curcumin. Curcumin rapidly degrades via two method, alkaline hydrolysis and autoxidation. The hydrolysis products are viz., vanillic acid, ferulaldehyde, ferulic acid and feruloyl methane which are minor products. On other hand, autoxidation results in a more stable and major product called bicyclopentadione formed via radical mediated process. Studies have shown that vanillin and ferulic acid do posses anti-cancer, anti-inflammatory activity but the concentration required to achieve this is quite high when compared with curcumin. Regardless, studies have found the traces of vanillin and ferulic acid when orally dosed with curcumin for desired activity. This indicates that curcumin does degrade *in vivo* and the degradation products might have some role in biological activity posed by curcumin. Shen et al., reported based on their experimental and theoretical findings propose that the degradation products are the main bioactive compounds rather than curcumin depending on its solubility and stability. Bicyclopentadione are not studied widely for their biological relevance but a report suggests it for the topoisomerase poisoning activity of curcumin [43–48]

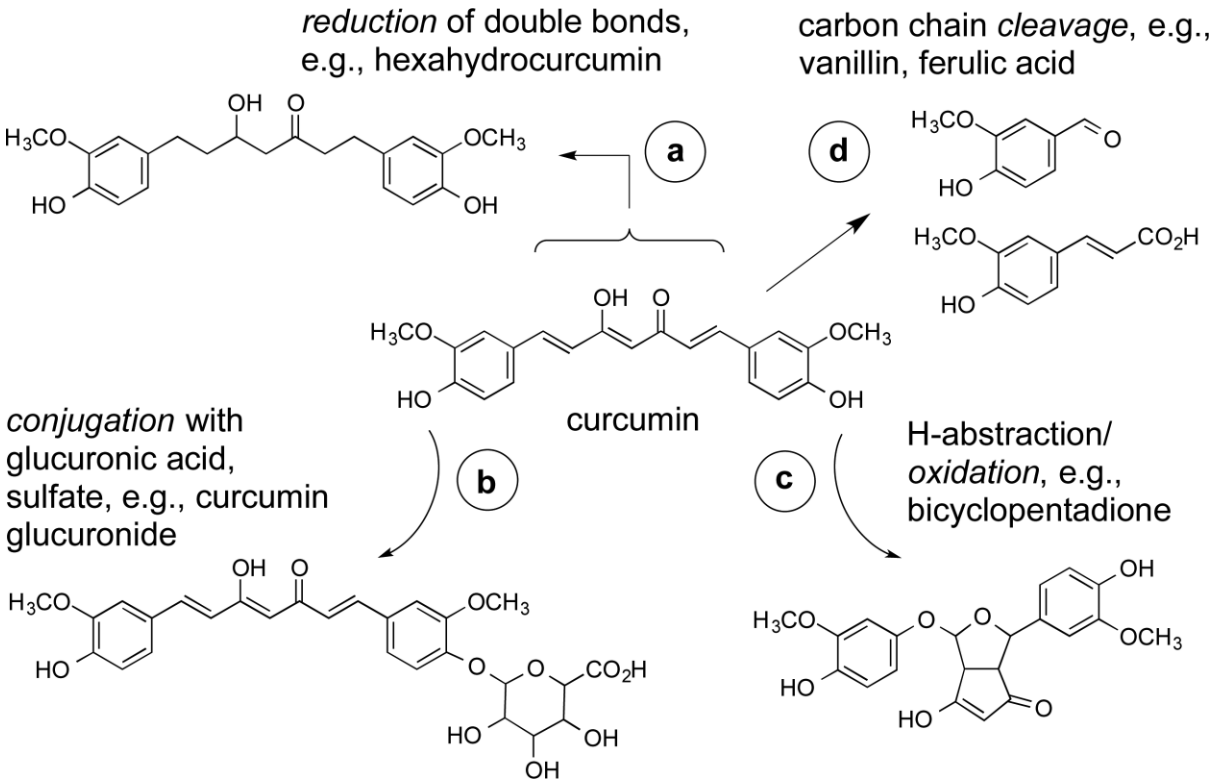

Fig 2: The metabolic and degradation pathways of curcumin. (a) Reduction; (b) conjugation; (c) oxidation; and (d) cleavage. [Image source: Claus Schneider**,** 2015[48]]

1.3. Sophorolipid

Sophorolipids are amphiphilic in nature with hydrophilic head made up of sophorose and hydrophilic tail made up of fatty acid chain. This property allows sophorolipid to solubilize into surface membranes and improves the bioavailability of any molecule such as a drug attached to it. Sophorolipids are made of sophorose head and fatty acid chain. The two glucose units in sophorose are linked via a unique β 1-2 linkage that may or may not is acetylated with one or two acetyl groups. The fatty acid chain is typically C16-18 long with varying degrees of saturation. During synthesis, if a hydrophobic carbon source is not provided, the organisms form fatty acids *de novo* via acetyl-CoA pathway. The fatty acids are then oxidized at the terminal (ω) or subterminal (ω − 1) position by a cytochrome P450 mono-oxygenase enzyme. These results into formation of hydroxylated fatty acids that are β-glycosidically linked to a first glucose molecule at the 1'-position by a glycosyltransferase I. A second glucose molecule is linked to the 2'-position of the first one by a glycosyltransferase II, yielding sophorolipid acid. [49-52] There are two basic structures of sophorolipid viz., the open chain acidic SL and the closed chain lactonic SL. The proportion

of acidic and lactonic in crude SL depends on many factors like organisms used for production, carbon, nitrogen and salt sources in medium, environmental conditions, temperature, agitation, pH, aerations, dissolved oxygen etc[49] Sophorolipids display properties and advantages which are comparable to or even better than other surfactants (chemical or biosynthesized). Some of these advantages are listed as follows [49,53]:

- Environmental compatibility.
- High biodegradability.
- Low toxicity.
- Higher tolerance to a broad range of temperature, pH and salinity conditions.
- Eco-friendly.
- Follow the approach of Green chemistry.

1.4. The Scope of the study

This study aims to create a Curcumin-Sophorolipid, a compound which will inhibit the setbacks of curcumin solubility to combine the properties of sophorolipid for enhanced medicinal and cosmetic benefits of curcumin. We also anticipate formation of novel compound of curcumin or rather a degradation product of curcumin combined with SL. This is due to the low stability of curcumin in aqueous solutions. The possibilities are immense and we are exploring this aspect to gain further insights in the fascinating molecule known as curcumin. The potential applications of such a compound will be highly beneficial and applicable in the fields of:

- Cosmetics.
- Food Preservation and Enhancement.
- Medical and Pharmaceutical uses.
- Agriculture.

A perfect summarization of the usefulness of this product can be understood by Andy Gescher's [2013][54] statement, "**There is plenty of research life left in the old yellow molecule,**" which clearly outlines the scientific potential that curcumin possesses.

2. Materials and Methodology:

All chemicals and solvents used in this study were of analytical grade and supplied by Himedia Pvt. Ltd. and Merck India Ltd respectively. Curcumin was procured from Sigma.

2.1 Maintenance of Micro-organisms:

For the study, non-pathogenic yeast species *Candida bombicola* (ATCC 22214) was used for the production of sophorolipid. The yeast was maintained on MGYP slants and kept at 4^{o}C until further use. The following composition is of MGYP broth and agar media [Joshi-Navare *et al* 2014][55]. This organism grows best at temperatures of 28^{o}C and is considered as a 'GRAS' organism i.e. 'generally regarded as safe organism'.

Malt Extract	0.3 g%
Glucose	2g%
Yeast Extract	0.3g%
Peptone	0.5g%
Agar	2g%

2.2. Production of Curcumin derived Sophorolipid (CSL)

This is a novel approach in the production of sophorolipid where typically fatty acid substrates are C16-18 in chain length viz., oleic acid, various seed oils, essential oils and other known fatty acids are used for production of SL. Here we will be providing curcumin as a hydrophobic substrate to initiate the synthesis process. For this, loopful of *Candida bombicola* (ATCC 22214) was inoculated in 10ml of MGYP broth and incubated overnight at 28^{o}C under shake flask condition. This pre-inoculum is then added to 90ml of sterile MGYP broth and again incubated at 28^{o}C for 48 hr at 180 rpm. This is to obtain higher cell mass [Joshi-Navare *et al* 2014] [55] Good aeration is an important condition for sophorolipid production as the yeast cells are highly sensitive to oxygen limitation during their exponential growth and therefore use of shake- flask is recommended.

2.3. Resting Cell Method

After 48 h of incubation, the broth containing the yeast cells was centrifuged at 10^{o}C for 20 mins at a speed of 5000 rpm. The cell pellet was collected and re-suspended in 10% of 100 ml glucose medium with addition of 10 mg of curcumin. The production occurs in the stationary phase. *De novo* synthesis of sophorolipid usually happens when *C. bombicola* are

provided with glucose and nitrogen deprived. The fatty acid for SL synthesis is self-synthesised by organism though the amount is very less. This method is called Resting Cell method. The incubation time is nearly 6-7 days after which yellow, viscous product formed, which was seen stuck to the walls of the flask. This product was named CSL and is used throughout this chapter. Fig 3 is the schematic for the production of CSL and the actual flask used for the study.

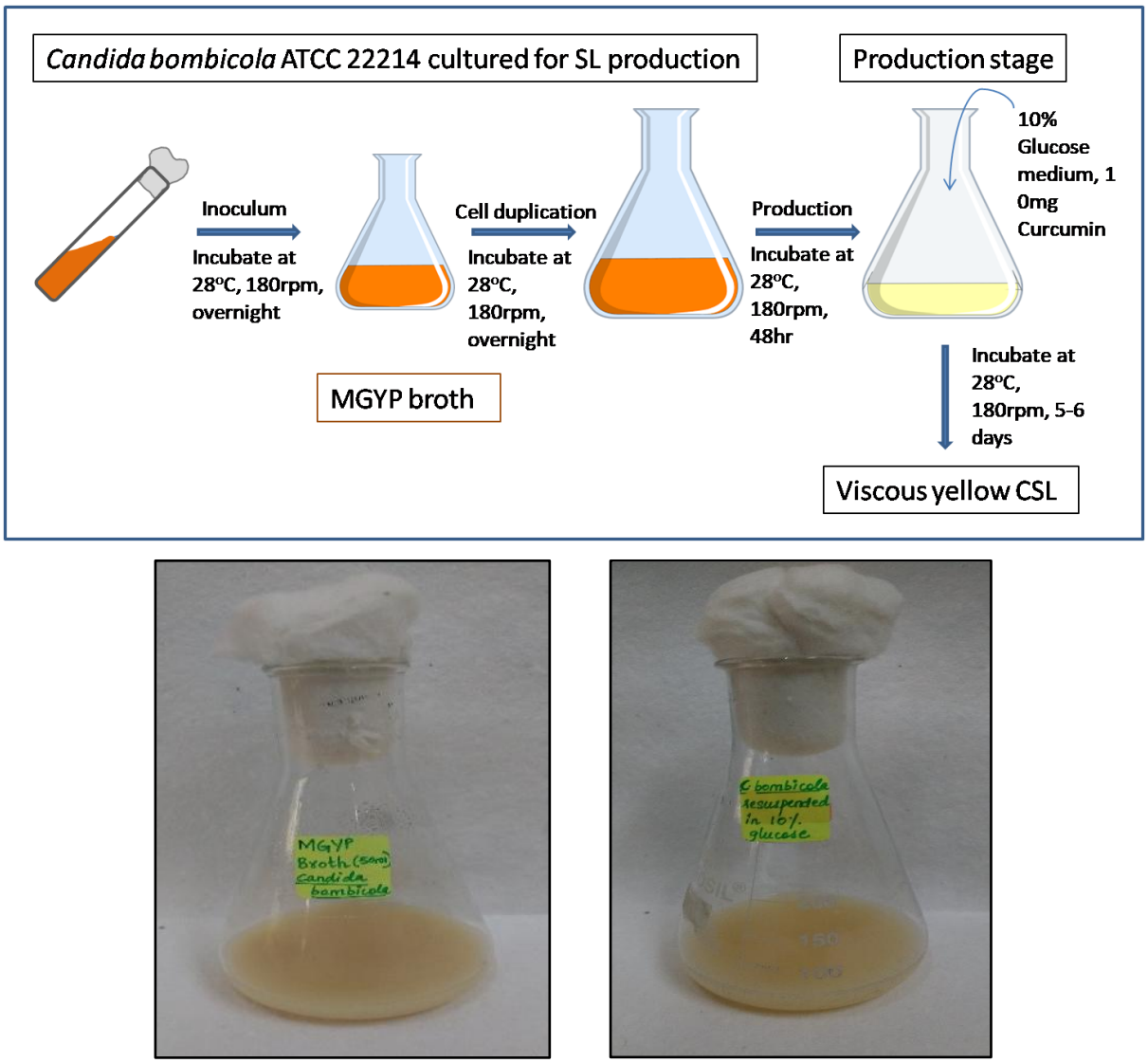

Fig 3: Schematic illustration of production method for CSL (a). Flask containing *C. bombicola* cells in MGYP broth incubated for 48 hours. (b). Re-suspended cells in 10% glucose medium with addition of 10mg Curcumin.

2.4 Extraction of CSL

After the production of CSL, the culture medium was subjected to centrifugation at 5000 rpm, 20mins at 10°C. The visible product i.e. stuck to the flask (Fig 4) is extracted with the

help of ethyl acetate. While the supernatant obtained after centrifugation of cells, containing trace amount of CSL was extracted with a co-solvent method, where a combination of Acetonitrile (ACN) and Ethyl Acetate was used. As ACN is polar in nature, it can extract CSL present in water in a much effective manner than ethyl acetate. Hence the supernatant was first mixed with ACN and then CSL was extracted from ACN into ethyl acetate. Phase separation was observed between water and the organic solvent layer as they are immiscible. The upper phase containing ethyl acetate mixed with CSL was collected and lower phase of water was discarded after repeated extractions. The extraction is carried out using separating funnel. Crystals of sodium sulphate was added to the solution to absorb the moisture content, if any.

Fig 4: The product (CSL) settled at the bottom of the flask

Fig 5: (a) Separation of cell mass from the solvent phase (b) Partially extracted CSL with sodium sulphate crystals.

2.5 Rota-Evaporation and Purging

The solvent was filtered of any sodium sulphate crystals and collected in a round bottom flask. The organic solvent, ethyl acetate was rota-evaporated at 45^{o}C under pressure and the crude CSL product was collected in amber bottles. Further purging was carried out using the inert gas argon to concentrate the product and remove any trace amount of solvent. Fig 6 shows the step wise process for rota-evaporation and Fig 7 represents the concentration and product after purging stored in amber bottle.

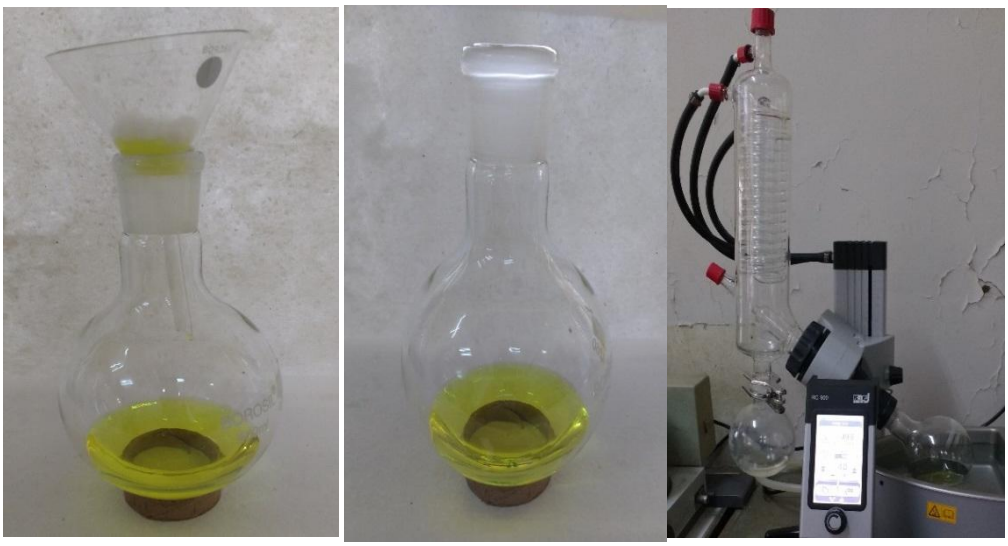

Fig 6: (a) Filtering the partially extracted CSL of any sodium sulphate crystals.(b)The solution before subjecting it to Rota-evaporation (c)Concentrating the extracted product by Rota-evaporation.

Fig 7: (a) The concentrated CSL after rota-evaporation. (b) The final product CSL.(c) Crystallization of CSL.

2.6. Characterization:

2.6.1 Oil displacement:

Oil displacement is a qualitative test used to confirm the surfactant property of the synthesized product. This assay is carried out in petri plate in which 20ml of distilled water is added approximately, and a thin film of oil is made by adding 0.5ml of Karanja oil. After the film was allowed to equilibrate for 1 minute, 40µl of varying concentration of CSL was dropped at the centre of the formed oil film. The diameter of the clear halo formed after displacement of oil was visualized and measured after 10 seconds. Same procedure was repeated for commercially available surfactant SDS. [51]

2.6.2 Thin Layer Chromatography (TLC)

To analyse the components of crude-CSL, TLC of the same was performed. Chromatography is defined as the partition or distribution co-efficient which describes the way in which the compounds distribute it-self between two immiscible phases. Thin layer chromatography is one of the modes of chromatography used to separate the components of the mixture. It consists of a stationary and a mobile phase. The stationary phase is attached to a suitable matrix and the mobile phase moves through the plate due to capillary action [56]. The solvent system used was a mixture of non-polar (chloroform) and polar solvents (Methanol) in the ratio of 90:10. The concentrated CSL was diluted by mixing it with methanol and was loaded on silica-coated plate (Merck DC Kieselgel 60 F254) with the help of a capillary. The plate was immersed in the solvent system. The compounds on the plate were located by charring at 120^{o}C for 4-5 sec after immersing the dried plate in anisaldehyde, a developing reagent. The reason behind using anisaldehyde as developing reagent is that it reacts with specific functional groups and gives a particular colour. Its reaction with allylic alcohols gives a green colour while Phenols react with anisaldehyde to give violet spots. Amines, aldehydes, ketones, carbohydrates and esters react to give blue/red spots.

2.6.3 Surface tension measurement and critical micelle concentration

Surface tension measurements were carried out using Data physics DCAT 11 tensiometer by using Wilhelmy plate method with an accuracy of ±0.2 mN/m at 25 ± 1°C. Initially the instrument was calibrated using water followed by measuring surface tension of different CSL solutions ranging from 0.001mg/mL to 0.2mg/mL (from stock solution of 3mg/mL) in triplicate and average values were taken. The critical micelle concentration (CMC) of CSL

was determined as the lowest concentration beyond which the surface tension value remained constant on the surface tension versus concentration graph.

2.6.4 High-Performance Liquid Chromatography (HPLC)

HPLC is a form of Column Chromatography consisting of a stationary Phase and a Mobile phase. Types of HPLC systems depend on the phase system used in the process. In normal phase chromatography, the stationary phase is hydrophilic and therefore has a strong affinity for hydrophilic molecules in the mobile phase. Reversed-phase high-performance liquid chromatography (RP-HPLC) involves hydrophobicity based separation of molecules. The separation occurs when hydrophobic solute molecules present in the mobile phase bind to the immobilized hydrophobic ligands that are attached to the stationary phase. Elution can proceed either by isocratic conditions where the concentration of organic solvent is constant or by gradient elution whereby the amount of organic solvent is increased over a period of time. The solutes are, therefore, eluted in order of increasing molecular hydrophobicity.

In order to separate individual components of CSL a Reverse Phase C-18 Column was used. The mobile phase comprised of two solvents, Acetonitrile (ACN) and MilliQ water. The sample was prepared by dissolving 10mg of CSL in 1 mL of Acetonitrile. An isocratic system was used with a flow rate of 0.5mL/min. RP-HPLC is a very powerful technique for this analysis because of a number of reasons.

(1) Closely related molecules can be excellently resolved using RP-HPLC under a wide range of chromatographic conditions.
(2) Recovery rate is generally high, so is the rate of productivity.
(3) Even after carrying out repetitive separation, the reproductivity rate is not affected. The credit for this excellent reproductivity rate partly goes to the stability of the sorbent materials under a wide range of mobile phase conditions [57].

Time	Acetonitrile	MilliQ	Flow rate ml/min
30 min	70%	30%	0.5 ml/min

2.6.5 High-Resolution Mass Spectroscopy (HRMS)

CSL synthesized as a mixture was resolved into its individual components using HPLC. The crude CSL and the collected peaks from HPLC were further resolved using LC-High Resolution Mass Spectrometer. Atomic mass nearest to 0.001 mass units can be easily

detected using this technique. Mathematically the mass resolution of a mass spectrometer is defined in parts per million (ppm). The instrument used in this studyis a Hybrid Quadrapole Q-Exactive orbitrap (Thermo Scientific). The sample was prepared by purging the collected peaks obtained from HPLC separation and dissolving them in 500µl of methanol. Operation parameters were as follows:

- Capillary temperature at 320 °C,
- Spray voltage at 3.6 kV,
- S-lens RF level at 50,
- Automatic gain control (AGC) at 1×106,
- Maximum injection time at 120ms, and
- Flow rate was set as 500µL/min [58].

1µl of prepared sample was injected to obtain a full HR-MS scan. Analysis of the mass spectra associated with chromatographic peaks was carried out using Thermo Scientific X calibur software. [M+H+] i.e. hydrogen adducts were calculated for peaks having highest relative abundance values. Putative identification of the mass-to-charge ratio of the CSL structure was possible.

2.6.6 Fourier Transform Infrared Spectroscopy (FTIR)

Fourier transform infrared spectroscopy is a technique used to obtain infrared spectrum of absorption, emission and photoconductivity of solids, liquid and gases. It contains a mathematical operation known as Fourier transformation which converts the time domain signal to frequency domain signal. The technique is less time consuming and has enhanced signal to noise ratio. In FTIR, frequency is conventionally displayed in the form of wave-number .The basic interpretation of an FTIR spectrum leads to the characterization and identification of the sample. The IR spectrum is formed as a result of absorption of electromagnetic radiation at frequencies that correlate to the vibration of specific sets of chemical bonds from within a molecule. Chemical bonds with different strength, bending and torsional characteristics are absorbed at different wavelength and the absorption maxima are specific for a particular linkage [56]. The fundamental requirement for IR activity is that there must be a net change in dipole moment during the vibration. FTIR analysis of CSL was done to analyse the chemical structures of the same.

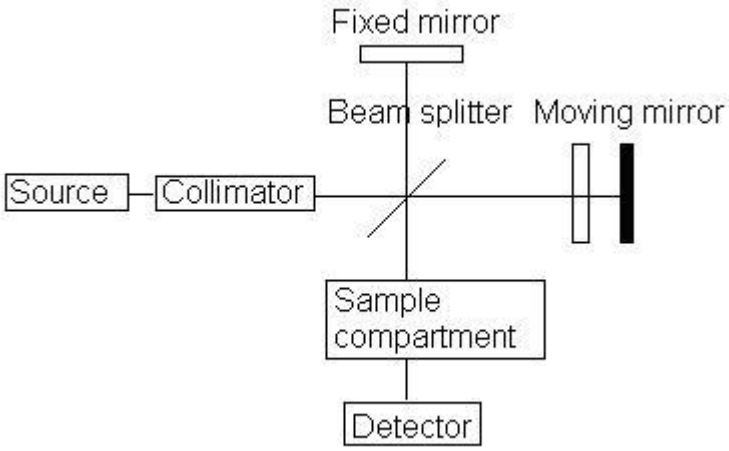

Fig 8: Block diagram of an FTIR spectrometer

2.6.7 Nuclear Magnetic Resonance (NMR)

10mg of CSL and curcumin were dissolved in 1 ml deuterated methanol. These samples were then transferred in NMR tubes and at 200Hz H1 NMR was carried out

2.6.8 Photoluminescence (PL):

Photoluminescence Spectroscopy is a study where the electronic structure of sample to be examined for photoluminescence study is probed in a manner that the sample does not get destructed and a contactless relationship is developed. In this method, light of excess energy is directed onto the sample and the energy is absorbed by the photons, a process called photo-excitation. The photon gets excited due to the absorbed energy. In order to return to this stable ground state, it has to dissipate the acquired energy through emission of light, or luminescence. In this case where photons are photo-excited, the luminescence is called photoluminescence. [59] 4 samples were prepared for carrying out the photoluminescence study. Sample 1 contained 3mg of CSL/3ml of distilled water. Sample 2 was prepared by dissolving 3mg curcumin/3ml of water. Sample 3 and 4 were ethanol preparations, where 3mg of curcumin was dissolved in 3ml of ethanol and 3mg of CSL was dissolved in 3ml of ethanol respectively

2.7. Fluorescence Microscopy

The fluorescence microscope is a technique based on the phenomenon that certain compounds are able to emit fluorescence when irradiated with light of specific wavelength. The basic idea behind the working of fluorescence microscope is to direct light through a filter that lets through the desired wavelength onto the sample that matches the fluorescing compound As a

result, the electrons present in the atoms of the compound get excited and reach a state of high energy level. On reaching the ground state they emit light in form of fluorescence. The regions that are fluorescing can be observed under the microscope and they stand out against a dark background with high contrast.

2.8 Bio-imaging

2 ml of 12 h grown cell culture of *E. coli* and *Cronobacter sakazakii* were taken in a microfuge tube and 1 mg/ml of CSL was added and incubated for 4 h. After incubation the tube was centrifuged and washed two times with water and re-suspended in 2 ml of water. On a slide 10 µl of the solution was drop casted and a cover-slip was placed on top and the edges were sealed. Confocal microscopy was carried out

2.9 Anti-biofilm assay

Pseudomonas aeruginosa was grown for 12 h in Luria bertani broth and diluted to attain an OD of 0.05 at 600 nm for further the experiment. 2 ml of the adjusted culture were added in a sterile petri plate containing a sterile cover-slip. To this CSL was added in concentration from 50, 100 and 150 µg/ml and incubated for 24 h. Control of prestine curcumin with same concentrations of 50, 100 and 150 µg/ml was carried out. After 24 h, the biofilm formed was loosely washed and crystal violet stain 0.1% was added for 5-10 mins. The stain was removed and gently washed with water. Then the cover-slip along with biofilm were placed in a test tube and 1ml of 30% acetic acid solution was added for destaining that can quantify the reduction of biofilm via CSL and Cur. Positive control was only organism while negative control was only media. The OD of the destained crystal violet was taken at 540 nm.

2.10 Antioxidant Activity [DPPH Assay]

The DPPH (2, 2-diphenyl-1-picrylhydrazyl) assay is an anti-oxidant assay based on the theory that the anti-oxidant acts as a hydrogen donor. This method is simple and sensitive. Antioxidants react with DPPH, which is a stable free radical and is reduced to the DPPH-H in presence of an anti-oxidant and as a consequence the absorbance is decreased from the DPPH to the DPPH-H form. The amount of disappearance of the purple colour is directly proportional to the scavenging potential of the anti-oxidant. A change in colour from purple to yellow occurs when DPPH is formed upon absorption of hydrogen from the anti-oxidant.[60]

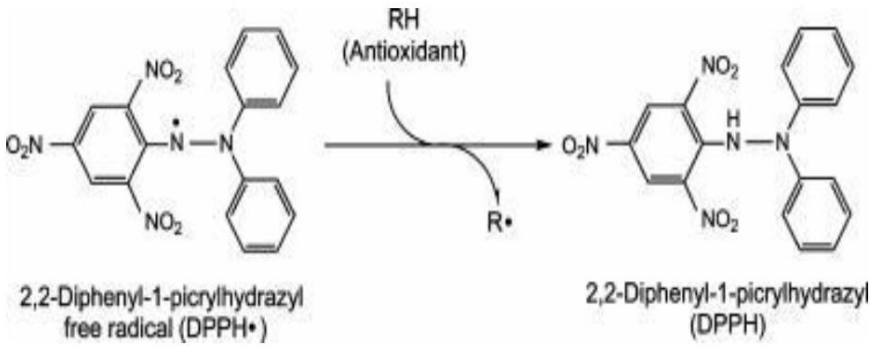

(Purple) (Yellow)

Fig 9: The scavenging reaction between DPPH and an antioxidant (R-H)

[Image source: MacDonald et al, 2006][60]

The reaction was carried out by adding 100µl of DDPH reagent and varying concentration of CSL compound (50µg/ml-500µg/ml) and the total volume of the sample was made 100µl by adding Distilled water. The 96-well microtitre plate containing the total mixture volume of 200µl was incubated for 30 minutes at room temperature in dark conditions. After 30mins of incubation the degree of reduction of the reagent was measured as absorbance using a micro-plate reader (Thermoscientific Varioskan Flash S.No:3001-1908) at 517nm.The reaction was carried out in triplicate and its average reading was calculated.

Percentage of scavenging activity was calculated as:
% scavenging rate= (Absorbance of Control - Absorbance of test/Absorbance of Control)*100

2.11 Anti-Tyrosinase Property

The determination of skin colour is mainly associated with the mix of carotenoids, oxy-/deoxy haemoglobin,types of melanin and its packaging and distribution under the skin layers [61]. Melanosomes are specific ovoid organelles where production of melanin takes place. They are produced in dendritic melanocytes [62]. The Melanin produced within melanosomes is transported with the help of dendrites to adjacent keratinocytes. Accumulation of melanin occurs in perinuclear areas within keratinocyete and melanocyetes as supranuclear “caps” [63].

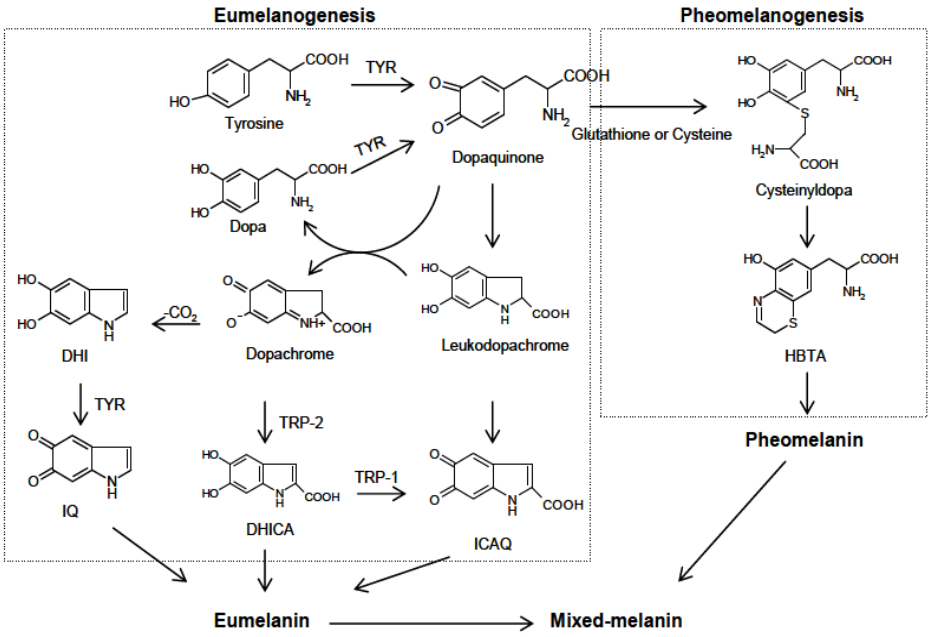

Fig 10: Biosynthetic pathway of melanin synthesis. [Image Source: Chang, T.S, 2009[64]]

TYR: tyrosinase; TRP: tyrosinase related protein; dopa: 3,4-dihydroxyphenylalanine; DHICA: 5,6-dihydroxyindole-2-carboxylic acid; DHI: 5,6-dihydroxyindole; ICAQ : indole-2-carboxylic acid-5,6-quinone; IQ: indole-5,6-quinone; HBTA: 5-hydroxy-1,4-benzothiazinylalanine.

Tyrosine is oxidized to dopaquinone in presence of enzyme Tyrosinase and this initiates the melanogenesis reaction. This reaction is followed by subsequent conversion of dopaquinone to dopa and dopachrome through auto-oxidation. Dopa, also being a substrate of tyrosinase is again oxidized to dopaquinone. Dihydroxyindole (DHI) and dihydroxyindole-2-carboxylic acid (DHICA), the reaction products from dopachrome undergo a series of oxidation reactions to give rise to eumelanin. Pheomelanin is synthesised when dopaquinone is converted to cysteinyldopa or glutathionyldopa in the presence of cysteine or glutathione[64-66]

2.11.1 Role of Melanin

Melanin protects the skin from UV rays and plays a role of photo-protective function in human skin. Melanin also determines our phenotypic appearance. An inverse correlation exists between skin pigmentation and the occurrence of sun-induced skin cancers [67]. The subjects with white skin are 70% more susceptible to develop a sun-induced skin cancer than people with black skin. Two types of melanins occur in mammals, the brownish black is known as eumelanin and the reddish yellow is called pheomelanin. Eumelanin has an excellent shielding property as it serves as a physical barrier that scatters UV rays and also

acts as an absorbent filter reducing the penetration of UV through the epidermis [68].

2.11.2 Deleterious Effect of Melanin

Melanin generally plays a photo-protective role and acts as an excellent protector against photo damage. But, accumulation of abnormal amount of Melanin in specific areas of skin can result in undesirable patches of pigmentation. Also Melanin acts as a photosensitizer and is known to produce ROS after UV radiation [69]. It also causes abnormal pigmentation.

The following are examples of hyper pigmentation:

- Lentigo/Lentigenes - Lentigo is a condition where one freckle is seen; lentigenes is condition where multiple freckles are seen.
- Solar Lentigenes –It is a condition widely known as ‘sun spots,’ ‘age spots’ and ‘liver spots,’ solar lentigenes are freckles caused by sun exposure. It usually appears near the eye region/cheek region due to exposure of sun. Commonly seen in fair skinned subjects.
- Melasma – It is commonly known as the ‘pregnancy mask, It is caused due to hormonal changes during pregnancy and is appears as brown, blotchy, patches.

Skin whitening cosmetics are part of a multi-billion dollar industry with a very high popularity, especially in Asian countries. The basic activity of these creams is to reduce the hyper pigmentation effects and lighten skin tone [70]. Depigmentation agents act at various stages of melanin synthesis. Many of the compounds in these chemicals are known to be competitive inhibitors of Tyrosinase, and they interfere in the synthesis pathway.

Addition of Curcumin as a yellow colour additive in food has been taking place for many years. Turmeric is applied topically as a natural anti-inflammatory agent for wounds, as a face pack for treating acnes and tanning; methods in use since traditional times. Curcumin, an essential component of turmeric has been approved as an additive for its anti-oxidant property in cosmetics for many years [71]. Application of curcumin is demonstrated to be effective against Vitiligo, a skin depigmenting condition and its colourless derivative, tetrahydrocurcumin, was recommended to be used in cosmetics as a lighting agent [72]. Furthermore, it has been reported that some formulated Curcumin analogues have exhibited inhibitory activity against tyrosinase enzyme [73]. Tropolone, L-mimosine, Kojic acid are commonly used as the positive control in the literature in finding new natural inhibitors [64]

2.11.3 Anti-Tyrosinase assay:

Anti-Tyrosinase activity of curcumin was determined according to the method of Rangkadilok with some modification [74]. Briefly, L-tyrosine solution (1.7 mM) was dissolved in phosphase buffer (pH 6.8; 10 ml; 0.1M) and a stock solution of mushroom tyrosinase (5771U) was prepared by dissolving in 500µL pH 6.5 phosphase buffer. Control 1 was prepared by adding 10mg of curcumin/ml of distilled water. Control 2 comprised of 10mg of curcumin dissolved in 1ml of ethanol. Control 3 was prepared by adding 10mg of CSL compound in 1ml of ethanol. Control 4 of ethanol (1ml) was also made. The inhibitor CSL was prepared by dissolving 10mg of CSL/ ml of distilled water. The reaction was carried out in 96 well microtitre plate. The reaction proceeded with addition of the inhibitor CSL of varying concentration (250µg/ml-500µg/ml) to the buffer (pH 6.5), followed by addition of 9µl of Tyrosinase enzyme (100units/500µl) from the enzyme stock solution. Control of Curcumin in ethanol and water, CSL in ethanol, control without inhibitor, and control without enzyme was carried out in the same way. After incubation for 10mins, 40µl of tyrosine was added and the mixture was incubated at room temperature for 30mins in dark. The absorbance of the reaction was recorded at 475nm using amicro plate-reader (Thermoscientific Varioskan Flash S.No:3001-1908)

The percentage inhibition of tyrosinase was calculated by the following equation:
Anti − tyrosinase activity (%) = (Abscontrol – Abs sample/Abs control)* 100
Where, Abs control is absorbance of control at 475 nm, Abs sample is absorbance of sample at 475 nm.

2.12 Anti-cancer activity

Curcumin has been extensively studied for its anti-angiogenic, anti-inflammatory, wound healing, antioxidant, and anti-cancer activities because of its medicinal proper ties in Indian and Chinese medicine. Furthermore, recent studies have revealed that curcumin, either alone or in combination with other anticancer agents, can efficiently induce apoptosis. Apoptosis is a closely regulated process of programmed cell death, where the activation of various molecules for initiating cell death occurs. Specific activation of apoptosis in cancer cells presents a potential approach for cancer therapy. Nonetheless, the mechanisms of curcumin-induced Cytotoxicity still remain a controversial topic, since curcumin is insoluble and less stable in solutions. [13, 75]

For the cell viability study, we chose L6 cell line (rat myoblasts) cultured in T75 tissue culture flasks and for anti-cancer activity HeLa a cervical cancer cell line and MCF-7 a breast cancer cell line were selected. All the mentioned cell lines were procured from National Centre for Cell Science (NCCS), Cell Repository, Pune. All cell lines were grown in Dulbecco's Modified Eagle's Medium (DMEM). The media were supplemented with 10% fetal calf serum and the cell lines were incubated in a humidified incubator containing 5% CO_2 at 37°C.

For the assay, cells were seeded at the density of 10000 cells/well in a 96 well plate. Once cells adhered (12 h), they were incubated with different concentrations (0.001, 0.010, 0.1, 1 and 10 µg) of CSL and Curcumin for 24 h. An untreated group was kept as a negative control. Wells containing culture medium and MTT solution with no cells was a blank. After the incubation the proliferation rate i.e. cell viability was assessed by MTT assay. Briefly 10 ml of MTT (3-(4, 5- Dimethylthiazol-2-yl)-2, 5-Diphenyltetrazolium Bromide, 5 mg/ ml) was added to each well and incubated at 37^oC for 4 h. The MTT solution was removed and blue formazan crystals were dissolved in 100 ml of DMSO (Dimethyl sulfoxide). The absorbance was recorded at 570 nm using a micro plate reader.

The percentage inhibition was calculated as: % Inhibition = [(OD of control well—OD of treated well)/ (OD of control well—OD of blank)] × 100. All experiments were conducted in triplicates and measurements were re-presented as the average ± standard deviation [77, 76]

3. Results and Discussion:

3.1 Oil displacement:

The oil displacement test helps to measure the diameter of the clear zone/halo that occurs after adding a surfactant-containing solution on an oil film. By measuring the zone diameter, the efficiency of surfactant sample can be found out. The surface activity of the crude CSL was analysed and compared with the standard surfactant such as SDS.

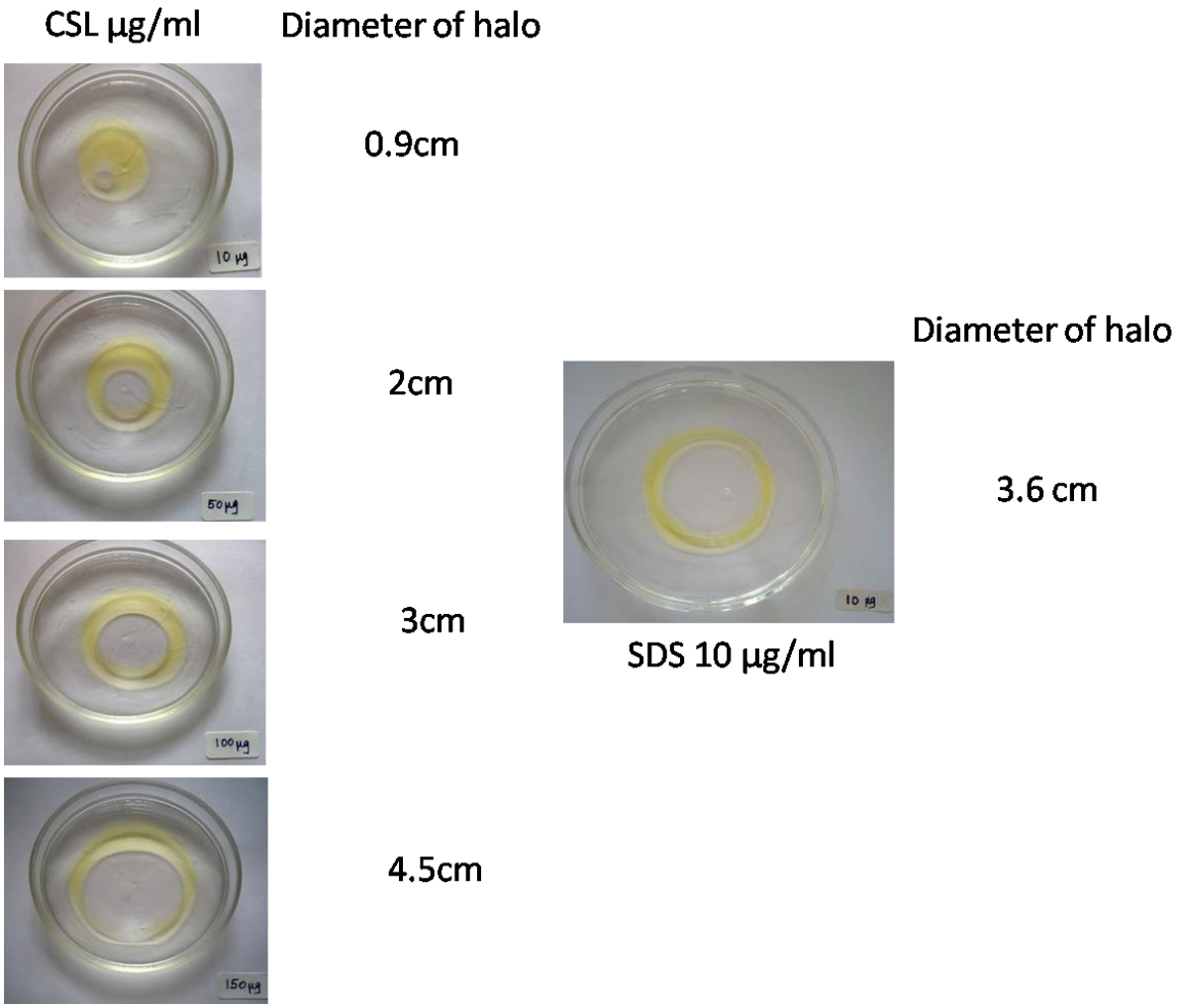

Fig 11: oil displacement activity of CSL, showing detergent property

3.2 Surface tension analysis:

Since the compound showed oil displacement activity, we further wanted to identify its surface tension and critical micelle concentration (CMC). When performed on a range of concentrations i.e. from 0.001 to 0.2 mg/ml, and observed the lowering of surface tension of water from 72mN to 56.75mN at 0.001mg/ml of CSL. The reducing surface tension trend remained till 0.05mg/ml, after which the surface tension remained more or less stable. The lowest concentration at which the surface tension started being stable is considered as its CMC value and this was achieved at 0.025mg/ml. When compared to the oleic acid SL (120mg/L), the CMC of CSL is at very low concentration i.e. 25mg/L. Fig. 12 represents the surface tension reduction and CMC of CSL.

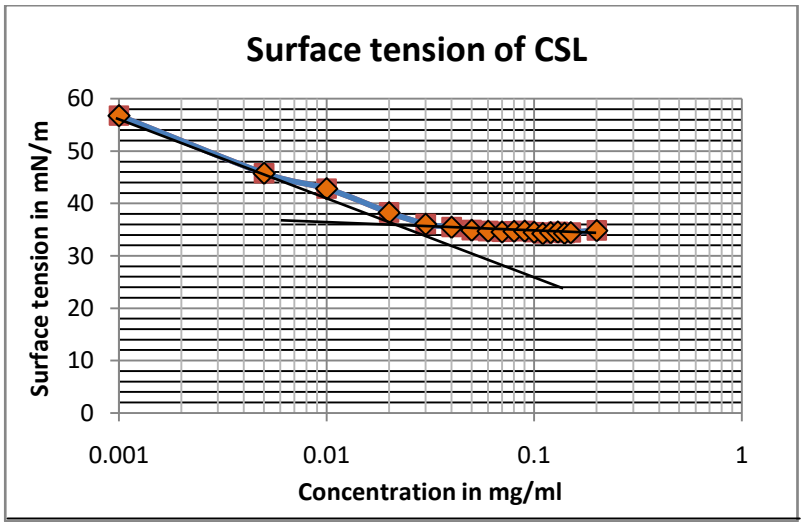

Fig 12: graph displaying the surface tension lowering property of CSL. The CMC was calculated by extrapolating graph to obtain the lowest surface tension started being stable.

3.3 TLC

The initial identification of the components present in CSL is essential to analyse the purity of compound. This primary analysis was completed using TLC.

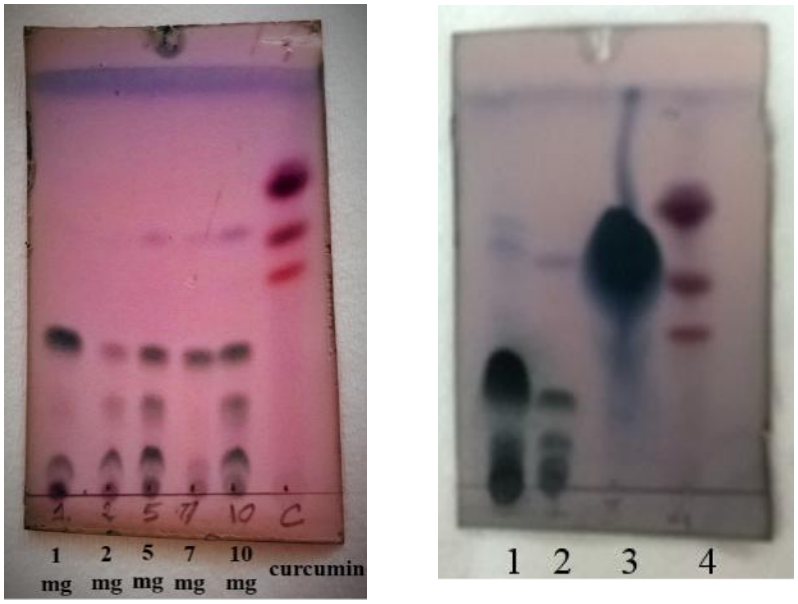

Fig 13 : (a) TLC of Curcumin-Sophorolipid (b) Comparative TLC of OASL and CSL (b) 1: Sophorolipid synthesised from oleic acid (OASL) 2: CSL 3: Oleic acid oil 4: Curcumin

The TLC analysis of crude CSL showed that it is a mixture consisting of different components. Non-polar components migrated more than the polar components. The CSL sample containing 5 mg and 10 mg curcumin showed 4 bands. The Rf value of curcumin obtained was 0.76, 0.63 and 0.51.The TLC plate (Fig 13: b) was a comparative analysis between sophorolipid derived from oleic acid and CSL.

3.4 HPLC:

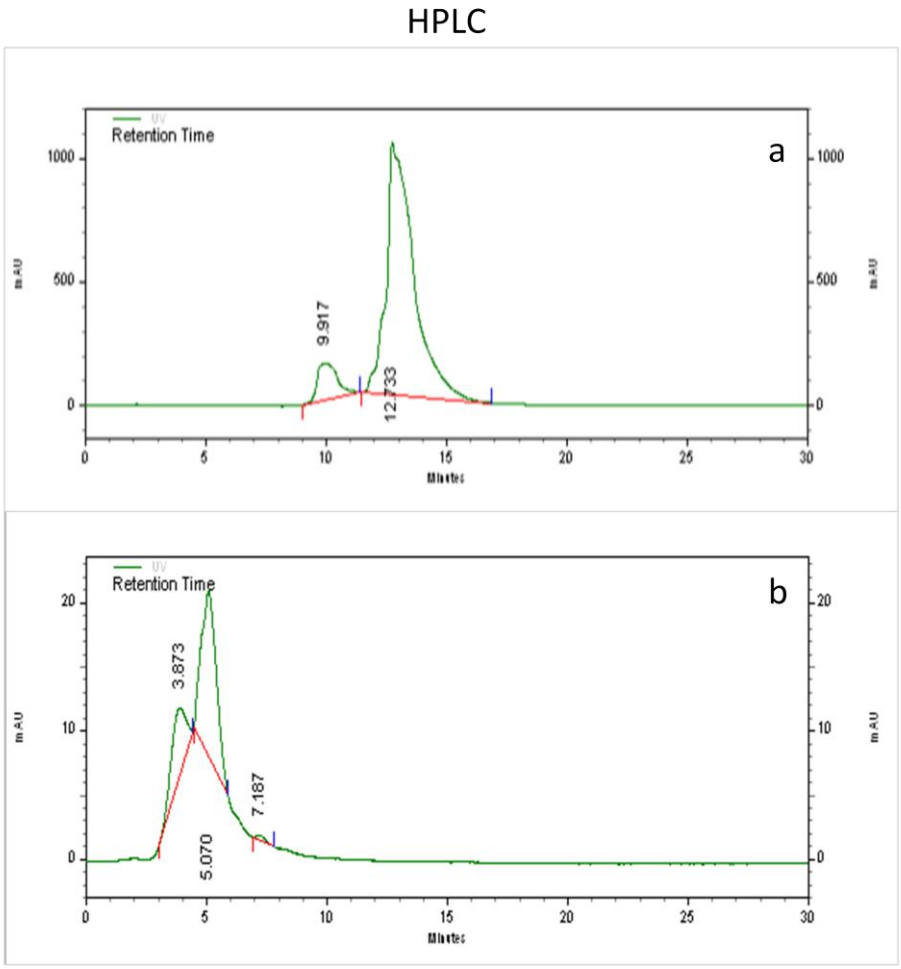

Figure:(a) Chromatogram of Standard Curcumin. (b) Chromatogram of CSL

Fig 14: (a) Chromatogram of Standard Curcumin. (b) Chromatogram of Crude-CSL.

The HPLC chromatogram of Standard curcumin shows a retention time at 12th minute, on the other hand, a shift in the retention time is seen in the CSL chromatogram observed at 5th minute. The CSL compound resolved to give 4 peaks that were collected at their specific retention time.

From the HPLC data it was observed that curcumin does not remain intact, and a different compound is synthesized instead. Based on literature, we assumed the product as degradation of curcumin. Since the literature supports that curcumin is unstable in water and quickly degrades in many forms, we suspect that the CSL synthesis process carried out in 10% glucose medium as detrimental for curcumins stability. So to identify the structure, HR-MS studies were conducted.

3.5 HRMS:

Before performing HR-MS, we did few structure predictions using software called ChemSketch. The molecular formulas were then searched in the chromatogram obtained in HR-MS while analysing. We observed the H+ adduct of seven predicted compounds. These were the known degradation products of curcumin but in conjugation with either deacetylated acidic oleic acid SL or diacetylated acidic oleic acid SL. Hence this became a novel approach in synthesizing a curcumin degradation product with acidic form of SL. The HR-MS graph are given bellow with the predicted structure and probable name.

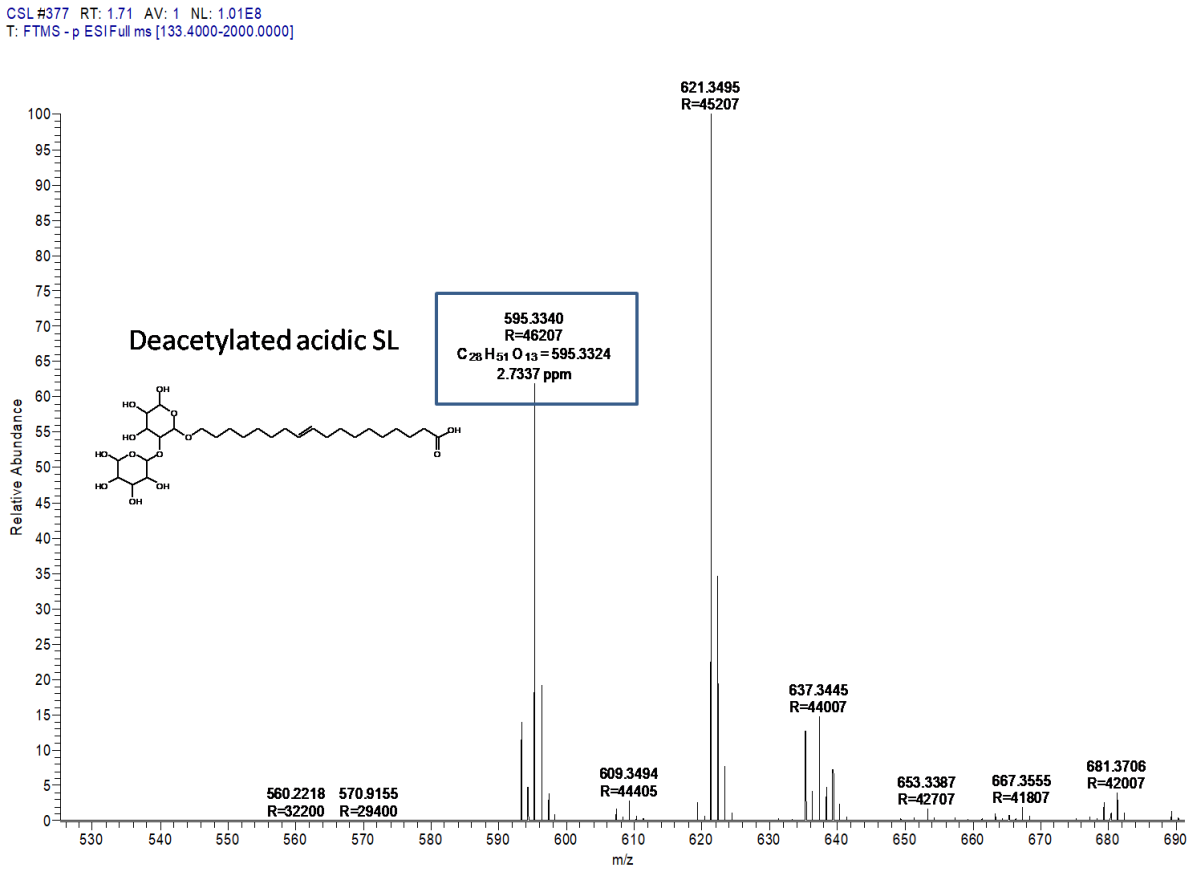

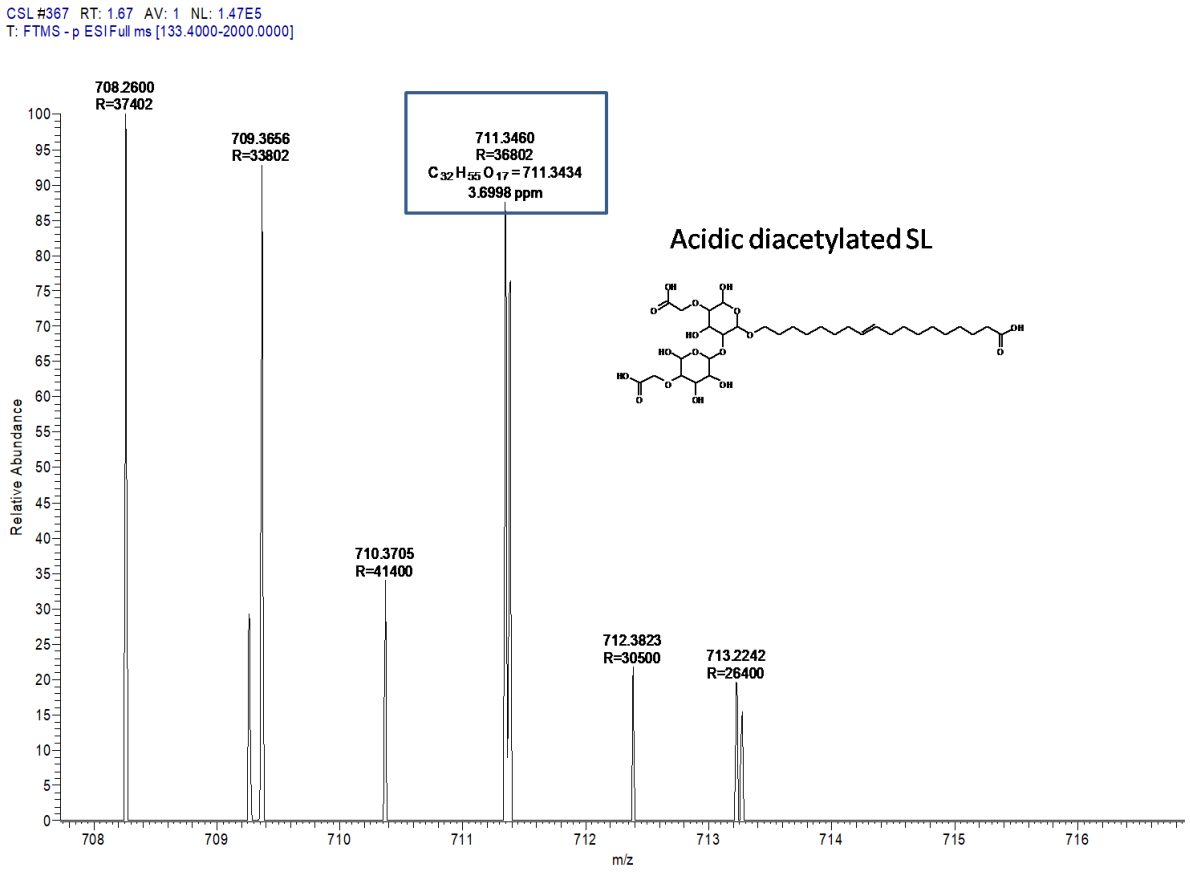
CSL #367 RT: 1.67 AV: 1 NL: 1.47E5
T: FTMS - p ESI Full ms [133.4000-2000.0000]
708.2600
R=37402
709.3656
R=33802
711.3460
R=36802
C32 H55 O17 = 711.3434
3.6998 ppm
710.3705
R=41400
712.3823
R=30500
713.2242
R=26400
Acidic diacetylated SL
Relative Abundance
m/z

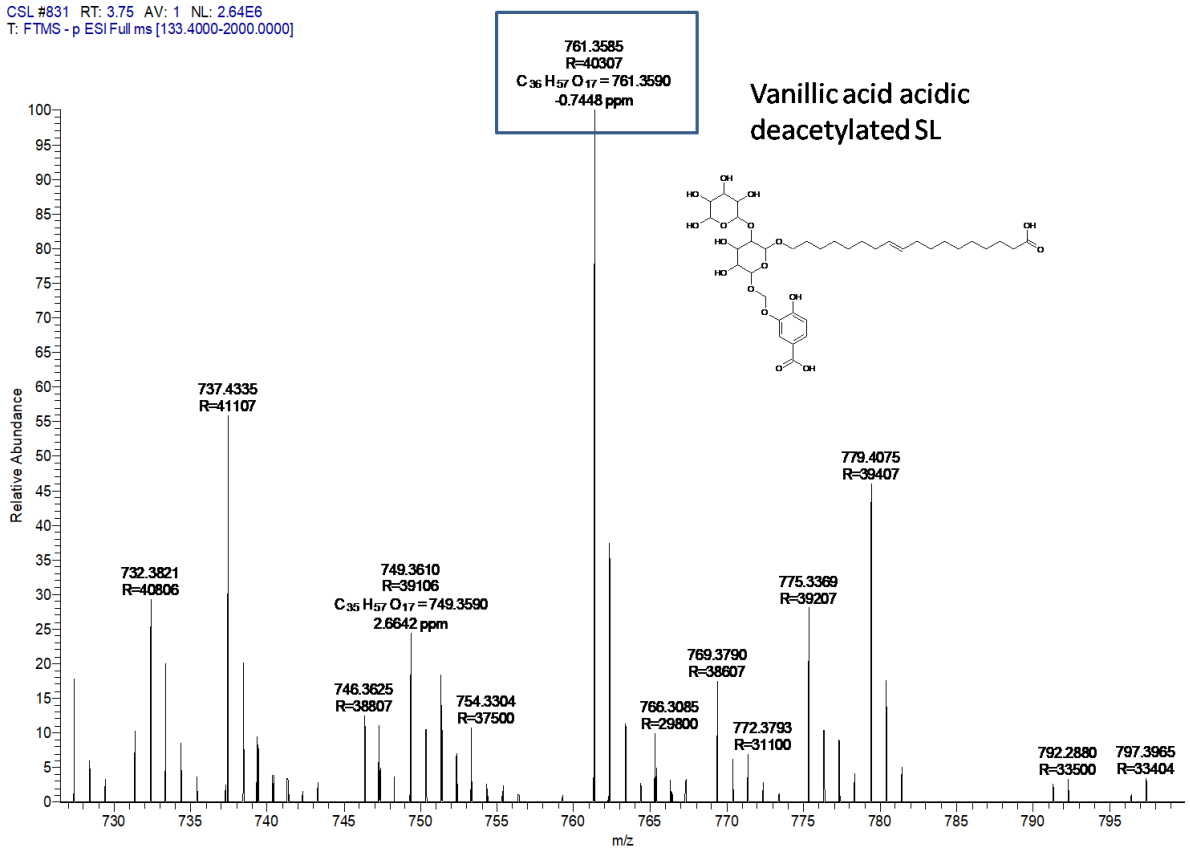
CSL #831 RT: 3.75 AV: 1 NL: 2.64E6
T: FTMS - p ESI Full ms [133.4000-2000.0000]
761.3585
R=40307
C36 H57 O17 = 761.3590
-0.7448 ppm
Vanillic acid acidic
deacetylated SL
737.4335
R=41107
732.3821
R=40806
749.3610
R=39106
C35 H57 O17 = 749.3590
2.6642 ppm
746.3625
R=38807
754.3304
R=37500
766.3085
R=29800
769.3790
R=38607
772.3793
R=31100
775.3369
R=39207
779.4075
R=39407
792.2880
R=33500
797.3965
R=33404
Relative Abundance
m/z

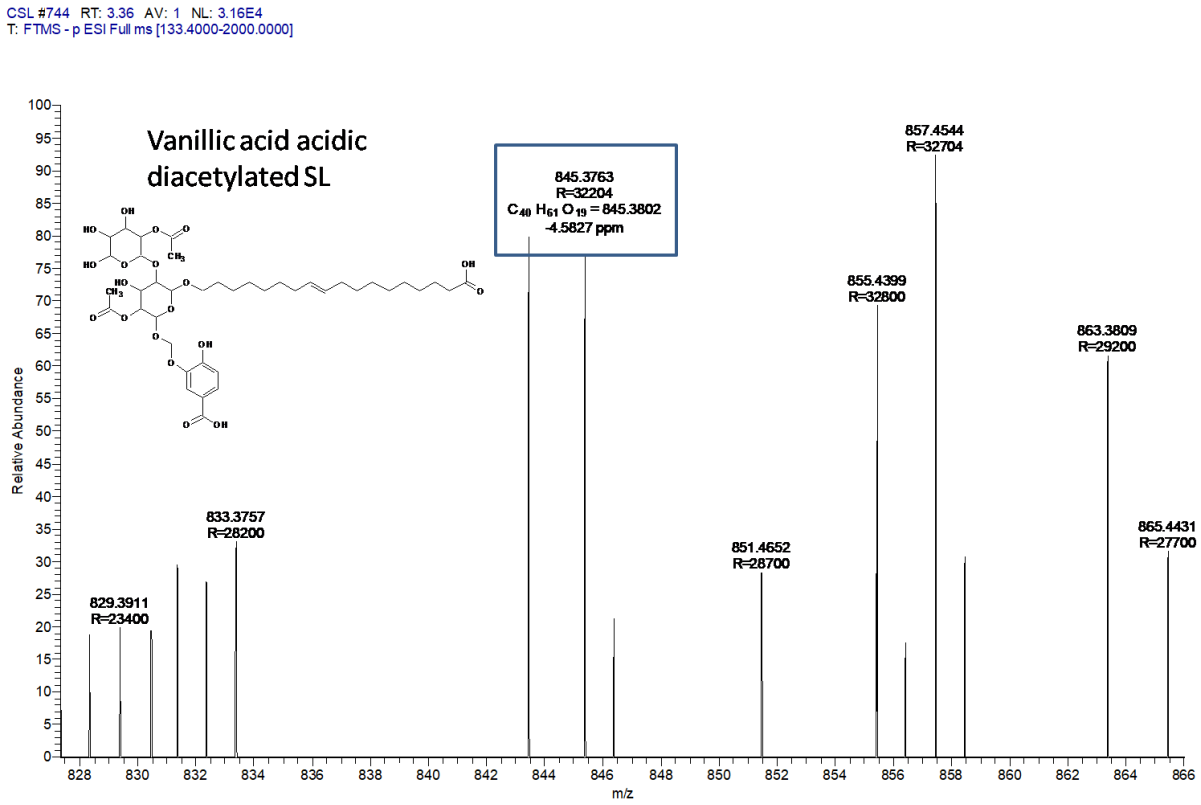
CSL #744 RT: 3.36 AV: 1 NL: 3.16E4
T: FTMS - p ESI Full ms [133.4000-2000.0000]
Vanillic acid acidic diacetylated SL
845.3763
R=32204
C40 H61 O19 = 845.3802
-4.5827 ppm
857.4544
R=32704
855.4399
R=32800
863.3809
R=29200
865.4431
R=27700
851.4652
R=28700
833.3757
R=28200
829.3911
R=23400
Relative Abundance
m/z

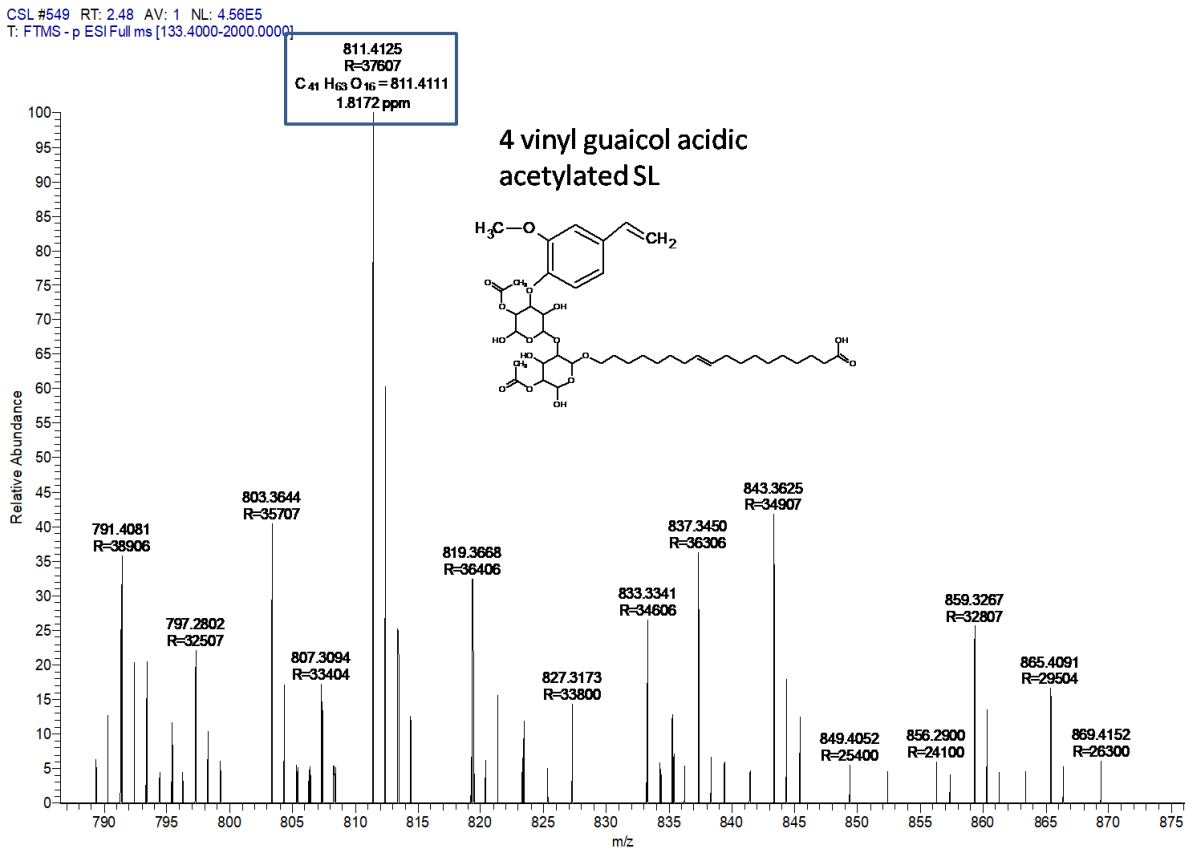
CSL #549 RT: 2.48 AV: 1 NL: 4.56E5
T: FTMS - p ESI Full ms [133.4000-2000.0000]
811.4125
R=37607
C41 H63 O16 = 811.4111
1.8172 ppm
4 vinyl guaicol acidic acetylated SL
803.3644
R=35707
791.4081
R=38906
843.3625
R=34907
837.3450
R=36306
819.3668
R=36406
833.3341
R=34606
859.3267
R=32807
797.2802
R=32507
807.3094
R=33404
865.4091
R=29504
827.3173
R=33800
849.4052
R=25400
856.2900
R=24100
869.4152
R=26300
Relative Abundance
m/z

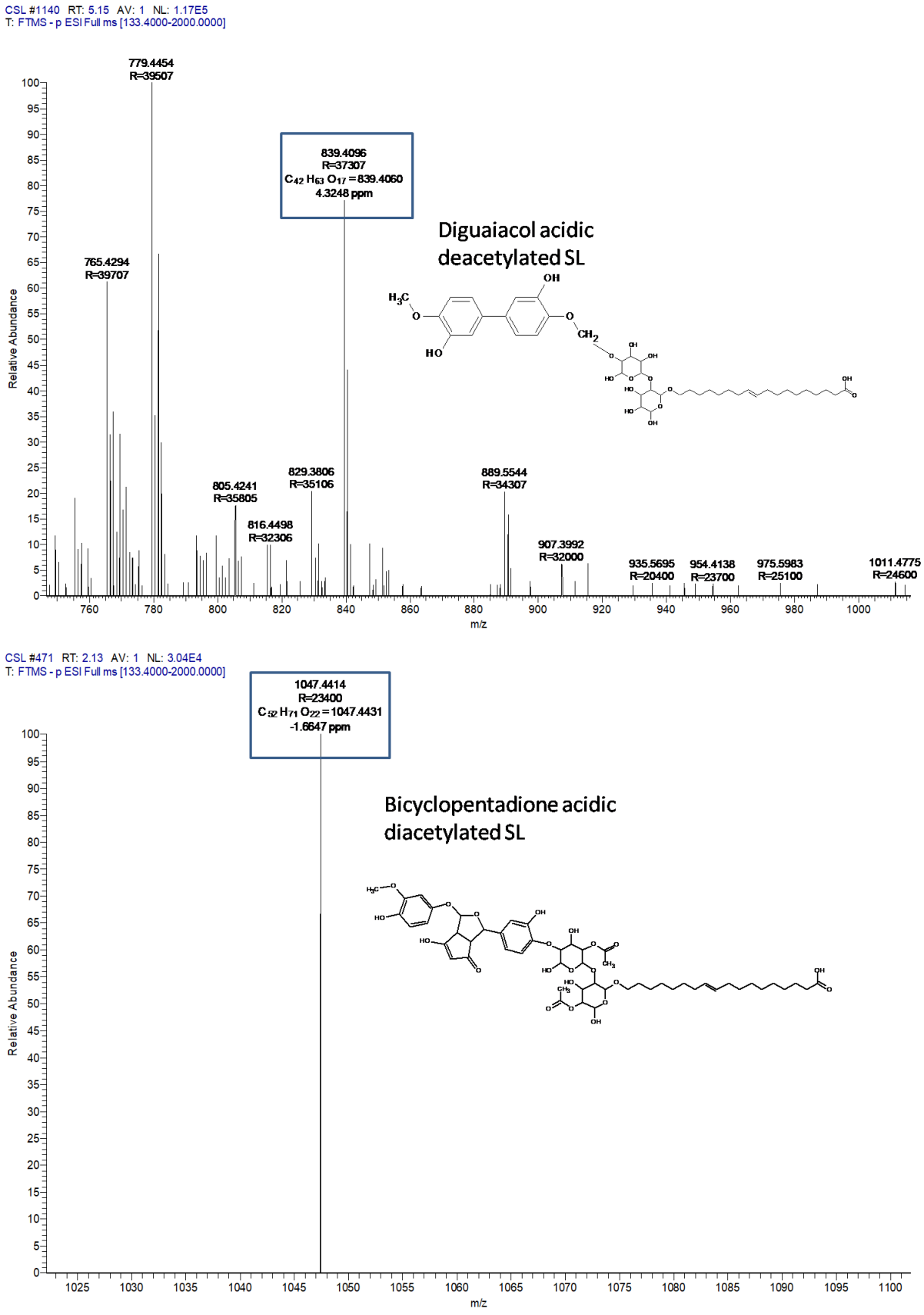

Fig 15: HR-MS spectra showing molecular weight of the seven predicted compounds viz., Deacetylated acidic SL, Acidic diacetylated SL , Vanillic acid acidic deacetylated SL, Vanillic

acid acidic diacetylated SL, 4-vinyl guaicol acidic acetylated SL, Diguaiacol acidic deacetylated SL, and Bicyclopentadione acidic diacetylated SL

In order to obtain further confirmation FTIR and NMR studies was carried out.

3.6 FTIR:

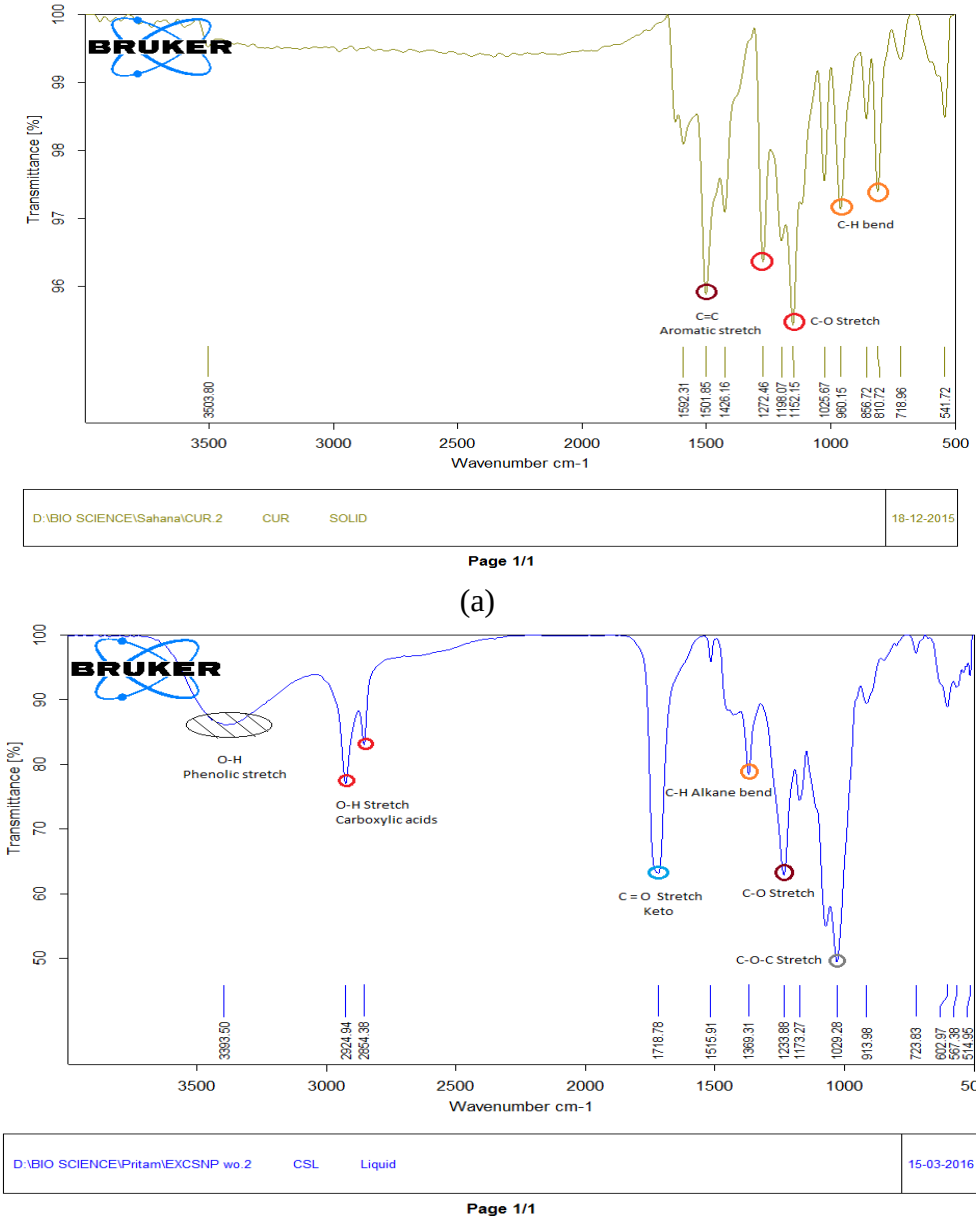

Fig 16: (a) FTIR of Standard Curcumin. (b) FTIR of CSL compound

The FTIR spectra of curcumin and CSL were compared. All essential bonds of curcumin are present in the synthesized CSL molecule. In addition to the curcumin bonds, there are two new bonds observed at 1233^{-1} and 2854^{-1}, 2924^{-1} frequencies which are corresponding to C-O-H bend and OH stretch respectively. This indicates that the parent molecule curcumin has

been modified but not to the greater extent, leaving all the active groups intact. The additional bonds are proposed to be related to the sugar moiety. This makes the CSL soluble in water.

The following **Table 2** gives us the individual peaks and their representation:

Curcumin	**OASL**	**CSL**	**Bonds**
717, 886, 976	783,896	723, 913,	C-H bend
1014, 1119, 1179	1125,1179	1029, 1173,	C-O stretch
		1233	C -O-H bend
1301	1313		C-O stretch
	1380	1369	C-H alkane bend
1412			C-O enol bending
1556	1503,1574	1515	C-C aromatic
1628, 1717		1718	C=O stretch of Keto
	1840		Acid stretch
	2909,2980		Alkane stretch
		2854, 2924	OH stretch
3526	3410	3393	OH phenolic stretch

3.7 NMR

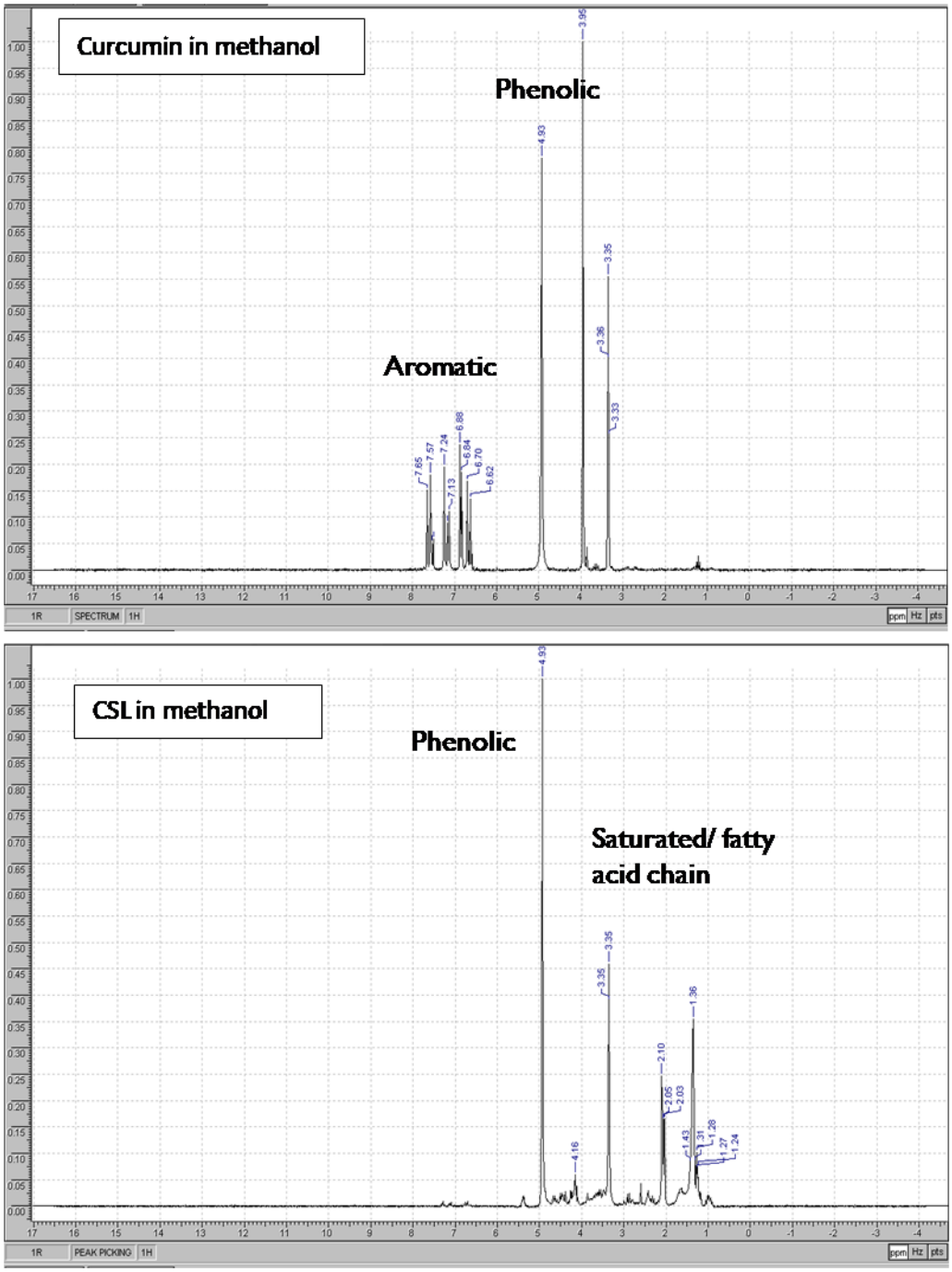

Fig 17: H1 NMR spectra of curcumin and CSL in deuterated methanol

10mg of CSL and curcumin were dissolved in 1 ml deuterated methanol. These samples were then transferred in NMR tubes and at 200Hz nmr was carried out. We could observe phenolic peak present in both Cur and CSL spectra, while an addition of saturated fatty acid peaks observed in CSL indicate the formation of degraded product. The newly formed SL was further tested for activities.

3.8 Photoluminescence:

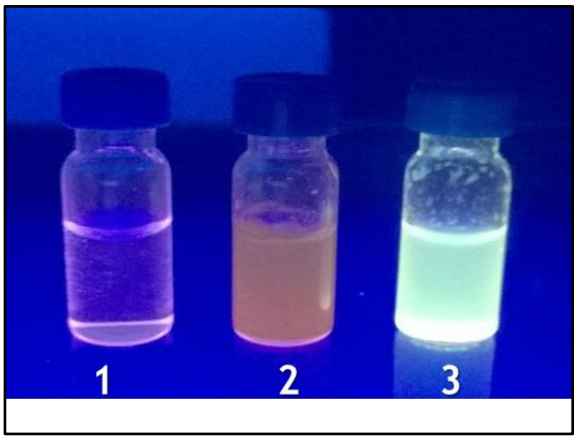

Fig 18: Vials containing sample observed under Ultra-violet light.

1: Only distilled water sample (1mL) 2: Curcumin (5mg) in distilled water (1ml) 3: CSL (5mg) in distilled water (1ml)

Sample 2 containing Curcumin being hydro-phobic in nature, when dissolved in water showed no fluorescence under ultra-violet light due to its low-solubility. Whereas, When CSL is dissolved in water, it emits green fluorescence as the structure of CSL helps in better solubility of the complex in water.

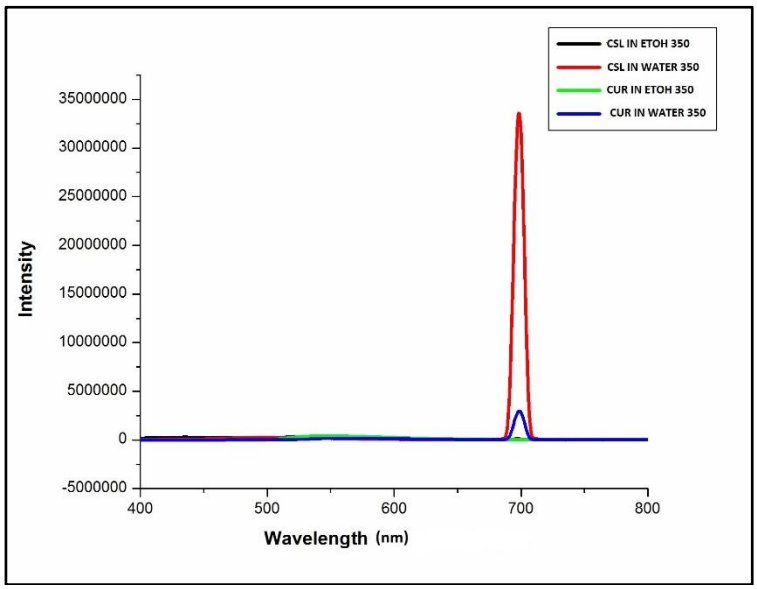

Fig 19: Photoluminescence study of Curcumin and CSL in water and ethanol.

Photoluminescence of CSL sample (1mg/ml in distilled water), CSL (1mg/ml in ethanol), Curcumin (1mg/ml distilled water), curcumin (1mg/ml ethanol) were recorded for comparison on excitation at the same wavelength of 350nm. Curcumin and CSL in ethanol exhibited no PL. Curcumin in water showed low emission at 700 nm, whereas CSL in water

showed strong emission at 700nm. Form previous studies and reports, curcumin is known to show strong emission at 540 nm when excited at 400-420nm[9]. This is due to curcumins absorption at 420nm and when excited near this range, the emission is observed at 520nm. But in case of CSL, the compound is a degraded product and the evidence for PL of such compound is still not available, we need to further confirm these readings.

3.9 Fluorescence Microscopy:

The PL reading of CSL shows strong emission in the range of 700nm when excited at 365nm. A green fluorescence is observed when aqueous solution of CSL is observed under UV light. The fluorescence is not seen in aqueous solution of curcumin. This property of CSL was used for labelling *E. coli* cells as a probe so that green fluorescent organisms can be seen under UV light. For this study, stock solution of 5 mg CSL in distilled water and 5 mg of curcumin in distilled water were prepared. 10 µl of *E. coli* cells was inoculated in 10 ml of Nutrient broth and it was incubated at 37°C for 12- 16 h in shake-flask condition. The pellet obtained after centrifugation of 1 ml of cell culture was re-suspended in 0.5 ml of sterile distilled water. 100 µl of cell culture was added along with 200 µl of CSL solution. A control of curcumin solution with cell culture was also made. The tubes were incubated for 3 h at 37°C and the slides were observed under microscope.

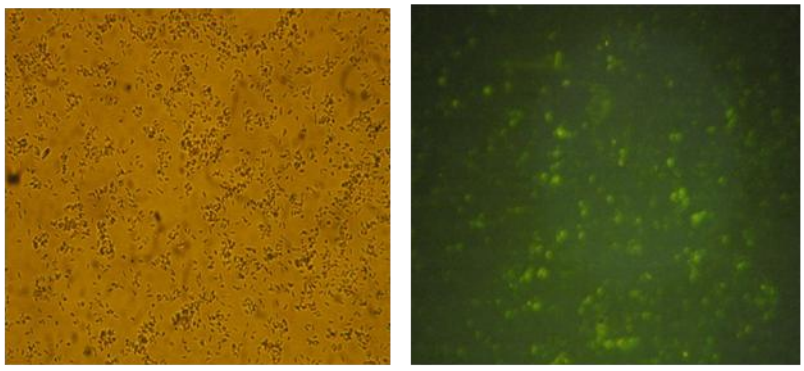

E. coli with CSL in (a) simple and (b) fluorescent microscopy

Fig 20: (a). View of under light microscope (40x) (b) View under blue filter for fluorescent imaging (40x)

The CSL compound was observed to be fluorescent and CSL tagged *E. coli* cells were also fluorescing

3.10 Bio-imaging

For bio-imaging purpose, we chose a food pathogen and an opportunistic pathogen i.e. *Cronobacter sakazakii* and *Escherichia coli* respectively.

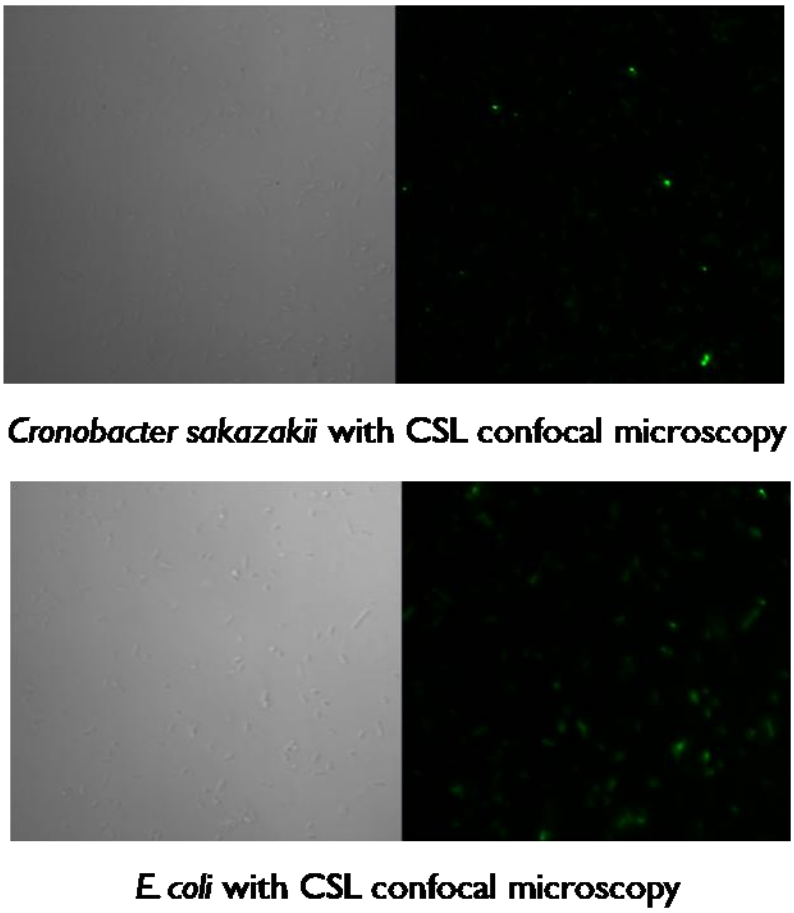

Fig 21: Confocal microscopy

The fluorescence activity of CSL can be explored as bio-imaging dye like material for tracking the progress of drug molecules/nanoparticles towards the target destination. 1mg/ml of CSL was dissolved in water and organisms like *Escherichia coli* and *Cronobacter sakazakii* were individually incubated for 4 h and imaged using confocal microscopy. The results show that the derivatized curcumin goes inside the cells and gives bright fluorescence.

3.11 Anti-biofilm

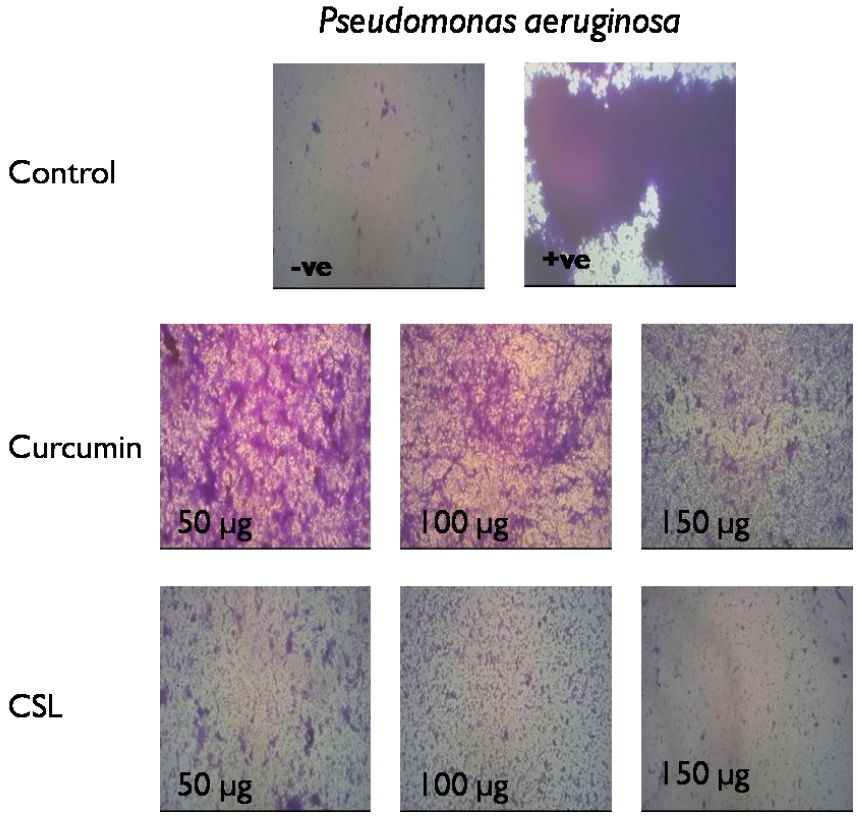

Fig 22: anti-biofilm activity of CSL and Curcumin

From the above figure it can be clearly seen that CSL has better anti-biofilm property than only curcumin. This may be due to curcumins lower solubility and stability in water. The quantitative data is tabulated in following **Table 3**:

Sample µg/ml	Percentage inhibition of biofilm
Negative	100
Positive	0
Cur 50	39.2 ±0.03
Cur 100	48.7±0.02
Cur 150	**51.1**±0.05
CSL 50	65.4±0.03
CSL 100	66.9±0.05
CSL 150	**79.7**±0.02

The quantitative analysis of the stain indicated that at highest concentration studied for the anti-biofilm study i.e. 150µg/ml for both curcumin and CSL, curcumin showed ~50% biofilm

inhibition while CSL could achieve ~80% inhibition at same concentration. Again this can be attributed to the solubility of curcumin in water as opposed to CSL's solubility.

3.12 Anti-Oxidant activity

To check the anti- oxidant activity DPPH assay was performed. 2, 2-dipenyl-1-picrylhydrazyl (DPPH) is a biological free radical violet in colour. The magnitude of anti-oxidation ability of sample can be expressed by their ability to scavenge the free radical. Based on this property, antioxidants present in the sample will turn the free radical into yellow colour. This change of colour from violet to yellow thus indicates that the sample possesses anti-oxidant activity.

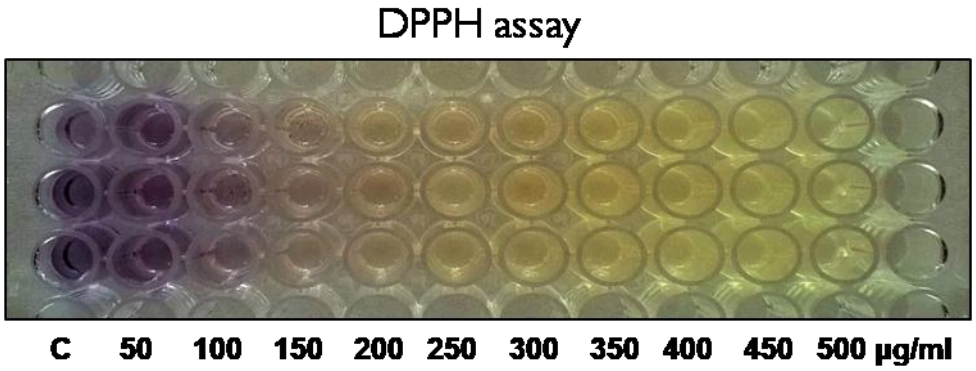

Fig 23: DPPH activity of CSL compound.

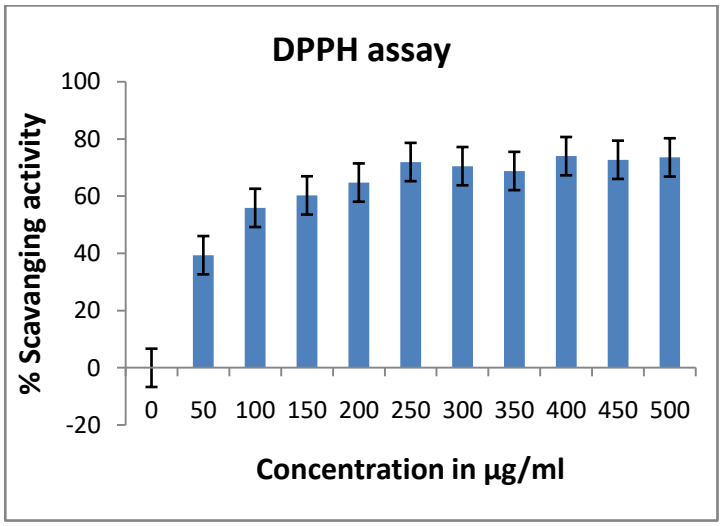

Fig 24: graph representing percent scavenging activity of CSL.

The scavenging activity of more than 60% starts at concentration 200µg/ml remains in increasing trend. The highest concentration tested i.e. of 500 µg/ml showed nearly 75% scavenging activity.

3.13 Anti-Tyrosinase assay

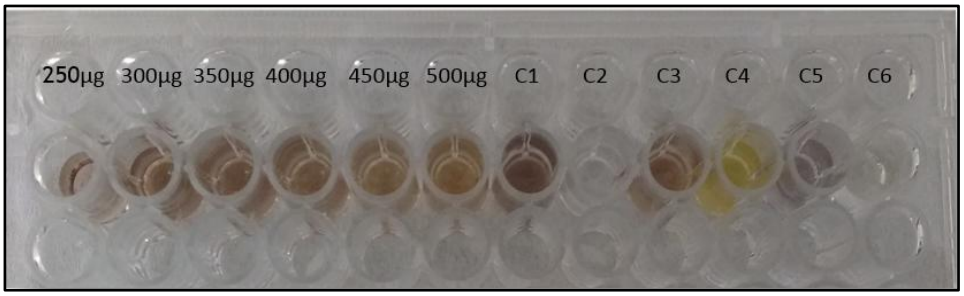

(a)

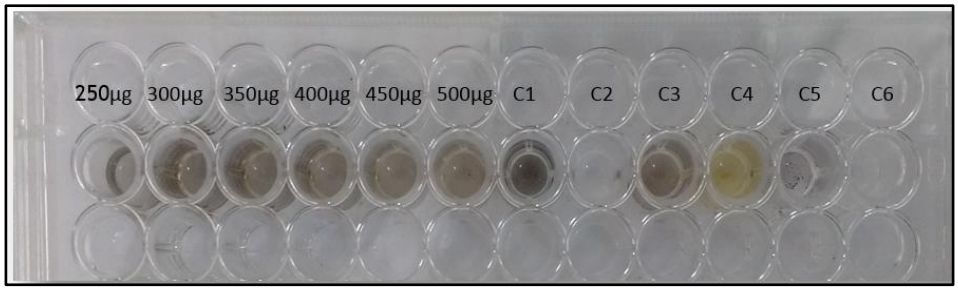

(b)

Fig 25: (a) The plate observed after 30 mins (b) The plate observed after 24 hours. C1: No inhibitor C2: No enzyme C3: Curcumin in water C4: Curcumin in ethanol C5: Ethanol C6: CSL in ethanol

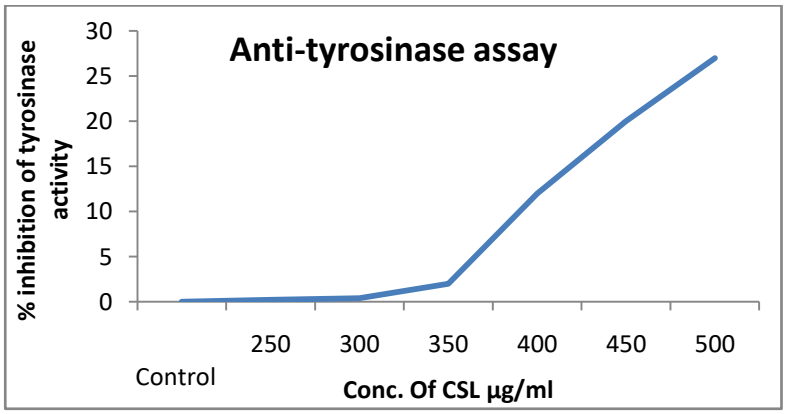

Fig 26: percent inhibitory activity graph of Tyrosinase activity of CSL.

The percent inhibitory activity of tyrosinase at the highest concentration of CSL compound (500 µg/ml) was observed to be 27%. The inhibitory activity of the CSL is effective even after 24 hours [Fig 25 (b)].

CSL is synthesized by natural method without use of any toxic chemicaland both Curcumin and sophorolipid are bio-compatible with human keratinocytes and fibroblasts. This compound with further modification can be used in formulations for preparation of lotions and face-washes acting as a depigmenting agent.

3.14 Cell viability and anti-cancer study

For the study, we used very low concentrations of curcumin and CSL (0.001, 0.01, 0.1, 1 and 10 µg) and observed that, CSL was actually helping the L6 cells to proliferate while curcumin showed some toxicity towards L6 cells. The IC50 values were calculated and observed that curcumin had IC50 of 56.52 µg/ml and comparatively normal cells can tolerate slightly higher concentration of 81.145 µg/ml of CSL. Fig 25 represents the cell viability of CSL and curcumin on L6.

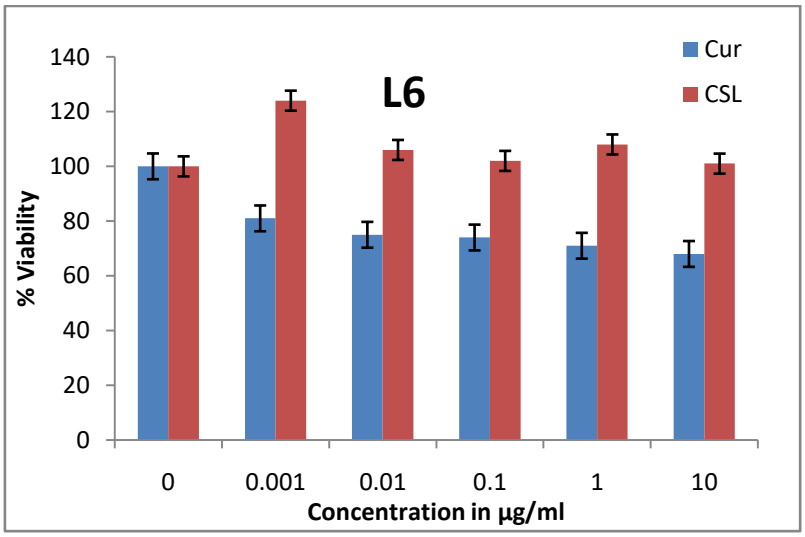

Fig 27: Toxicity study on L6 cell line. Curcumin shows detrimental effect with increasing concentration, while CSL helps in cell proliferation.

When same concentrations were tested on MCF-7 and HeLa cell lines, quite the opposite trend was observed. Curcumin actually helped in proliferation of MCF-7 cells while showed slight inhibition on HeLa cells. While, the CSL showed inhibition activity on both the cell lines indicating its effectiveness against cancer. The IC50 of curcumin for MCF-7 and HeLa were 224.62 and 32.37 µg/ml respectively. The IC50 for CSL were 40.782 and 17.94 µg/ml for MCF-7 and HeLa.

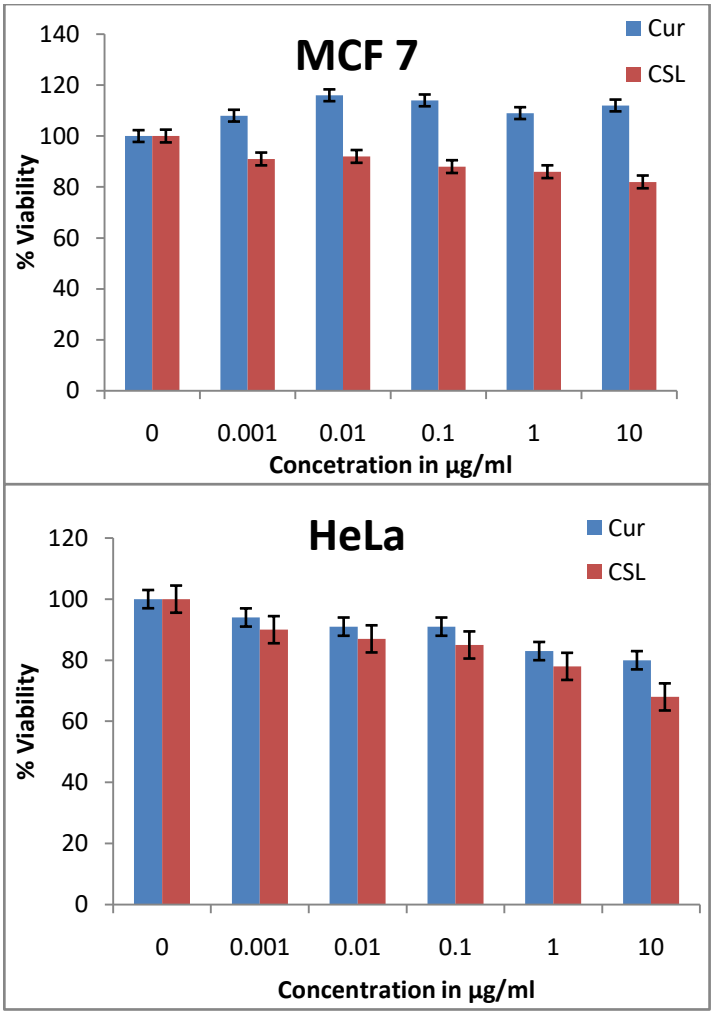

Fig 28: MTT assay of curcumin and CSL against cancer cell line MCF-7 and HeLa

From this study, we observed that more detailed cell studies are required on this compound. Although we confirmed the compound as degradation product of curcumin attached to SL, the reports for activity and this kind of study are scarce.

Conclusion:

To conclude, we were able to successfully bio-transform curcumin into sophorolipid attached molecule. It is quite possible that curcumin got degraded within few hours of addition into the production medium, but the organism *C. bombicola* was able to attach the degraded product to *de novo* synthesized acidic form C18 of sophorolipid. This in a way value added the degradation product and showed application as an anti-oxidant, anti-tyrosinase, anti-cancer and for theranostic application like microbial bio-imaging and anti-biofilm activity. The compound was identified as five degradation products and two forms of SL viz., diguaiacol acidic deacetylated SL , 4 vinyl guaicol acidic acetylated SL , Vanillic acid acidic diacetylated SL, Vanillic acid acidic deacetylated SL, Bicyclopentadione acidic diacetylated SL,

Deacetylated acidic SL, and Acidic diacetylated SL. Although all the activities and characterization done in this chapter are a collective effect of these compounds, a more detailed study needs to further the understanding of CSL.

References:

1. Hatcher H, Planalp R, Cho J, Torti FM, Torti S V. Curcumin: From ancient medicine to current clinical trials. *Cell Mol Life Sci*. 2008;65(11):1631-1652. doi:10.1007/s00018-008-7452-4.
2. MacGregor HE. Out of the spice box , into the lab.2006:1-3.
3. Nair KPP. Neutraceutical Properties of Turmeric. *Agron Econ Turmeric Ginger*. 2013:179-204. doi:10.1016/B978-0-12-394801-4.00012-0.
4. Pandeya NK. Old Wives ' Tales : Modern Miracles — Turmeric as Traditional Medicine in India. *Trees Life J*. 2005;1:3.
5. Aggarwal BB, Bhatt ID, Ichikawa H. Curcumin-Biological and Medicinal Properties. *Tumeric: The Genus Curcuma*. 2006:297-368.
6. Tilak JC, Banerjee M, Mohan H, Devasagayam TPA. Antioxidant availability of turmeric in relation to its medicinal and culinary uses. *Phyther Res*. 2004;18(10):798-804. doi:10.1002/ptr.1553.
7. Verma SP, Goldin BR, Lin PS. The inhibition of the estrogenic effects of pesticides and environmental chemicals by curcumin and isoflavonoids. *Environ Health Perspect*. 1998;106(12):807-812.
8. Payton F, Sandusky P, Alworth WL. NMR study of the solution structure of curcumin. *J Nat Prod*. 2007;70(2):143-146. doi:10.1021/np060263s.
9. Singh PK, Wani K, Kaul-Ghanekar R, Prabhune A, Ogale S. From micron to nano-curcumin by sophorolipid co-processing: highly enhanced bioavailability, fluorescence, and anti-cancer efficacy. *RSC Adv*. 2014;4(104):60334-60341. doi:10.1039/C4RA07300B.
10. Naksuriya O, van Steenbergen MJ, Torano JS, Okonogi S, Hennink WE. A Kinetic Degradation Study of Curcumin in Its Free Form and Loaded in Polymeric Micelles. *AAPS J*. 2016;18(3):777-787. doi:10.1208/s12248-015-9863-0.
11. Ishita C, Khaushik B. Turmeric and Curcumin: Biological Actions and Medical Applications (Review). *Curr Sci*. 2004;87(1):44-50.
12. Jagannathan R, Abraham PM, Poddar P. Temperature-Dependent Spectroscopic Evidences of Curcumin in Aqueous Medium: A Mechanistic Study of Its Solubility and Stability. *J Phys Chem B*. 2012;116(50):14533-14540. doi:10.1021/jp3050516.
13. Duvoix A, Blasius R, Delhalle S, et al. Chemopreventive and therapeutic effects of curcumin. *Cancer Lett*. 2005;223(2):181-190. doi:10.1016/j.canlet.2004.09.041.
14. Morimoto T, Sunagawa Y, Kawamura T, et al. The dietary compound curcumin inhibits

p300 histone acetyltransferase activity and prevents heart failure in rats. *J Clin Invest*. 2008;118(3):868-878. doi:10.1172/JCI33160.

15. Garcea G, Jones DJL, Singh R, et al. Detection of curcumin and its metabolites in hepatic tissue and portal blood of patients following oral administration. *Br J Cancer*. 2004;90(5):1011-1015. doi:10.1038/sj.bjc.6601623.
16. Anand P, Kunnumakkara AB, Newman RA, Aggarwal BB. Bioavailability of Curcumin: Problems and Promises. *Mol Pharm*. 2007;4(6):807-818. doi:10.1021/mp700113r.
17. Gao Y, Li Z, Sun M, et al. Preparation and characterization of intravenously injectable curcumin nanosuspension. *Drug Deliv*. 2011;18(2):131-142. doi:10.3109/10717544.2010.520353.
18. Pandey MK, Kumar S, Thimmulappa RK, Parmar VS, Biswal S, Watterson AC. Design, synthesis and evaluation of novel PEGylated curcumin analogs as potent Nrf2 activators in human bronchial epithelial cells. *Eur J Pharm Sci*. 2011;43(1-2):16-24. doi:10.1016/j.ejps.2011.03.003.
19. Gao Y, Li Z, Sun M, et al. Preparation, characterization, pharmacokinetics, and tissue distribution of curcumin nanosuspension with TPGS as stabilizer. *Drug Dev Ind Pharm*. 2010;36(10):1225-1234. doi:10.3109/03639041003695139.
20. Wang BL, Shen YM, Zhang QW, et al. Codelivery of curcumin and doxorubicin by MPEG-PCL results in improved efficacy of systemically administered chemotherapy in mice with lung cancer. *Int J Nanomedicine*. 2013;8:3521-3531. doi:10.2147/IJN.S45250.
21. Zhongfa L, Chiu M, Wang J, et al. Enhancement of curcumin oral absorption and pharmacokinetics of curcuminoids and curcumin metabolites in mice. *Cancer Chemother Pharmacol*. 2012;69(3):679-689. doi:10.1007/s00280-011-1749-y.
22. Nair KL, Thulasidasan AKT, Deepa G, Anto RJ, Kumar GSV. Purely aqueous PLGA nanoparticulate formulations of curcumin exhibit enhanced anticancer activity with dependence on the combination of the carrier. *Int J Pharm*. 2012;425(1-2):44-52. doi:10.1016/j.ijpharm.2012.01.003.
23. Dandekar P, Dhumal R, Jain R, Tiwari D, Vanage G, Patravale V. Toxicological evaluation of pH-sensitive nanoparticles of curcumin: Acute, sub-acute and genotoxicity studies. *Food Chem Toxicol*. 2010;48(8-9):2073-2089. doi:10.1016/j.fct.2010.05.008.
24. Mohan Yallapu M, Ray Dobberpuhl M, Michele Maher D, Jaggi M, Chand Chauhan S.

Design of Curcumin loaded Cellulose Nanoparticles for Prostate Cancer. *Curr Drug Metab*. 2012;13(1):120-128. doi:10.2174/138920012798356952.

25. Sanoj Rejinold N, Muthunarayanan M, Divyarani V V., et al. Curcumin-loaded biocompatible thermoresponsive polymeric nanoparticles for cancer drug delivery. *J Colloid Interface Sci*. 2011;360(1):39-51. doi:10.1016/j.jcis.2011.04.006.
26. Peng SF, Lee CY, Hour MJ, et al. Curcumin-loaded nanoparticles enhance apoptotic cell death of U2OS human osteosarcoma cells through the Akt-Bad signaling pathway. *Int J Oncol*. 2014;44(1):238-246. doi:10.3892/ijo.2013.2175.
27. Li H, Zhang N, Hao Y, et al. Formulation of curcumin delivery with functionalized single-walled carbon nanotubes: Characteristics and anticancer effects in vitro. *Drug Deliv*. 2014;21(5):379-387. doi:10.3109/10717544.2013.848246.
28. Marrache S, Dhar S. Engineering of blended nanoparticle platform for delivery of mitochondria-acting therapeutics. *Proc Natl Acad Sci*. 2012;109(40):16288-16293. doi:10.1073/pnas.1210096109.
29. John MK, Huan XIE, Bell EC, Liang D. Development and pharmacokinetic evaluation of a curcumin co-solvent formulation. *Anticancer Res*. 2013;33(10):4285-4292. doi:0250-7005/2013.
30. Gong C, Deng S, Wu Q, et al. Improving antiangiogenesis and anti-tumor activity of curcumin by biodegradable polymeric micelles. *Biomaterials*. 2013;34(4):1413-1432. doi:10.1016/j.biomaterials.2012.10.068.
31. Feng R, Song Z, Zhai G. Preparation and in vivo pharmacokinetics of curcumin-loaded PCL-PEG-PCL triblock copolymeric nanoparticles. *Int J Nanomedicine*. 2012;7:4089-4098. doi:10.2147/IJN.S33607.
32. Kumar SSD, Surianarayanan M, Vijayaraghavan R, Mandal AB, Macfarlane DR. Curcumin loaded poly(2-hydroxyethyl methacrylate) nanoparticles from gelled ionic liquid - In vitro cytotoxicity and anti-cancer activity in SKOV-3 cells. *Eur J Pharm Sci*. 2014;51(1):34-44. doi:10.1016/j.ejps.2013.08.036.
33. Agarwal NB, Jain S, Nagpal D, Agarwal NK, Mediratta PK, Sharma KK. Liposomal formulation of curcumin attenuates seizures in different experimental models of epilepsy in mice. *Fundam Clin Pharmacol*. 2013;27(2):169-172. doi:10.1111/j.1472-8206.2011.01002.x.
34. Hegge AB, Andersen T, Melvik JE, Bruzell E, Kristensen S, Tønnesen HH. Formulation and bacterial phototoxicity of curcumin loaded alginate foams for wound treatment applications: Studies on curcumin and curcuminoides XLII. *J Pharm Sci*.

2011;100(1):174-185. doi:10.1002/jps.22263.

35. Pawar YB, Purohit H, Valicherla GR, et al. Novel lipid based oral formulation of curcumin: Development and optimization by design of experiments approach. *Int J Pharm*. 2012;436(1-2):617-623. doi:10.1016/j.ijpharm.2012.07.031.
36. Thuillier R, Allain G, Giraud S, et al. Cyclodextrin curcumin formulation improves outcome in a preclinical pig model of marginal kidney transplantation. *Am J Transplant*. 2014;14(5):1073-1083. doi:10.1111/ajt.12661.
37. Mourtas S, Canovi M, Zona C, et al. Curcumin-decorated nanoliposomes with very high affinity for amyloid-β1-42 peptide. *Biomaterials*. 2011;32(6):1635-1645. doi:10.1016/j.biomaterials.2010.10.027.
38. Saengkrit N, Saesoo S, Srinuanchai W, Phunpee S, Ruktanonchai UR. Influence of curcumin-loaded cationic liposome on anticancer activity for cervical cancer therapy. *Colloids Surfaces B Biointerfaces*. 2014;114:349-356. doi:10.1016/j.colsurfb.2013.10.005.
39. Sun J, Bi C, Chan HM, Sun S, Zhang Q, Zheng Y. Curcumin-loaded solid lipid nanoparticles have prolonged in vitro antitumour activity, cellular uptake and improved in vivo bioavailability. *Colloids Surfaces B Biointerfaces*. 2013;111:367-375. doi:10.1016/j.colsurfb.2013.06.032.
40. Singh R, Kristensen S, Tønnesen HH. Influence of vehicle properties and excipients on hydrolytic and photochemical stability of curcumin in preparations containing Pluronics: Studies of curcumin and curcuminoids XLVIII. *Pharmazie*. 2013;68(3):160-169. doi:10.1691/ph.2013.2136.
41. Anuchapreeda S, Fukumori Y, Okonogi S, Ichikawa H. Preparation of lipid nanoemulsions incorporating curcumin for cancer therapy. *J Nanotechnol*. 2012;2012. doi:10.1155/2012/270383.
42. Prasad S, Tyagi AK, Aggarwal BB. Recent developments in delivery, bioavailability, absorption and metabolism of curcumin: The golden pigment from golden spice. *Cancer Res Treat*. 2014;46(1):2-18. doi:10.4143/crt.2014.46.1.2.
43. Shen L, Ji HF. The pharmacology of curcumin: Is it the degradation products? *Trends Mol Med*. 2012;18(3):138-144. doi:10.1016/j.molmed.2012.01.004.
44. Shen L, Liu C, An C, Ji H. How does curcumin work with poor bioavailability ? Clues from experimental and theoretical studies. *Nat Publ Gr*. 2016;(February):1-10. doi:10.1038/srep20872.
45. Sanidad KZ, Zhu J, Wang W, Du Z, Zhang G. Effects of Stable Degradation Products

of Curcumin on Cancer Cell Proliferation and In fl ammation. 2016. doi:10.1021/acs.jafc.6b04343.

46. Tsuda T. Curcumin: An Effective or Deceptive Dietary Factor? Challenges for Functional Food Scientists. *J Agric Food Chem*. 2018;66(5):1059-1060. doi:10.1021/acs.jafc.7b05878.
47. Tsuda T. Curcumin as a functional food-derived factor: Degradation products, metabolites, bioactivity, and future perspectives. *Food Funct*. 2018;9(2):705-714. doi:10.1039/c7fo01242j.
48. Schneider C, Gordon ON, Edwards RL, Luis PB. Degradation of Curcumin: From Mechanism to Biological Implications. *J Agric Food Chem*. 2015;63(35):7606-7614. doi:10.1021/acs.jafc.5b00244.
49. Oliveira MR De, Magri A, Baldo C, Camilios-neto D. Review : Sophorolipids A Promising Biosurfactant and it ' s Applications. 2015;6:161-174.
50. Delbeke EIP, Movsisyan M, Van Geem KM, Stevens C V. Chemical and enzymatic modification of sophorolipids. *Green Chem*. 2015;18(1):76-104. doi:10.1039/c5gc02187a.
51. Darne P, Mehta M, Dubey P, Prabhune A. Bauhinia Seed Oil, a Novel Substrate for Sophorolipid Production. *World J Pharm Pharm Sci*. 2014;3(11).
52. Marchant R, Banat IM. Biosurfactants: A sustainable replacement for chemical surfactants? *Biotechnol Lett*. 2012;34(9):1597-1605. doi:10.1007/s10529-012-0956-x.
53. Banat IM, Franzetti A, Gandolfi I, et al. Microbial biosurfactants production, applications and future potential. *Appl Microbiol Biotechnol*. 2010;87(2):427-444. doi:10.1007/s00253-010-2589-0.
54. Gescher A. Curcumin : Recent insights , novel developments , new. 2013;(paper 5):2013.
55. Joshi-Navare K, Khanvilkar P, Prabhune A. Jatropha oil derived sophorolipids: production and characterization as laundry detergent additive. *Biochem Res Int*. 2013;2013:169797. doi:10.1155/2013/169797.
56. Wilson and Walker. Principles and techniques of biochemistry and molecular biology, seventh edition. *Biochem Mol Biol Educ*. 2011;39(3):244-245. doi:10.1002/bmb.20499.
57. Aguilar M-I. HPLC of Peptides and Proteins. In: *Current Protocols in Protein Science*. Vol 251. Hoboken, NJ, USA: John Wiley & Sons, Inc.; 2001:8.7.1-8.7.40. doi:10.1002/0471140864.ps0807s23.

58. Dubey P, Selvaraj K, Prabhune A. PHYSICO-CHEMICAL, ANALYTICAL AND ANTIMICROBIAL STUDIES OF NOVEL SOPHOROLIPIDS SYNTHESIZED USING CETYL ALCOHOL. 2014;3(3):993-1010. http://www.wjpps.com/admin/assets/article_issue/1396438041.pdf. Accessed September 28, 2014.
59. Sharma A, Schulman SG. Introduction to fluorescence spectroscopy. *Microchem J*. 2000;65(3):353. doi:10.1016/S0026-265X(00)00048-5.
60. MacDonald-Wicks LK, Wood LG, Garg ML. Methodology for the determination of biological antioxidant capacityin vitro: a review. *J Sci Food Agric*. 2006;86(13):2046-2056. doi:10.1002/jsfa.2603.
61. Stamatas GN, Zmudzka BZ, Kollias N, Beer JZ. Non-invasive measurements of skin pigmentation in situ. *Pigment cell Res*. 2004;17(6):618-626. doi:10.1111/j.1600-0749.2004.00204.x.
62. Haass NK, Herlyn M. Normal human melanocyte homeostasis as a paradigm for understanding melanoma. *J Investig Dermatol Symp Proc*. 2005;10(2):153-163. doi:10.1111/j.1087-0024.2005.200407.x.
63. Montagna W, Carlisle K. The architecture of black and white facial skin. *J Am Acad Dermatol*. 1991;24(6):929-937. doi:10.1016/0190-9622(91)70148-U.
64. Chang TS. An updated review of tyrosinase inhibitors. *Int J Mol Sci*. 2009;10(6):2440-2475. doi:10.3390/ijms10062440.
65. Cooksey CJ, Garratt PJ, Land EJ, et al. Evidence of the indirect formation of the catecholic intermediate substrate responsible for the autoactivation kinetics of tyrosinase. *J Biol Chem*. 1997;272(42):26226-26235. doi:10.1074/jbc.272.42.26226.
66. Schallreuter KU, Bahadoran P, Picardo M, et al. Vitiligo pathogenesis: Autoimmune disease, genetic defect, excessive reactive oxygen species, calcium imbalance, or what else? *Exp Dermatol*. 2008;17(2):139-140. doi:10.1111/j.1600-0625.2007.00666_1.x.
67. Gilchrest BA, Eller MS. DNA photodamage stimulates melanogenesis and other photoprotective responses. *J Investig Dermatology Symp Proc*. 1999;4(1):35-40. doi:10.1038/sj.jidsp.5640178.
68. Kaidbey KH, Agin PP, Sayre RM, Kligman AM. Photoprotection by melanin—a comparison of black and Caucasian skin. *J Am Acad Dermatol*. 1979;1(3):249-260. doi:10.1016/S0190-9622(79)70018-1.
69. Korytowski W, Pilas B, Sarna T, Kalyanaraman B. Photoinduced Generation of Hydrogen Peroxide and Hydroxyl Radicals in Melanins. *Photochem Photobiol*.

1987;45(2):185-190. doi:10.1111/j.1751-1097.1987.tb05362.x.

70. Briganti S, Camera E, Picardo M. Chemical and Instrumental Approaches to Treat Hyperpigmentation. *Pigment Cell Res*. 2003;16(2):101-110. doi:10.1034/j.1600-0749.2003.00029.x.
71. Gonçalves GMS, Da Silva GH, Barros PP, et al. Use of Curcuma longa in cosmetics: Extraction of curcuminoid pigments, development of formulations, and in vitro skin permeation studies. *Brazilian J Pharm Sci*. 2014;50(4):885-894. doi:10.1590/S1984-82502014000400024.
72. Asawanonda P, Klahan S-O. Tetrahydrocurcuminoid Cream Plus Targeted Narrowband UVB Phototherapy for Vitiligo: A Preliminary Randomized Controlled Study. *Photomed Laser Surg*. 2010;28(5):679-684. doi:10.1089/pho.2009.2637.
73. Lee KH, Farida FH, Syahida A, et al. Synthesis and biological evaluation of curcumin-like diarylpentanoid analogues for anti-inflammatory, antioxidant and anti-tyrosinase activities. *Eur J Med Chem*. 2009;44(8):3195-3200. doi:10.1016/j.ejmech.2009.03.020.
74. Rangkadilok N, Sitthimonchai S, Worasuttayangkurn L, Mahidol C, Ruchirawat M, Satayavivad J. Evaluation of free radical scavenging and antityrosinase activities of standardized longan fruit extract. *Food Chem Toxicol*. 2007;45(2):328-336. doi:10.1016/j.fct.2006.08.022.
75. Koohpar ZK, Entezari M, Movafagh A, Hashemi M. Anticancer Activity of Curcumin on Human Breast Adenocarcinoma : Role of Mcl-1 Gene. 2015;8(3). doi:10.17795/ijcp2331.
76. Nawale L, Dubey P, Chaudhari B, Sarkar D. Anti-proliferative effect of novel primary cetyl alcohol derived sophorolipids against human cervical cancer cells HeLa. 2017:1-14.
77. Sanap A, Chandravanshi B, Shah T, et al. Herbal pre-conditioning induces proliferation and delays senescence in Wharton's Jelly Mesenchymal Stem Cells. *Biomed Pharmacother*. 2017;93:772-778. doi:10.1016/j.biopha.2017.06.107.

Chapter 4

Synthesis of biocompatible Calcium carbonate ($CaCO_3$) microparticles as a drug delivery system using sophorolipid as a capping agent to increase the porosity of synthesized particles

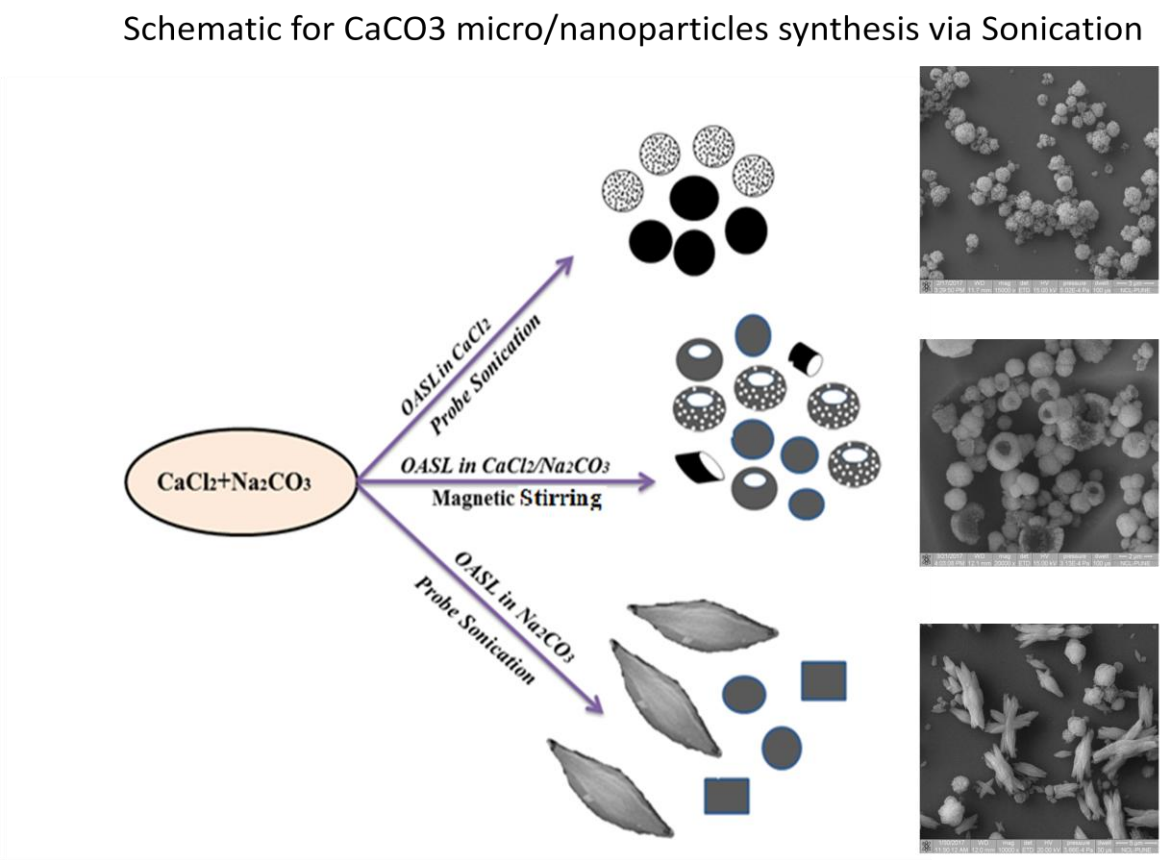

Summary

A simple yet effective method is developed for the synthesis of calcium carbonate micron-sized particles. The 0.1M aqueous solution of calcium chloride is drop-wise added in a 0.1M solution of sodium bicarbonate under probe sonication for 30 minutes to obtain spindle-shaped 2-3 micron particles. To reduce the particles size, we added a biologically synthesized glycolipid (sophorolipid) during the synthesis by two different approaches. In one method sophorolipid is solubilized in aqueous calcium chloride solution and probe sonicated for 10 minutes. To this mixture, drop-wise sodium bicarbonate solution was added and further

sonicated for 20 minutes. This approach leads us to produce spherical and porous calcium carbonate nanoparticles in the size range of 100-400nm. While in the second method, sophorolipid was solubilized in sodium bicarbonate solution and sonicated for 10 minutes. Here, calcium chloride solution is added gradually and sonicated for 20 minutes. The particles observed here were spindle shaped with size 1-3μm. Scanning electron microscopy and EDS have confirmed the shape, size, and composition of these particles. Also when using these two approaches if we change the method to magnetic stirring, porous and spherical microparticles of CaCO3 obtained. The sizes of these were also in the range of 1-2μm. The nucleation of the particles was studied via time-dependent SEM analysis. These particles can be an effective host for the fabrication of biocompatible composite materials as they are natural biomineral available in nature and can be used for oral drug delivery.

1. Introduction:

1.1 Calcium carbonate:

Calcium Carbonate ($CaCO_3$) is a naturally occurring inorganic biomaterial. It is a white, insoluble solid that occurs in nature in form of chalk, limestone, marble, and calcite, and is the main component of shells of marine organisms, snails, pearls, and eggshells [1]. In the chemical industry, it acts as raw material owing to its varied applications such as to produce cement, mortars, plasters, refractories, and glass as building materials. It also is used to produce quicklime, hydrated lime and a number of calcium compounds. The latter consists of finer particles of greater purity and more uniform in size. Diverse calcium carbonate forms are currently being used in several commercial products, like textiles, papers, paints, plastics, adhesives, sealants, and cosmetics [2].

1.2 Synthesis methods for $CaCO_3$ particles

Calcium carbonate has three polymorphic forms: calcite, aragonite, and vaterite based on the synthesis condition [3]. The conditions during synthesis can influence the particles shape, size, and morphology [4]. For the synthesis of calcium carbonate micron or nanosized particles, many studies have used the bottom-up approach via precipitation process, either through carbonation or through solution route as a raw material in chemical industry over the past few years [1]. The two existing method of carbonation are spray carbonation and batch carbonation. The spary method gives monodispersed and small nanoparticles but their are difficulties with the control of reacton like mass fraction of Ca $(OH)_2$ suspension, carbonation temperature, ratio of amount of CO_2 gas to that of $Ca(OH)_2$ suspension in a spraying tower, and the size of solution drop sprayed etc. Also this method is expensive and requires regular maintenance. Batch carbonation is preferred method in industries due to its high rate of production and efficient control over the crystal shape and size during the process. This comes with a drawback of particles having relatively larger size with wider particle size distribution. Also the process needs strict control of temperature, purified raw materials, and strenuous gas (CO_2 or combination of CO_2 and N_2) bubbling phases which is complicated and that incurs time results in expensive process [5–7]

Another method used to produce $CaCO_3$ particles from cockleshell is by using high pressure homogenizer (HPH) technique through a microemulsion route in the presence of a surfactant like polysorbate 80 (Tween 80). The particles showed good results as drug delivery system,

but the requirement of equipment is quite complex and expensive along with high energy inputs to operate. [8]

The physical process of ultrasound (sonication) seems to be a promising and greener method over the use of harsh temperatures and carbonation, etc for the synthesis of $CaCO_3$ nanoparticles [4].

1.3 Applications of Calcium carbonate:

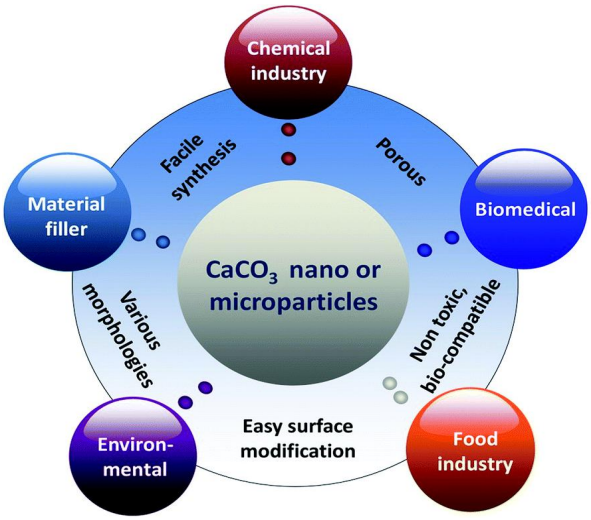

Image Source: Boyjoo et al., 2014[6]

Nano calcium carbonate synthesis has received significant importance due to their industrial applications in the quantum dots, catalysis, flame retardant, clean-up of toxic contamination from chemical warfare, and bone replacement [9]. The applications of nanoparticles of $CaCO_3$ strictly depend on parameters such as morphology, size, specific surface area, oil adsorption capacity, and chemical purity. Therefore, the control of particle morphology via its shape and size is crucial from the perspective of the technical applications [10].

1.4. Sophorolipids:

Sophorolipid is one of the most promising and attractive biosurfactants. SL has numerous properties that make them superior to synthetic surfactants including stability in the wide range of pH, temperatures, and salinity, low-foaming and excellent detergent properties, water hardness (a high concentration of divalent cations does not affect their interfacial properties) [11].

SL can be produced in large quantities based on renewable resources, agro-industrial by-products and residues and easy and simplified product recovery [11,12] . Interest in

sophorolipids is not limited to the production of surfactants because of their highly attractive characteristic and wide range application [13].

2. The scope of work:

$CaCO_3$ nanoparticles show unique advantages due to their ideal biocompatibility and are ideal as the potential drug delivery systems offering a range of drug loading options [3]. This chapter deals with the synthesis of the calcium carbonate particles using a milder approach. Here we have used oleic acid sophorolipid as a capping agent along with a bottom-up method. We have used few combinations for the addition of sophorolipid and starter salt solutions. For the synthesis, magnetic stirring and probe sonication methods were used and based on the particle shape and size, a suitable candidate was studied for drug loading and release study. The particles obtained were further characterized using a different technique like UV-VIS, DLS, Zeta, SEM, and TEM.

2. Materials and Methods:

All chemicals used in this study are of analytical grade. Calcium chloride ($CaCl_2.H_2O$) was purchased from Merck, Sodium Carbonate (Na_2CO_3) was purchased from Qualigens.

Oleic acid sophorolipid (OASL) was synthesized using the method described in chapter 1 of this thesis. The sonication method reported here is simple, cheap, and efficient for the synthesis of $CaCO_3$ (nano) particles [10]. Probe sonicated using a Branson Digital Sonifier 250 at amplitude of 70 Hz with a constant pulse of 10 seconds at an interval of 3 seconds each for 30 minutes reaction.

2.1. Synthesis of $CaCO_3$ particles:

2.1.1. Probe sonication for the synthesis of $CaCO_3$ particles

The synthesis was carried out in a 50ml beaker. The nano-micro sized $CaCO_3$ were synthesized by a modified in situ deposition technique. Briefly, 0.1M $CaCl_2$ was added to 10ml of distilled water. Likewise, 0.1M Na_2CO_3 was added to 10 ml of distilled water. There were two sets of experiments carried out in the presence of biosurfactant oleic acid sophorolipid (OASL), and it was added in varying amounts to the aqueous calcium chloride and sodium carbonate solutions in the concentrations of 10mg, 30mg and 50mg per ml.

2.1.1a: Set I: In this set OASL was introduced in the 0.1M Na_2CO_3 solution before mixing with a 0.1M $CaCl_2$ solution. After subjecting the Na_2CO_3 solution containing sophorolipid for 10minute of probe sonication, calcium solution 10ml was introduced in a dropwise manner and the sonication was continued for another 20minutes

2.1.1b: Set II: In the second set, sophorolipid was introduced into the 0.1M $CaCl_2$ solution prior to mixing with 0.1M sodium carbonate solution. Calcium solution containing sophorolipid was subjected for 10min sonication and later sodium carbonate solution was introduced and sonication was continued for 20 more minutes.

For both the set of experiments, after completion of sonication, the resulting solutions were centrifuged at 8000rpm for 20mins and the pellet was twice washed with double distilled water to remove un-reacted salts and biosurfactant. The precipitate was dried overnight at 60^oC and the particles were characterized using SEM.

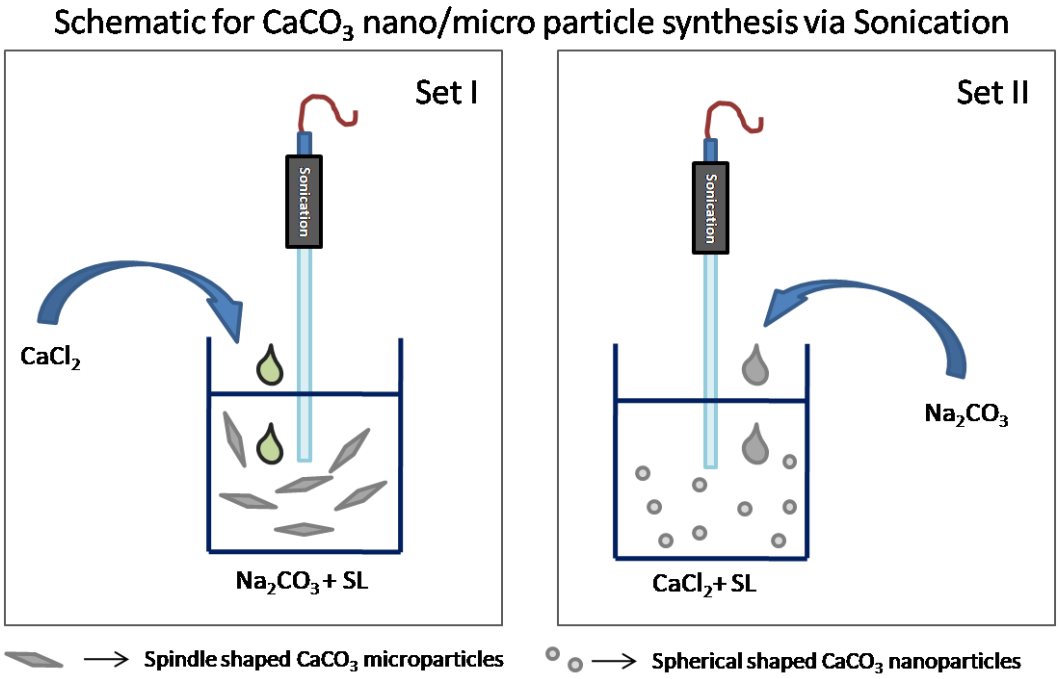

Fig 1: Schematic representation of $CaCO_3$ particle formation by sonication method

2.1.2. Magnetic stirring for the synthesis of $CaCO_3$ particles

After probe sonication, another one of the milder physical method of magnetic stirring was employed for the synthesis of $CaCO_3$ particles. Two methods (set I, II) similar to probe sonication were employed as follow:

2.1.2a: Here, 0.1M of $CaCl_2$ was solubilized in 20mg/ml OASL aqueous solution (10ml) and 0.1M Na_2CO_3 10ml solution was added drop-wise.

2.1.2b: 0.1M Na_2CO_3 was mixed with 20mg/ml OASL aqueous solution (10ml) and gradually 0.1M calcium solution 10ml was added.

These sequence of addition resulted in the different morphological forms of $CaCO_3$ particles studied via SEM.

2.2. Nucleation of Calcium carbonate particles in presence of sophorolipid

For the study, SEM was employed. The samples were taken in a timely fashion after the addition of Na_2CO_3 in the OASL-$CaCl_2$ solution. The time points were 0min, 2min, 5min, 10min, 15min, and 20min. Elemental mapping was carried out to confirm the formation of $CaCO_3$ particles

2.3. Determining the presence of SL on $CaCO_3$ particles

In the previous study from our group, we had observed the synthesis of gold nanoparticles using sophorolipid [14]. Therefore to ascertain the presence of sophorolipid on the $CaCO_3$ particles, 10^{-3} M $HAuCL_3$ solution was added to 1mg per ml of thoroughly washed and powdered $CaCO_3$ particles. The mixture was incubated overnight at 60^oC at 50rpm in a water bath. The particles were later analyzed via TEM.

2.4. Drug loading and release study

Based on the SEM data, we chose the $CaCO_3$ particles synthesized using set two of the method via probe sonication. Here furosemide a drug used for treating fluid build-up caused due to heart failure, liver scarring or kidney disease procured from Sigma Aldrich was selected as a candidate for drug loading study. This drug is hydrophobic in nature and its solubility is a difficulty that many are trying to tackle. In this study, we are attempting to provide a drug carrier that can release the drug over time thus prolonging the stay of the drug in the body. 1 mg of drug and 1 mg of $CaCO_3$ nanoparticles were weighted and transferred to a 5ml glass beaker. 2 ml water: ethanol 1:1 ratio was added and the solution was stirred at 50rpm overnight on a magnetic stirrer to allow drug adsorption/absorption in CaCO3 nanoparticles. Next day, the solution was centrifuged at 10000rpm and the pellet obtained was re-suspended in 2ml of phosphate buffer pH 7.4 and kept under magnetic stirring to study the drug release profile. To check any unbound drug, the immediate supernant after drug-CaCO3 incubation was subjected for UV-vis analysis. Later, 1 ml of solution was timely removed and fresh 1ml buffer added to maintain the volume. UV-vis spectroscopy was employed (full spectrum) to analyse any traces of drug. The time points taken in this study are 1 hr, 2 hr and 24 hr.

3. Results and Discussion

Studies have showed the use of ultrasonication can improve the supersaturation of Ca^{2+} ions and induce rapid nucleation. This results in smaller nanoparticles and size distribution. [5]

3.1.1 Set I of sonication

The influence of additives or modifiers during the crystallization of $CaCO_3$ particles is an interesting area to study. The orientation of Ca^{2+} and CO_3^{2-} ions around the organic additive results in various shaped and sizes observed in crystal formation of $CaCO_3$. Self assemblies of polymers, surfactants, polymer/surfactants and other organic molecules have been reported for various morphological aggregation based crystal formation of $CaCO_3$. These in turn provide the particles with different physico-chemical and mechanical properties[15]. The sonication method used in the formation of $CaCO_3$ particles in this chapter along with the addition of sophorolipid, a bio-surfactant influences the shape and size of particles. We observed two distinct shapes of $CaCO_3$ micro particles based on the addition of SL in the particular salt solution ($CaCl_2$ and Na_2CO_3) and by the way of mixing these two solutions. When SL is mixed with Na_2CO_3 solution and drop-wise added to solution of $CaCl_2$, a striated spindle shaped microparticles were observed. The shape of spindle evolved into a mixed shape of cuboids, spheres and forked spindles as the concentration of sophorolipid is increased. The shaped evolution can be probably caused by the addition of SL. Due to chemical electrostatic interactions between SL and the salts may be arranging the crystal in such formation that they appear as spindles. The Fig.2 depicts the probable mechanism by which spindle shape is formed during the first set of sonication experiments. The SEM studies (Fig. 3) of the synthesized particles revealed the development of mixed population of micro-particles with increasing SL concentration of 10, 30 and 50mg. The control study, in which SL was not added, showed sharp spindles. The size of particles more or less remained constant in case of 10 and 30mg SL addition i.e. ~2-5 µm length and 1-2µm diameter, while 50mg showed a mixed population of particle formation with sizes for spindle ~5µm length and 2.5-3µm diameter and spheres with 2-4µm in diameter.

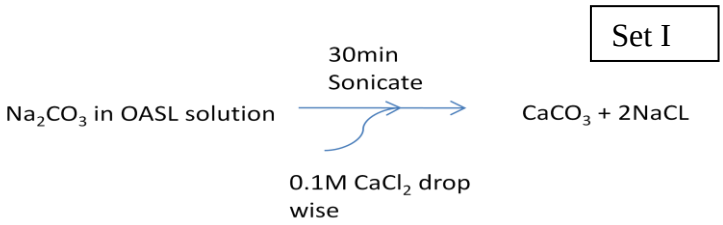

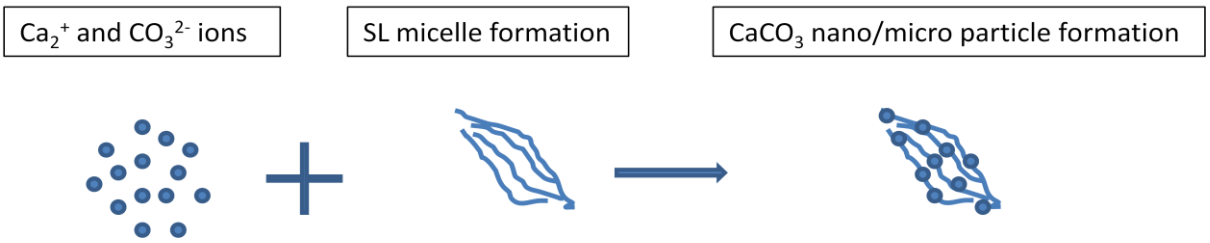

Fig. 2: An illustration of the probable mechanism for spindle shape formation.

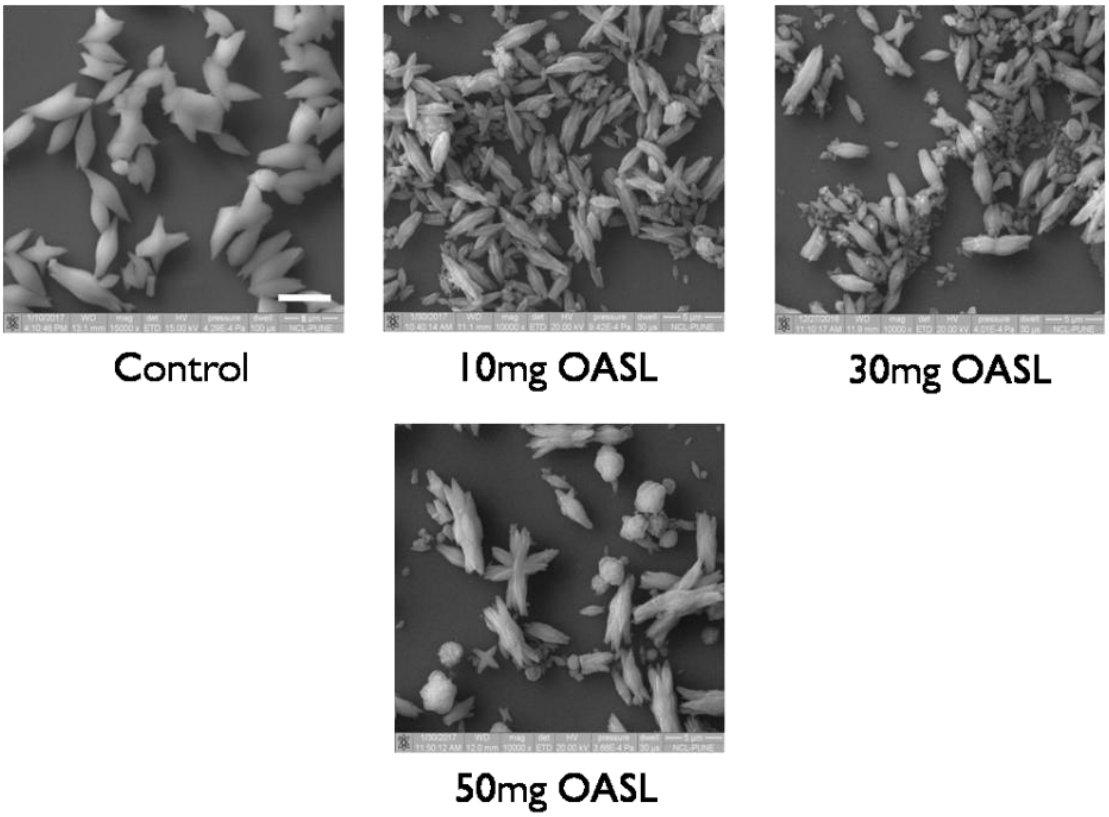

Fig.3: SEM of Control $CaCO_3$ and SL influenced $CaCO_3$ micro particles.

3.1.2 Set II of sonication

Likewise, when SL is added to a $CaCl_2$ solution and gradually mixed under sonication with Na_2CO_3 solution spherical nano-micro mixed particles were observed. In this case it can be said that calcium salt allows the SL to self assemble in a round matrix and when it comes in contact with carbonate solution, the $CaCO_3$ starts nucleating and crystallizing into a spherical shape. The schematic illustration of the formation is given in Fig. 4. It is seen from SEM (Fig.5) studies of synthesised particles, with increasing SL concentration (10, 30, and 50 mg/ml) the random structures it start converting into prefect spheres. The porosity of the particles also improves with the set II experiments. The sizes vary with each concentration, i.e. for 10mg SL the CaCO3 size was around 4-5 µm in length and 1-2 µm in diameter, 30mg

SL showed compact spindles under 3µm length and 1µm diameter and spheres of 600nm to 1µm sizes, 50mg SL showed almost all the particles as spheres with sizes ranging from 500nm to 2µm.

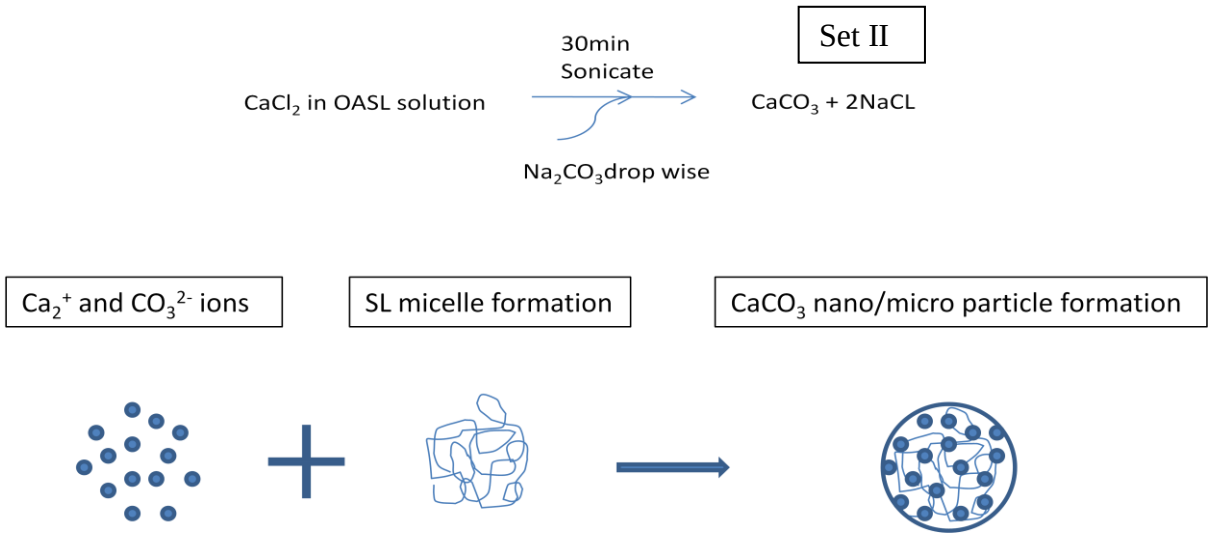

Fig. 4: An illustration of the probable mechanism for spherical shape formation.

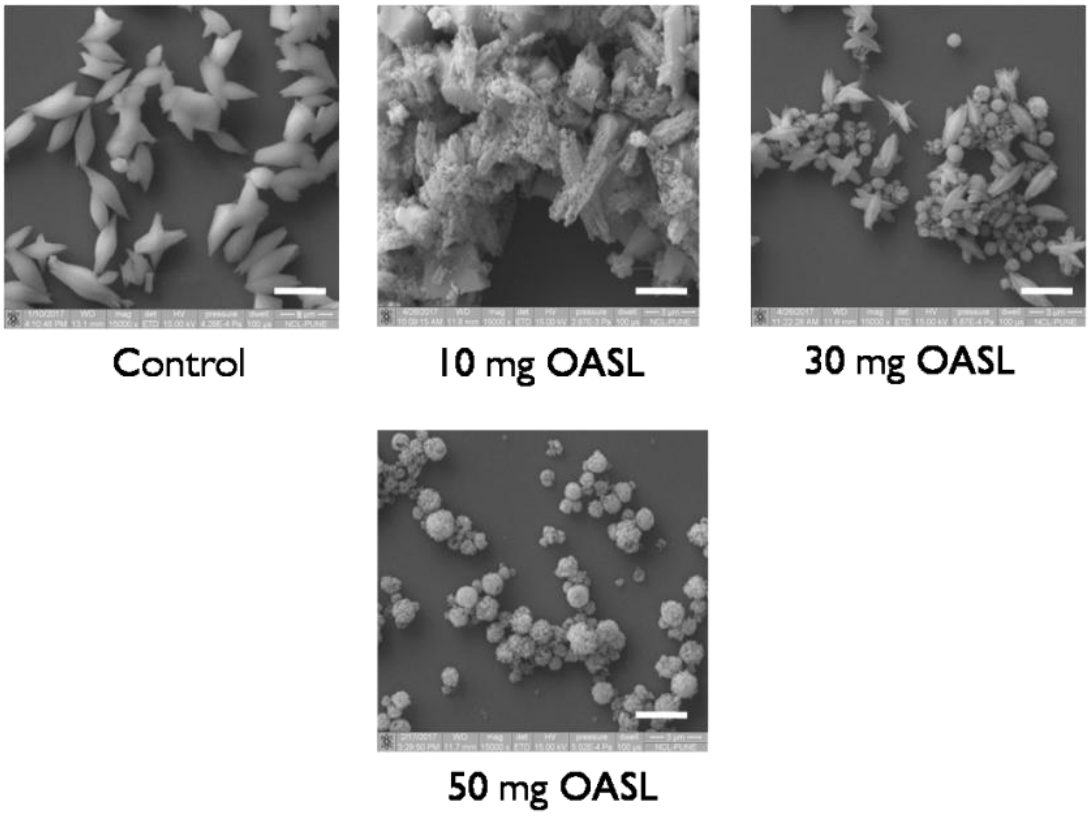

Fig. 5 SEM image of control CaCO3 micro-particle and change in the morphological form of $CaCO_3$ with increasing SL concentration in set II experiment.

3.2. Magnetic stirring for the synthesis of $CaCO_3$ particles

We have used another physical method for the synthesis of $CaCO_3$ particles. By simple stirring of solutions via magnetic stirrer, we could achieve porous, spherical, hollow $CaCO_3$ micro particles. In this study we adapted the similar methodology as in set I and set II of sonication stated in methods section of this chapter but instead of increasing amounts of SL we kept the concentration same i.e. 20mg/ml and performed the experiment. Here we observed that both sets presented with spherical micro-particles but the size of hollow in both cases varied. This could be attributed to the orientation of SL micelle in the solubilising salt solutions that later helped in crystallization of $CaCO_3$. Fig 6 is the schematic for better understanding the role of SL in shape formation of $CaCO_3$ particles. SEM data (Fig 7) gave us the morphological evidence. The size of these particles was between 800nm to 2µm. The reports suggest the addition of additive like surfactant provides with active site for nucleation of $CaCO_3$ and also they prevent the further growth of crystals limiting their size which is desired. Work with SDS and SDBS at higher concentrations than CMC values lead to the formation of micelles that helps the nuclei of $CaCO_3$ to attach to its surface causing the spherical particle formation. Also the hollow spheres observed were attributing to the bubble effect of SDS [6]. Similar results were seen in case of SL suggesting us that similar mechanism must have worked.

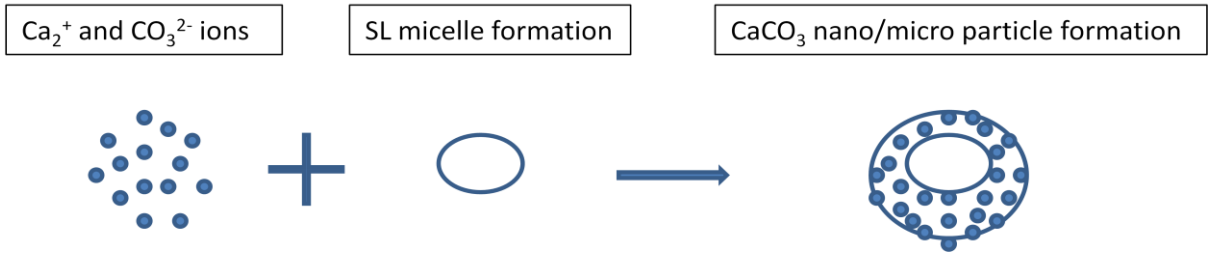

Fig 6: illustration for CaCO3 particle formation by magnetic stirring

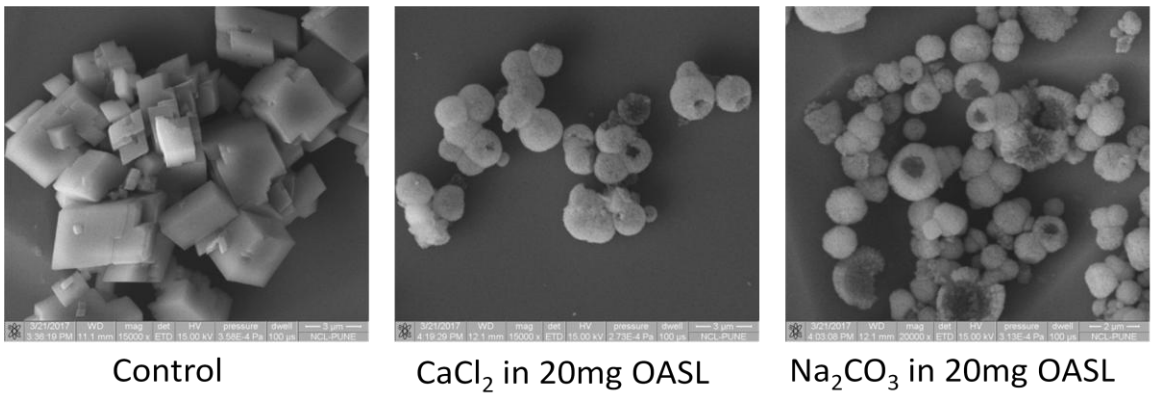

Fig 7: SEM images of the particles formed by magnetic stirring

3.3. Nucleation of Calcium carbonate particles in presence of sophorolipid

As we have understood from the literature and our synthesis process, an additive can cause the morphological changes and porosity in particles during crystallization process. To get the evidence of same we conducted a time bound SEM study of the nucleation process. Here from the two stated methods sonication and magnetic stirring with variation in SL addition, we chose set II of sonication. As this method yields spherical particles, their growth right from 0min was studied. Time intervals 0min, 2min, 5min, 10min, 15min and 20min was recorded via SEM. Fig 8 shows the sheet like formation on silicon chip at the beginning of the experiment and as the drop-wise addition of CO_3^{2-} ion starts, nucleation and small crystal formation is observed. This trend continues till 10min and the shape remains constant after the end of experiment at 20min. We also did elemental mapping (Fig 9) to confirm the formed particles as $CaCO_3$ and presence of carbon, oxygen as a indication of presence of SL.

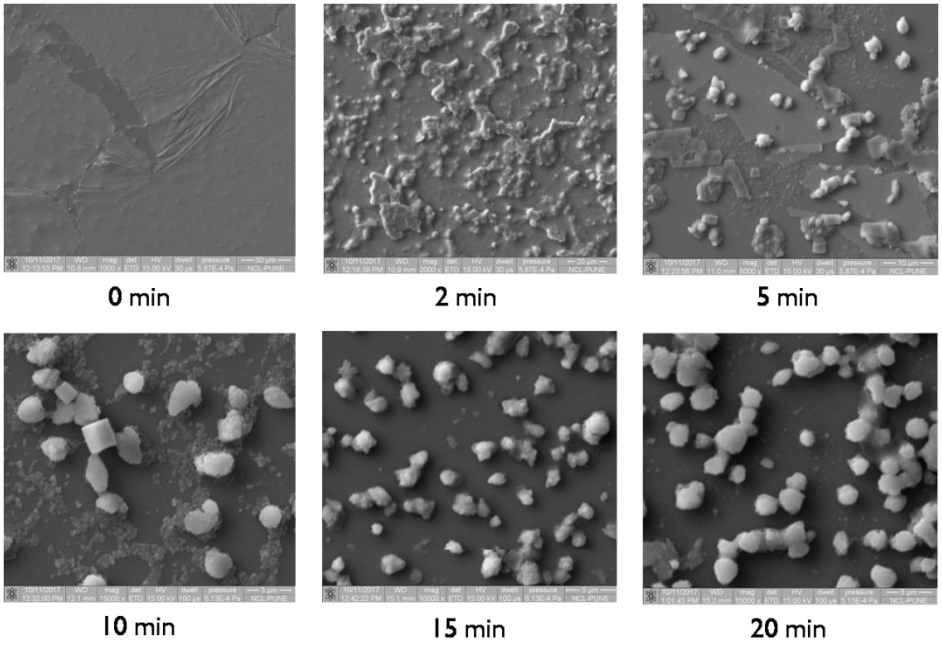

Fig 8: SEM study for the nucleation and formation of particles

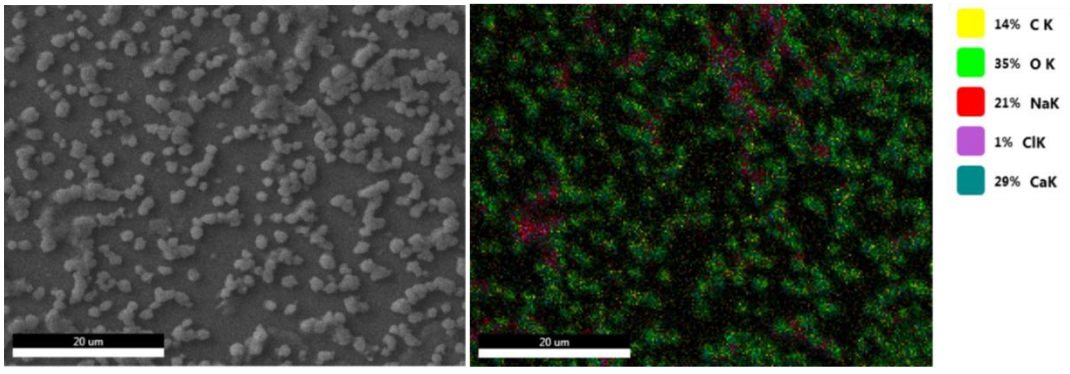

Fig 9: Elemental mapping of the formed micro-particles

3.4. Determining the presence of SL on $CaCO_3$ particles

From the above study it is apparent that SL is incorporated with the $CaCO_3$ micro-particles, but to confirm the presence, we conducted an experiment where chloroauric acid ($HAuCl_4$) 10^{-3} M was added with the 1mg of washed, dried and re-suspended $CaCO_3$ particles and incubated overnight at 60^oC at 50rpm in a water bath. We observed change in colour from turbid white to pale pink. It is a direct indication that SL convetred $HAuCl_4$ solution to Au^0 resulting in formation of gold nanoparticles. The particles were analyzed using TEM and gold nanoparticles were detected on the periphery and crevices of the CaCO3 particles. The confirmatory Energy Dispersive X-Ray Analysis (EDAX) Fig 11 (inset showing the SAED pattern indicating crystalline nature of the whole assembly) validated the results by indicating the presence of Au in the $CaCO_3$ sample. The formed GNPs were found to be of 5-10nm in size Fig 10 (arrows)

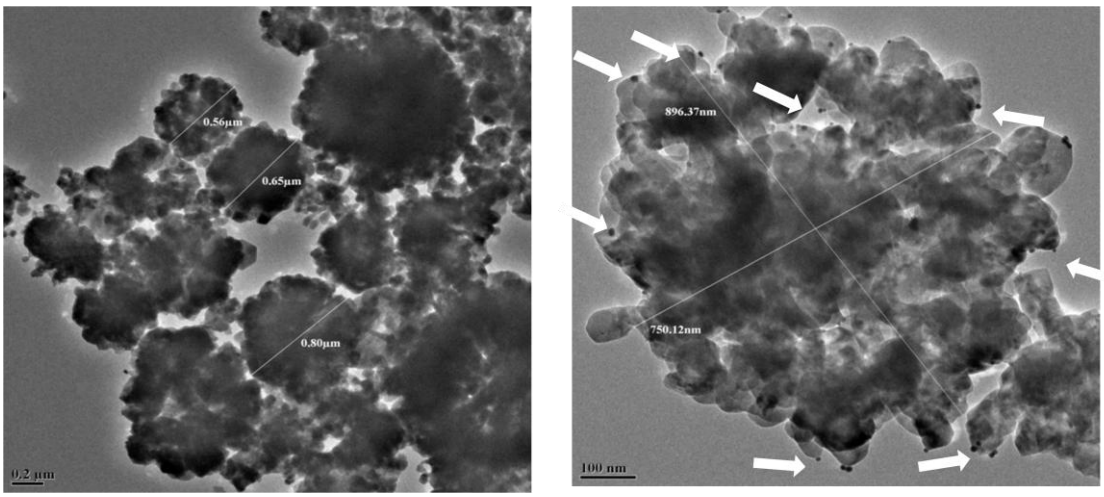

Fig 10: TEM study validating the presence of SL on $CaCO_3$ particles.

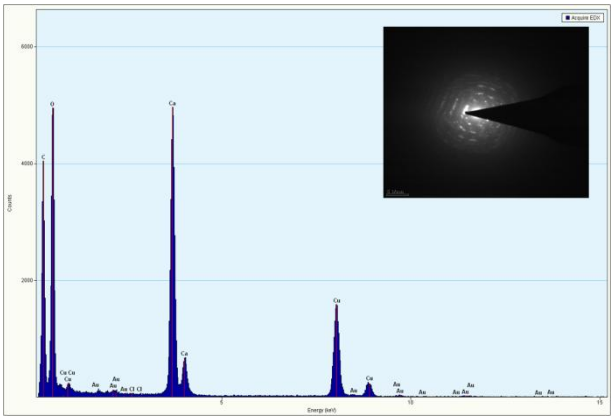

Fig 11: EDAX graph showing elemental presence on the TEM grid, inset showing a SAED pattern indicating crystalline nature of whole assembly.

3.5. Drug loading and release study

As stated above, for the drug loading and release study we chose the $CaCO_3$ microparticles obtained from set II of sonication method. The drug furosemide which is hydrophobic in nature was chosen as the candidate for this study. This is a simple experiment, where drug and $CaCO_3$ micro-particles were allowed interacting overnight on a magnetic stirrer. This enabled the drug to adsorb on the surface and interior of the particles, this was evident from the TEM images (Fig 12) of bare and drug loaded particles. The image reveals the empty cavities in bare particles and a perfect solid filled particle in case of drug. When we studied the release profile, it was observed that the drug releases in a burst at start i.e. after 1 hr, and at 2 hr we observed some traces of drug in the solution. But when drug release was tested at 24 hr, we could hardly see the drug. This lead us to an understanding that $CaCO_3$ can act as drug carrier but since the drug is adsorbing loosely on the surface, release up to 2 hr can be seen.

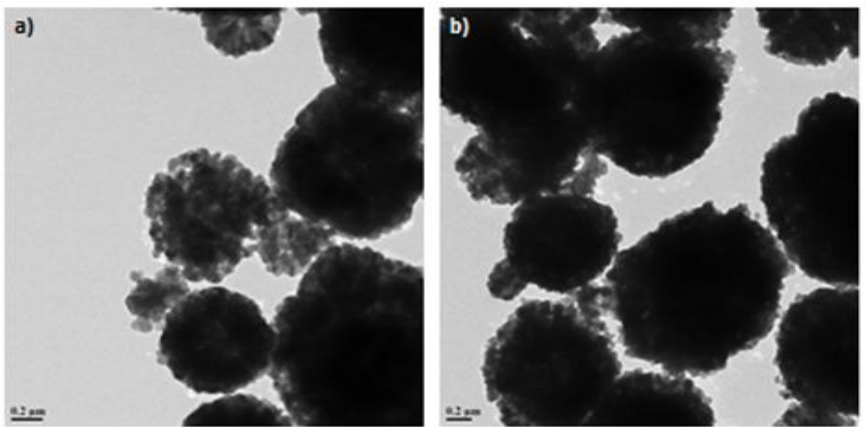

Fig 12: a. Bare $CaCO_3$ and b. $CaCO_3$ loaded with drug furosemide

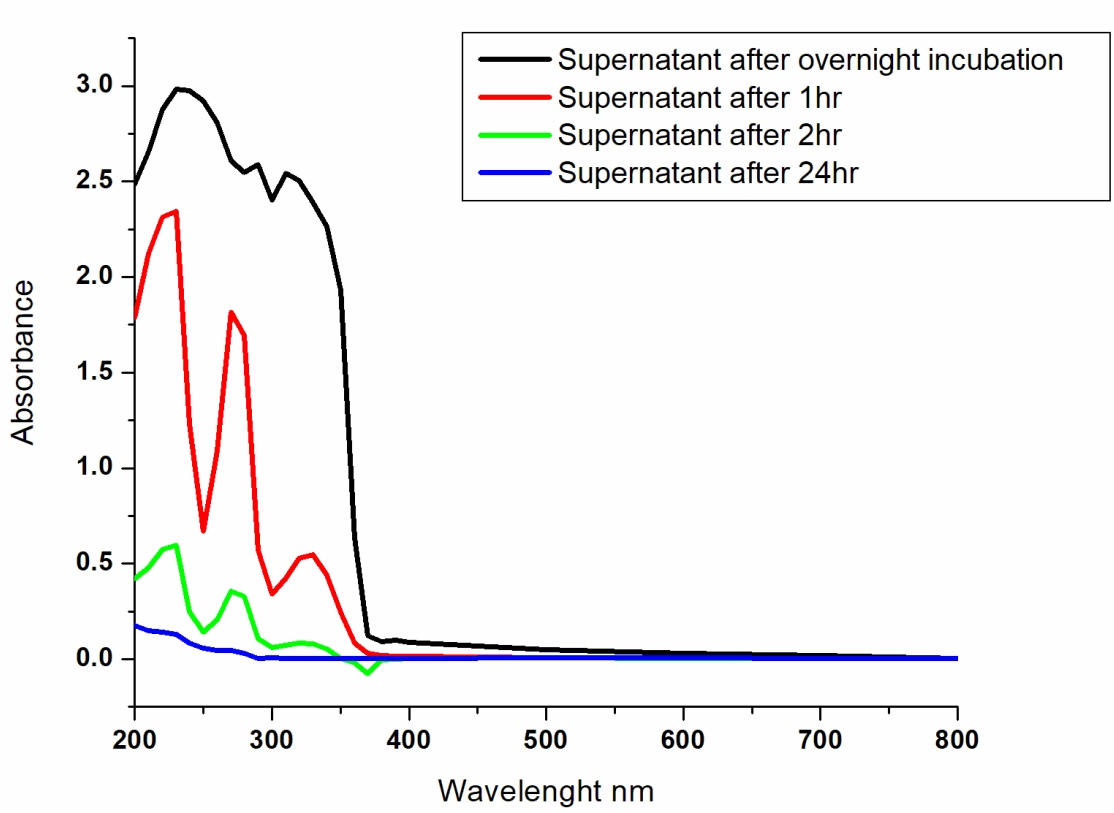

Fig 13: Furosemide drug release profile from $CaCO_3$ microparticles

Conclusion

We have successfully established the role of SL in the synthesis of $CaCO_3$ micro-particles were SL makes the particles more porous and helps in determining the shape of particles based on the sequence of addition. In probe sonication method, when SL is added in sodium carbonate, it helps in formation of spindle shaped $CaCO_3$ particles. This happens due to lamellar micelle formation of SL causing the $CaCO_3$ crystallization in layered formed. The spindles when compared with bare $CaCO_3$ spindles i.e. without SL, the surface is quite rough and structured. This increases the surface to volume ration and can be used in application like paints, paper or even fillers in cement for dentistry. While, when SL mixed with calcium chloride, SL leads to spherical particle formation. Again this can be attributed to spherical miceller formation helping the $CaCO_3$ crystallization around them. The final particles have porous structure.

The magnetic stirring method shows spherical particles formation in both the sequences of SL addition. This can be due to the less forceful method of stirring helps SL to interact more and form spherical micelles and bubbling in biosurfactant, causing open spheres to form. The diameter of opening again varies with the addition of SL in particular salt solution, like when

SL is in sodium carbonate, larger opening is observed. In case of SL in calcium salt solution smaller opening and tighter spheres are formed.

These experiments easily establish the role of sophorolipid and the method in which it is added can immensely influence the formation of $CaCO_3$ particles. Hence from these two physical method and variation in addition of SL, we chose the best suited particles for drug loading assay. The furosemide drug loading and release profile observed from spherical $CaCO_3$ microparticles obtained from set II of sonication method, also ascertain the notion of $CaCO_3$ as a good drug delivery system.

References:

1. Hariharan M, Varghese N, Cherian AB, et al. Synthesis and Characterisation of CaCO3 (Calcite) Nano Particles from Cockle Shells Using Chitosan as Precursor. *Int J Sci Res Publ*. 2014;4(10):1-5. www.ijsrp.org.
2. Devamani RHP, Kavitha M, Bala BL. Synthesis and characterization of Calcium Carbonate nanoparticles. *J Environ Sci Comput Sci Eng Technol*. 2015;4(1):112-120.
3. Dizaj SM, Barzegar-Jalali M, Hossein Zarrintan M, Adibkia K, Lotfipour F. Calcium carbonate nanoparticles; Potential in bone and tooth disorders. *Pharm Sci*. 2015;20(4):175-182. doi:10.5681/PS.2015.008.
4. Kirboga S, Oner M, Akyol E. The effect of ultrasonication on calcium carbonate crystallization in the presence of biopolymer. *J Cryst Growth*. 2014;401:266-270. doi:10.1016/j.jcrysgro.2013.11.048.
5. He M, Forssberg E, Wang Y, Han Y. Ultrasonication-Assisted Synthesis Of Calcium Carbonate Nanoparticles. *Chem Eng Commun*. 2005;192(11):1468-1481. doi:10.1080/009864490896025.
6. Boyjoo Y, Pareek VK, Liu J. Synthesis of micro and nano-sized calcium carbonate particles and their applications. *J Mater Chem A*. 2014;2(35):14270-14288. doi:10.1039/C4TA02070G.
7. Jaji AZ, Abu Bakar MZ Bin, Mahmud R, et al. Synthesis, characterization, and cytocompatibility of potential cockle shell aragonite nanocrystals for osteoporosis therapy and hormonal delivery. *Nanotechnol Sci Appl*. 2017;10:23-33. doi:10.2147/NSA.S113030.
8. Mohd Abd Ghafar SL, Hussein MZ, Abu Bakar Zakaria Z. Synthesis and Characterization of Cockle Shell-Based Calcium Carbonate Aragonite Polymorph Nanoparticles with Surface Functionalization. *J Nanoparticles*. 2017;2017:1-12. doi:10.1155/2017/8196172.
9. Islam A, Teo SH, Rahman MA, Taufiq-Yap YH. Seeded growth route to noble calcium carbonate nanocrystal. *PLoS One*. 2015;10(12):1-13. doi:10.1371/journal.pone.0144805.
10. Atchudan R, Na H Bin, Cheong IW, Joo J. Facile Synthesis of Monodispersed Cubic and Spherical Calcite Nanoparticles in the Presence of Cetyltrimethylammonium Bromide. *J Nanosci Nanotechnol*. 2015;15(4):2702-2714. doi:10.1166/jnn.2015.9154.
11. Oliveira MR De, Magri A, Baldo C, Camilios-neto D. Review : Sophorolipids A Promising Biosurfactant and it ' s Applications. 2015;6:161-174.

12. Dolman BM, Kaisermann C, Martin PJ, Winterburn JB. Integrated sophorolipid production and gravity separation. *Process Biochem*. 2017;54:162-171. doi:10.1016/j.procbio.2016.12.021.
13. Kurtzman CP, Price NPJ, Ray KJ, Kuo T-M. Production of sophorolipid biosurfactants by multiple species of the Starmerella (Candida) bombicola yeast clade. *FEMS Microbiol Lett*. 2010;311(2):140-146. doi:10.1111/j.1574-6968.2010.02082.x.
14. Singh S, D'Britto V, Prabhune AA, Ramana C V., Dhawan A, Prasad BL V. Cytotoxic and genotoxic assessment of glycolipid-reduced and -capped gold and silver nanoparticles. *New J Chem*. 2010;34(2):294. doi:10.1039/b9nj00277d.
15. Kanoje B, Patel D, Kuperkar K. Morphology modification in freshly Precipitated Calcium Carbonate particles using surfactant-polymer template. *Mater Lett*. 2017;187(October 2016):44-48. doi:10.1016/j.matlet.2016.10.043.

Chapter 5

Sericin based synthesis of Tunable, Monodispersed and Stable Gold nanoparticles: Role of Temperature and pH

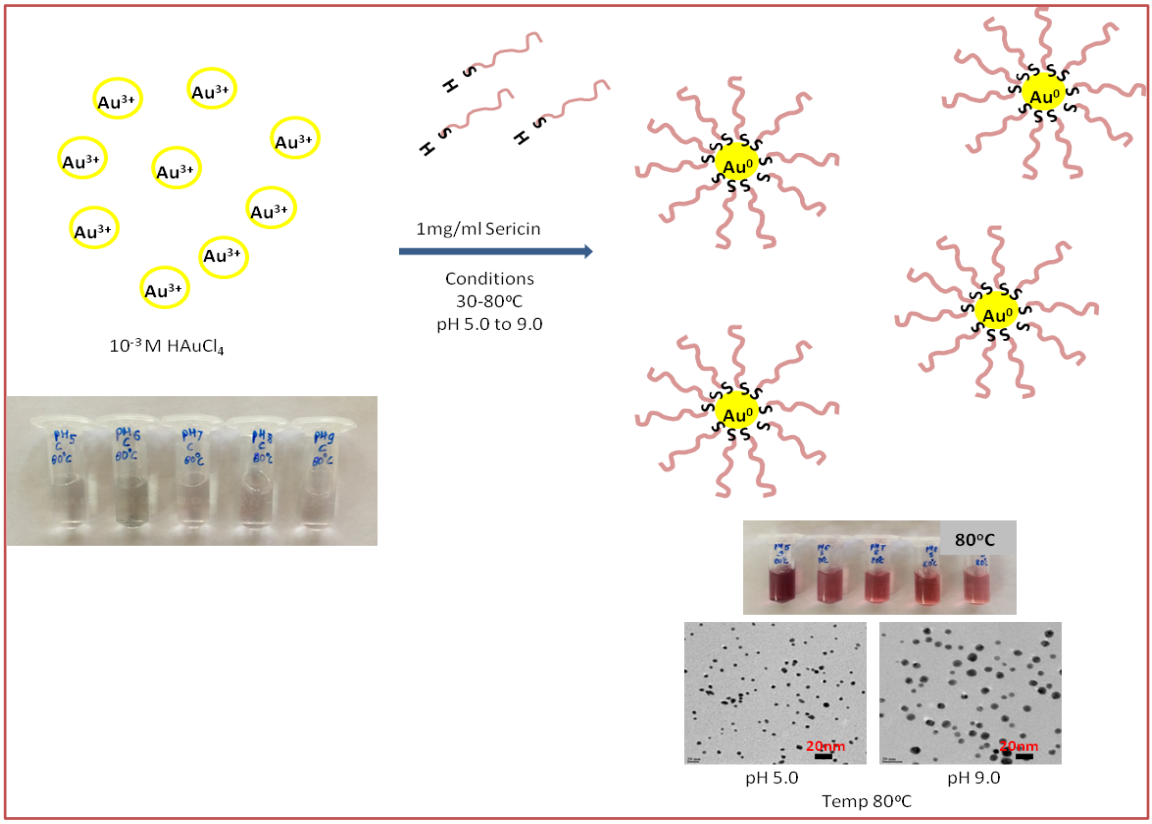

Summary

Sericin is a biocompatible and biodegradable protein with many biological properties and applications yet sericin based nanoparticles remains a less explored area. Gold nanoparticles are generally studied for their nontoxic carrier properties for drug and gene delivery. Many studies are conducted to obtain gold nanoparticles using greener approaches with lesser chemicals. Therefore, the synthesis of sericin based gold nanoparticles offers us a new way toward gold nanoparticle synthesis and also understanding the role of pH and temperature in the synthesis process. Here, sericin is extracted from the silk cocoon of *Bombyx mori* and lyophilized to obtain a powder. Conditions from pH 5.0 to pH 9.0 at varying temperatures ranging over 30^{o}C to 80^{o}C were employed for gold nanoparticle (GNP) synthesis. The formation of GNP was observed via characteristic color change from colorless to pink-red

color after 12-hour incubation. UV-vis spectroscopy confirmed the typical surface plasmon band of gold nanoparticles while FTIR analysis revealed the presence of sericin on GNPs indicating that sericin not only reduces but also caps the particles. Zeta potential of particles at 80^{o}C of pH range 5.0 to 9.0, showed highly stable particles particularly at pH 5.0. DLS and Transmission electron microscopy data confirmed the size of particles broadly between 10-40nm. XRD analysis of particles synthesized in pH 5.0 and pH 9.0 at 80^{o}C corroborated the TEM data, indicating smaller nanoparticles at pH 5.0 compared to pH 9.0. In this study, we observed a trend, as the temperature increases the size of GNP reduces while acidic conditions at every temperature tested favors to the synthesis of smaller nanoparticles.

Introduction

1.1 Gold Nanoparticles (GNPs)

Gold nanoparticles (GNPs) have gained a lot of interest in recent years because of its wide range of applications and unique electronic, magnetic, optical, mechanical, physical and chemical properties. Most metal nanoparticles synthesized in different shapes and sizes are being used in diagnostics and therapeutics because of its high acceptability to the living cells, stability at high temperatures, easy translocation into the cells, inertness, relatively less cytotoxicity and biocompatibility to both in-vitro as well as in-vivo environments [1,2]. Other biomedical applications being: Targeted delivery of drugs, Gene delivery, Cancer diagnostic and therapeutic agents, Biosensors, Detection of biological molecules, Immobilization of enzymes, Immunoassay and Metal sensors. [3]

1.2 Synthesis Methods:

Synthesis of gold nanoparticles has been reported by various chemical methods where many stabilizing agents like sodium citrate, transferrin, and cetyltrimethylammonium bromide are used for stabilization of GNPs [4]. The chemically synthesized nanoparticles pose slight toxicity towards biological systems hence are limited for non-biological applications. Since GNPs have a lot of potential in the field of drug delivery; it is essential to synthesize GNPs free of the chemicals. All GNP preparation methods are based on the reduction of gold ion and require a capping agent to prevent further growth and particle agglomeration. To overcome the limitations of the chemical synthesis of GNPs, alternative synthesis methods are gaining a lot of importance.

These synthesis methods include the use of biomolecules that reduce gold ions and act as a capping agent for the formed nanoparticles. This includes plant extract, extract of spices, proteins, and amino acids etc are reported with such activity. In our approach, we have used silk protein “sericin” as a reducing and capping agent.

1.3. Sericin:

Silk is a continuous protein fiber produced by the silkworm and consists of two main groups of proteins, sericin, and fibroin. Fibroin constitutes the fibrous component and has great tensile strength and property to withstand wear and tear (Agarwal P et al., 2012). Fibroin is being used in textile manufacturing and for several biomaterial applications. Whereas sericin

is a natural macromolecular protein, that serves as an adhesive binding the fibroin threads.

Sericin is a glue-like protein that binds the silk fibers in a cocoon of *Bombyx mori*. It is highly hydrophilic in nature due to the higher content of hydrophilic amino acids like serine (35%) and threonine (10%). This also means they are rich in hydroxyl groups due to serine and this is expected to have a major role in its structure conformation. Sericin is secreted by the middle silk gland of *B. mori* larvae as a watery solution during spinning. Afterward, it solidifies to give toughness to cocoon. [5]

Sericin is considered as waste material in the textile industry, with nearly 250 to 300 tons of sericin per year being discarded [6]. Recently sericin has been found to activate the proliferation of several cell-lines and has also shown various biological activities [7] like Anti-oxidant [8], Anti-tyrosinase [9], Anti-bacterial [10]and Anti-aging [11]. Nanoparticles capped with sericin can have these advantageous properties as well and this needs to be further studied.

2. Materials and Method

Sericin was extracted from silk cocoons of *Bombyx mori*, brought from local market. Chloroauric acid ($HAuCl_4$) was purchased from Sigma Aldrich. All chemical used to prepare buffers were of analytical grade. Cellulose tubing for dialysis (12kDa) was purchased from Sigma Aldrich.

2.1. Extraction of Sericin

Bombyx mori cocoons were weighed 5 grams and cut into small pieces about $5mm^2$. Silk sericin was recovered by subjecting the cocoons in 200 ml of distilled water to a high temperature of 121°C under a high pressure of 15 psi for 60 mins as described by Aramwit et al., 2010. The insoluble fibers of Fibroin proteins were separated by filtration using a muslin cloth and aqueous sericin was collected.

Dry sericin powder was obtained by freeze-drying the filtrate using lyophilization (Scanvac cool safe lyophilizer). This powder was stored at 4^oC and used for further experiments. MALDI analysis for molecular weight determination was carried out over pH range of 5.0 to 9.0 at a temperature 80^oC.

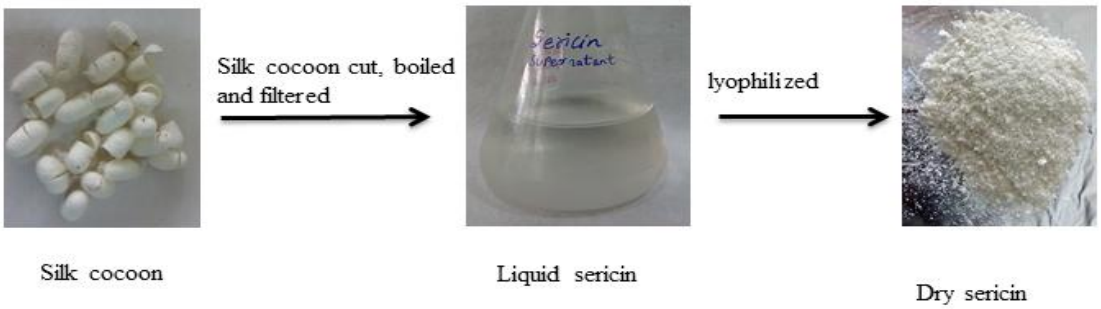

Fig 1: process used for obtaining sericin in this thesis

2.2 Synthesis of Sericin Gold Nanoparticles (Seri-GNPs) and Characterization

To ascertain the role of pH in sericin mediated gold nanoparticles, different pH values of solutions were studied. The following buffers were used: 0.1M acetate buffer (pH 5.0), 0.1M phosphate buffer (pH 6.0- pH 8.0) and 0.1M carbonate-bicarbonate buffer (pH 9.0). Sericin was dissolved in each buffer solution at 0.1mg/ml along with the addition of 1mM chloroauric acid. For determining the effect of temperature on the synthesis of gold nanoparticles, 10ml of this mixture was incubated respectively over the temperature range 30-80^oC for 12-hour in shaking water bath at 50rpm. The nucleation process of gold

nanoparticles was observed by the conversion of white color broth to the characteristic ruby-red color. This biologically synthesized Seri-GNP was further dialyzed using a dialysis membrane of the size of 12 kDa against de-ionized water to remove the un-reacted salts, ions, and protein.

UV-Vis Spectroscopy (Jasco V-630 spectrophotometer) and DLS (Brookhaven 90 plus particle size analyzer) were used for characterizing the synthesized Seri-GNPs along with its Zeta potential (based on UV-spectrum, samples of temperature 80^{o}C were studied) to understand its stability. TEM was used to determine the particle size of the synthesized particles (based on the spectroscopy results, a sample of pH 5.0 and pH 9.0 of temperature range 30-80^{o}C were studied). Both FTIR on a Bruker, Tensor 27 Platinum ATR with a resolution of 4 cm^{-1}over the spectral range of 450-4000 cm^{-1}, 40 scans per sample were recorded, which were present in their aqueous solution and XRD on Philips X'PertPRO were carried out for particles synthesized at pH 5.0 and pH 9.0 of temperature 80^{o}C as representational samples.

3. Results and Discussion

3.1. UV-Vis spectroscopic and MALDI

Sericin is environmentally friendly as it is derived from silk cocoons and has been reported to have biological applications. We report here the use of sericin for green synthesis of gold nanoparticles by reducing gold chloride ($HAuCl_4$). This process is a one-step synthesis reaction in which the non-toxic silk protein, having many effective functional groups is observed as capable of reducing as well as stabilizing the Au^{3+} ions at differing acidic and alkaline conditions. In this study, we extracted sericin and subjected this sericin in different conditions from acidic to alkaline pH (5.0 to 9.0) at temperature 80^{o}C, where we observed many small peptides ranging from 999-1900 dalton weight (Fig. 2 MALDI analysis). When sericin at pH 5.0 to pH 9.0 is subjected at different degrees of temperature i.e. 30^{o}C to 80^{o}C, causes the protein to orient in a fashion where it exposes the amide bonds responsible for the reduction of Au^{3+} to Au^{0}. Eventually, the protein also caps the nanoparticles stabilizing the gold nanoparticles colloid in the aqueous environment. Fig. 3 represents the observation of nucleation of Seri-GNPs at respective conditions.

MALDI of sericin suspended in different buffers ranging in pH 5.0 to 9.0 at temperature 80^{o}C.

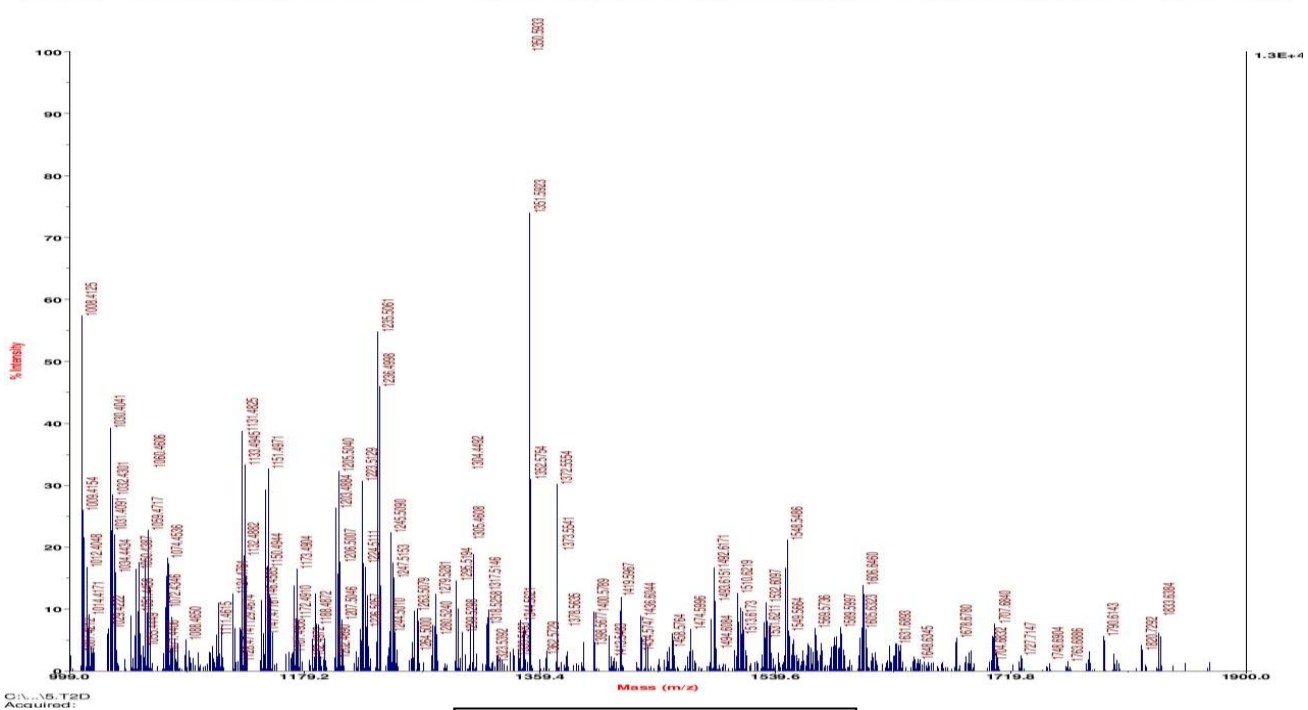

Sericin in pH 5.0 at 80^{o}C

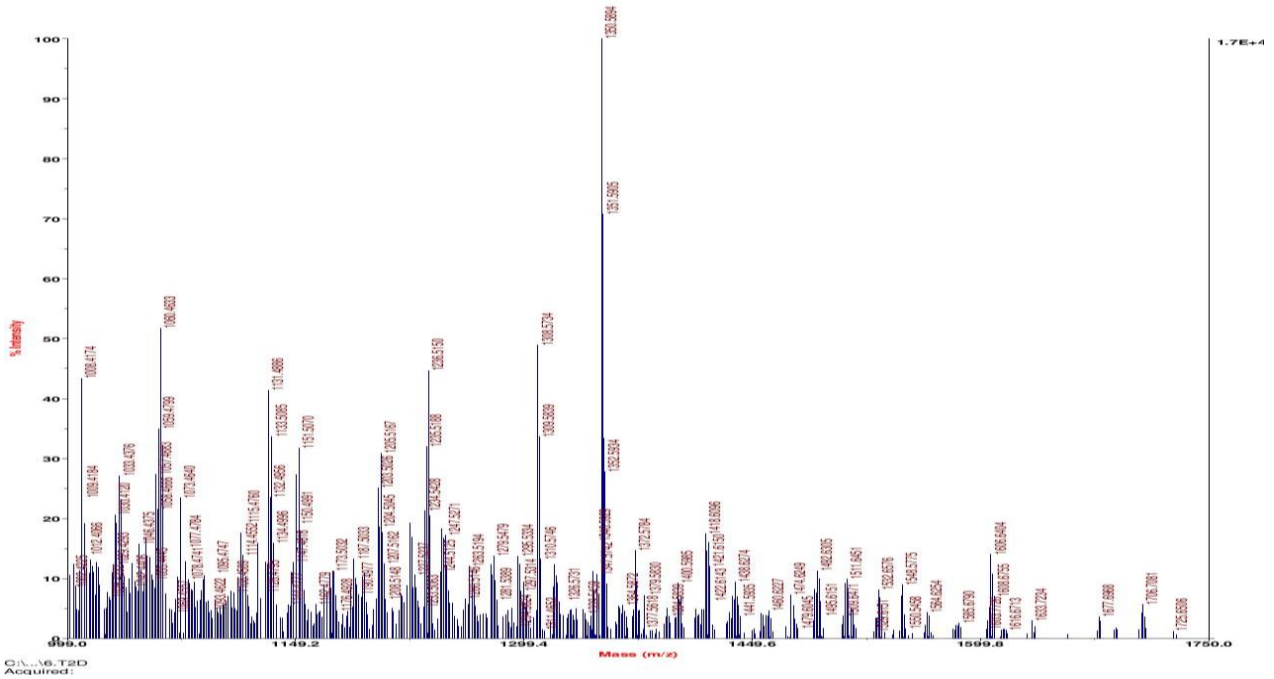

Sericin in pH 6.0 at 80^{o}C

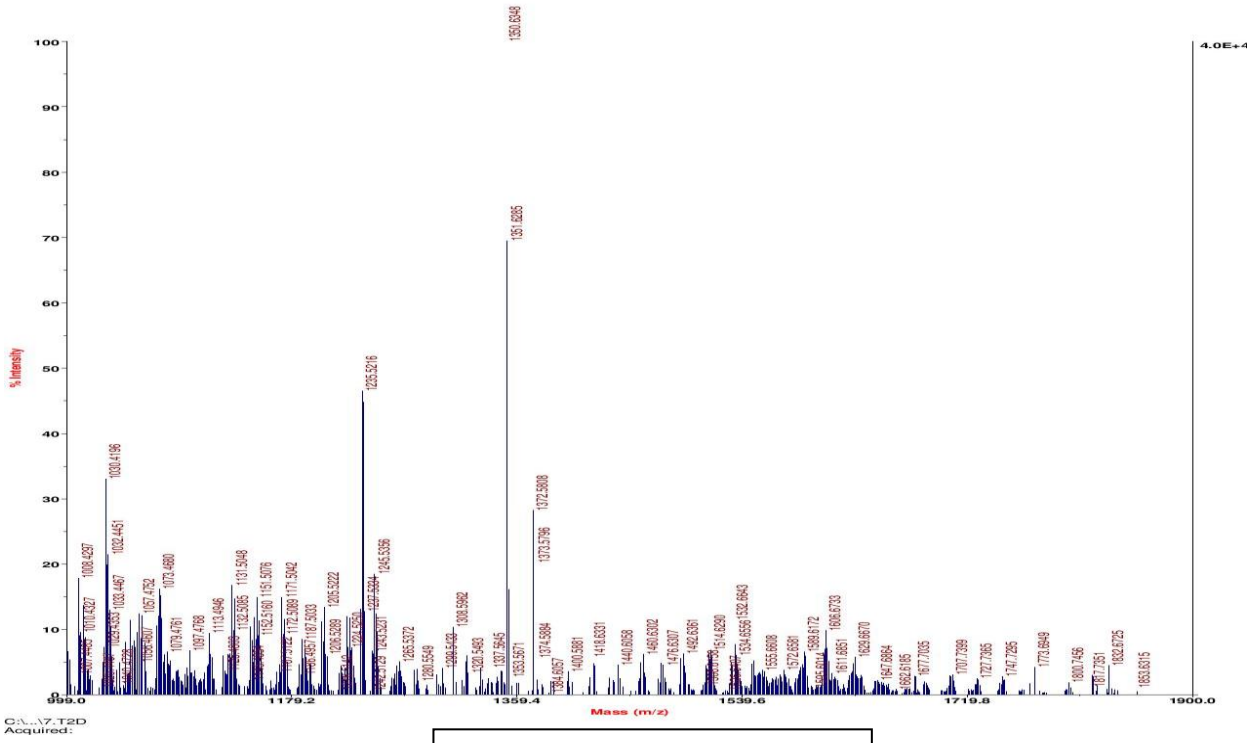

Sericin in pH 7.0 at 80^{o}C

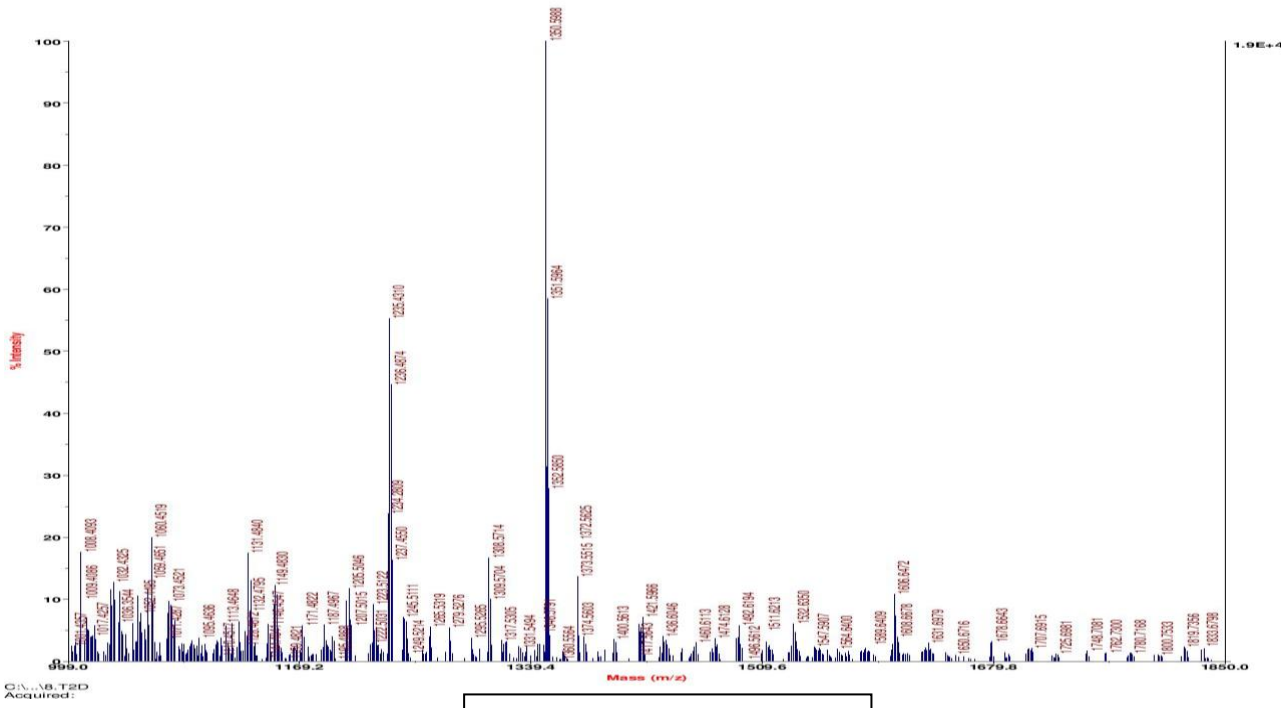

Sericin in pH 8.0 at 80^{o}C

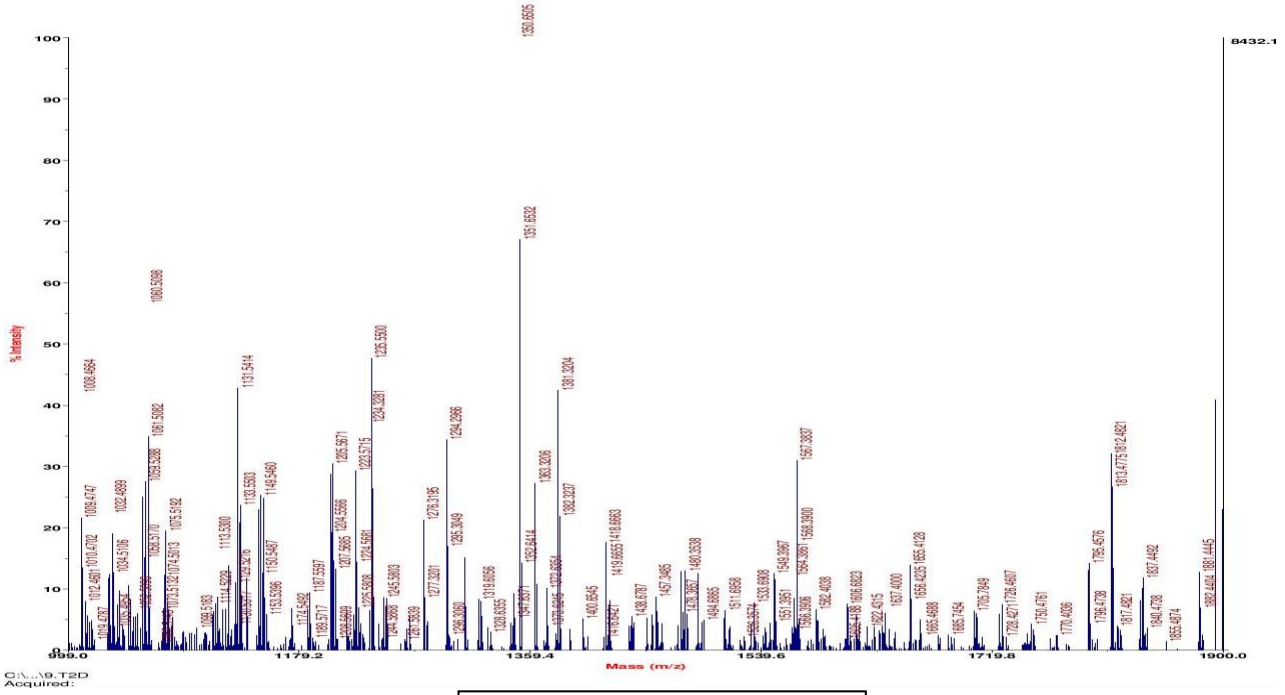

Sericin in pH 9.0 at 80^{o}C

Fig 2: MALDI of sericin in different pH (5.0 to 9.0) at 80^{o}C

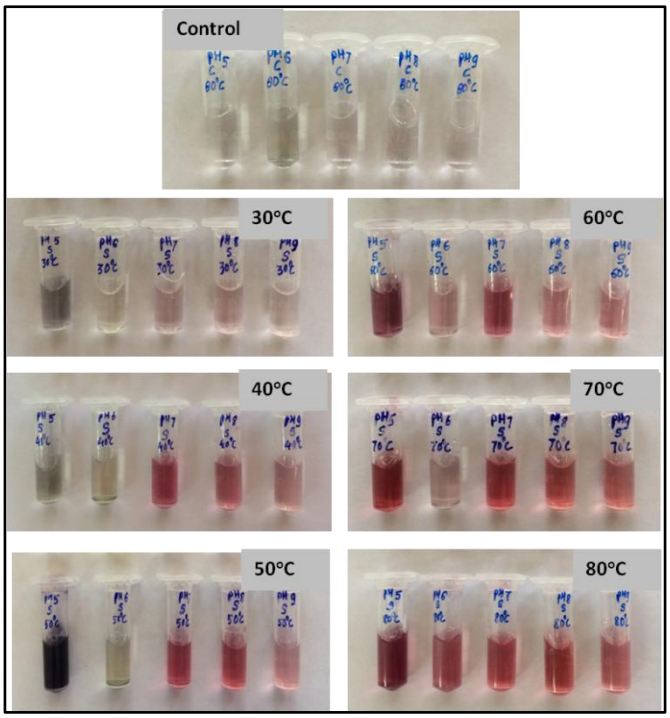

Fig.3: Seri-GNP synthesis in different conditions. Control represents $HAuCL_4$ in pH buffers 0.1M (pH 5.0 to pH 9.0) without sericin at 80°C. Rest represents Sericin-$AuCL_4$ sample in different buffers of 0.1M (pH 5.0 to pH 9.0) at respective temperatures (30°C to 80°C).

Sericin is a hydrophilic polypeptide rich in serine and aspartic acid with side chains made up of strong polar groups comprising of hydroxyl, amino and carboxyl groups [12]. Degradation of sericin under high temperature exposes these polar groups that are responsible for the reduction of gold ions [13]. It is quite clear from the image above, that pH and temperature definitely play an important role in synthesis observed via the change of characteristic ruby red colored appearance of gold nanoparticles solution. It has been reported that the apparent isoelectric point of silk sericin is at pH 3.7 [14]. Therefore when sericin is subjected to higher pH, it gains a negative charge, causing repulsion between molecules and possibly leading to delayed interaction with gold ions that get reduced into gold nanoparticles. It is observed that as the pH of sericin-$HAuCL_4$ solution progressively increases, the relative sizes of Seri-GNPs also proportionally increases. This phenomenon of sericin at different pH can be attributed to the effects of electrostatic repulsion, hydrogen bonding, and Van der Waals attractive force [12].

The free electrons present in the final or penultimate orbitals of Au^0 resonate when a light is incident on the particles exhibiting the characteristic ruby-red color [15]. This property known as surface plasmon resonance (SPR) was explored to determine the absorbance and scattering measured by the UV-vis spectroscopy. These values are a function of shape, size, aggregation characteristic and dielectric constants of both the metal and also the surrounding material [16]. Fig. 3 is representational of all the Seri-GNPs synthesized in different conditions. Here only temperature 80°C with pH ranging from pH 5.0 to pH 9.0 is given as an example.

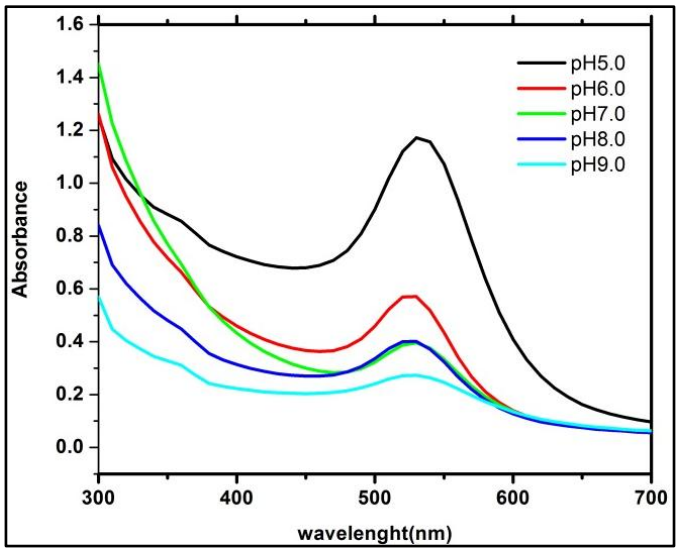

Fig.4: Seri-GNP synthesized at 80°C with varying pH 5.0 to pH 9.0. SPR band was observed at 540nm typical of gold nanoparticles.

It is observed that Seri-GNP synthesized at pH 5.0 has a sharp peak at a maximum intensity of 540 nm. As the pH of the working solution is increased systematically up to pH 9.0, a gradual band broadening trend is observed in the SPR bands. While the λ maximums of all the peaks are in the range of 530 - 540 nm their respective intensities go on decreasing. Generally, the difference in the intensity of SPR bands is attributed to diverse levels of the size distribution of particles as well as their shape in the solution along with their aggregation [17]. An intense, sharp band is indicative of high monodispersity, with negligible aggregation and extremely small particle size [16,18]. Based on these observations, samples from pH 5.0 and pH 9.0 were further characterized for DLS and TEM studies. And the interpretations of size are in

accordance with the particle sizing analysis discussed below where the similar trend is seen for DLS and TEM.

3.2. Particle size distribution and Analysis via DLS and TEM

The particle size of the synthesized gold nanoparticles in colloidal dispersions was studied. As Seri-GNP was synthesized in an aqueous dispersion of buffer solutions, they were individually dialyzed before further analysis to avoid any noise due to the presence of salts. For all the analysis using DLS, the shutter opening diameter was kept constant. As discussed in the prior section, the DLS measurements of Seri-GNPs at pH 5.0 and 9.0 were studied as two extreme opposites of the same temperature. They exhibited hydrodynamic sizes as represented in Table 1 below. The polydispersity of these particles were nearly 0.2 to 0.3.

Table 1:

Temperature	Hydrodynamic diameter (nm) of pH 5.0	Hydrodynamic diameter (nm) of pH 9.0
30°C	344.4	349
40°C	286.6	330
50°C	255.5	323
60°C	167.2	199
70°C	80	137
80°C	59.7	83.6

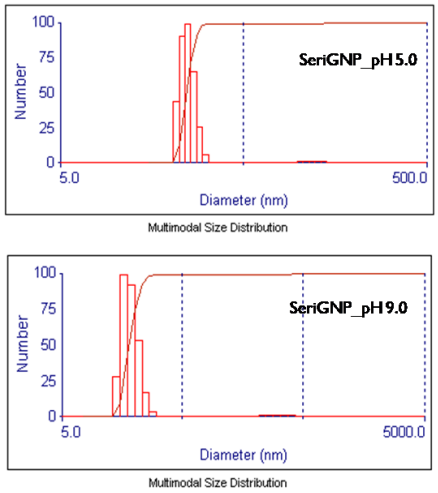

Fig.5. DLS size distribution of temperature 80°C, pH 5.0 and pH 9.0.

The values are in agreement with TEM analysis and aligning with our spectroscopic observations (Fig. 6). The particle sizes observed in TEM were almost 10 times less than the hydrodynamic diameter obtained in DLS analysis. The smallest nanoparticles were obtained at pH 5.0 and pH 9.0 at 80°C temperature which is nearly or less than 10nm. Sericin is rich in serine and aspartic acid and provided with heat, the polypeptide starts degrading. This exposes amide groups which are known to reduce Au^{3+} ions to Au^{0} [13]. Therefore, when subjected to different temperature, the degree of degradation varies leading to change in shape and size of gold nanoparticles. As many

functional groups are exposed with increasing temperature, the time required for gold nanoparticles formation also reduces. This is evident from studies conducted at 80°C where the smallest sizes (~10nm) are observed but the time required is drastically reduced from 12-hour to merely an hour. This trend is observed from 50°C onwards and remains consistent with increasing temperatures.

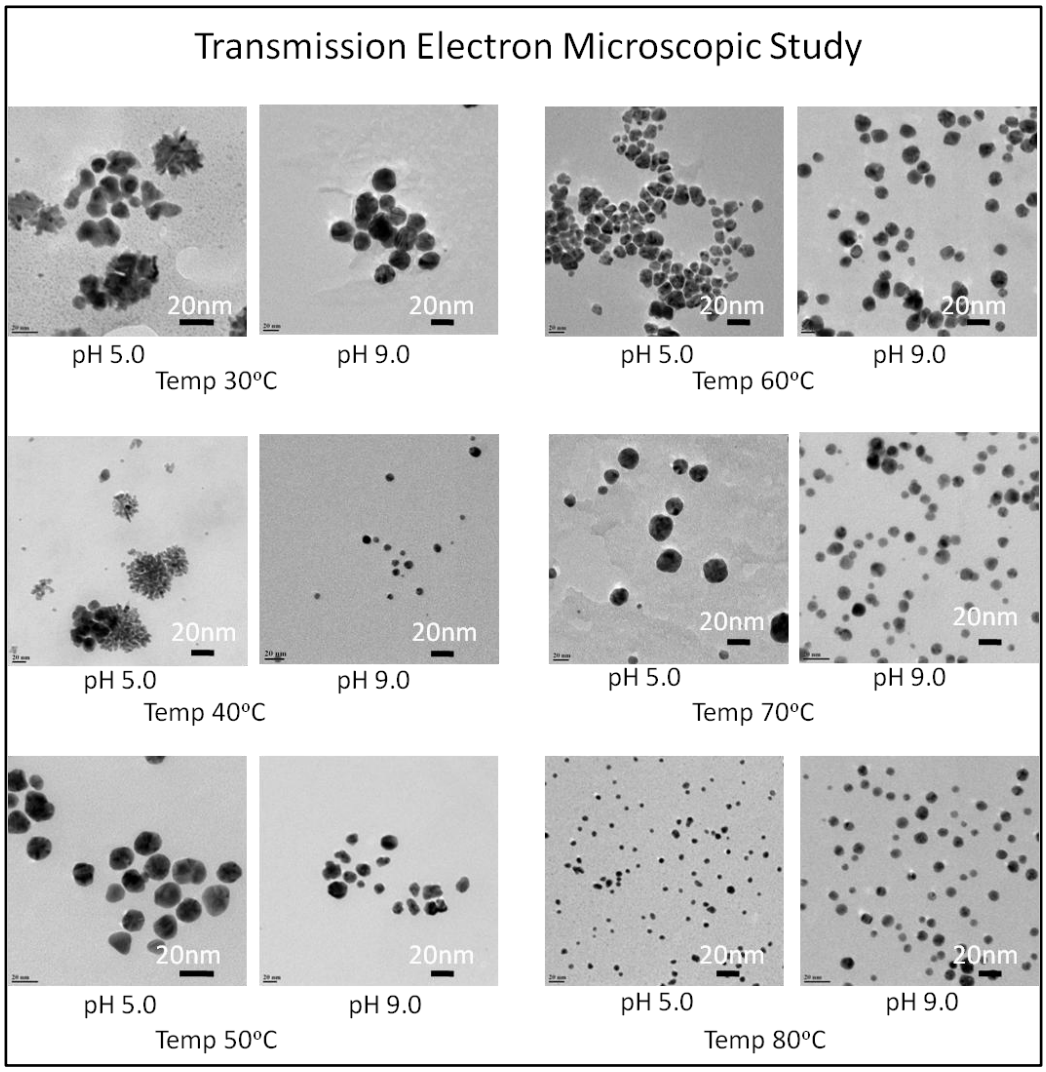

Fig. 6: TEM of Seri-GNPs synthesized at different conditions

When the stability over the range of pH was analyzed of Seri-GNPs synthesized at 80°C, we observed the charge highest in lower pH i.e. at pH 5.0 as -60.06 mV. As the pH increases, the stability of Seri-GNPs decreases. This is represented in Table 2 given below:

pH	Zeta potential (mv)
5.0	-60.86

6.0	**-52.95**
7.0	**-43.42**
8.0	**-51.14**
9.0	**-30**

Table 2: Zeta potential of Seri-GNPs synthesized at temperature 80^{o}C at varying pH

3.3. X-Ray Diffraction Analysis XRD

To further understand the crystalline nature of Seri-GNPs, XRD study was carried out for a sample of pH 5.0 and pH 9.0 synthesized at 80^{o}C. The XRD pattern recorded from the drop cast film of an aqueous solution of dialyzed and concentrated GNPs showed the signature of characteristic Bragg's reflex ions for crystalline gold as observed in Fig. 5. The diffraction peaks were indexed for [111], [200], [220] and [311] crystal planes of gold. The XRD peaks appear to be broadened, suggesting the presence of very small (few nanometers) particles constituting the major population of GNPs. When peaks of GNPs produced at pH 5.0 and pH 9.0 were analyzed; pH 5.0 GNPs had broader peak suggesting that particle size of GNPs was smaller when compared to Seri-GNPs at pH 9.0. The data corroborates the results of particle sizing and TEM data. The characteristic peaks corresponding to [111], [200] [220] and [311] of Au are located at 2θ = 38.37˚, 44.34˚, 64.56˚, and 77.80 respectively. The results indicate the sample is composed of crystalline gold [19–21].

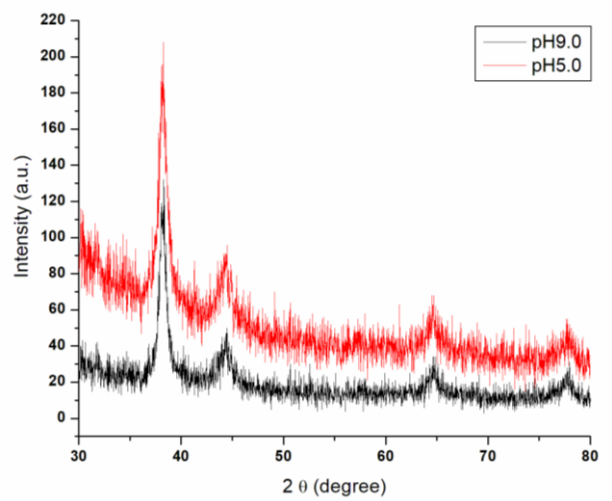

Fig. 7: XRD pattern of Seri-GNPs synthesized at 80^{o}C and pH 5.0 (red) and pH 9.0 (black).

3.4. Fourier Transform Infrared Spectroscopy (FTIR)

Later, for better understanding the interactions between sericin and gold nanoparticles Fourier Transform Infrared Spectroscopy was employed. For the study, pH 5.0 and pH 9.0 Seri-GNPs of 80^{o}C were selected as model and sericin acted as a control. In Fig. 6, the spectrum of extracted sericin has two peaks at 1530 cm^{-1} and at 1620cm^{-1} corresponding to mono-substituted amides in solution (-RCONR$_2$), secondary amines (R$_2$NH) and conjugated cyclic polypeptides all of which are characteristic of sericin [22]. Bands observed between 1610 cm^{-1} and 1625cm^{-1} generally denote thermally denatured proteins [5]. In case of Seri-GNPs synthesized at pH 5.0 and pH 9.0, a narrowly spaced doublet was observed at 1363cm^{-1} and 1620cm^{-1} while a broad band was seen at a wavelength of 3050cm^{-1}. The FTIR spectra of nanoparticles synthesized at pH 9.0 showed an additional peak at 2372cm^{-1}. In this case, the bands at 1363cm^{-1} and 1620cm^{-1} are assigned to hydroxyl (OH) and amine (NH$_2$) group respectively. The hydroxyl group came into existence only after stabilization of Au nanoparticles, unlike seen in sericin, mainly due to the reduction of gold chloride by moieties such as amides and amines. Apart from these, a week peak observed at 2372cm^{-1} indicates weak interaction of amines present within the amino acid which is not always present. Another broad peak at 3050cm^{-1} is indicative of medium or weak vibration because of stretching in O-H group present in carboxylic acids [5,22]

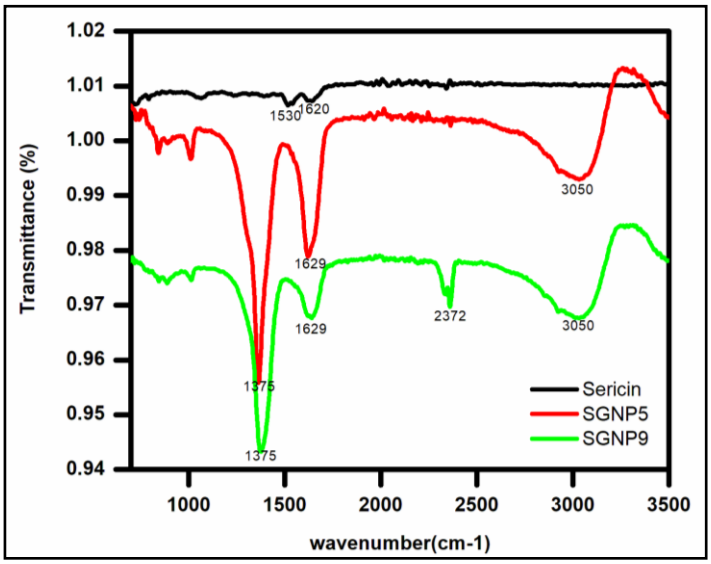

Fig. 8: FTIR of Sericin, legends SGNP5 and SGNP9 indicate Seri-GNP pH 5.0 and Seri-GNP pH 9.0 respectively synthesized at 80^{o}C.

4. Conclusions

From the current study, we were able to establish the synthesis of gold nanoparticles using Sericin, an industrially waste protein. We observed that sericin reduces $AuCl_4$ more efficiently with increasing temperature. At temperatures 30^oC and 40^oC, the gold nanoparticles form in aggregates at pH 5.0 and monodispersed at pH 9.0 with ~30-40nm size. But a drastic size reduction (<30nm) was observed from temperature 50^oC onwards which is supported by DLS and TEM data. The stability of particles was also observed to be decreasing with more alkaline synthesis condition at 80^oC. At pH 5.0 sharp surface plasmon resonance of Seri-GNPs was observed to be at 540nm, typical for gold nanoparticles and gradual peak broadening was observed with increasing pH indicating wide particle size distribution. While the FTIR data suggested that Seri-GNPs had a capping of sericin and XRD profile confirmed the crystalline nature of GNPs. Since sericin is a biologically compatible molecule, the gold nanoparticles synthesized by them will have considerably lower toxicity. These GNPs thus can be used as a novel drug delivery vehicle owing to the size and biological synthesis.

References

1. Das SK, Dey T, Kundu SC. Fabrication of sericin nanoparticles for controlled gene delivery. *RSC Adv*. 2014;4(5):2137-2142. doi:10.1039/C3RA44990D.

2. Shah M, Fawcett D, Sharma S, Tripathy S, Poinern G. Green Synthesis of Metallic Nanoparticles via Biological Entities. *Materials (Basel)*. 2015;8(12):7278-7308. doi:10.3390/ma8115377.

3. GHOSH P, HAN G, DE M, KIM C, ROTELLO V. Gold nanoparticles in delivery applications. *Adv Drug Deliv Rev*. 2008;60(11):1307-1315. doi:10.1016/j.addr.2008.03.016.

4. Zeiri Y, Elia P, Zach R, Hazan S, Kolusheva S, Porat Z. Green synthesis of gold nanoparticles using plant extracts as reducing agents. *Int J Nanomedicine*. 2014;9:4007. doi:10.2147/IJN.S57343.

5. Teramoto H, Kakazu A, Yamauchi K, Asakura T. Role of Hydroxyl Side Chains in Bombyx mori Silk Sericin in Stabilizing Its Solid Structure. *Macromolecules*. 2007;40(5):1562-1569. doi:10.1021/ma062604e.

6. Aramwit P, Siritientong T, Srichana T. Potential applications of silk sericin, a natural protein from textile industry by-products. *Waste Manag Res*. 2012;30(3):217-224. doi:10.1177/0734242X11404733.

7. Mondal, M KT and SNK. The silk proteins, sericin and fibroin in silkworm, Bombyx mori Linn., - a review. *Casp J Env Sci*. 2007;5(2):63-76. http://www.sid.ir/en/journal/ViewPaper.aspx?FID=120920070208.

8. TAKECHI T, WADA R, FUKUDA T, HARADA K, TAKAMURA H. Antioxidant activities of two sericin proteins extracted from cocoon of silkworm (Bombyx mori) measured by DPPH, chemiluminescence, ORAC and ESR methods. *Biomed Reports*. 2014;2(3):364-369. doi:10.3892/br.2014.244.

9. Aramwit P, Damrongsakkul S, Kanokpanont S, Srichana T. Properties and antityrosinase activity of sericin from various extraction methods. *Biotechnol Appl Biochem*. 2010;55(2):91-98. doi:10.1042/BA20090186.

10. Rajendran R, Balakumar C, Sivakumar R, Amruta T, Devaki N. Extraction and application of natural silk protein sericin from Bombyx mori as antimicrobial finish for cotton fabrics. *J Text Inst*. 2012;103(4):458-462. doi:10.1080/00405000.2011.586151.

11. Kitisin T, Maneekan P, Luplertlop N. In-vitro Characterization of Silk Sericin as an Anti-aging Agent. *J Agric Sci*. 2013;5(3):54-62. doi:10.5539/jas.v5n3p54.

12. Aramwit P, Bang N, Ratanavaraporn J, Ekgasit S. Green synthesis of silk sericin-capped silver nanoparticles and their potent anti-bacterial activity. *Nanoscale Res Lett*. 2014;9(1):79. doi:10.1186/1556-276X-9-79.

13. Lalit Jajpura AR. The Biopolymer Sericin: Extraction and Applications. *J Text Sci Eng*. 2015;05(01):1-5. doi:10.4172/2165-8064.1000188.

14. Wu LP1, Leng XJ, Sun Y, Ren FZ NS. Analysis of the effects of pH and salt on the conformation of the sericin particles by DLS and TEM measurements. 2010. doi:https://doi.org/10.3964/j.issn.1000-0593(2010)05-1391-05.

15. Rai A, Prabhune A, Perry CC. Antibiotic mediated synthesis of gold nanoparticles with potent antimicrobial activity and their application in antimicrobial coatings. *J Mater Chem*. 2010;20(32):6789. doi:10.1039/c0jm00817f.

16. Eustis S, El-Sayed MA. Why gold nanoparticles are more precious than pretty gold: Noble metal surface plasmon resonance and its enhancement of the radiative and nonradiative properties of nanocrystals of different shapes. *Chem Soc Rev*. 2006;35(3):209-217. doi:10.1039/B514191E.

17. Rechberger W, Hohenau A, Leitner A, Krenn JR, Lamprecht B, Aussenegg FR. Optical properties of two interacting gold nanoparticles. *Opt Commun*. 2003;220(1-3):137-141. doi:10.1016/S0030-4018(03)01357-9.

18. Guide To Dynamic Light Scattering Measurement and Analysis. Guide To Dynamic Light Scattering Measurement and Analysis. *NanoComposix*. 2012:1-7.

19. Syed A. Extracellular Biosynthesis of Monodispersed Gold Nanoparticles, their Characterization, Cytotoxicity Assay, Biodistribution and Conjugation with the Anticancer Drug Doxorubicin. *J Nanomed Nanotechnol*. 2012;04(01):1-6. doi:10.4172/2157-7439.1000156.

20. Parida UK, Bindhani BK, Nayak P. Green Synthesis and Characterization of Gold Nanoparticles Using Onion (Allium cepa) Extract. *World J Nano Sci Eng*. 2011;01(04):93-98. doi:10.4236/wjnse.2011.14015.

21. Bindhani BK, Panigrahi AK. Green Synthesis of Gold Nanoparticles Using Neem (Azadirachta indica L .) Leaf Extract and Its Biomedical Applications. *Int J Adv Biotechnol Res*. 2014;5(3):457-464.

22. Turbiani FRB, Tomadon J, Seixas FL, Gimenes ML. Properties and structure of sericin films: Effect of the crosslinking degree. *Chem Eng Trans*. 2011;24:1489-1494. doi:10.3303/CET1124249.

Chapter 6

Conclusion and Future work

From the curcumin solubility chapter i.e. Chapter 2 we can clearly establish the aspects for curcumin solubilization with its properties maintain without altering its structure and chemical bonds. We have successfully solubilized curcumin in a micellar aqueous solution of sophorolipids resulting in the synthesis of curcumin nanoconjugates in this chapter. By employing the physical force of sonication, we were able to form CurSL nanoconjugates of size in the range of 40-60nm confirmed by SEM and DLS. During their synthesis, significant chemical bonds were retained indicating no chemical modifications with respect to standard curcumin as indicated by FTIR signatures. This data is of great significance as any structural and chemical changes in curcumin can result in the loss or modification of activity. The synthesis of CurSL-GNPs was also achieved at ambient temperatures unlike that of the earlier reported studies by Singh et al 2013, where they have used 90^{o}C temperature which may lead to a loss in activity of curcumin. The rate determining step for oral drug formulation is absorption by the gastrointestinal tract with respect to the dissolution and solubility in aqueous solution. The synthesized CurSL nanoparticles when administered to Wistar rats for bioavailability study, showed a remarkable increase in retention time of curcumin in blood plasma up to 2hours. The concentration of curcumin in blood plasma was 0.015% which was calculated using the HR-MS data of standard curcumin of 1 µg/ml and which is much higher than 0.00011% and 0.00025% of previous reports.

The CurSL bioconjugate acts as a reducing and capping agent for the formation of gold nanoparticles. The distribution of CurSL-GNPs in rat showed presence in all vital organs. The size of particles is very small and in future studies, they can be functionalized and loaded with hydrophobic drugs which can be targeted to specific organs for slow release and delivery of drugs which may even carry them and cross BBB. Our method of solubilization of curcumin can become a solution for the use of curcumin as a therapeutic drug in modern science.

After solubilization, we were able to successfully bio-transform curcumin into a new assembled molecule (chapter 3). It is quite possible that curcumin got degraded within few hours of addition into production medium, but the organism *C. bombicola* was able to attach the degraded product to de novo synthesized acidic form C18 of sophorolipid. This in a way

value added the degradation product and showed application as an anti-oxidant, anti-tyrosinase, anti-cancer and for Theranostic application like microbial bio-imaging and anti-biofilm activity. The compound was identified as five degradation products and two forms of SL viz., diguaiacol acidic deacetylated SL , 4 vinyl guaicol acidic acetylated SL , Vanillic acid acidic diacetylated SL, Vanillic acid acidic deacetylated SL, Bicyclopentadione acidic diacetylated SL , Deacetylated acidic SL, and Acidic diacetylated SL. Although all the activities and characterization done in this chapter are a collective effect of these compounds, a more detailed study needs to further the understanding of CSL.

The part of this thesis work was to develop drug delivery system, and we have successfully established the role of SL in the synthesis of $CaCO_3$ micro-particles (chapter 4) were SL makes the particles more porous and helps in determining the shape of particles based on the sequence of addition. In probe sonication method, when SL is added in sodium carbonate, it helps in formation of spindle shaped $CaCO_3$ particles. This happens due to lamellar micelle formation of SL causing the $CaCO_3$ crystallization in layered formed. The spindles when compared with bare $CaCO_3$ spindles i.e. without SL, the surface is quite rough and structured. This increases the surface to volume ration and can be used in application like paints, paper or even fillers in cement for dentistry. While, when SL mixed with calcium chloride, leads to spherical particle formation. Again this can be attributed to spherical miceller formation helping the $CaCO_3$ crystallization around them. The final particles have porous structure.

The magnetic stirring method shows spherical particles formation in both the sequences of SL addition. This can be due to the less forceful method of stirring helps SL to interact more and form spherical micelles and bubbling in biosurfactant, causing open spheres to form. The diameter of opening again varies with the addition of SL in particular salt solution, like when SL is in sodium carbonate, larger opening is observed. In case of SL in calcium salt solution smaller opening and tighter spheres are formed.

These experiments easily establish the role of sophorolipid and the method in which it is added can immensely influence the formation of $CaCO_3$ particles. Hence from these two physical method and variation in addition of SL, we chose the best suited particles for drug loading assay. The furosemide drug loading and release profile observed from spherical $CaCO_3$ microparticles obtained from set II of sonication method, also ascertain the notion of $CaCO_3$ as a good drug delivery system.

Apart from $CaCO_3$ particles, many reports suggest use of gold nanoparticles for drug delivery. Therefore, in chapter 5 we were able to establish the synthesis of gold nanoparticles using Sericin, an industrially waste protein. We observed that sericin reduces $AuCl_4$ more efficiently with increasing temperature. At temperatures 30^oC and 40^oC, the gold nanoparticles form in aggregates at pH 5.0 and monodispersed at pH 9.0 with ~30-40nm size. But a drastic size reduction (<30nm) was observed from temperature 50^oC onwards which is supported by DLS and TEM data. The stability of particles was also observed to be decreasing with more alkaline synthesis condition at 80^oC. At pH 5.0 sharp surface plasmon resonance of Seri-GNPs was observed to be at 540nm, typical for gold nanoparticles and gradual peak broadening was observed with increasing pH indicating wide particle size distribution. While the FTIR data suggested that Seri-GNPs had a capping of sericin and XRD profile confirmed the crystalline nature of GNPs. Since sericin is a biologically compatible molecule, the gold nanoparticles synthesized by them will have considerably lower toxicity. These GNPs thus can be used as a novel drug delivery vehicle owing to the size and biological synthesis.

Future Work

We would like to continue the CSL work for the synthesis of nanoparticles like zinc oxide (ZnO). ZnO nanoparticles are broad spectrum anti bacterial agent and are synthesized at low cost with less toxicity towards human cells. Their UV blocking and anti-biofilm activity makes them as a suitable coating material for medical and other devices, and it is approved by the Food and Drug Administration (FDA) in the treatment of disease and ingredients in food additives (Felix et al, 2015).

Because of its distinct properties ZnO are widely used in many fields such as rubber industry, pharmaceutical and cosmetic industries, textile industries, electronic and electro technology industries. Towards this aspect we have got some interesting leads, we have synthesized ZnO nanoparticles using CSL as capping agent through different ways of addition (methodology similar to chapter 4)

The nanoparticles obtained were further characterized by SEM and TEM.

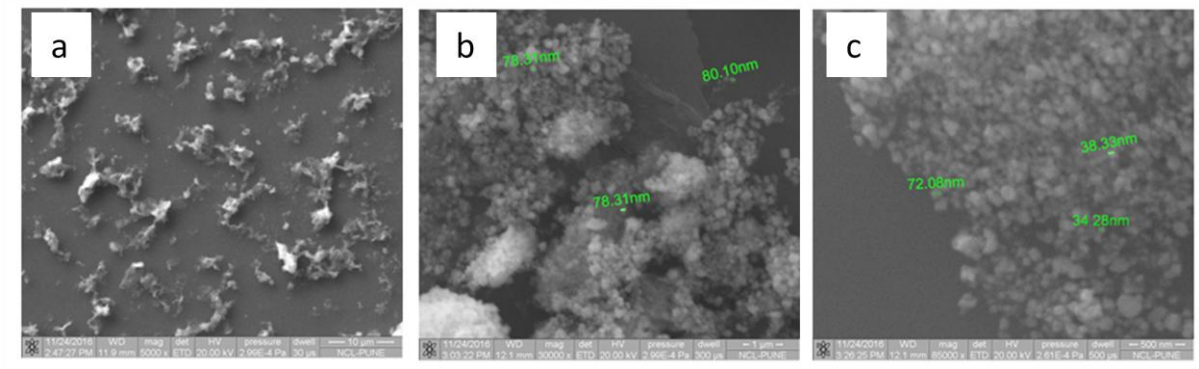

Fig 1 SEM images (a) Control solution of ZnO nano-material in aggregates (scale 10µm) (b) CSL reduced/capped ZnO particles as separate (scale 1µm) (c) CSL reduced/capped ZnO particles as separate (scale 500 nm)

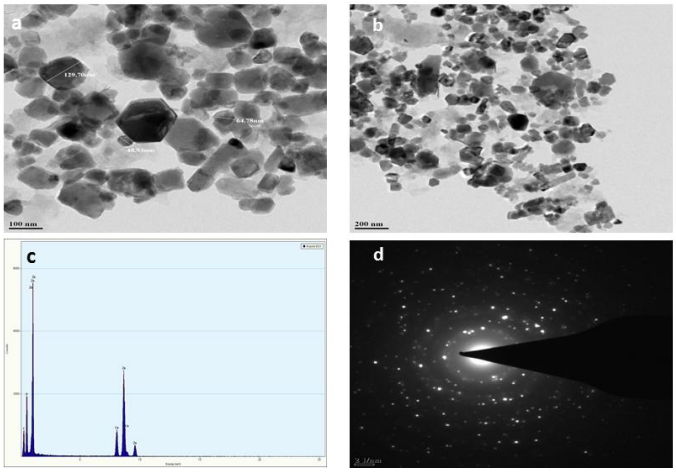

The above figure indicates the formation of ZnO particles and is represented with SAED pattern indicating the crystalline nature of particles and EDX confirming the composition.

We performed the antibacterial assay of the synthesized particles to check their anti-bacterial potential and observed a very good bactericidal activity.

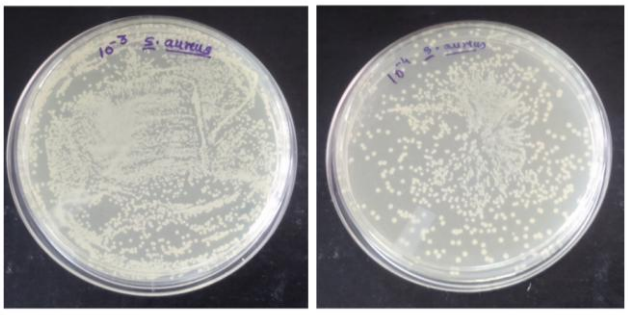

Control 10^{-3} dilution, (*S.aureus*)

control 10^{-4} dilution, (*S.aureus*)

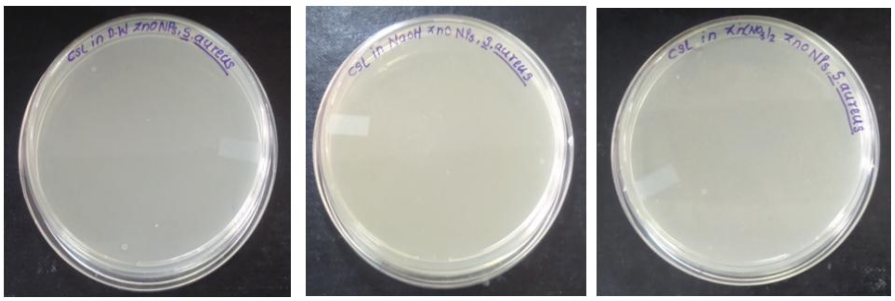

20 mg CSL in D/W, 1mg/ml, (*S.aureus*)

20 mg CSL in NaOH, 1mg/ml, (*S.aureus*)

20 mg CSL in Zn(NO3)2, 1mg/ml, (*S.aureus*)

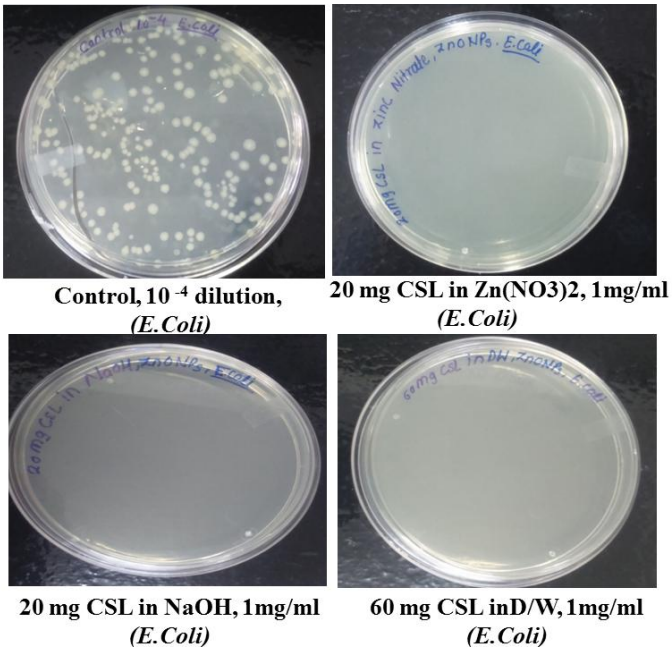

Fig 2: Anti bacterial activity of ZnO against *S.aureus* and *E. coli*

Although the particles when synthesized in different conditions gave good anti-bacterial activity, the concentrations used for the study were high and detailed works needs to be done.

List of Publication:

- **Priti A. Darne**, Mihir R. Mehta, Sachin B. Agawane and Asmita A. Prabhune, Bioavailability studies of curcumin–sophorolipid nano-conjugates in the aqueous phase: role in the synthesis of uniform gold nanoparticles. ***RSC Adv***., 2016, 6, 68504.

- **Priti Anand Darne**, Pradnya Chandane, Arun Puranikmath and Asmita Prabhune, Sericin mediated size modulation of Gold nanoparticles: Role of pH and Temperature. ***RSOS*** **(Manuscript under review)**

- **Priti Anand Darne**, Pradnya Chandane and Asmita Prabhune, Synthesis of biocompatible Calcium carbonate ($CaCO_3$) microparticles as a drug delivery system using sophorolipid as a capping agent to increase the porosity of synthesized particles **(Manuscript under preparation)**

- **Priti Anand Darne**, Pradnya Chandane and Asmita Prabhune, Derivatization of curcumin via biotransformation and exploring its applied aspects **(Manuscript under preparation)**

Patent: Provisional filing CSIR no.: 2016-NF-0143

Seminar and Workshop attended:

1. "**Green synthesis of porous and diverse shaped Calcium carbonate micro and nanoparticles**" accepted for oral presentation at the 21st Annual Green Chemistry and Engineering Conference held on June 13-15, 2017, Reston, VA, USA.

2. International Symposium on "**Microbial Ecology and Systematic**" held on 16-17 September 2016, at CSIR-National Chemical Laboratory, Pune, India.

3. "**Sericin based synthesis of Tunable, Monodispersed and Stable Gold nanoparticles: Role of Temperature and pH**" poster presentation held 26-27 February 2016 as a part of National Science Day celebration, at CSIR-National Chemical Laboratory, Pune, India.

4. "**Multifold increase in bioavailability of curcumin using a safe biocompatible and promising method**" poster presentation held 26-27 February 2015 as a part of National Science Day celebration, at CSIR-National Chemical Laboratory, Pune, India.